VRLA Battery Float Charge: Analysis and Optimisation

A Thesis Submitted for the
Fulfilment of the Requirement for the Degree of
Doctor of Philosophy of Engineering (Electrical and Electronic)

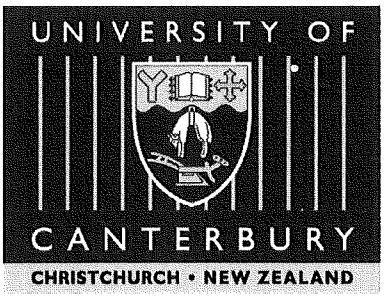

Electrical and Electronic Engineering Department
University of Canterbury
New Zealand

Phillip M. Hunter, B.E. (Hons), M.E.

July 2003

Abstract

This thesis investigates the float charge operation of Valve Regulated Lead Acid (VRLA) batteries in standby power applications. While the telecommunication standby power system is the targeted application, the results are applicable in any situation where VRLA batteries are subjected to long periods of float charge. The goals of float charge are identified and a test and analysis procedure is developed to provide a means of assessing the effectiveness of the applied float charge. The primary goal of float charge is to counteract the natural self-discharge of the battery and indefinitely maintain it in a fully charged state. A secondary goal of float charge is to maximise the life of the battery. This is achieved by ensuring that ageing mechanisms such as positive grid corrosion and gas venting are maintained at minimum levels.

The problems associated with conventional float charge control are investigated and, in particular, the electrode imbalance problems associated with some long life VRLA cells are detailed. These electrode imbalance problems can result in the cell suffering a gradual discharge of the negative electrode while the cell appears healthy and on a float charge. This ultimately results in reduced cell capacity and is identified as a major cause of the premature failure of long life VRLA cells.

Float charge analysis and the subsequent optimisation relies heavily on knowledge of the polarisation distribution between the positive and negative electrodes within a cell. Conventionally, this is determined with the aid of a reference electrode, although such testing is only possible in a well-controlled laboratory environment. By modelling the steady state and transient features of both the positive and negative electrodes, a test and analysis procedure is developed to estimate the polarisation distribution within a conventional 2 V VRLA cell, in effect creating a virtual reference electrode. The developed procedure exploits differences in the transient response of each electrode to estimate their polarisations at the applied float voltage. The polarisation estimations are typically accurate to within 10 mV, the window of polarisation relating to minimal positive grid corrosion is approximately 40 mV wide, and the total polarisation applied to a VRLA cell is around 130 mV. The test requires only a very low rate constant current discharge, and cell terminal voltage measurements. This test may be automated and applied to cells in field service, and provides the necessary measure to gauge float charge

optimisation. The developed test is able to verify that a cell on float charge is indeed fully charged, and assists in determining the optimal float voltage for maximum cell life.

Extended Summary

A continuous power supply is critical to the success of many applications. Telecommunication systems are a prime example of this, as they are expected to function continuously in the event of a power outage. A typical telecommunications power system converts the AC-grid power to 48 V DC, and then uses this to charge storage batteries and supply the load. In the event of a disruption to the AC-grid power, critical plant is supplied directly from the storage batteries. Depending on the load size and required back-up time, large amounts of energy storage are often necessary. Lead acid batteries are traditionally used as the storage element due to their relatively low cost, high energy density, and reliability. There has been a recent trend towards the use of Valve Regulated Lead Acid (VRLA) batteries due to perceived savings from reduced maintenance and ventilation requirements. The chemistry of a VRLA battery is the same as a conventional flooded lead acid battery, but the physical construction of a VRLA cell has been optimised to allow the gases produced during overcharge to be recombined back into water. Periodic addition of water to replace that lost through gas venting is therefore not required (or possible) with a VRLA battery. In situations where there is a reliable AC power supply, years can pass before the power supply might be interrupted, during this time the storage batteries must be maintained in a fully charged state. All lead acid batteries have a natural self-discharge, so a float charge must be supplied in order to maintain the battery in a fully charged state. Constant voltage float charge is normally recommended, and may be specified as a function of the battery temperature.

In this thesis, the goals of optimal VRLA battery float charge management are identified, and the requirements for measuring or verifying the achievement of these goals are also established. An investigation into the problems associated with present float charge methods and existing float charge optimisation and analysis techniques is also undertaken. The problems and suspected mechanism leading to the premature failure of some long life VRLA batteries is described, and a test procedure for the early detection of this failure mechanism is developed. Analysis of the developed test procedure, applied to the terminals of a standard 2 V VRLA cell, provides an estimation of the polarisation distribution within the cell. As the procedure reveals information that traditionally could only be obtained through the careful use of an additional reference electrode, the test and analysis may be used as a virtual reference electrode for float optimisation.

An equivalent electrical model of the float charge region of a VRLA battery is also developed. This model reproduces both the steady state and transient responses of a VRLA cell on float charge. Two goals of float charge have been identified:

1) Ensure the battery remains fully charged indefinitely.
2) Maximise the life of the battery by maintaining ageing effects at minimum levels.

To ensure that a cell remains fully charged, both electrodes within the cell must be sufficiently polarised[1] (raised above their fully charged open circuit rest-potential). To maximise the life of a VRLA cell, grid corrosion and gas loss (venting) must be minimised. The traditional (designed) failure mechanism of lead acid batteries is excessive corrosion of the positive grid. The grid forms a low resistance path within the electrode, allowing large currents to be drawn from it. Grid corrosion reduces the cross-sectional conductor area, which increases its resistance. Eventually this resistance rises to a point where the cell can no longer supply the necessary current at the required terminal voltage. At this point the cell is said to have reached the end of its life. Due to the potentials involved, positive grid corrosion can never be completely eliminated, but it can be optimised to ensure the lowest possible rate. It is commonly accepted that the rate of positive grid corrosion is a function of the polarisation on the positive electrode, and has a minimum rate occurring at a polarisation slightly greater than the open circuit rest potential. While there is some debate on the actual voltage at which the grid corrosion minima occur[2,3], a window of acceptable grid corrosion occurs between 40 and 80 mV. The polarisation associated with minimum grid corrosion may vary with cell chemistry.

A typical fully charged open circuit rest voltage for a VRLA cell is 2.14 V. For such a cell a float voltage of 2.27 V may be recommended. At this float voltage, a total polarisation of 130 mV must exist. If, for example, the optimal positive electrode polarisation for minimum corrosion exists at 50 mV, the negative electrode must then support the remaining polarisation of 80 mV. As both electrodes are raised above their open circuit potentials, the primary goal of float charge will also be satisfied, and the cell will be maintained in its fully charged state indefinitely.

Traditionally, an optimal (recommended) float charge voltage is determined on sample cells in a laboratory with the aid of a reference electrode. This recommended float voltage is then applied (largely unchecked) to cells in service in the field. A further complication is that 2 V cells are

connected in series to produce the desired system voltages (typically 24 or 48 V). A single supply is then used to charge the series connected cells. Small differences between cells (resulting from manufacturing variance) may produce a distribution of cell voltages, despite all cells receiving an identical float current due to the series connection.

With an industry trend towards reducing battery maintenance, longer life batteries are desirable. However it is becoming increasingly apparent with many long life VRLA batteries that either poor design or poor quality manufacturing results in the cells failing prematurely in the field. This is believed to be due to internal electrode balance problems, and in particular negative plate discharge. As grid corrosion is the traditional failure mechanism, an obvious way to improve the battery life is to reduce the rate of grid corrosion. This may be achieved by altering the grid alloy. However for balanced float charge operation, the current associated with corrosion of the positive grid must balance the current associated with (impurity related) hydrogen evolution at the negative electrode. If the grid corrosion rate is reduced and the purity of the negative electrode is not appropriately compensated, polarisation of the negative electrode will be reduced by the excess current required for hydrogen evolution. If the current associated with hydrogen evolution at the negative electrode is sufficiently large when compared to the current associated with positive corrosion, the positive electrode will support the entire polarisation applied to the cell. A gradual discharge of the negative must result in order to supply the current required for the hydrogen evolution. While this rate of negative electrode discharge may be extremely low, the cumulative effects over months or years of float charge can be significant. Furthermore, as the applied polarisation is supported entirely by the positive electrode, increased rates of grid corrosion, gassing, and possible dryout must result.

Analysis and subsequent optimisation of the float charge relies heavily on knowledge of the polarisation distribution between the positive and negative electrodes within a cell. Conventionally, an optimal float voltage is determined by the cell manufacturer and is applied virtually unmonitored to all cells of that type in field use. However, due to the importance polarisation plays in float charge optimisation, a number of schemes have been published[4 5 6 7] that require varying designs of reference electrodes or reference cells for float polarisation analysis and subsequent control purposes. Without exception, all of these systems require cell modifications to facilitate the use of the reference electrode or reference cell. As VRLA cells basically function as a sealed unit, it is difficult to insert a reference electrode without disturbing the seal and modifying the cells' characteristics.

A test and analysis procedure is developed to produce an estimate of the distribution of polarisation between the positive and negative electrodes within a cell. This test is applied to the terminals of a conventional 2 V VRLA cell, and no reference electrode or cell modifications are required. Provided the battery is properly designed and manufactured, optimal float charge requires the polarisation on the positive electrode to be maintained within a defined (minimum corrosion) window. The estimated polarisation distribution may be used to determine whether the test cell is fully charged, and if so, how optimal the float voltage is. It can also be used to determine whether the test cell is suffering from imbalance problems, such as positive or negative plate discharge. In effect, the test and analysis procedure produce a virtual reference electrode, as information on the polarisation of each electrode is obtained. The test can be performed with only a small amount of low-power electronic hardware. The size and cost of this hardware lends itself well to automated field use. Based on significant differences in the transient decay of the polarisation on each electrode, the test requires only cell terminal voltage measurements and a low-rate constant current discharge (of a similar magnitude to the normal float current). With a typical test duration being less than ten minutes, the test has negligible impact on cell health, as the depth of discharge is typically less than 0.01%.

With the aid of a reference electrode, a thorough investigation of the float charge characteristics (steady state and transient) of a VRLA battery has been undertaken. The results of this testing have allowed the development of an equivalent electrical-model of each electrode. For each applied current, the developed electrode models reproduce the voltage response seen at both electrodes within a cell, or, for an applied voltage, the models will draw the correct current. Combining the models of the positive and negative electrodes reproduces the overall terminal response of the cell.

While the electrical-equivalent model has not been developed to represent chemical reactions occurring within a cell, the physical layout of the model is linked closely with the physical construction of a cell. The model's component values and transition points may be interpreted as features of the chemical reactions, however the model is not based on, or intended to represent, the actual chemical processes occurring within a cell. As the target region of battery operation is at or near float charge, to avoid confusion and minimise calibration requirements, the model's representation of the bulk storage is limited. Should a complete battery model be required, further investigation and development of the bulk charge storage region will be necessary.

Although the developed float charge model is not strictly required for the developed polarisation estimation test and analysis, it does simplify the understanding of the processes occurring within a cell. This may be beneficial if the present float charge operating point is to be used as a basis for further optimisation of the float charge voltage. There are many other applications that may benefit from the developed VRLA battery float charge model. Such applications may include a battery simulator to aid the development, optimisation, and modelling of cell equalisation hardware, or the overall control of the power system. Battery chemists and manufacturers may also benefit from the float charge model or the polarisation estimation test, as non-intrusive verification testing may be performed on new and existing products. The float model may provide a simple method of tracking or characterising the internal operation of a cell during natural or accelerated ageing. Furthermore, the float charge model and associated polarisation estimation test may be used to determine the internal characteristics (Tafel plots etc) of cells that are identified as problem cells during field-testing. With knowledge of the actual root of the problem, the most appropriate corrective action may be taken.

References

[1] D. Berndt, U. Teutsch, *Float Charging of Valve-Regulated Lead-Acid Batteries: A Balancing Between Secondary Reactions,* Journal of the Electrochemical Society, Vol. 143, No. 3, March 1996.

[2] J. Jergl, B. Cole, & S. Purcell, *Real World Effects on VRLA Batteries in Float Applications,* Proceedings of INTELEC, 1996, 11-4.

[3] W.B. Brecht, D.O. Feder, J.M. McAndrews, A.J. Willlamson, *The Effect of Positive Polarisation on Grid Growth, Cell Performance and Life "Willihnganz Revisited – 20 Years Later",* Proceedings of INTELEC, 1988, 5-7.

[4] S. C. Chalasani, V. J. Thottuvelil, *Recharging Circuit and Method for Recharging a Battery Having a Reference Electrode,* United States Patent 6,137,266, October 24, 2000.

[5] T. D. O'Sullivan, C. F. Leung, *Field Test of a Polarisation Controller on a Mixed Battery String,* Proceedings of INTELEC, 1992, 9-2.

[6] K. M. Mistry, T. D. O'Sullivan, *Electrical Storage Cell Life Extender,* United States Patent 4,935,688, June 19, 1990.

[7] E. A. Willihnganz, *Method and Apparatus for Measuring the State of Charge of a Battery Using a Reference Battery,* United States Patent 3,657,639, April 18, 1972.

Acknowledgements

There are many people whom I must thank for their assistance to me while conducting this research into the analysis and optimisation of VRLA battery float charge. First and foremost, I would like to thank my supervisors, Dr. Adnan H. Anbuky at *Powerware NZ*, and Associate Professor Harsha R. Sirisena at the *University of Canterbury* for their assistance and support throughout this project.

I would like to make special mention of Adnan's guidance, direction, and motivation. The formation, success, and stability of the research group at *Powerware NZ*, in which this project has been supported, is almost entirely due to his dedication and persistence in the area of battery management research, throughout many changes in our workplace. Adnan's knowledge, advice, and technical supervision have been fundamental to the success and completion of this research.

Many of the staff at *Powerware NZ* have been of assistance to me during the course of this research. There are too many to name individually, so I would like to acknowledge all of those people who have made a contribution be it large or small. *Powerware NZ* must also be thanked for facilitating this research, and for the provision of the facilities and resources required for its completion.

I would also like to thank the *Foundation for Research, Science, and Technology* for their financial support of both this project and myself over the past three years. Without this support, this research would not have been undertaken.

Lastly, and certainly not least, I would like to thank Bronwyn Charles for her unwavering love, support, and patience, as well as her tolerance of my focus on this work. I am also extremely grateful for the countless hours Bronwyn has spent proof reading and correcting my novel use of the English language.

Table of Contents

Table of Figures

Table of Tables

Abbreviations

A	Amp
AC	Alternating Current
AGM	Absorbent Glass Mat
°C	Degrees Celsius
DC	Direct Current
DLL	Dynamic Link Library
DSO	Digital Storage Oscilloscope
DUT	Device Under Test
EIS	Electrochemical Impedance Spectroscopy
GPIB	General Purpose Instrumentation Bus
GΩ	Giga-Ohm
Hz	Hertz
kPa	kilo-Pascals
K	Kelvin
mA	milli-Amp
mHz	milli-Hertz
ms	milli-seconds
mV	milli-Volt
MΩ	Mega-Ohm
nA	nano-Amp
ODE	Ordinary Differential Equation
pA	pico-Amp
PCB	Printed Circuit Board
PLC	Power Line Cycles
PPP	Positive Plate Polarisation
S.H.E.	Standard Hydrogen Electrode
SOC	State of Charge
SOH	State of Health
μA	micro-Amp
μF	micro-Farad

μH	micro-Henry
μV	micro-Volt
UPS	Uninterruptible Power Supply
V	Volts
VPC	Volts Per Cell
VRLA	Valve Regulated Lead Acid
W	Watt
w.r.t	With Respect To
Ω	Ohm

1 Introduction

1.1 The Telecommunication Power System

The modern electronic age in which we live has an ever-increasing reliance on telecommunications. Communication, via wire, fibre-optic, or radio frequency, is no longer regarded as a luxury, but as part of everyday life and a requirement for business. To support the increasing demands and reliance on communication systems, Uninterruptible Power Supplies (UPS) have been developed. These are designed to supply continuous power to the telecommunication system, even in the event of a mains power failure.

A typical telecommunication power system is shown in Figure 1.1. The rectifier converts the AC mains power to 12, 24, or 48 V DC. Both the telecommunication equipment and storage batteries are supplied directly from the rectifier's DC voltage. In the event of an AC mains power failure, the communications equipment is supplied directly with the energy stored in the battery. Depending on the importance of the load, a generator may also be used to provide power during a mains failure, however the batteries are still required to bridge power during the generator's start-up period, and as a back-up should the generator fail to start.

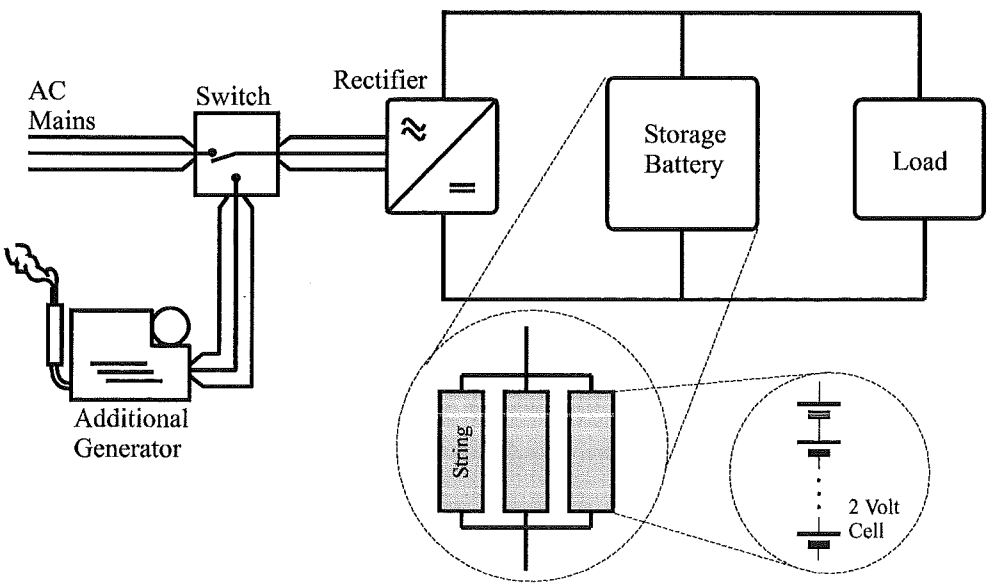

Figure 1.1 A Typical Telecommunication Power System

Due to considerations such as cost, reliability, safety, energy density, and life expectancy, the lead acid battery is by far the most popular storage device in standby power systems. More recently, there has been a trend towards Valve Regulated Lead Acid (VRLA) batteries due to the perceived reduction in associated maintenance costs. If operated correctly, the VRLA battery does not require any additional water throughout its life, as the design of the battery allows the hydrogen and oxygen produced during overcharge to be recombined back into water. The VRLA battery is effectively sealed, with only a one-way pressure relief valve to prevent explosion should the battery be operated beyond its design limits. As there is no access to allow electrolyte replacement, the VRLA battery is less tolerant than a flooded battery to overcharge abuse. The VRLA battery requires greater care and more precise charge-control than conventional flooded lead acid batteries if its full useful life is to be realised.

With the lead acid chemistry having a nominal voltage of 2 V per cell, cells are stacked in series to achieve the voltages (12, 24, or 48 V) required by the telecommunications equipment. Often with smaller capacity cells, two, three, four, or six cells are combined into a 'mono-block', where the terminals of the block produce the series sum of the individual cells within it. The capacity of the battery must be suitably sized and store sufficient energy to power the load until an alternative power supply can be established, or the primary supply is restored. Typical standby lead acid battery sizes may range from tens to thousands of amp-hours capacity. When greater capacity or increased reliability is required, parallel strings are often used.

1.1.1 Standby Battery Operational Phases

There are three distinct phases of standby battery use - discharge, recharge, and float charge. The discharge phase normally occurs during an AC mains power failure, when the battery supplies energy to the load to ensure continuous operation. Depending on availability of a secondary power supply such as a generator, the physical location, accessibility, and significance of the load, discharge time may range from a few minutes to several days. When the AC power is re-established, the energy taken from the battery during the discharge must be replaced. This is commonly known as the recharge phase, and continues until the battery is returned to a fully charged state. Typically, 80% of the recharge is complete within ten hours, however the remainder may take up to 72 hours to complete. When the battery has reached a fully charged state, it enters the float charge. Float charge attempts to maintain the battery in a fully charged

state indefinitely, counteracting the effects of self-discharge that occur when a battery is left to stand for a period of time. Depending on the quality of the primary power supply, a standby battery may remain in the float charge phase for months or even years before an interruption to the primary power supply requires the battery to supply power to the load in another discharge phase. During this sometimes lengthy period of limited battery activity, the cumulative effects of minor imbalances within a cell, or imbalances between cells, may have a large influence on the charge state or readiness of the battery. If the battery is not properly maintained during this float period, only a fraction of the alleged battery capacity may be available when discharge is required.

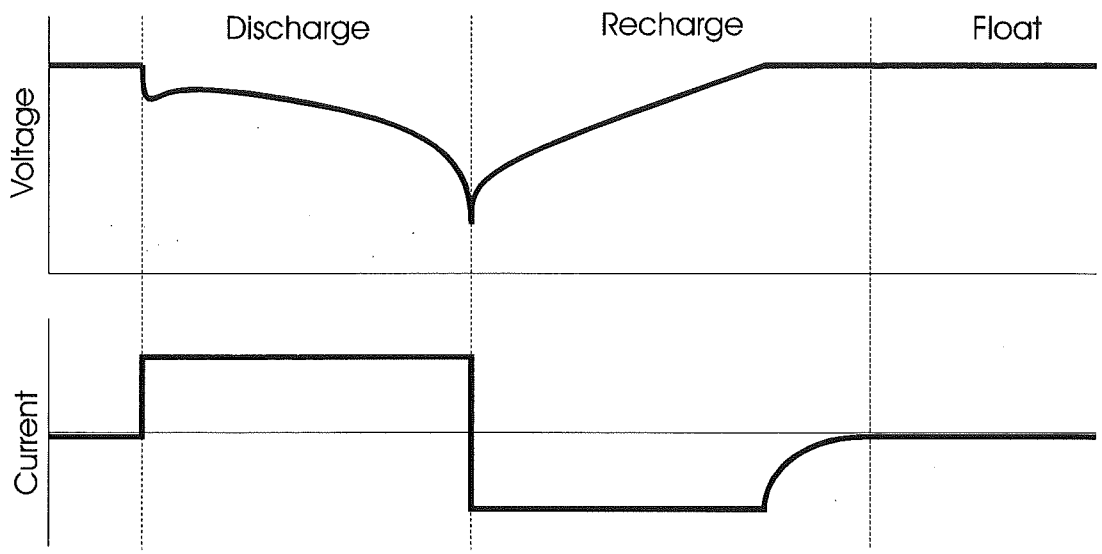

Figure 1.2 Standby Battery Operational Phases

1.2 Thesis Purpose and Structure

The VRLA battery is by far the most common energy storage device used in telecommunication power systems. However, even when these batteries are operated within the manufacturer's guidelines, a large number appear to fail prematurely, well short of their designed life.

The purpose of this thesis is to investigate the float operation of VRLA batteries in telecommunication standby applications. The investigation identifies possible causes of premature cell failure and highlights deficiencies in present float charge management techniques.

A simple field useable test has been developed to identify whether a cell on float charge is indeed fully charged and operating as designed, or whether it is suffering from an internal charge imbalance. This test may also be used to select the most appropriate float voltage of each individual cell as they age or are subjected to various (thermal) operating conditions.

Prior work by the author[1] [2] has investigated the recharge phase of VRLA battery operation and works by Pascoe[3] [4] have investigated the discharge phase. These works, together with that presented in this thesis cover the complete operational cycle of a VRLA battery.

A brief introduction into the operational phases and use of VRLA batteries in telecommunication power systems has been given in Chapter 1 of this thesis. Chapter 2 provides an in-depth introduction to VRLA batteries, and details the underlying cell chemistry and the requirements for satisfactory continuous float service. Two goals of float charge are drawn from this. Through review of relevant literature, an analysis of float charge operation is undertaken and the failure modes linked to float operation are highlighted. Chapter 2 also examines existing methods of float charge and various control and optimisation schemes. Chapter 3 describes the test system and equipment constructed and used throughout the course of this research. Chapters 4 and 5 detail the testing and analysis that lead to the development of an electrical equivalent model of the float charge operational characteristics for VRLA cells. From this model, a test and analysis procedure was developed, allowing covert information about the internal operation of a cell to be extracted. This test does not require any modification to the cell, and may be easily applied to a standard 2 V VRLA cell in field service. Chapter 6 verifies the developed model and the associated test and analysis procedure through testing of a cell with vast differences in size, type, and construction. Chapter 6 also discusses possible applications of the model and the test and analysis procedure. Chapter 7 concludes this work through a brief description of the achievements and outcomes of the research.

1.3 References

[1] P. M. Hunter, *Advanced Battery Management and Control,* M.E. Thesis, University of Canterbury, New Zealand, 1999.

[2] P. M. Hunter, A. H. Anbuky, *VRLA Battery Rapid Charging Under Stress Management,* IEEE Transactions on Industrial Electronics, Vol. 50, No. 6, December 2003.

[3] P. E. Pascoe, *VRLA Battery State of Charge Estimation,* M.E. Thesis, University of Canterbury, New Zealand, 1998.

[4] P. E. Pascoe, *Standby VRLA Battery Behavioural Prediction,* Ph.D. Thesis, University of Canterbury, New Zealand, 2001.

2 The Standby VRLA Cell

Raymond Gaston Planté developed the first practical lead acid battery 143 years ago, in 1860. Since then there have been many developments and improvements in the understanding and design of lead acid batteries. A significant development was made in the 1970s with the production of the 'sealed' lead acid battery. While termed 'sealed', these batteries contain a small pressure relief valve to prevent possible explosion, and hence are also commonly referred to as Valve Regulated Lead Acid (VRLA) batteries. The VRLA battery operates on the same basic chemistry as a flooded lead acid battery, however its physical construction provides a mechanism for the gasses produced during overcharge to be recombined into water, thus eliminating the need for periodic water replacement throughout the life of the cell.

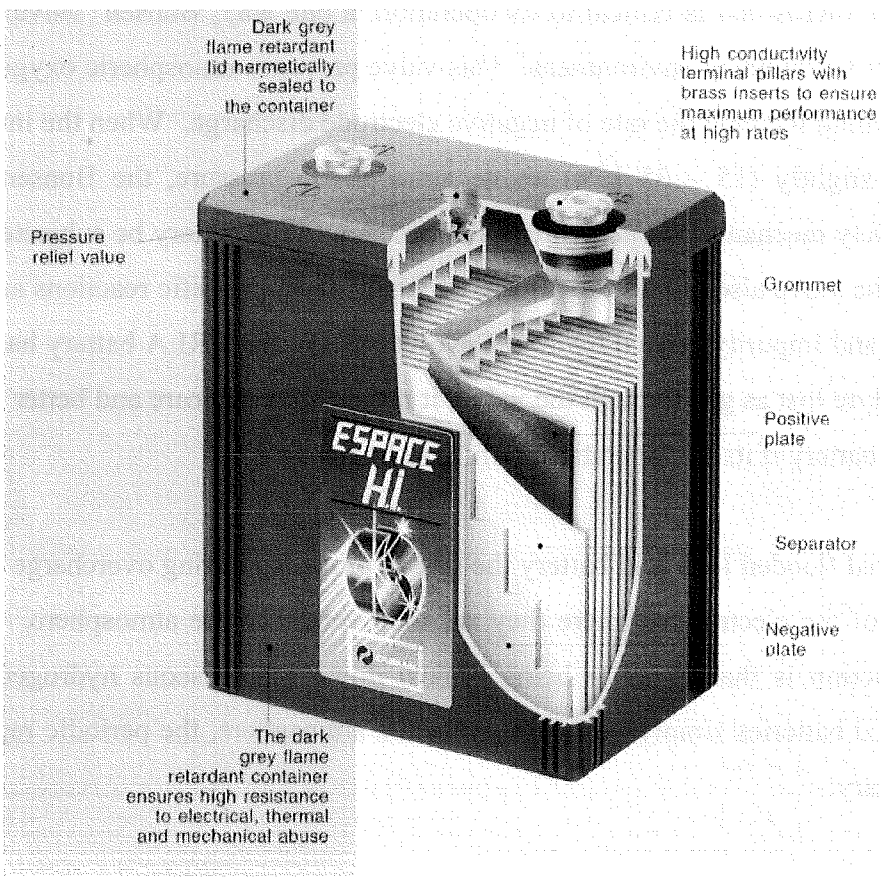

Figure 2.1 A Typical Absorbent Glass Mat (AGM) VRLA Cell [1]

In all VRLA batteries the electrolyte is immobilised. There are two common methods of achieving this; the electrolyte is either 1) suspended in an Absorbent Glass Mat (AGM Cell) separator between the plates, or 2) immobilised by a fumed silica gel (Gel-Cell). Typically, new VRLA batteries are supplied with excess electrolyte. This over-wet state reduces the oxygen transport between the positive and negative electrodes, resulting in gas venting. The VRLA cell functions as a flooded cell until sufficient water is lost through the gas venting process and the cell dries out sufficiently to produce the necessary gas transport paths through the separator. These paths allow the overcharge gasses produced at the positive electrode to migrate through the separator to the negative electrode, where they are recombined into water. VRLA cells have only a minimum amount of electrolyte immobilised in the separator, and are therefore often described as having a 'starved' electrolyte.

Figure 2.1 shows the internal components of an AGM VRLA cell. Because the balance of gasses within a VRLA cell is critical to its operation, a one way 'Bunsen' valve is used to seal the cell from its surrounding environment. This valve prevents atmospheric oxygen entering the cell, where it would increase the rate of negative electrode discharge. When the internal pressure of the cell is slightly (15 – 35 kPa) above atmospheric pressure, the Bunsen valve opens, providing a safety mechanism to prevent explosions should the battery be subjected to excessive overcharge. The valve also allows the release of gasses from parasitic reactions such as positive grid corrosion and impurity-related hydrogen evolution. As the VRLA battery has no facility to replace electrolyte lost as gas through the valve, it requires greater care and better charge control than a flooded battery if its full operational life is to be realised.

In a conventional flooded lead acid battery the gasses produced during overcharge simply bubble to the surface of the electrolyte, where they are then vented to the atmosphere. The dominant overcharge reaction is that of water being broken down into gaseous hydrogen and oxygen. Because flooded batteries simply vent this gas to the atmosphere, the periodic replenishment of water is necessary.

2.1 VRLA Cell Chemistry

The primary energy storage reactions occurring during charge and discharge of a VRLA cell are identical to the charge and discharge reactions of a conventional flooded lead acid cell. The two types of cells have differing physical constructions, and as a result react differently when they are fully charged. For a VRLA cell to function satisfactorily, not only does the main charge-discharge reaction have to be properly designed and balanced, but the overcharge and unwanted (but unavoidable) parasitic reactions must also be considered and balanced appropriately.

2.1.1 Main Charge-Discharge Reaction

The electrochemical storage of a VRLA cell is achieved by converting lead sulphate ($PbSO_4$) to lead dioxide (PbO_2) at the positive electrode, and to spongy lead (Pb) at the negative electrode. This reversible process has been summarised in Equations 1) and 2), with the overall cell reaction shown in Equation 3). In the concentration range applied with batteries, the electrolyte of dilute sulphuric acid (H_2SO_4) is dissociated mainly into H^+ and HSO_4^-. Only about one percent of the H_2SO_4 molecules dissociates into $2H^+$ and SO_4^{2-} [(2)]. This is the same basic 'double sulphate' reaction of a traditional flooded lead acid battery[3].

The reaction at the positive electrode is:

$$PbO_2 + 3\,H^+ + HSO_4^- + 2e \underset{charge}{\overset{discharge}{\rightleftharpoons}} 2\,H_2O + PbSO_4 \qquad 1)$$

And at the negative electrode:

$$Pb + HSO_4^- \underset{charge}{\overset{discharge}{\rightleftharpoons}} PbSO_4 + H^+ + 2e \qquad 2)$$

With the overall reaction being:

$$PbO_2 + Pb + 2\,H_2SO_4 \underset{charge}{\overset{discharge}{\rightleftharpoons}} 2\,PbSO_4 + 2\,H_2O \qquad 3)$$

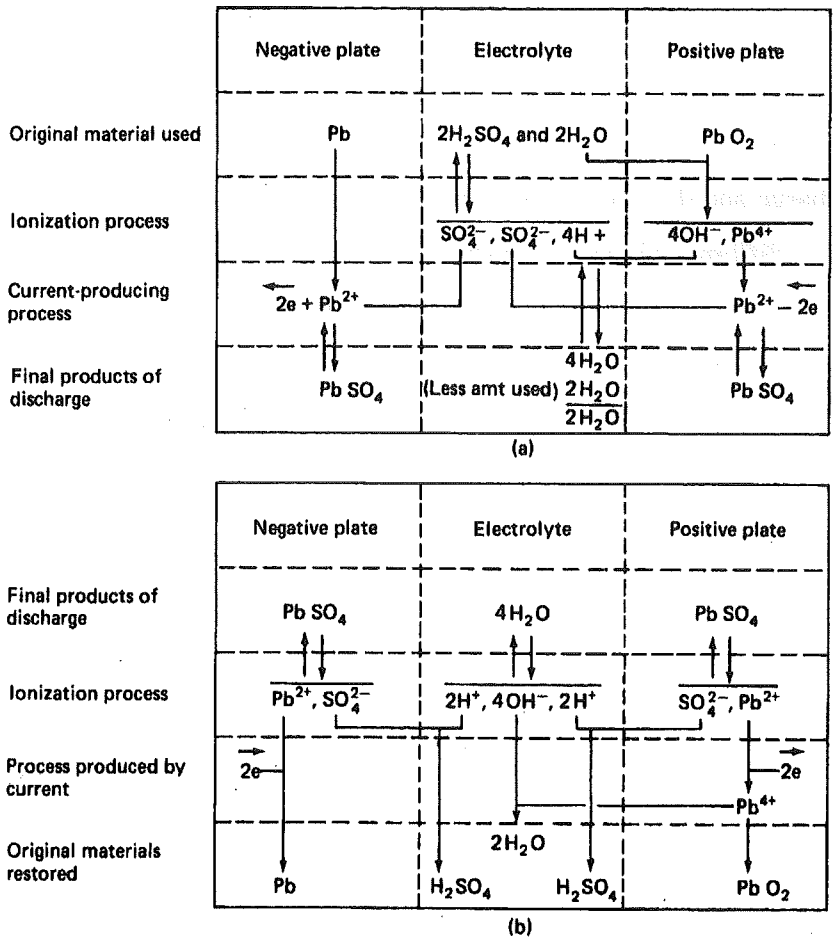

Figure 2.2 Lead Acid Cell (a) Discharge and (b) Recharge Reactions [4]

As the double sulphate reaction is reversible, the cell is either discharged or recharged depending on the direction of the current passing through it. The double sulphate reaction is shown graphically for both discharge and recharge in Figure 2.2. During discharge both spongy lead and lead oxide are converted into lead sulphate, and the concentration of the sulphuric acid electrolyte is reduced as it is consumed and water is produced. During recharge the lead sulphate is converted back into spongy lead at the negative electrode, and into lead dioxide at the positive. The concentration of the sulphuric acid electrolyte is increased as the cell is recharged.

During the recharge process, the species involved in the chemical reactions are consumed. When the majority of the lead sulphate has been converted to spongy lead at the negative electrode and lead oxide at the positive, the cell is near its fully charged state. When insufficient reacting species are available to absorb the supplied recharge current, the excess current supplied

to the cell is consumed by the overcharge reactions. As VRLA batteries are said to be positive limited[5], the positive electrode is normally the first to enter the overcharge region of operation.

2.1.2 Overcharge reaction

When the main recharge reactions, as described in the previous section, can no longer store the energy supplied to the cell by the charge current, the excess current is consumed by the overcharge reactions. In a flooded lead acid cell, water is broken down into hydrogen and oxygen through the overcharge reactions at each electrode (Equations 4) and 5)). The overall reaction is shown in Equation 6). The hydrogen and oxygen produced during overcharge bubbles up through the electrolyte and is vented to the atmosphere.

At the negative electrode:

$$2H^+ + 2e^- \rightarrow H_2 \qquad 4)$$

And at the positive electrode:

$$H_2O - 2e^- \rightarrow \tfrac{1}{2}O_2 + 2H^+ \qquad 5)$$

The overall reaction is:

$$H_2O \rightarrow H_2 + \tfrac{1}{2}O_2 \qquad 6)$$

In a VRLA battery, the internal design ensures that the oxygen produced at the positive diffuses toward the negative plate. Here, it reacts chemically with the spongy lead negative active material to form lead oxide. The sulphuric acid electrolyte then reacts with the lead oxide to form lead sulphate and water. This lead sulphate is then further electrochemically reduced into lead and sulphuric acid. This state of equilibrium will continue as long as the battery remains fully charged. This process has been symbolically shown below in Equations 7) - 9).

As a VRLA battery approaches its fully charged state, overcharging commences and oxygen is released from the positive plate in a process identical to that of a flooded cell (Equation 5)). The released oxygen then diffuses across the separator to the negative plate, where it reacts chemically with the spongy lead to form lead oxide, as shown in Equation 7).

$$Pb + \tfrac{1}{2}O_2 \rightarrow PbO \qquad 7)$$

The sulphuric acid reacts with the lead oxide to give lead sulphate and water, and some of the spongy lead is chemically discharged to a lead sulphate state. The water consumed at the positive plate is regenerated at the negative.

$$PbO + H_2SO_4 \rightarrow PbSO_4 + H_2O \qquad 8)$$

The float current then recharges the spongy lead chemically discharged at the negative.

$$PbSO_4 + 2H^+ + 2e^- \rightarrow Pb + H_2SO_4 \qquad 9)$$

As these reactions occur an equilibrium is achieved. While this 'chemical recombination' process is commonly shown in literature[6], it has been suggested that there is an alternative path for the direct reduction of oxygen at the negative, with the same result[7]. It has been said that the 'chemical recombination' of Equation 7) can only occur above the equilibrium potential of the negative electrode[8]. In proper float conditions, the negative electrode potential should always be kept slightly more negative than its equilibrium value to secure the state of full charge of the negative electrode. 'Direct recombination' must occur through Equations 10) and 11).

At the positive electrode:

$$2H_2O \rightarrow O_2 + 4H^+ + 4e^- \qquad 10)$$

And at the negative electrode:

$$O_2 + 4H^+ + 4e^- \rightarrow 2H_2O \qquad 11)$$

These recombination reactions allow the VRLA cell to function in what is effectively a sealed environment. However small continually occurring parasitic reactions, such as corrosion of the positive grid and hydrogen evolution at the negative, produce gasses that cannot be internally recombined. Small amounts of gas venting will always result, as these reactions can never be eliminated, although they normally proceed at relatively slow rates.

2.1.3 Parasitic Reactions – Grid Corrosion and Hydrogen Evolution

The charged products of each electrode (lead and lead dioxide) are thermodynamically unstable in the sulphuric acid electrolyte. Because mixed potentials exist at each electrode, a true equilibrium is never formed, and gradual self-discharge results from local action at each electrode, with no current flow required. Self-discharge occurs when the float charger is removed and the cell left to stand open circuit. For each electrode there are several mechanisms that result in the self-discharge. These are briefly summarised in Sections 2.1.3.1 and 2.1.3.2. The rate of self-discharge can be controlled through cell design and construction materials, although designing cells with low self-discharge rates does have side effects. Typically, the self-discharge rate of a VRLA cell is around 4% per month at 20 °C. As the cell ages, the self-discharge rate is influenced, and may increase by a factor of 2 – 5.

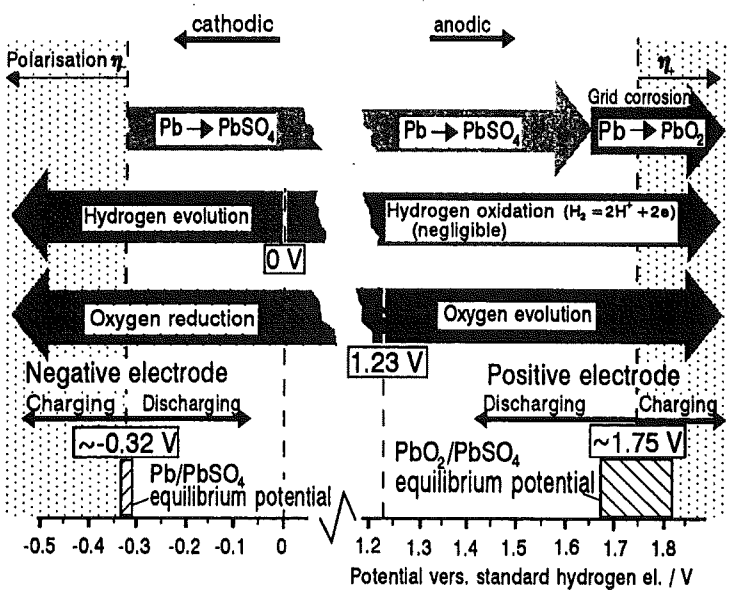

Figure 2.3 Reactions Possible at Various Electrode Potentials of Lead Acid Battery Systems[9]

Figure 2.3 depicts the thermodynamically possible reactions for various positive and negative electrode potentials in a lead acid battery system. The range of equilibrium potentials indicated by the crosshatched regions at each electrode shows their dependence on acid concentration. The values of –0.32 V and 1.75 V correspond to acid concentration of 1.23 g/cm^3. It can be seen that lead is stable only below the equilibrium potential of the negative electrode (approximately

–0.32 V w.r.t. S.H.E). Above this point, lead is converted into lead sulphate or corroded into lead dioxide. While the by-product of corrosion (lead dioxide) provides some protection for the underlying grid, corrosion will always occur at potentials commonly encountered for the positive electrode. This corrosion occurs above, at, and below the equilibrium potential of the positive electrode. Hydrogen evolution occurs at electrode potentials lower than the standard hydrogen reference. The reverse of this, hydrogen oxidation, can occur above this reference point, but it is hindered so much so at the lead dioxide surface that it may be neglected. The evolution of oxygen occurs at potentials greater than 1.23 V w.r.t S.H.E. Below this potential, oxygen is reduced as it comes in contact with the surface of the electrode.

2.1.3.1 Self-Discharge of the Negative Electrode

Several mechanisms may result in a gradual unwanted discharge of the negative electrode. The evolution of hydrogen and the reduction of oxygen both produce a gradual discharge of the negative electrode while no net current is passed through the cell. Hydrogen evolution is strongly influenced by foreign metals, which reduce the hydrogen over-voltage of the electrode. Self-discharge of the negative electrode through oxygen reduction can result from either: 1) Air entering the cell through case leaks or defective valves, or 2) Unbalanced float conditions caused by high levels of hydrogen evolution at the negative electrode.

Hydrogen Evolution

Although no current flows from the negative electrode as the cell sits open circuit, a gradual self-discharge of the electrode still occurs. Self-discharge is produced by the mixed potentials of the two reactions occurring at the negative electrode in the presence of sulphuric acid, as shown in Equations 12) - 14). Overall, this results in the conversion of lead to lead sulphate (discharging the electrode) and the production of hydrogen gas, as shown in Equation 15).

$$H_2SO_4 \rightarrow 2H^+ + SO_4^{2-} \qquad 12)$$

$$Pb \rightarrow Pb^{2+} + 2e^- \qquad 13)$$

$$2H^+ + 2e^- \rightarrow 2H_2 \qquad 14)$$

$$Pb + H_2SO_4 \rightarrow PbSO_4 + H_2 \quad 15)$$

Oxygen Reduction

Self-discharge of the negative electrode may also occur through the oxidation of lead (Equation 13)) and the reduction of oxygen (Equation 16)) which in turn produces lead oxide, as shown by Equation 17). In the presence of sulphuric acid, this lead oxide is converted to lead sulphate and water. The overall process is shown by Equation 18).

$$1/2\ O_2 + 2\ e^- \rightarrow O^{2-} \quad 16)$$

$$Pb + 1/2\ O_2 \rightarrow PbO \quad 17)$$

$$PbO + H_2SO_4 \rightarrow PbSO_4 + H_2O \quad 18)$$

2.1.3.2 Self-Discharge of the Positive Electrode

The open circuit self-discharge of the positive electrode results from one of two mechanisms: either 1) The mixed potential of the electrode produces a gradual self-discharge through the evolution of oxygen, or 2) The unavoidable corrosion of the positive grid.

Hydrogen Oxidation

Hydrogen oxidation at the positive electrode, shown in Equation 19), is the reverse of the hydrogen evolution occurring at the negative electrode. While hydrogen oxidation is possible at the positive, it is hindered by the lead dioxide surface and may therefore be neglected. As no significant hydrogen oxidation occurs, any gaseous hydrogen produced within the cell cannot be electrochemically removed and therefore must be vented from the cell.

$$H_2 \rightarrow 2\,H^+ + 2\,e^- \quad 19)$$

Oxygen Evolution

Oxygen evolution must occur at common potentials encountered for the positive electrode in a VRLA battery, as shown in Equation 20). The evolution of oxygen and the discharge of lead dioxide to lead sulphate (Equation 21)) produce a mixed potential at the positive electrode. This

ultimately results in the gradual discharge of the positive electrode through the evolution of oxygen. The overall process is shown in Equation 22).

$$H_2O \rightarrow 1/2\,O_2 + 2\,H^+ + 2\,e^- \quad 20)$$

$$PbO_2 + H_2SO_4 + 2\,H^+ + 2\,e^- \rightarrow PbSO_4 + 2\,H_2O \quad 21)$$

$$PbO_2 + H_2SO_4 \rightarrow 1/2\,O_2 + PbSO_4 + H_2O \quad 22)$$

Lead Corrosion (Positive Grid)

When in a charged state, the active material of the positive electrode is lead dioxide, which is physically supported on a lead grid. As well as providing mechanical strength, the grid provides a low resistance path from the active material through the plate to a connection point. At potentials commonly encountered for the positive electrode in a VRLA cell, the lead grid gradually corrodes. While various grid alloys and construction methods may reduce the rate of corrosion, it can never be eliminated. Corrosion of the positive grid discharges the electrode, and produces lead oxide and water, as shown in Equation 24). Equations 21) and 23) are the reaction couples that allow this to occur.

$$Pb + H_2O \rightarrow PbO + 2\,H^+ + 2\,e^- \quad 23)$$

$$PbO_2 + Pb + H_2SO_4 \rightarrow PbO + PbSO_4 + H_2O \quad 24)$$

When the lead oxide produced in Equation 24) comes in contact with the sulphuric acid electrolyte, it is converted to lead sulphate (Equation 18)). The final grid corrosion reaction is shown in Equation 25).

$$PbO_2 + Pb + 2\,H_2SO_4 \rightarrow 2\,PbSO_4 + 2\,H_2O \quad 25)$$

Grid corrosion gradually consumes the lead dioxide passivating layer that protects the underlying grid when a battery is stored at open circuit. For this reason, refreshing charges are required periodically in order to rebuild the protective layer.

2.1.4 Temperature Effects

Battery temperature has a large influence on almost every aspect of battery operation. Temperature affects both kinetic parameters (transport of reacting species to and from the reaction site), and the rates at which chemical reactions within the cell proceed. This effect is described by the Arrhenius equation[10]. As the activation energy in the Arrhenius equation is often approximated as a constant, the equation is simplified to the common approximation that for every 8 – 10 °C increase in cell temperature, the rate of the chemical reactions (or kinetic parameters) doubles.

Self-Discharge

As the rate at which chemical reactions occur is expected to double when battery temperature increases by 10 °C, it is expected that unwanted side reactions, such as self-discharge, will also be affected by the increase in temperature. Figure 2.4 shows how the open circuit storage time is reduced through increased self-discharge as the temperature of the battery is increased. It can be seen that for each 10 °C increase in storage temperature, the time taken to reach a given remaining capacity is approximately halved. This is due to the increased rate of self-discharge.

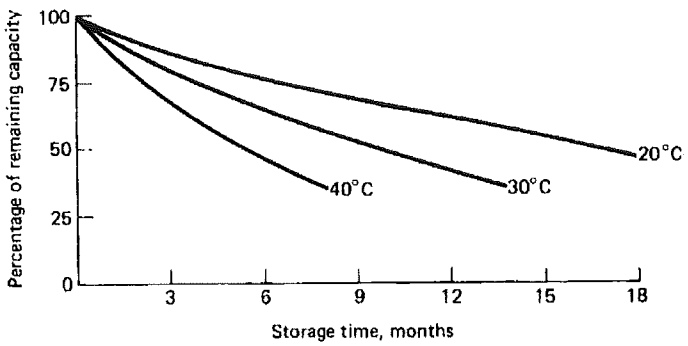

Figure 2.4 Temperature Effects on Rate of Charge Loss[11]

Float

It can be seen in Figure 2.4 that the rate of self-discharge increases with the temperature of the battery. For a given float voltage, the float current drawn by the battery is approximately doubled for every 10 °C increase in battery temperature. As the temperature of the battery rises, the increased float current should compensate for the increased rate of self-discharge. While this

effect should ensure that the battery remains fully charged at various temperatures, reactions such as grid corrosion and hydrogen and oxygen production are also increased when the temperature is raised. It is commonly accepted that the service life of a lead acid battery is halved with a temperature increase of 8 - 10 °C due to the increased rate of grid corrosion. The life of a battery designed to operate for 10 years at 20°C will be reduced to 5 years at 30°C. However, at elevated temperatures, cell failure through excessive dryout may pre-empt the designed failure mode of grid corrosion. If the rate of oxygen production increases to the point where gas production exceeds the maximum recombination rate, gas venting will occur and premature failure due to dryout may result.

Discharge

Battery kinetics control the rate at which reacting species are transported to and from the reaction site. It is commonly accepted that the available capacity of a fully charged lead acid battery is dependent on the discharge rate. As the discharge rate is increased, the available capacity is reduced, largely due to the battery's kinetic parameters limiting the rate at which reacting species are transported to the reaction site. If the available capacity of a battery is discharged at a high rate, and the battery is then left to stand open circuit, some of the previously 'unavailable' capacity will become available as the battery settles to a uniform state. Similar to reaction rates, battery kinetic parameters are also temperature dependent, with the available capacity of a battery decreasing as the temperature is reduced. This capacity-temperature dependence is exaggerated for high rate discharges where kinetics plays a greater role.

Recharge

Similar to the way in which a battery's discharge characteristics are influenced by temperature through its kinetic parameters, the maximum rate at which a VRLA cell can be recharged is also limited by cell kinetics. As cell temperature is reduced, the maximum current able to be consumed in the desired recharge reactions is also reduced. If the selected recharge rate is too high for the battery temperature, the available active material may become fully charged and force excess current to be consumed in overcharge reactions. However, the overall battery state of charge (SOC) may be significantly less than full.

2.2 Float Charge Analysis

While the basic chemical reactions occurring in lead acid batteries described in Section 2.1 appear simple and straightforward, the design and optimisation of a battery for a particular application is an extremely complex process. There are many parameters that can be controlled by the battery designer in order to produce a battery that is best suited to a particular application. Basic parameters available to the designer may include grid alloy, size and shape, plate thickness (active material depth), expanders, separator type and size, the ratio of positive and negative active material, and electrolyte volume and concentration. As application requirements differ, so too must the battery designs in order to provide the best solution for the application. Batteries used in cyclic applications, such as electric vehicles or solar energy storage, must be able to be charged or discharged at high rates repeatedly, but are not expected to spend significant periods of time on float charge. Batteries used in standby applications with the intention of bridging a primary power supply failure have a very different life to cyclic batteries, and therefore require very different characteristics. Depending on the location and quality of the primary power supply, a standby battery might be discharged at a low (10 - 20 hour) rate only a handful of times in its entire life. During the large majority of its life, a standby battery must be maintained in a fully charged (float) state.

In the remainder of Section 2.2 the requirements for successful or optimal float charge will be discussed through literature analysis. It will be shown that for satisfactory standby float charge operation, overcharge reactions have to be appropriately designed, and parasitic side reactions must be adequately catered for to ensure that the cell remains fully charged. These reactions must be suitably accounted for in addition to ensuring that the underlying main charge-discharge reaction is appropriately designed.

2.2.1 Tafel Plots

Tafel plots are often used to analyse the steady state float behaviour of a VRLA cell (J. Tafel was the first to describe the hydrogen over-voltage relation of noble metals[12].). A Tafel plot shows the polarisation (the potential above the fully charged rest potential) for both the positive and negative electrodes as a function of the float current passed through the cell. Typically, a straight line is produced for each electrode when the polarisation is plotted against current on a

linear-log graph. In order to measure electrode polarisation, a reference electrode must be used to determine the potential of both electrodes. The fully charged rest potential of each electrode must also be known before the polarisation can be calculated. While this thesis targets the float charge region of VRLA battery operation, to aid understanding Tafel plots of both flooded lead acid and VRLA batteries have been described below.

Figure 2.5 shows a typical Tafel plot of a conventional flooded lead acid battery. When the battery is fully charged, only secondary (overcharge and parasitic) reactions occur. The zero polarisation point of each electrode represents the fully charged rest (equilibrium) potential for that electrode. The total current from the negative electrode is accounted for by that associated with hydrogen evolution and oxygen reduction. The total current from the positive electrode is accounted for by grid corrosion and oxygen evolution. It can be seen that both oxygen and hydrogen evolution have constant Tafel slopes, while the current associated with corrosion of the positive grid has a minimum point at a polarisation of approximately 50 mV. As the polarisation is increased or decreased from this minimum point, the current consumed by corrosion increases with a constant Tafel slope. It can also be seen in Figure 2.5 that the current associated with oxygen reduction at the negative electrode is unaffected by the polarisation of the electrode. This is due to the flooded electrolyte cell design, which permits only very small amounts of oxygen (produced at the positive electrode) to diffuse through the electrolyte to the negative electrode. The majority of the oxygen produced simply bubbles to the surface of the electrolyte, where it is freely dissipated into the atmosphere.

In order for either the positive or negative electrode to begin to polarise, the float current applied to the cell must be greater than the sum of the currents consumed by the secondary reactions at that electrode. In the Tafel plot shown in Figure 2.5, the minimum float current required to compensate for the secondary reactions of the positive electrode is slightly greater than 2 mA per 100 Ah. The negative electrode requires just over 3 mA per 100 Ah before it begins to polarise. As the float current passes through both electrodes, the sum of currents at the positive must equal the sum of currents at the negative. The distribution of the total polarisation (float voltage minus the open circuit voltage) between the positive and negative electrodes is determined by the slope and location of the total current required to polarise each electrode. Polarisation of the positive and negative electrodes within a flooded lead acid battery is largely determined by hydrogen and oxygen evolution[13].

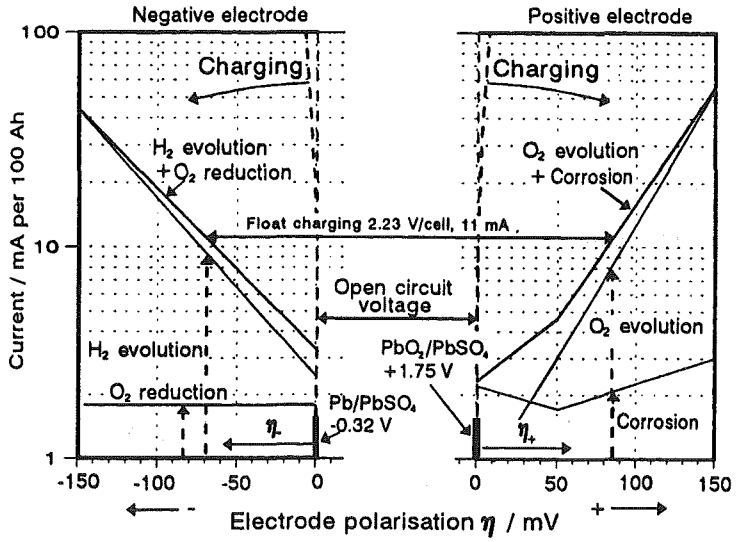

Figure 2.5 Tafel Plot of a Flooded Lead Acid Battery Showing the Currents Associated with the Reactions Occurring at Each Electrode[14]

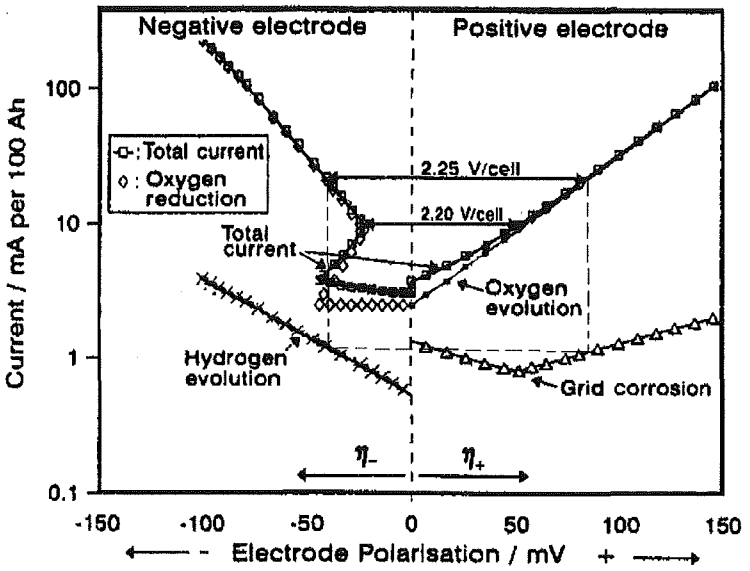

Figure 2.6 Tafel Plot of a VRLA Cell Showing Individual Reaction Currents and Total Current at Each Electrode[15].

Figure 2.6 shows a typical Tafel plot for a VRLA cell. The main point of difference between the Tafel plots of flooded and VRLA batteries relates to oxygen reduction at the negative electrode. A VRLA cell has only a minimum ('starved') amount of electrolyte, which is suspended between the positive and negative electrodes in an absorbent glass matt or a fumed silica gel. Small pathways are created through the electrolyte to provide oxygen transport between the positive

and negative electrodes. Unlike hydrogen evolution, grid corrosion, and oxygen evolution, the reduction of oxygen at the negative electrode does not have a defined Tafel slope. As the main overcharge reaction at the negative electrode, oxygen reduction does not depend on the electrode polarisation, but rather it is determined by the oxygen evolution at the positive electrode and its subsequent transport to the negative[16].

Polarisation of the positive electrode in a VRLA cell is determined by the total current applied to the cell. As the electrode is polarised, the current is consumed through oxygen evolution and corrosion of the positive grid. As the internal oxygen cycle of a standard VRLA cell approaches 100%, the current associated with oxygen reduction at the negative electrode is essentially equal to the oxygen evolution current at the positive. However, oxygen reduction at the negative does not cause or require the negative electrode to polarise. Polarisation of the negative electrode is only required to complement the gap between current flow and oxygen reduction. As the recombination efficiency approaches 100%, polarisation of the negative electrode is determined by a hydrogen evolution current equivalent to the corrosion current at the positive electrode. Essentially, the total polarisation applied to a cell is distributed between the positive and negative electrodes by the currents associated with grid corrosion and hydrogen evolution, i.e. $\eta_{Total} = \eta_{H2} + \eta_{Corrosion}$ and $I_{H2} = I_{Corrosion}$. The dashed lines in Figure 2.6 show this relationship.

It is standard practice when plotting figures to have the controlled parameter on the X-axis, and the resultant parameter on the Y-axis. A Tafel plot is normally produced by maintaining a constant voltage on the terminals of the cell, and waiting for the current and electrode potentials to stabilise before measurements are taken and the voltage is incremented. Because of this, the controlled parameter of cell voltage is not directly plotted. The currents involved in the various reactions are shown to be functions of electrode polarisations, however the polarisation on each electrode is not directly controlled. The fully charged rest potential of each electrode should not change, and therefore the total polarisation ($\eta_+ - \eta_-$) for a given float voltage should be controlled. At steady state, the float current should be a direct function of the float voltage and is directly measured. It is therefore more logical to plot float current on the X-axis.

Tafel plots in literature are typically displayed with polarisation on the X-axis, as shown in Figure 2.6. However, plots with the float current on the control axis (X) are also common[17 18]. A possible reason for the differing plot rotations may be the intended user of the plot. The

battery designer has the ability to control or manipulate individual reactions, such as those shown in Figure 2.6, and it is therefore convenient to see the effects of these reactions as functions of polarisation. Once a battery is manufactured, the cell's chemistry is fixed and cannot be altered. The only method of optimising the float charge is manipulation of the float voltage or current. Because of this, it is more convenient to see how the polarisation applied to the cell is distributed between the positive and negative electrodes as a function of the float current. As this thesis targets float charge analysis and optimisation of standard VRLA batteries in field service, Tafel plots produced during this work have been plotted with float current on the control axis.

When a fully charged VRLA cell is left to stand open circuit, the mixed potentials and parasitic reactions present at each electrode cause a gradual self-discharge of the electrodes. To combat this, a float charge is normally applied to the cell. It can be seen in Figure 2.6 that a minimum current (approximately 3 mA in this case) must be applied to the cell before the electrodes begin to polarise ('Total current' trace). Below this minimum, the current applied to the cell reduces the cell's rate of self-discharge. However, as the effective self-discharge current is greater than the current applied to the cell, the self-discharge continues. At the point where each electrode begins to polarise, the current applied to the cell is identical to the effective self-discharge current of that electrode. At higher float currents that result in considerable polarisation on the electrodes, more current is applied to the cell than is necessary to compensate for the self-discharge. The additional current is largely consumed by the overcharge gas production and reduction reactions.

When a cell is fully charged, no further energy can be absorbed by the main charge reaction. If a float current is applied to a fully charged cell, the current into and out of the cell must balance. At the positive electrode the secondary reactions of oxygen evolution, grid corrosion, and the self-discharge of lead dioxide are present, while hydrogen evolution, oxygen reduction, and the self-discharge of spongy lead are seen at the negative. As the current into and out of each electrode must balance, Equations 26) and 27) can be written[19].

At the positive electrode:

$$I_{float} = I_{O2\ evolution} + I_{corrosion} - I_{PbO2\ discharge} \qquad 26)$$

At the negative electrode:

$$I_{float} = I_{O2\ reduction} + I_{H2\ evolution} - I_{Pb\ discharge} \qquad 27)$$

If no float current is applied, lead dioxide is discharged through oxygen evolution and grid corrosion, while spongy lead is gradually discharged through oxygen reduction and hydrogen evolution. In Figure 2.6 the curves for the discharge of lead dioxide and spongy lead are not shown, as they would be near vertical lines at polarisations very close to zero. For each electrode, the discharge curve will intercept the zero polarisation point at the current at which electrode polarisation begins.

In a properly designed VRLA cell charging under normal float conditions, recombination efficiency approaches 100% and the discharge reactions do not occur. If the float voltage is insufficient to maintain the current balance described by Equations 26) and 27), it will be maintained through the discharge of active material at the positive or negative electrodes. Assuming that a cell has 100% recombination efficiency, and a float voltage that ensures discharge reactions are not present, the sum of Equations 26) and 27) indicates that the current associated with positive electrode corrosion must be equal to that associated with hydrogen evolution at the negative. This is shown in Equation 28).

$$I_{O2\ evolution} = I_{H2\ evolution} \qquad 28)$$

If the design of the cell is such that Equation 28) is not satisfied, or that the float voltage is not sufficient to overcome the electrode's self-discharge reactions, a gradual discharge of the active material will occur in order to satisfy Equations 26) and 27). If hydrogen evolution is greater than oxygen evolution, a gradual discharge of the negative electrode will result until the point at which equilibrium is found and Equation 28) is satisfied. Similarly, if the oxygen evolution is greater than hydrogen, a gradual discharge of the positive electrode will result.

When oxygen reduction efficiency is close to 100%, the hydrogen evolution current must be approximately equal to the grid corrosion current. The kinetics of hydrogen evolution and grid corrosion govern the electrode polarisation at a given float voltage[20]. The float voltage must be high enough to ensure sufficient polarisation of both electrodes in order to keep them fully charged i.e. $\eta_- < 0$ and $\eta_+ > 0$ [19 21 22], where η_x represents positive or negative electrode polarisation.

2.2.1.1 Grid Corrosion Rates

At positive electrode potentials commonly encountered in a lead acid battery, corrosion of the positive electrode's current conducting grid must occur. As this can never be completely eliminated, grid corrosion is the traditional (designed) failure mode of a lead acid battery. A new lead acid battery has a grid with greater cross-sectional area than necessary, to allow for a reduction in size as the grid corrodes with time. At the end of the battery's life, the grid will have corroded to the minimum value allowed by the battery specification. In the Tafel plot of Figure 2.6, the current associated with grid corrosion is shown as a function of positive polarisation. It can be seen that as the positive electrode's polarisation is increased from zero, the current consumed by grid corrosion is reduced. This reduction continues until the electrode reaches a polarisation of approximately 50 mV. Further increasing the polarisation increases the current consumed through grid corrosion. Two straight lines represent the grid corrosion current in Figure 2.6, however the Y-axis of this plot has a logarithmic scale. If this corrosion current were plotted on a linear axis, the plot would be bowl shaped. Figure 2.7 shows the grid corrosion acceleration factor in comparison with the Positive Plate Polarisation (PPP). The minimum corrosion acceleration factor occurs at a PPP of approximately 75 mV. This indicates the minimum possible corrosion rate. Increasing or decreasing the PPP from this value has the effect of increasing the grid corrosion rate, which in turn leads to decreased cell life. While Figure 2.7 does not have a symmetrical logarithmic rise either side of the minimum point, the basic trends of the corrosion current (Figure 2.6) and the corrosion acceleration factor are similar.

It is generally well accepted that as the polarisation of the positive electrode is increased from open circuit, grid corrosion will initially decrease to a minimum point, and then increase as the polarisation continues to increase. However, the specific point at which grid corrosion is minimised has been questioned. Ultrasonic-reflection measurements of grid growth caused by the by-products of corrosion[24] have shown that minimal plate growth occurs at 40 mV rather at 70 – 80 mV as previously reported and universally accepted. Figure 2.8 shows the results of the (ultrasonic-reflection) measured grid growth rate at various electrode polarisations. The plot is again bowl shaped, however these measurements indicate minimum corrosion occurs at a positive electrode polarisation of approximately 40 mV.

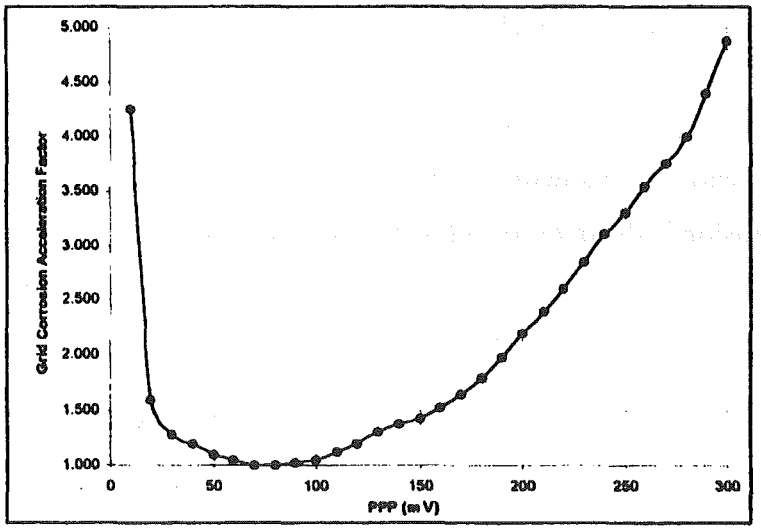

Figure 2.7 Positive Grid Corrosion Acceleration with Positive Plate Polarisation (PPP)[23]

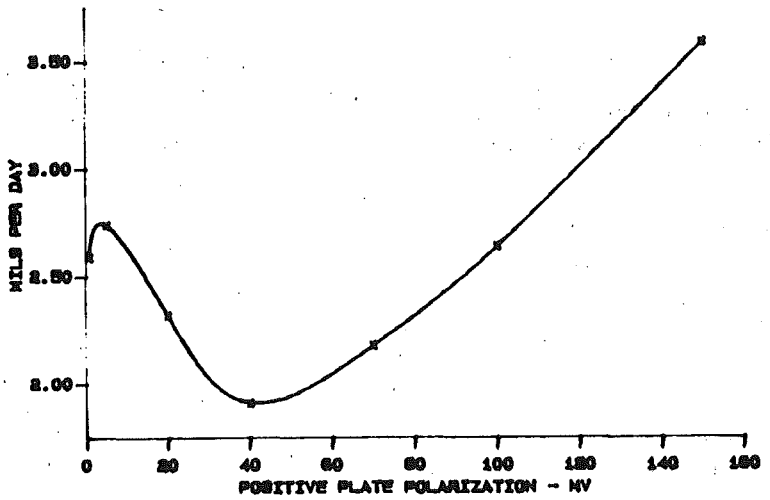

Figure 2.8 Grid Growth Rate Measured by Ultrasonic-Reflection vs Positive Plate Polarisation[24]

The precise electrode polarisation resulting in minimum corrosion may vary with cell design, grid alloy, and grid manufacturing method. Most studies have found that as the polarisation is increased from low values there is an initial decrease in the rate of corrosion to the minimum value. Any further polarisation past this point results in increased corrosion rates. For optimum cell life, the electrode polarisation should be maintained at the value giving minimum corrosion. As the positive electrode is polarised at this minimum corrosion point, it should remain fully charged indefinitely.

2.2.1.2 Hydrogen Evolution

The traditional (designed) failure mechanism of lead acid batteries is excessive corrosion of the positive grid. Attempts to reduce the overall corrosion rate should therefore result in a longer-life battery. However, it was shown in Section 2.2.1 that for a recombining VRLA cell to function correctly and maintain both electrodes in a fully charged state, the current associated with corrosion of the positive electrode must balance with that associated with hydrogen evolution at the negative. If the grid corrosion rate is lowered without appropriately reducing the hydrogen evolution rate at the negative electrode, the cell may suffer from a gradual discharge of that electrode.

In comparison with other metals, lead has a relatively high over-voltage for hydrogen evolution. This should result in the production of extremely low levels of hydrogen evolution at the equilibrium potential of the negative electrode. However, the high hydrogen evolution over-voltage of lead is reduced as soon as metals with a lower hydrogen over-voltage contaminate its surface. Contamination occurs when metals with an equilibrium potential above that of the lead electrode are precipitated at the electrode surface, and remain there as stable metals. This concerns not only impurities of the electrolyte, but also additives that are leached out from the corrosion products of the positive grid alloy[25]. While metallic contamination lowers the hydrogen over-voltage, some organic substances impede the evolution of hydrogen and as such raise the required over-voltage. These organic substances (often wood based) are added in low quantities to the negative active material as 'expanders', with the aim of increasing the surface area of the active material and preserving its fine crystal structure.

2.2.2 Temperature Effects

Section 2.2.1 shows that the currents associated with the parasitic reactions of positive grid corrosion and hydrogen evolution at the negative must balance for both electrodes to be maintained in a fully charged state indefinitely. Although there is some debate over the precise polarisation value at which minimum positive grid corrosion occurs, it is generally accepted to be at a polarisation of 40 - 80 mV. The rate of hydrogen evolution at the negative electrode during float charge is largely determined by the metallic impurities present at the surface of the electrode. While these parasitic reactions occur independently, the currents consumed at each

electrode by these reactions must balance in order to ensure satisfactory float charge is achieved. Section 2.1.4 suggests that the Arrhenius equation explains many temperature dependant characteristics of a VRLA battery. Generally, reaction rates (and their associated currents) are increased by a factor of two for every 8 – 10 °C increase in battery temperature. While a temperature increase produces an increase in the rate of self-discharge (through increased grid corrosion and hydrogen evolution), the float current is naturally increased by a similar ratio and largely compensates for the increased self-discharge rate. Because a rudimentary balance occurs, the battery should remain fully charged at the normal float voltage and be independent of the battery's operating temperature.

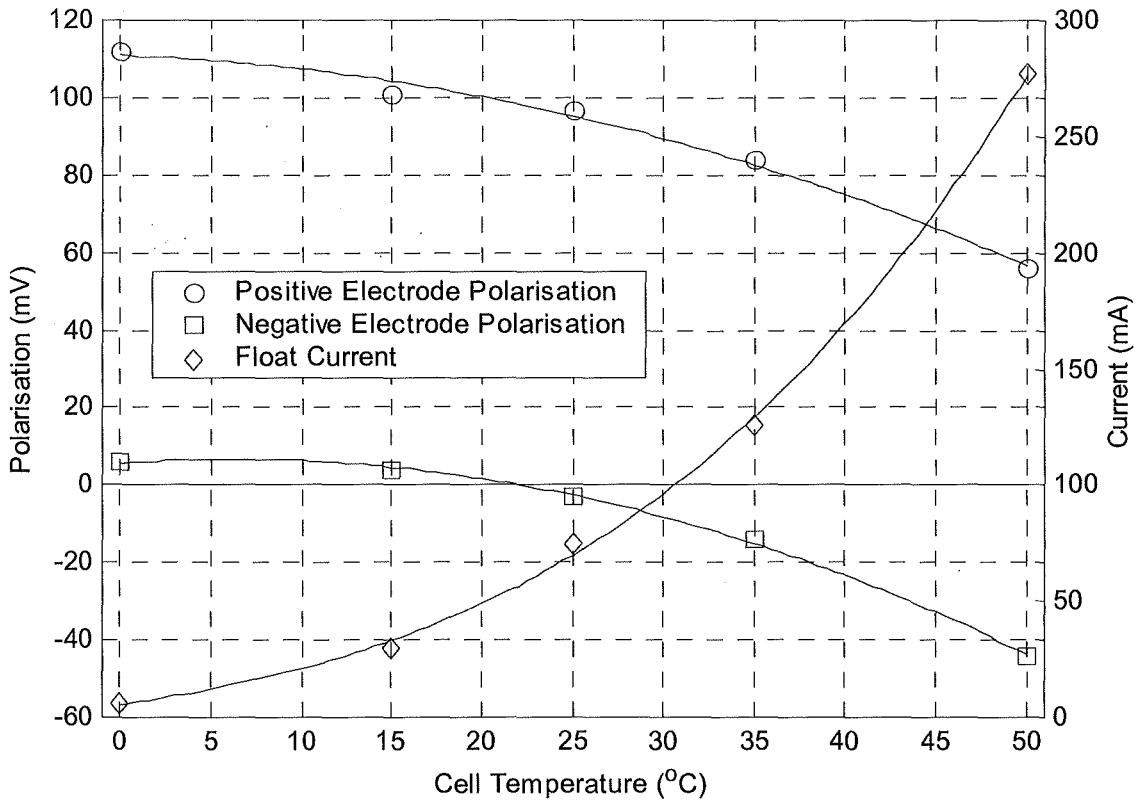

Figure 2.9 Temperature Influence on Electrode Polarisations and Float Current[26]

Overall, the lead acid system has a temperature coefficient of only 0.23 mV/K[27]. However, when the float voltage is held constant, the polarisation of the positive electrode (η_+) decreases with increasing temperature, while the polarisation of the negative electrode (η_-) increases[28]. For a vented lead acid battery with constant float voltage, η_+ is reduced by about -6 mV per 10°C with increasing temperature, while η_- is increased correspondingly[29]. Experimental measurement of the polarisation shift favouring the negative electrode with increased

temperature is shown in Figure 2.9. This figure also shows the expected increase in float current as the temperature is raised. The redistribution of polarisation results from differences in the activation energy of hydrogen evolution at the negative electrode, and oxygen evolution at the positive[30].

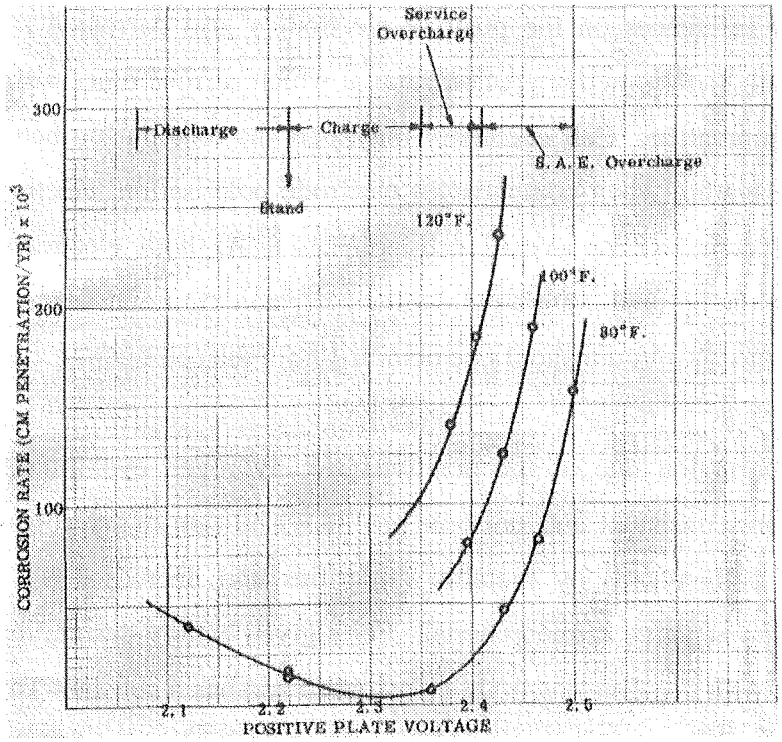

Figure 2.10 Changes in Positive Electrode Corrosion Rates with Temperature and Plate Voltage[32] (Positive Plate Voltage plotted w.r.t. a Cadmium Reference Electrode, Temperatures 26.6, 37.8, and 48.9 ℃))

Section 2.2.1.1 highlights how the positive electrode's grid corrosion rate passes through a minimum value at potentials slightly greater than its open circuit rest potential. While the precise polarisation at which the minimum corrosion occurs is not universally agreed upon (as it may be a function of chemistry), for any given cell, the temperature of that cell influences the point at which minimum corrosion occurs. It has been shown through model simulations[31], that at voltages between the positive electrode's rest potential and the minimum corrosion point, the polarisation of the positive electrode has increased sensitivity to temperature. Consequently, the lower limit of the float voltage should correspond to the voltage of the corrosion minimum. With increasing temperature, the cell voltage producing minimum corrosion is shifted to more positive values[31]. However, these simulation results appear to differ from the early experimental

work on grid corrosion rates shown in Figure 2.10[32]. While Figure 2.10 plots the corrosion minimum for a single temperature (constructed from several series of experiments over a significant time period), extrapolation of results at other temperatures would indicate that the electrode voltage relating to the corrosion minimum decreases with increased temperature.

As there are many influences on the positive electrode's grid corrosion rate, it may not be possible to generically determine the precise point at which corrosion occurs, and how this point is influenced by temperature. Cell chemistry may alter the relationship between the corrosion minimum and temperature when compared to electrode polarisation, electrode potential (w.r.t various reference electrodes), or overall cell potential. As both electrode and overall cell chemistry may alter the optimal point at which the corrosion minimum occurs, cell specific data relating to the corrosion minimum should be obtained from the cell manufacturer.

Compared to the corrosion rate of the positive grid, hydrogen evolution from the negative electrode has a more consistent and uniform profile. The rate of hydrogen evolution at the negative electrode is increased by metallic impurities and decreased by the proportion of expanders used in the negative active material. For a given battery design, the rate of hydrogen evolution increases with negative electrode polarisation and has a constant Tafel slope. As with grid corrosion, the rate of hydrogen evolution is approximately doubled for every 10 °C increase in battery temperature. The polarisation shift favouring the negative electrode at increased temperatures may further increase the level of hydrogen evolution at the negative electrode.

The main overcharge reaction involving the evolution of oxygen at the positive electrode, and its reduction at the negative, is also approximately doubled with every 10 °C increase in battery temperature. There is an upper limit to the rate at which oxygen can be transported from the positive to the negative electrode, and exceeding this transport limit will cause excess gas to be vented from the battery. Due to the finite amount of electrolyte contained within a VRLA cell and the lack of facility for replenishment of any water lost through gas venting, excessive venting may result in premature cell failure through dryout.

2.2.3 Long Life Battery Problems

At positive electrode potentials commonly encountered in lead acid battery systems, corrosion of the current conducting positive grid can never be avoided. For this reason, grid corrosion is the traditional and designed failure mechanism of a lead acid cell. To increase battery life it is logical to either reduce the rate of grid corrosion, or increase the grid size so that a longer period of time passes before the grid corrodes to the minimum cross-sectional area. Over-sizing the grid is usually avoided as this increases both weight and cost. Additionally, the end product of corrosion (lead sulphate) consumes more volume than the starting material, causing further problems. The rate of grid corrosion may be reduced through the addition of various alloys during manufacture, or through the physical manufacturing process (casting, or rolling and stamping). These variations in construction method and materials are often used to make long life batteries.

For a traditional flooded cell, oxygen evolution at the positive electrode and hydrogen evolution at the negative largely dominates the electrodes' polarisation. Lowering the rate of positive grid corrosion through the use of various grid alloys does not significantly alter the float charge operation, although the float life of the battery will be increased. While it may appear logical to apply this concept of increasing battery life by decreasing the grid corrosion rate to a VRLA cell, the delicate balance of the parasitic float charge reactions needs to be considered before life gains will be realised. Section 2.2.1 indicates that as the internal oxygen cycle of a VRLA cell approaches 100%, the polarisation distribution between the positive and negative electrodes is determined by the parasitic reactions. These involve corrosion of the positive electrode's grid and hydrogen evolution from the negative. While these reactions are completely unrelated, for a VRLA cell to function satisfactorily, the currents consumed in each of these reactions must balance, as shown in Equation 28).

Optimal float charge of a VRLA battery requires the currents associated with the parasitic reactions of each electrode in the cell to balance. If these currents do not balance, or an attempt is made to extend the life of a previously balanced cell by reducing positive grid corrosion without adequate consideration of the negative electrode, one of the cell's electrodes may gradually discharge while the cell appears to be float charging. This gradual discharge occurs to balance the float current (total current) and the secondary reactions at each electrode. If the grid

corrosion current is less than that of hydrogen evolution, the negative electrode will gradually discharge. Similarly, if grid corrosion is greater than hydrogen evolution, the positive electrode will gradually discharge. While it is theoretically possible for a suitable mix of reaction currents to cause the positive electrode to gradually discharge on float, negative electrode discharge is by far the most common single electrode discharge mode[33]. This is due to the purity of lead required to achieve very low rates of hydrogen evolution, and the negative electrode's high susceptibility to surface contamination, which lowers its hydrogen evolution over-voltage.

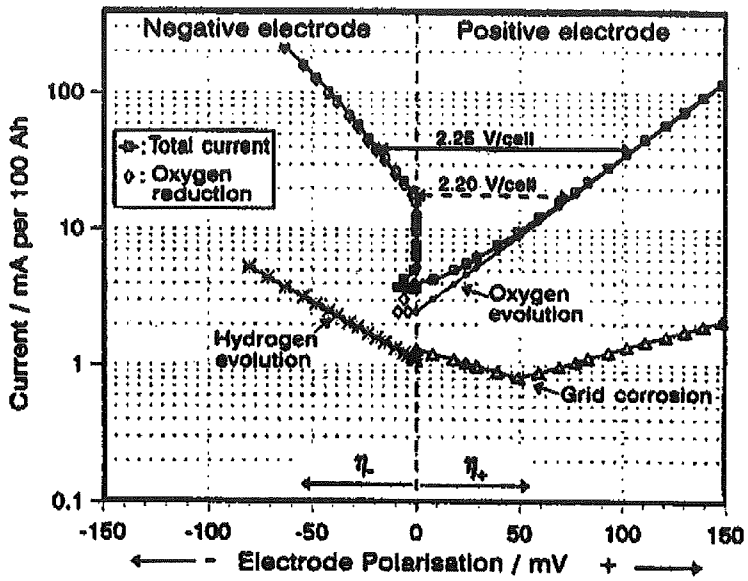

Figure 2.11 Tafel plot of a VRLA Cell with Hydrogen Evolution Current Greater than Grid Corrosion Current[34]

Figure 2.11 shows a Tafel plot of a VRLA cell that has unbalanced parasitic reactions. It can be seen that the current consumed by hydrogen evolution at the negative electrode is greater than the current consumed by grid corrosion at the positive. As the recombination efficiency approaches 100%, the distribution of the total polarisation (float voltage minus the fully charged rest voltage) applied to the cell is determined by the current consumed by parasitic reactions. The negative electrode of the cell depicted in Figure 2.11 does not show any significant polarisation until the cell voltage is raised above 2.2 V. Below this voltage the positive electrode supports the entire polarisation applied to the cell. This occurs because the current consumed by positive grid corrosion is less than the minimum hydrogen evolution current (hydrogen evolution Tafel intercept) at the negative electrode. Because the hydrogen evolution current does not balance the grid corrosion current, an equivalent current must be supplied by the negative

electrode (through the main discharge reaction) in order to balance the total (float) current at each electrode. Hydrogen evolution continues to decrease below the equilibrium potential of the negative electrode, and the gradual discharge of the negative continues until a balance between the rates of hydrogen evolution and grid corrosion is found[35].

When compared to the Tafel plot of a balanced VRLA cell (Figure 2.6), the plot in Figure 2.11 shows a small increase in the current required for hydrogen evolution, from approximately 0.5 mA per 100 Ah, to 1 mA per 100 Ah. This small rise produces an increase in the minimum float current required to ensure both electrodes are polarised, from approximately 4 mA per 100 Ah, to 11 mA per 100 Ah. If the current required for hydrogen evolution was further increased (due to the presence of impurities) or the current consumed by grid corrosion was further decreased (thus improving cell life), the float current and voltage required to polarise both electrodes would be expected to rise further.

The requirements and influences of VRLA battery electrode polarisation presented in this thesis are largely based on work by Teutsch et al[36 37 15] (published between 1994 and 1996), who identified the need to balance parasitic reactions. It is claimed that the world's first rechargeable sealed lead acid cell was made commercially available in 1973[38]. Until Teutsch's recent work, it was commonly accepted and stated in the literature that VRLA batteries operate with low or no negative electrode polarisation[39 40 41 42]. While some previous studies indicate significant negative electrode polarisation at high float currents, the common reason given for reduced negative electrode polarisation in VRLA cells is the depolarising effect of oxygen recombination. To reduce the level of recombination depolarisation, alternative recombination sites may be provided through the use of catalysts[40 43], however the effectiveness of these has been questioned[44].

The presence of parasitic reaction imbalance problems is supported by claims that statistically, long life designs (20 year life) appear to have greater problems than shorter life batteries (5 - 10 year life)[45]. In an attempt to extend the life of VRLA cells by reducing the rate of positive grid corrosion, the level of parasitic reaction imbalance is increased by the reduction in corrosion current. This results in increased rates of negative plate discharge, which eventually reduce the cell capacity below a satisfactory limit. "It is an irony that, if an attempt is made to improve a balanced cell by incorporating a better positive grid (i.e. one with a lower corrosion rate), that the

cell will no longer be balanced, will suffer negative plate discharge and quite likely have a shorter life than before."[46]

The problems associated with unbalanced parasitic reactions may be temporarily masked in new VRLA cells as they are typically supplied in an 'over-wet' state, with excess electrolyte suspended in the separator between the plates. The excess electrolyte restricts the transport of oxygen from the positive electrode to the negative, where it normally recombines with hydrogen to produce water. As the efficiency of the internal oxygen cycle is reduced by this restriction, both oxygen and hydrogen are produced and not recombined, and are therefore vented from the cell. In this state, the VRLA cell temporarily functions as a flooded cell. When oxygen is vented and not recombined, the current consumed by oxygen recombination at the negative is reduced. Current balance between the electrodes is achieved through polarisation of the negative electrode and the associated increase in hydrogen evolution, as would occur in a flooded cell. An over-wet VRLA cell will temporarily function as a flooded cell, until sufficient water is lost through gas venting and the separator dries to the point where oxygen transport is unrestricted, allowing recombination efficiency to approach 100%. When high rates of recombination efficiency are achieved, positive and negative electrode polarisation levels are determined by the parasitic reactions of grid corrosion and hydrogen evolution. Imbalances in these reactions result in a gradual discharge of either electrode, and will be temporarily masked in a new VRLA cell due to its over-wet state.

Accelerated life testing is often used to estimate the expected life of VRLA cells. Techniques used to perform this testing may mask problems associated with unbalanced parasitic reactions. As the Arrhenius equation predicts that the rate of grid corrosion will increase as the operating temperature of the battery is raised, elevated temperatures are used to artificially age the battery in a significantly shorter time than would be experienced in normal field service. Using the Arrhenius equation, the measured life at an elevated temperature is extrapolated to estimate life at conventional temperatures. Failure mechanisms evident at elevated temperatures may not replicate the true failure mechanism seen to occur at conventional operating temperatures. The experimental data plotted in Figure 2.9 indicates that below approximately 22 °C, the negative electrode in the tested cell is not polarised. Below this temperature, the negative electrode will gradually discharge to compensate for the unbalanced grid corrosion and hydrogen evolution reactions. As the temperature is increased, polarisation of the negative electrode is increased at

the expense of the positive. The negative electrode will be gradually discharged at a typical operating temperature of 20 °C, while the positive electrode must support the entire polarisation applied to the cell (approximately 100 mV). With this high level of positive polarisation, the rate of grid corrosion will be significantly greater than the minimum corrosion rate of polarisations between 40 – 80 mV. For example, if accelerated life testing were undertaken at 50 °C, the polarisation of the negative electrode would be artificially increased to approximately 45 mV, and the polarisation of the positive correspondingly decreased to approximately 55 mV. Due to the polarisation shift with temperature the negative electrode is well polarised, and will therefore remain fully charged indefinitely. The polarisation on the positive electrode is in the middle of the range generally accepted to produce minimum grid corrosion. Due to the redistribution of polarisation with temperature, care must be taken that failure modes identified and measured by thermally accelerated testing replicate the failure modes experienced at designed operating temperatures. Thermally accelerated life testing can mask imbalance problems that typically result in the negative plate discharge of long life VRLA batteries.

2.3 Float Charge Goals

When lead acid batteries are used as the storage element in standby power systems, float charging is necessary to counteract their relatively high rate of self-discharge. During the design and manufacture of the battery, materials and design parameters may be optimised to reduce the rate of self-discharge, however it can never be completely eliminated. For this reason, some form of float charge is always necessary to indefinitely maintain the battery in a high SOC. If the float current is greater than the self-discharge current of both the positive and negative electrodes, they will be raised above their fully charged open circuit (rest) potentials, and will remain fully charged. Ensuring that each cell in a battery is kept in a high SOC may be seen as the primary goal of float charge.

From the day a lead acid cell is manufactured, parasitic reactions gradually corrode the current carrying path of the positive electrode. While the design and materials used in the construction of the cell may be optimised to reduce the rate of corrosion, it can never be completely eliminated. For this reason, all lead acid batteries have a finite life. The overall rate of grid corrosion is largely determined by cell design, although for a given cell the rate of corrosion can be minimised by controlling operational variables such as float voltage. As the rate of grid

corrosion is a function of positive electrode polarisation, which in turn is a function of float voltage, an operational mechanism is available to maximise cell life.

Flooded lead acid cells require water to be periodically added to the electrolyte in order to replace that which is lost through overcharge gas production. The design of VRLA cells provides a mechanism that allows the gas produced during overcharge to be internally recombined back into water, eliminating the need for periodic water replacement. VRLA cells contain only a finite amount of electrolyte, and there is no facility for water replacement. It is therefore necessary to ensure that the rate of overcharge gas production is sufficiently well controlled to prevent excessive gas venting. Loss of electrolyte through excessive overcharge and gas venting may result in premature cell failure through dryout.

Both positive grid corrosion and gas venting have the ability to reduce the life of a VRLA cell. To some extent the rates of these processes can be controlled through manipulation of operational variables. The primary goal of float charge has been identified as ensuring that each cell within a battery remains fully charged indefinitely. A secondary goal of float charge is to ensure that the maximum life of each cell (and therefore battery) is realised. The priority of these goals is important. Attempts to maximise the life of the battery should not be at the expense of reducing its charge state. However, if a particular failure mode is identified for a certain cell design, and can be minimised by operating the cell in an almost full state, continuous operation in this state may be tolerated so long as sufficient reserve time is provided. This situation requires very detailed knowledge of both the battery and the application. As a general rule, the float charge goals identified below should be considered in order of priority.

1) Ensure each cell in a battery remains fully charged (counteract the effects of self-discharge)
2) Maximise cell life by minimising a) grid corrosion, and b) gassing and dryout

Many complex electrochemical reactions occur in VRLA cells during discharge, recharge, and float charge. The cell designer must ensure that all of these reactions are balanced, and occur at appropriate rates. Satisfactory float charge of VRLA batteries relies heavily on a delicate balance between the parasitic reactions occurring at the positive and negative electrodes. For a well designed VRLA cell, both the primary and secondary float charge goals may be realised simultaneously. Assuming a typical fully charged rest voltage of 2.14 V, and a float voltage of 2.27 V, a total polarisation of 130 mV is applied to the cell. If the positive electrode polarisation

that produces minimum grid corrosion occurs at 50 mV, the remaining 80 mV of polarisation must be supported by the negative. As both electrodes are raised above their open circuit potentials, they will remain fully charged. Because the positive electrode is operating at the polarisation for minimum grid corrosion, maximum cell life will be realised. If a cell has balanced parasitic reactions, both float charge goals may be achieved simultaneously.

Although VRLA batteries have been available since 1973[38], the requirement for parasitic reactions to be balanced between electrodes was only modelled and explained in works published between 1994 and 1996[36 37 15]. Until this recent revelation, it was commonly accepted that VRLA cells operating with high recombination efficiency did so with little or no polarisation on their negative electrodes. While the parasitic reactions of hydrogen evolution and grid corrosion are independent and unrelated, the currents consumed at each electrode by these reactions must balance for the overall float charge balance to be maintained. The identified imbalance problems explain the premature failure of many VRLA cells, and in particular, long life cells that have reduced rates of positive electrode corrosion.

Assuming a typical fully charged rest voltage of 2.14 V and a float voltage of 2.27 V, a total polarisation of 130 mV is applied to the cell. If the cell has unbalanced parasitic reactions that result in little or no negative electrode polarisation, the positive electrode must support the total polarisation applied to the cell. The 130 mV positive polarisation would result in significantly increased rates of positive grid corrosion, and high levels of oxygen evolution. Although the presence of little or no negative polarisation is common, "...the current practice of floating VRLA cells at positive polarisations of 100 to 150 mV seems illogical."[47] A gradual discharge of the unpolarised negative electrode will occur in order to provide the necessary current balance between the positive and negative electrodes. It is obvious that unbalanced parasitic reactions may result in neither of the float charge goals being achieved.

Until the publication of papers identifying the need for the electrodes' parasitic reactions to be balanced, it was commonly accepted that VRLA cells with high recombination efficiency operated with the positive electrode supporting the bulk of the polarisation applied to the cell. In contrast to the 50 – 100 mV values previously accepted as the minimum corrosion point for the positive electrode, work in 1988[24] suggested that it occurs as low as 40 mV. Despite the suggestion that minimum grid corrosion occurs at relatively low positive electrode polarisations, and the apparent acceptance of VRLA batteries operating with no significant negative electrode

polarisation, high float voltages ranging from 2.23 - 2.38 V are often prescribed[48]. The reason for these high float voltages is said to be the provision of sufficient polarisation for both electrodes during float charge, and compensation for voltage scatter between individual cells when a series connected string is float charged from a single voltage supply. If the negative electrode were operating with no significant polarisation, at the float voltages suggested above the positive electrode would experience increased rates of grid corrosion and oxygen evolution. In this situation, the secondary goal of float charge identified earlier in this Section will not be achieved, and it is not guaranteed that the primary float charge goal will be satisfied.

The distribution of polarisation within a cell is largely determined by the cell design, although to some extent, the float voltage may be used to optimise or manipulate the level of polarisation on a particular electrode. If cell design results in the gradual discharge of the negative electrode, the float voltage must be raised to the point at which the maximum gas recombination rate is exceeded in order to recharge and polarise the negative. As excess oxygen is vented through the pressure relief valve, the current required for oxygen recombination at the negative electrode is reduced. The superfluous current is then directed into recharging the negative. Although this forced gas venting will reduce the liquid content of a cell, if a cell is becoming negative limited through a gradual discharge of the active material, periodic capacity recovery through forced gas venting may temporarily extend cell life.

For both float charge goals to be achieved, a battery must be designed appropriately with balanced positive grid corrosion and hydrogen evolution reactions. An appropriate float voltage must be applied to the cell so that the optimal positive electrode polarisation is produced. While specific float voltages are normally recommended by the battery manufacturer for a particular design, due to the 'sealed' nature of VRLA batteries, there is no practical means of verifying that either of the float charge goals have or have not been achieved. This verification has traditionally been undertaken with polarisation measurements using a reference electrode. However, reference electrodes have a fragile nature, and require high maintenance and a stable environment. Because of this, and due to the lack of electrolyte access, reference electrodes are not commonly used with VRLA cells in the field. At present, the best an end user can do to maximise the life of a battery is to ensure that the appropriate (recommended) float voltage is applied to each cell.

2.4 Existing Float Charge Solutions

Ideally, the float charge of VRLA batteries requires an environment with well controlled temperature, and a charger that can maintain each cell's voltage. In practice, 2 V VRLA cells are connected in series and charged from a single supply. They are often installed in environments with an uncontrolled temperature. Many differing float charge analysis techniques and practices may be used when attempting to improve battery life or reliability, compensate for temperature variations, or provide sufficient float charge for each cell within a battery. Cell models are often used as a basis for improving the design of a battery, or to aid the understanding of operational characteristics. These characteristics may include remaining life or discharge time. In this Section, commonly used float charge practices and analysis techniques are described, and their advantages and disadvantages are outlined. Cell models developed to describe float charge operational characteristics or assist with the optimisation of VRLA battery float charge are also discussed in this Section.

2.4.1 String Level Float Charge Methods

Traditionally, constant voltage float charge has been recommended by manufacturers of flooded and VRLA batteries. For a given operating temperature, a specific voltage or voltage window is normally recommended. This may be supplemented with temperature compensation, and possibly a periodic boost or equalisation charge. Due to the design and operational requirements of conventional standby power systems, constant current float charge is not easily implemented, and therefore not commonly used.

2.4.1.1 Constant Voltage Float

The use of a constant voltage is by far the most popular method for the float charge of VRLA batteries. In most standby power systems, cells are connected in a series string to produce the required system voltage (typically 12 or 24 cells are used to produce a 24 or 48 V system). A single supply is used to provide the float charge for the entire string. This supply is normally set at the manufacturer's recommended float voltage per cell, multiplied by the number of cells in the string. As all cells are connected in series, they must all receive an identical float current. Although it is highly likely that each cell in a string was manufactured at a similar time on the

same production line, small differences between the cells produce some variance in their terminal voltages, despite all cells receiving an identical float current. Throughout the life of the battery, variations in the level of voltage spread between cells may be experienced. When the cells are new, it is expected that the spread in terminal voltages will be significant, but reduce as the cells dry out sufficiently to operate in a fully recombinant mode. As a battery nears the end of its life, it is expected that the voltage spread will increase. While small variances between the terminal voltages of cells in the same string are expected, large differences may indicate potential problems. In general, float voltage alone is not a good indication of SOC or state of health (SOH).

Constant voltage float charge relies on the assumption that the cells are adequately designed and operate correctly over the entire life of the battery. However, ensuring that the correct float voltage is applied to the string does not ensure that all cells receive the correct or sufficient voltage required to remain fully charged. Likewise, constant voltage float charge does not ensure that the maximum life of the battery will be realised. Providing a cell is adequately designed, both of the identified floats charge goals may be achieved through constant voltage float charge. However, the imbalance problems previously described in this Chapter may not be identified with a constant voltage float charge until reductions in capacity and/or life have occurred.

2.4.1.2 Maximum Cell Voltage and Cell Pressure

Battery float voltage is conventionally set based on the number of cells in the string, and the recommended voltage per cell. Small tolerance differences between cells result in a spread between individual cell voltages. As the rate of overcharge gassing is largely a function of cell voltage, internal pressure measurements have shown that the cells with higher float voltages regularly vent gas to the atmosphere through the pressure relief valve[49]. It has also been shown that by controlling the overall battery voltage so that the maximum voltage of any individual cell does not exceed a reference value, gas loss through venting is almost completely eliminated. This new method of charging is said to effectively avoid excessive overpotentials at the electrodes, therefore preventing gassing and accelerated corrosion.

It may be expected that this method of charge control could result in some cells receiving insufficient charge. Tests that artificially unbalanced the cells by discharging a single cell by 10%, showed that with sufficient time (60 hours) the cells' capacities were equalised. While initial impressions of this charge method appear promising, only the initial stages of float charge have been assessed[49]. The effects of long-term float have not been investigated, however it is suggested that further protection of the battery is achieved by separating it from the charger when fully charged. This charge method may work satisfactorily for cells that are appropriately designed and manufactured, however it does not ensure that the primary goal of float charge is achieved. As the maximum voltage on any cell is controlled through manipulation (lowering) of the overall battery voltage, any cell with a naturally lower float voltage must become more susceptible to problems relating to insufficient float charge. This will be further influenced by the parasitic reaction imbalance problems apparent in many VRLA cells.

2.4.1.3 Temperature Compensation

Assuming that a cell is adequately designed, continuous float charge at the recommended voltage and temperature should result in acceptable battery life. However, as it is not always possible to operate the battery in an environment where the temperature is controlled, temperature compensation of the float voltage is often recommended.

There are a number of reasons given for the use of temperature compensation. These range from preventing thermal runaway at high temperatures and assuring adequate charging at low temperatures[50], to maintaining a constant current as the operating temperature is varied[51]. The given reasons may explain the wide range of temperature compensation factors recommended by VRLA cell manufacturers. These range from 2 - 5.5 mV/°C[52] (decreasing float voltage with increasing temperature). As all VRLA batteries operate on basically the same principles and chemical reactions, it cannot be said that this wide range of compensation values is linked to battery design or type. It is suspected that the compensation values are based on plausibility rather than experience[53].

One reason commonly given to explain the need for temperature compensation of VRLA batteries is to prevent thermal runaway. The float current of a VRLA cell has been said to increase twice as fast (doubling for every 5 °C increase in temperature) in comparison to a

flooded cell[54]. Eventually, all the energy supplied to the cell through the float charge must be dissipated as heat, or lost from the system through gas venting. For these reasons the VRLA battery is commonly believed to be more susceptible to thermal runaway than a flooded cell. The increasing float current leads to increased heating, which in turn leads to a further increase in float current, and so on. It has been shown that increased temperature alone is not a trigger for thermal runaway, and that this process may be better linked to a combination of events, such as extended discharges or shorted cells resulting in an increased applied voltage[55 56 57]. There is a possibility that as the battery temperature is increased, the associated increase in float current will result in elevated levels of overcharge gas production. If this exceeds the maximum recombination rate, excess gas will be vented to the atmosphere. Ultimately, this will result in premature battery failure through dryout.

Another reason commonly used to justify temperature compensation is in order to maintain a constant rate of a particular chemical reaction, or series of reactions. If float current doubles for every 8 °C increase in temperature, and is halved for every 24 mV decrease in float voltage, temperature compensation of -3 mV/°C will maintain a constant float current as the temperature is varied[51]. On an individual reaction level, it has been shown that -2.7 mV/°C is required to keep oxygen evolution at a constant rate, while -3.6 mV/°C is required to keep hydrogen evolution constant. Depending on the slope of the Tafel lines representing the grid corrosion current, for polarisations greater than the corrosion minimum, temperature compensations between -4 mV/°C and -9 mV/°C are necessary. At polarisations lower than this minimum point, positive temperature compensation is required[58]. It is not possible to universally compensate for temperature variance through float voltage manipulation. Suitable compromises are therefore required to ensure that no single failure mechanism proceeds at an unacceptable rate.

In keeping with the wide range of recommended temperature compensation factors, many differing implementations also exist. These range from simple fixed compensation factors that extend over the entire thermal operating range of the battery, to curves that gradually alter the level of temperature compensation based on battery temperature. Other compensation schemes use a piecewise approach to achieve different levels of compensation at various operating temperatures. Figure 2.12 shows a typical temperature compensation curve[59] with a slope of -4 mV/°C between 0 - 40 °C. As the temperature is lowered below 0 °C or raised above 40 °C, the

float voltage is maintained at a constant level. The reason for this bounding is to prevent gassing (at low temperatures) or insufficient polarisation (at high temperatures)[59]. However, in direct contrast to this limitation on the maximum and minimum float voltages, it is said that a number of battery manufacturers only recommend temperature compensation outside 10 - 30 °C[53]. If the temperature of the battery remains within the 10 - 30 °C window, no temperature compensation is necessary, as the increased self-discharge rate is naturally compensated for by an increase in float voltage.

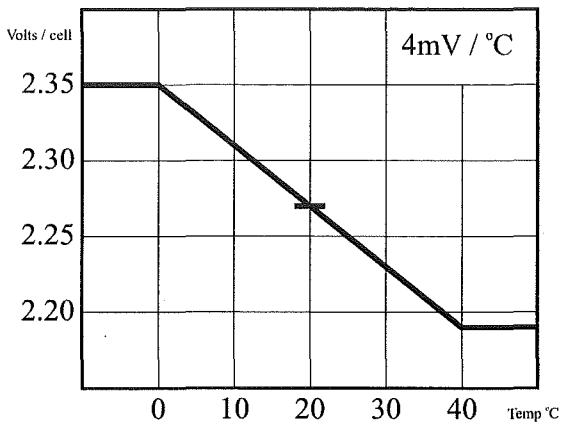

Figure 2.12 Typical Temperature Compensation Scheme

An alternative temperature compensation scheme has also been suggested[60]. This involves increasing the float voltage at low temperatures only, and maintaining a constant float voltage at conventional and elevated operating temperatures. This scheme has been depicted over a temperature range of -10 - 45 °C in Figure 2.13. The temperature coefficient for the equilibrium voltage (open circuit terminal voltage) of a lead acid cell is only 0.23 mV/K, and in practice may be neglected[58]. Due to the reduction of positive electrode polarisation with elevated temperatures, as described in Section 2.2.2, float voltage should be increased with temperature in order to maintain a constant positive polarisation. This would increase the internal oxygen cycle that eventually results in increased heating, and also promotes gas venting. If the positive electrode polarisation relating to minimum corrosion is reduced with temperature, as indicated by Figure 2.10, maintaining a constant float voltage with increasing temperature should not promote an unnecessary increase in grid corrosion. Providing cell design allows the internal oxygen cycle to proceed at increased rates associated with elevated temperatures, the persistence of the nominal float voltage at elevated temperatures should not have a detrimental effect on the

cell. Polarisation of the negative electrode reduces with cell temperature. To enable the negative electrode to remain sufficiently polarised, the temperature compensation scheme shown in Figure 2.13 increases the float voltage at low temperatures. As the level of float current is reduced with temperature, so too are the rates of the internal oxygen cycle and positive grid corrosion. The elevated float voltage at low temperatures should not result in excessive gassing or grid corrosion.

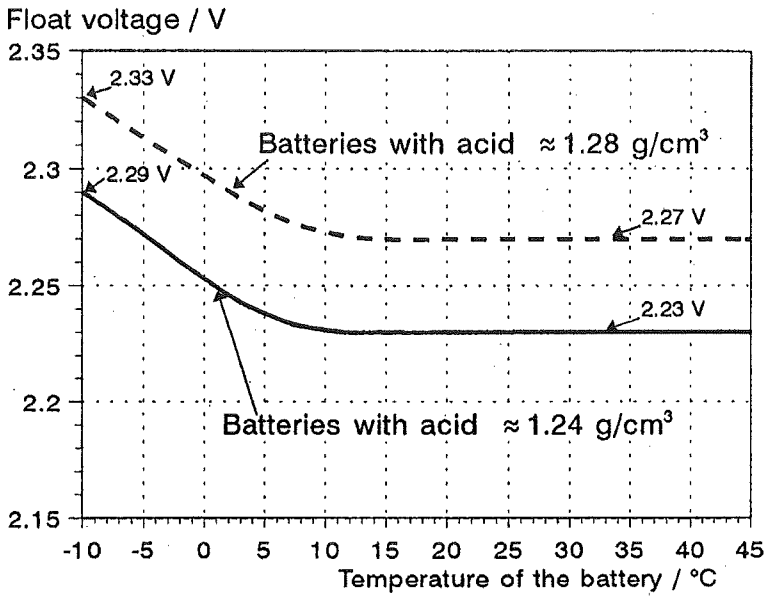

Figure 2.13 Alternative Temperature Compensation Scheme[60]

It is believed that temperature compensation is a compromise between the two ageing mechanisms of grid corrosion and gas venting. If the level of temperature compensation is too large, there is a risk that the battery will be supplied with insufficient current, and not maintained in a fully charged state. If the level of temperature compensation is too small, the increased float current may result in excessive gas production, which may lead to venting. Temperature compensation is based on compromise between two failure modes (corrosion and gas venting). It is important that the primary goal of ensuring that the battery remains fully charged is not neglected in achieving this compromise. Providing VRLA cells are adequately designed, appropriate levels of temperature compensation might improve cell life for operation outside the nominal temperature range. However, the underlying influence of temperature on reaction rates is always present. Increased rates of grid corrosion will result at elevated temperatures, and a

reduced life must therefore be expected. Temperature compensation does not ensure or verify that either of the identified float charge goals will be achieved.

2.4.1.4 Equalisation and Boost Charges

When a string of series connected cells is float charged from a single power supply, slight differences between the cells can result in a scattering of their terminal voltages. This scatter may result in some cells not receiving a sufficiently high float voltage to ensure that they remain fully charged. An equalise charge attempts to reduce or eliminate the charge imbalance problems between cells in the same string. This generally involves raising the float voltage of the entire string to increase the float current through it. This increased float current should be sufficiently high to allow the lesser-charged cells to be bought up to a fully charged state. However, the recharge of these cells through increased float current can only be achieved at the expense of fully charged cells. During the course of an equalise charge, gas venting from the already fully charged cells may occur.

Although it has been stated that periodic equalisation is not normally required to correct cell/unit imbalance[61], scattering of plate potentials can lead to non-uniform ageing[62]. As the potentials of the positive and negative plate within a cell produce its terminal voltage, it must be expected that voltage differences between cells will promote dissimilar ageing. While dissimilar ageing of cells due to terminal voltage variations may be possible, of far greater concern is the recently identified parasitic reaction imbalance problem. This typically results in the gradual discharge of the negative electrode, despite the cell outwardly appearing to be fully charged by the float. While this gradual discharge of the negative electrode stems from problems with cell design, the condition may be temporarily corrected by applying a boost charge.

Depending on the application, 'boost charging' has several meanings. When describing standby applications 'boost charging' implies a short-term elevated float charge that attempts to correct cell problems. When used in traction applications 'opportunity charging' is sometimes described as a 'boost charge'. This involves using partial recharges (when and where available) to extend the operational duration of a battery.

A well designed VRLA cell or battery should not normally require boost charging. However, if it is determined that the battery capacity is reducing through negative limitation, or its negative electrode is operating in a depolarised state, a boost charge may be used to temporarily correct this problem. With a boost charge of sufficient magnitude and duration, it should be possible to recharge a partially discharged negative electrode, albeit at the expense of excessive overcharge of the positive, and the resulting increased corrosion and gas production. To allow the negative electrode to be recharged, the float current must be raised to the point where gas venting occurs. Gas venting reduces the current consumed by oxygen recombination at the negative, and produces a surplus current that is used to recharge the negative electrode. While gas venting is undesirable, intentional boost charging to recover a discharged negative electrode may temporarily correct imbalance problems. Due to the shift in the polarisation distribution with temperature, at extreme temperatures individual plate discharge or overcharge problems may occur. In addressing thermal runaway concerns, it may be necessary to provide periodic boost charges, or accept reduced life due to overcharging[63].

2.4.1.5 Intermittent Charge

Intermittent float charge involves charging a battery until a fully charged sate is reached, and then removing the charger to allow the natural self-discharge to proceed until a lower SOC threshold is reached. At this point, the charger is reconnected to the battery and the battery is returned to a full state. This cycle is repeated indefinitely to ensure that the battery is continuously maintained in a high SOC. The charger used during intermittent charging may either be constant voltage (maintained for a specified time, or until a current threshold is achieved), or constant current (maintained until a maximum voltage threshold is obtained). There are several claimed benefits of intermittent float charging, including the prevention of continuous thermal stress[64] that may lead to thermal runaway[65], and the reduction of failure modes, such as positive grid corrosion, by reducing continuous overcharge and therefore extending the operating life of the battery[66].

Intermittent charge of lead acid batteries in standby applications was first investigated after it was realised that automobile batteries in automobile service were outlasting sealed lead acid standby batteries on a constant voltage float charge[67]. It was determined that the intermittent charge typical of automobile service is easier on batteries than the constant voltage float charge

used in standby applications. Accelerated life testing of sealed lead acid batteries revealed that if the float charge is applied for only 50% of the time, the expected life is double that for a continuous float charge.

With regards to grid corrosion, a VRLA battery operating as designed should outlast a battery on intermittent float charge. It is shown in Section 2.2.1.1 that the rate of grid corrosion increases below the optimal PPP (including open circuit). However, the open circuit corrosion rate is an upper bound value, which is significantly lower than the corrosion rate when the entire polarisation is supported by the positive electrode, as would be the case with a poorly designed or manufactured cell. In relation to gassing and dryout, the reduction in float current and associated overcharge gas producing reactions with intermittent charge may have some advantages over constant voltage float charge. However, if the rate of hydrogen evolution from the negative electrode is reduced to the level necessary for balanced cell design at the recommended (constant) float voltage, the level of gas venting should be negligible. It has been shown recently that there are no life advantages from intermittent charging at recommended operating temperatures, however at elevated temperatures (>35 °C) intermittent charging may be beneficial[68].

Numerous claims have been made regarding increases of battery life through the use of intermittent charge[67 69 70]. From a theoretical point of view, a properly designed cell that is continuously float charged at a voltage corresponding to the corrosion minimum should have its life maximised. In practice however, a cell's design and actual operating point will dominate the float charge operation. A poorly designed cell may have an operating point (at a constant float voltage) far from optimal, and the adverse effects for intermittent charge may indeed be less than those imposed by constant float voltage. Therefore, under certain conditions, life improvements may be realised with intermittent float charge techniques. In a recent study[71], no clear correlation between charging modes and premature failure of VRLA cells was found. It was suggested however, that the reduced life of VRLA batteries may be related to shortages in the charging procedure, rather than to the continuous float charge.

2.4.1.6 Float Current Monitoring

Flooded lead acid batteries have traditionally had their charge state determined through the use of electrolyte specific gravity measurements. While this technique may give an approximation of a cell's SOC, due to the relatively narrow window of specific gravity that a lead acid battery typically operates over, highly accurate measurements are unlikely. As the electrolyte in a VRLA cell is immobilised, with no simple means of accessing it, specific gravity measurements of VRLA batteries are not possible. Estimations of specific gravity are made using measurements of the stabilised open circuit voltage, and the application of a basic rule of thumb where specific gravity ≈ open circuit voltage – 0.85. While this technique gives a basic estimate of the SOC for a VRLA cell, 12 – 36 hours open circuit stand is required for voltage stabilisation[72]. This is not practical for standby power applications, and as specific gravity based estimates of SOC are not precise, alternative methods of determining if or when a battery is fully charged are required.

It has been said[73] that a VRLA battery is charged when the float current has stabilised at the charging voltage, and there is less than a ±10% change in battery current over a three hour period. While this technique will provide an indication that the battery is fully charged, it does not ensure that every cell within the battery is fully charged. Also, the technique may not provide an indication that any cells are suffering from float charge imbalance problems, which result in the discharge of a single electrode. Due to the large differences seen in the magnitude of float currents and in discharge/recharge currents, accurate measurement of float current with conventional current shunts (very low value resistance) is difficult. Systems are available for resolving low level float current measurement[74 75], although these are not commonly used.

A single precise float current measurement is unlikely to detect float charge problems. Appropriate trending of the current drawn by a string throughout its life may highlight problems that develop over time. It is expected that float current changes gradually throughout the life of a battery[76], and is expected to increase with age[75]. Any sudden variance in float current may highlight potential problems that would otherwise go unnoticed. As an increase in float current must accompany thermal runaway, it has been suggested that float current monitoring may be used to prevent this[77].

While trending of float current does hold potential for the early detection of float charge problems, the wide range and accuracy of current sensors makes measurement difficult. As each cell in a series string receives an identical float current, string based current sensing will only indicate problems within a string. Further investigation would be required to determine whether these problems are related to a particular cell or mono-block. Furthermore, as the detection of float problems through float current measurement is largely comparison based, the technique can not ensure that the string or individual cells within the string are fully charged. Similarly, float current measurement does not determine that the battery is operating in a state that will maximise its life.

2.4.2 Cell Level Float Improvement Schemes

As the battery in a typical standby power system is constructed from a string of series connected cells charged from a single power supply, all cells in the string must receive an identical float current. Despite all cells being of an identical type, with a strong possibility that they were manufactured on the same production line, small variances between cells may result in a distribution in their terminal voltages. If left unchecked, this may result in charge imbalance between cells. Attempts made at the string level to correct this imbalance through boost or equalise charges normally impose unnecessary stress on the cells that have a higher charge state. To reduce this stress, the correction of charge imbalance problems may be implemented at a cell or mono-block level, although additional hardware is required for this.

2.4.2.1 Individual Voltage Equalisation

To force an even distribution of the applied float voltage between all cells within the string, individual cell voltage equalisation may be implemented with some additional hardware. While there are many possible hardware schemes for achieving cell voltage equalisation, all schemes must either bypass excess float current around higher voltage cells, or supply additional current to lower voltage cells.

The simplest individual equalisation schemes simply limit the maximum voltage on a cell (or mono-block) by installing a high-power zener-like bypass unit across every cell[78]. This scheme may prevent excessive overcharge of an individual cell, but because the bypass voltage is pre-set

it may not work in conjunction with temperature compensation, or with the elevated voltages sometimes used to accelerate recharge. Additionally, the scheme will not assist with unit equalisation during the discharge or recharge phases of battery operation.

An improvement over simple voltage limit based bypass units involves hardware that balances (equalises) the voltage between two adjacent cells. By overlapping these units so that every cell is equalised with both its neighbours, the overall battery voltage becomes evenly distributed between all cells in the string over time. Advantages of these neighbouring cell equalisation systems are that accurate voltage references are not required, and also that equalisation occurs during all phases of battery operation. Although this type of voltage equalisation is active, no control is necessary. A disadvantage of neighbouring cell equalisation is that while cell voltage differences are eliminated, the current required to achieve this is not monitored, and the indicators of problem or defective cells are therefore removed. Examples of these types of equalisation systems include switched capacitor[79] designs, and switched inductor[80] designs. Similar free-running equalisation systems use multiple output fly-back type DC/DC converters. Diode action and the multiple output transformer ensures that cells with the lowest voltage receive the equalisation charge.

As complexity of equalisation hardware increases, the configurations for controlled active cell or unit equalisation become essentially unlimited. Controlled equalisation involves the use of DC/DC converters to transfer energy between cells in a string, or between individual cells and the battery as a whole. These systems typically have either permanently connected charge and/or discharge hardware dedicated to each cell/unit, or at least one floating charge/discharge unit that connects to unbalanced cells when equalisation is required. With controlled active equalisation, microprocessors are typically used to determine which cells require equalisation, and to what level. Logging of the currents required to equalise voltages may also be implemented in the microprocessor. This information may assist with the identification of defective cells in a similar fashion to extreme float voltage divergences, when no voltage equalisation is used.

Almost invariably for a given temperature, VRLA battery manufacturers recommend a float voltage per cell. The string voltage is simply calculated using the given voltage and the number of cells in the string. If all cells were identical, it would be expected that the cells would evenly distribute the voltage applied to the string. However, slight tolerance differences between cells result in a spread of their terminal voltages. The distribution of cell voltages tends to increase as

the length of the string increases. Additional hardware may be used to force an even distribution of the applied float voltage between all cells, in order to ensure that the manufacturer's recommended float voltage is applied to every cell. However, voltage equalisation does not guarantee that each or every cell in the string is fully charged. In the absence of suitable knowledge of a cell's charge state, forced voltage equalisation should ensure that each cell is float charged as recommended by its manufacturer. Provided that the cell is designed and manufactured properly, optimal float charge should result. The fact that equalisation is necessary when all cells in the string receive identical float current highlights the fact that all cells are not created equally. This raises questions about the feasibility and appropriateness of having one universal recommended float voltage for all cells of a given design.

2.4.2.2 Catalysts

Section 2.2 details how imbalances in the currents required to support the parasitic reactions of grid corrosion (at the positive electrode) and hydrogen evolution (at the negative) may result in either of the electrodes discharging while the cell appears to be on float charge. Alone, the currents that are required to support the internal oxygen cycle at the positive and negative electrodes must balance when the cycle is complete. This oxygen cycle should approach 100% efficiency, and the currents at the positive and negative electrodes should be approximately equal. Due to the float current entering one electrode and exiting from the other, both electrodes must account for identical currents. When the internal oxygen cycle currents at both electrodes are equal, the balance of the float current consumed by parasitic reactions at both electrodes must also be identical. Attempts to increase battery life by reducing positive grid corrosion, coupled with the negative electrode's sensitivity to impurities, results in an imbalance in the parasitic reaction currents between the electrodes. To rebalance these currents, the excess current drawn by the highest consuming parasitic reaction is supplied by the energy stored in the primary reaction at that electrode. This typically results in VRLA cells suffering from a gradual discharge of the negative electrode while on a long-term float charge.

Ideally, negative plate discharge should be rectified by appropriate cell design in which the parasitic reaction currents at each electrode are balanced. Due to the cost of raw materials, manufacturing methods, and battery life requirements, this may not be possible. One solution to the problem of unbalanced parasitic reactions is compensation through the unbalancing of the

internal oxygen cycle. This may be achieved by placing a catalyst in the head (gas) space of each cell. When a catalyst, made from a noble metal (such as palladium), is placed in the atmosphere of a VRLA cell, a site is created that allows small amounts of excess oxygen to be combined with hydrogen, which is always available.

Cells used in traction (cyclic, deep-cycle service) applications are often charged at relatively high voltages, causing electrolysis that produces significant quantities of hydrogen and oxygen. Catalysts may be used to recombine these bulk hydrogen and oxygen gasses[81]. While analysis has shown that the gas vented from VRLA cells contains less than 5% oxygen, some recombination will still occur within a cell when a catalyst is installed. When oxygen and hydrogen are recombined to form water vapour at the catalyst instead of at the negative electrode, the efficiency of the internal gas cycle is reduced from 100% (with regards to both electrodes). In relation to the electrodes, this oxygen cycle imbalance is similar to gas venting, although the production of water vapour at the catalyst avoids dryout. The end result of adding a recombination catalyst into the headspace of a VRLA cell should be an increase in the negative electrode's polarisation, and a corresponding reduction at the positive.

There have been many claims of improved negative polarisation and reduced gas emission[40 82 83] when a catalyst is added to a conventional VRLA cell. Other testing[84] found that the addition of catalysts did not improve the polarisation of the negative electrode at 25 °C, although cells fitted with a catalyst did show a reduction in float current at elevated temperatures. While the use of catalysts in VRLA cells goes some way towards correcting float charge parasitic reaction imbalance problems, improving cell design to eliminate these problems would be preferable. It has been suggested that a balanced design is technically possible, although high material costs and the problems associated with the use of recycled lead may make this impractical[85]. The application of oxygen recombining catalysts in VRLA cells is a relatively new concept. Initial fears of catalytic poisoning[83] have recently been acknowledged[86], resulting in the use of suitable materials to absorb catalyst-poisoning contaminants. Because the recombination of oxygen and hydrogen is exothermic, catalysts may also suffer from heat dissipation problems if high rates of recombination are encountered.

The addition of oxygen recombining catalysts into the headspace of VRLA cells directly targets the negative plate discharge problems common to many VRLA battery designs. This solution

does not directly correct the root cause of the problem. Correcting the problem at its source may not be financially viable, and the use of catalysts may prove to be a more economic alternative. However, as the addition of a catalyst does not guarantee polarisation of the negative electrode[84], it does not ensure that either of the two float charge goals identified in Section 2.3 will be fulfilled.

2.4.2.3 Sensed Polarisation Float Control

Successful and optimal float charging relies almost entirely on the distribution of polarisation between each electrode within a cell, and in particular, on the magnitude of the positive electrode's polarisation. To ensure optimal polarisations, several systems have been developed to sense or measure the electrode's polarisation[87 88(&89) 90]. The measured results may then be used to appropriately adjust the float voltage or current in order to achieve the desired polarisations. Of these systems, only the most recent[90] describes control of VRLA batteries. This also suggests that the output voltage of the rectifier be adjusted so that the reference electrode to either the positive or the negative is set at a desired value.

As conventional laboratory reference electrodes for lead acid systems (such as cadmium or mercurous-sulphate) are fragile and require regular maintenance and calibration, they are not suitable for long-term polarisation control. Willihnganz's polarisation measuring system[87] overcomes this problem with the use of a complete 'reference cell'. The electrolyte from this reference cell is electrically connected to the electrolyte of the test cell via a porous plug that allows current to pass, but impedes electrolyte flow. By connecting like terminals of the reference and test cells, the reference cell is charged. When fully charged, the reference cell's terminals are isolated from the test cell, and it is allowed to settle for 24 – 48 hours to its normal open circuit potential. When the reference cell's potential has stabilised, voltmeter measurements between like terminals of the reference and test cells may be made. These measurements are the polarisations of the positive and negative electrodes in the test cell. Periodically, the reference cell must be recharged by reconnecting it in parallel with the main test cell. The measurement of the positive electrode's polarisation is shown in Figure 2.14

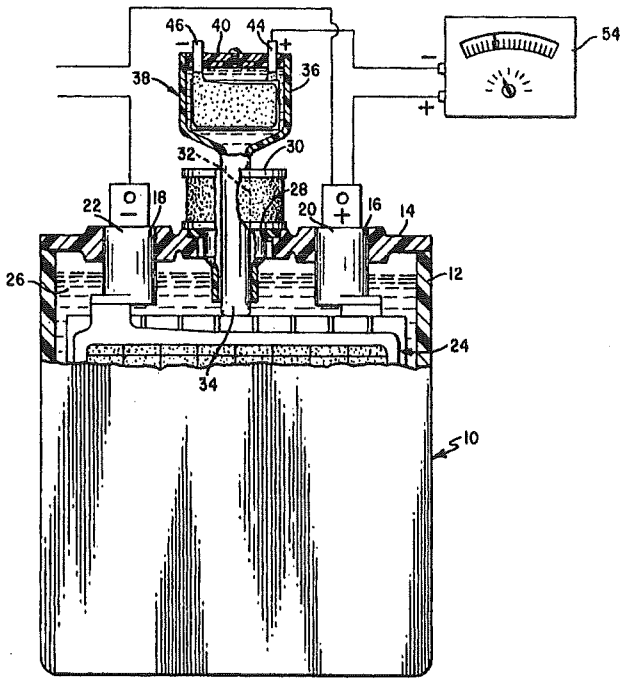

Figure 2.14 Willihnganz's Polarisation Measurement System[87]

The polarisation measurement system shown in Figure 2.14 allows direct measurement of both the positive and negative electrodes' polarisations, however as a complete additional cell is required, the system has significant complexity and expense. A simplification of this system that provides only positive electrode polarisation measurements, for the purpose of float charge polarisation control, is described by Mistry et al[88] [89]. In this system, an additional piece of positive electrode is used as a reference. It is inserted into the test cell so that it is in contact with the electrolyte. This reference electrode requires periodic recharging (every four to six months), which is achieved by shorting the reference electrode to the positive electrode for a period of time, followed by a 10 - 15 hour open circuit stand. Mistry's work also describes an electronic controller that uses the reference electrode polarisation measurements to determine the necessary additional charge current required to achieve a desired positive electrode polarisation. This system allows the level of positive electrode polarisation to be directly set, and maintained indefinitely. While not specifically stated, it is understood that this system targets flooded lead acid batteries.

A polarisation based charge control system that specifically targets VRLA batteries has been described by Chalasani et al[90]. Again, the reference is lead, or an alloy of lead, with a similar

fabrication to the main electrode. The system contains a three-position switch for charging, rest, and measurement periods. The installation of the reference electrode is not described. Considering the difficulties of adding reference electrodes to finished VRLA cells due to the immobilised electrolyte and sealed construction, it is assumed that the reference electrode must have been added during the cell's manufacture. By applying either a positive or negative charge to the reference electrode during the charge phase, the polarisation of the positive or negative electrode may be measured.

All of the systems described in this Section directly measure the amount of polarisation on one or both electrodes within a cell. These measurements are then used as the basis for adjustment of either the overall battery voltage, or an additional charge current at the cell level, allowing optimal float charge at specified electrode polarisations to be achieved. With this direct control of electrode polarisation, both of the float charge goals described in Section 2.3 should be realised. While a level of complexity is still associated with the charge maintenance of these lead based reference electrodes, this process is significantly less labour intensive than some traditional reference electrode systems. The system described by Chalasani et al[90] specifically targeted VRLA batteries, however its use may be restricted by the inability to easily insert the required reference electrode into commercially available VRLA cells.

2.4.3 Existing Float Analysis

Besides common voltage, current, and temperature measurements, the analysis of conventional flooded lead acid batteries is able to draw on many additional parameters, such as electrolyte level, electrolyte specific gravity, individual electrode potentials and polarisations, and observations of the physical condition of the cell's electrodes. As VRLA batteries are effectively sealed, there is no facility to access a cell's internal elements. While conventional voltage, current, and temperature measurements are still available, alternative methods of assessing internal parameters (based largely on a cell's terminal response) have been developed to provide increased knowledge about the internal (and/or external) operation of a VRLA cell.

Cell models are produced to replicate a cell's characteristics. These models may assist with the analysis of the cell's internal operation, with the aim of improving cell design. Similarly, a model may be used to assist with the understanding and prediction of operational characteristics.

Through suitable modelling, it is possible to predict available capacity, or the duration of a discharge for a given load. Predictions of a cell's SOH or remaining life may also be more accurately made when an appropriate model is used. While measurements of VRLA battery parameters are generally limited to voltage, current, and temperature, further information may be revealed through impedance based measurements at various frequencies. By probing a cell at a particular frequency, specific features or characteristics may be isolated, or more easily assessed. Direct identification of characteristic features of a transient response resulting from a particular physical occurrence may also provide an understanding of a cell's present state or condition, without requiring a model.

2.4.3.1 Models

Many different types of models are used in the description or analysis of lead acid and VRLA battery characteristics. Because different operational regions may be targeted, and each model's outputs are used for different purposes, no one model will satisfy all requirements. There are two general reasons for modelling; the verification or analysis of a particular cell design, and the prediction of operational characteristics. Correspondingly, there are two general types of models. These are derived from either an understanding of the cell's chemical operation, or a black box representation, in which the internal operation of the model is largely unimportant, provided that its response replicates the terminal response of the cell.

The primary purpose of any lead acid battery is energy storage. The majority of battery models therefore focus on the energy storage and extraction processes of recharge and discharge. However, as this thesis targets the analysis and subsequent optimised control of VRLA battery float charge, only models that describe this region of operation have been investigated. In particular, models that have been developed for the operational analysis and optimisation of a given cell (with and/or without design problems) have been considered. Many problems associated with long life VRLA batteries are largely due to fundamental design problems. Once a cell has been manufactured, deficiencies in design cannot be altered or corrected. Therefore, models that have been developed for the analysis and optimisation of cell chemistry will only be briefly described.

Models based on a present or presumed understanding of various chemical processes are used to gain a greater understanding of the dependencies and interactions of the possible chemical reactions occurring within lead acid cells. These may be compared with a measured response in order to gauge whether the reactions are occurring as understood, or whether other factors are involved. Previously published models are often improved or extended to provide a better representation of certain operational characteristics. However, due to the many possible reactions present in the lead acid system, large complicated models are required in order to adequately describe the cell's characteristics over its entire operational range. Targeting only specific regions of operation may reduce the complexity of the model. Teutsch et al[36 37 15] described a mathematical model based on balancing the float charge currents consumed by the reactions at each electrode during steady state float charge. Through the use of this model, a plausible explanation for the premature failure of many VRLA batteries in long-term float service is given. Because of this, the model has been used extensively within this Chapter. The Tafel plot analysis with this model has been used to demonstrate the steady state interaction of the many reactions involved in float charge. However, as this model deals only with steady state characteristics, and the differing scenarios are portrayed in terms of electrode polarisation (requiring some form of reference electrode) in several Tafel plots, the model does not offer a field useable mechanism for the detection of poor float charge.

The model by Teutsch et al is derived from a chemistry basis, and targets only a very small but extremely important region of VRLA battery operation. Other somewhat more complex chemistry based semi-analytical models have evolved over time. These rely more heavily on an understanding of chemical reactions, and the chemical and physical conditions required to support these reactions. These models tend to combine diffusion and mass-flow equations, electrical circuits, and semi-empirical laws. It has been said that "Although these models can give a better insight into the role of specific parameters, they are not very reliable due to the large number of parameters and assumptions involved"[91]. A model of this type, recently modified by Tenno et al[92], has shown a close correlation between measured and simulated results. This model specifically targets VRLA batteries, and covers transient behaviour over the full range of charge and discharge, including overcharge. While this model appears to be calibrated to the terminal response of a 12 V mono-block, subsequent analysis and plots detail profiles of parameters within a single 2 V cell. It is also stated that this model can distinguish between outwardly equal batteries with different back-up and cut-off times. However, because a 12 V mono-block is internally constructed from six 2 V cells, there is a possibility that one weak

cell may be masked by the remaining (stronger) cells. Verification of the calibrated model is shown through measured and simulated terminal response comparisons. While a plot of simulated 'Electrolyte overpotential vs. hydrogen electrode' is shown, this has not been compared to experimental reference electrode data. If this model (when calibrated to the terminal response of a 2 V cell) replicated experimental data measured with a reference electrode, it may be possible to use such a model as a means of determining whether float charge problems exist, or whether the float voltage is optimal. Two implementations of this model have been described: a 'Robust Distributed Parameter Model' used for fast discharge transients while ignoring overcharge gas formation processes, and a computationally faster 'Complete Lumped Parameter Model' that accounts for overcharge gas formation as well as charge and discharge. While this lumped parameter model is said to have high prediction accuracy for overcharge, the averaging process that must result from a 12 V characterisation may not detect any individual cells within the block suffering from problems associated with unbalanced parasitic reactions. Characterisation and assessment of the smallest series element is essential to ensure that no weak links in the chain exist.

Analysis using chemistry derived models can allow several batteries to be compared, and/or a battery's limiting factors to be determined, enabling design optimisation. However, the complexity of such models and the large number of parameters associated with them may be excessive when only a single region of operation is targeted. A reduced model, targeting only the float region of operation, may be more suitable for the comparatively simple task of determining individual electrode polarisations while the cell is in float service. A black box type model that replicates the potential of both electrodes (and hence the cell as a whole) would be sufficient for this purpose, and given its reduced complexity a reduction in computation time and/or necessary processing power should also result. Reduced model complexity may also allow assessment of the smallest element (a 2 V cell).

Because they are familiar and easily understood, electrical equivalent circuits are often used for 'black box' modelling of a cell's operational characteristics. Conventional, well-understood analysis tools and techniques may be used to construct and validate a model that replicates battery characteristics. These empirical models are commonly designed using standard (mainly passive) electrical components. Numerous electrical equivalent models have been developed, most of which attempt to replicate the terminal response of a battery over a wide range of operating conditions, covering the discharge and recharge phases of operation. Few models

describe the initial transient behaviour when a battery is discharged from a float charge. As the discharge of a float charging cell commences, the polarisation on the electrodes due to the float charge is eliminated. Noworolski et al[93] describes electrical equivalent models that specifically target this transition region. These models are shown in Figure 2.15. Figure 2.15 a) shows the basic model, which accounts for any increase in the imaginary part of impedance during float operation, and the subsequent decrease during discharge. This change of state is achieved by using the non-linear resistor 'Re'. Capacitor 'C1', described as double layer, is associated with electrode polarisation (it carries the voltage due to the float voltage[91]). Charge, discharge, and recharge conditions can be described by appropriate non-linear coefficients of 'Re'. However, because these coefficients also change sign from charge to discharge, the model shown in Figure 2.15 b) may be more attractive and convenient.

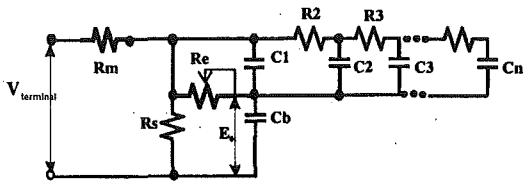

Rm – mechanical path resistance
Re – electrochemical resistance (time dependant) responsible for the *'coup de fouet'*
Rs – self discharge resistance
R_2 and R_3 – overcharge resistance
C_1, Double layer capacitance
C_2 and C_3 - overcharge capacitance
Vterminal - measurable terminal voltage
Cb - electrochemical capacitance
E_0 - open potential of the fully charged cell

a)

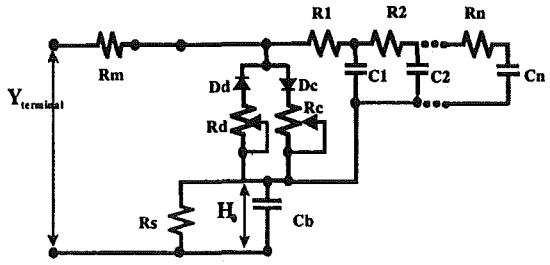

b)

Figure 2.15 Electrical Equivalent Models Targeting the Transition from Float to Discharge[93]

Figure 2.16 a) shows the measured voltage profile given when a 12 V battery is discharged from float. This profile has been separated into regions using the letters A–D. Figure 2.16 b) shows the model's simulated response with an enlarged X-axis (assumed to be regions A-C). The initial drop in voltage (A-B) is said to be due to the combined resistance of the connectors, plates, and electrolyte. Resistor 'Rm' models this combined resistance. Following the initial drop, the double layer capacitor 'C1' discharges with a linear profile, provided that the discharge current is constant. As the overcharge double layer capacitor is significantly smaller than the bulk electrochemical capacitance 'Cb', the voltage change of 'Cb' is negligible during the

discharge of 'C1'. When 'C1' discharges to 'V_{oc}' (open circuit voltage), an appropriately small resistance for 'Re' provides the path for 'Cb' to continue to discharge through.

If the fully charged rest voltage is assumed to be 2.14 volts per cell (VPC), the rest voltage of the six cell block will be 12.84 V. It can be seen in Figure 2.16 a) that the 'initial drop' falls below this open circuit rest voltage due to the resistive losses associated with high rate discharges. However, it is suggested that the voltage decay of the polarisation capacitance (above the float voltage) can still be resolved on a suitable time scale, as shown in Figure 2.16 b).

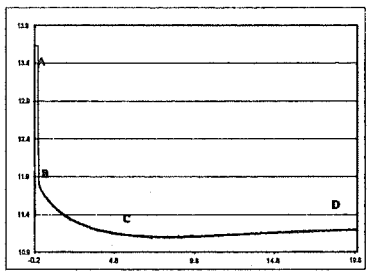

A-B initial voltage drop d
B-C voltage dip (*'coup de fouet'*)
C-D) voltage recovery,

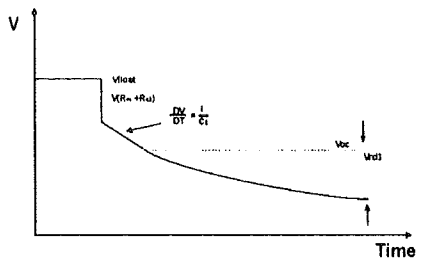

a) b)

Figure 2.16 a) Measured and b) Modelled Response (Enlarged X Axis) [93]

As the discharge rate is reduced, the resistive voltage drop will also decrease. The limiting case for this is a zero current (natural open circuit decay) 'discharge'. The parasitic discharge of polarisation capacitance causes the cell's voltage decay from the float to the rest voltage when the float charge is removed and no load is applied. It has been suggested that both electrodes within a cell have different time constants[97] [100] [94]. The differentiation of the polarisation capacitance 'C1' (and possibly C2, C3... Cn) associated with individual electrodes may, when coupled with an appropriate discharge rate, allow each electrode's polarisation-capacitance discharge to be identified. This would provide a mechanism to determine the distribution of polarisation between the positive and negative electrodes within a cell. Such a mechanism may be used for float analysis or optimisation control.

2.4.3.2 Impedance Analysis

With large numbers of VRLA batteries in field service failing well short of their designed life, a growing trend for the use of impedance based battery analysis techniques has been seen. These techniques are generally based on relationships between magnitude and phase measurements of voltage and current at a particular frequency. Ultimately, most of these techniques produce measurements that are a function of the cell's internal resistance, and for this reason, they may collectively be termed as 'Ohmic' testing. While many systems use one or more specific test frequencies, some systems derive the cell's internal resistance from its voltage response during a step change in load[95].

Increased internal resistance generally indicates that a cell is approaching the end of its life. This may result from either a reduction in cross-sectional area of the current carrying positive grid (due to corrosion), or a reduced amount of electrolyte caused by excessive dryout. Assessment of Ohmic data is largely comparison based, and requires the resistance to be tracked throughout the life of a cell or compared to the measurements of similar aged cells. While large differences may indicate possible problems, it has been suggested that if a cell's internal resistance increases by more than 25% from a base line value, the cell will be no longer be able to deliver 80% or more of its rated capacity[95]. Logging the impedance of individual cells as they age may provide timely indication of failure, however, at best, impedance techniques will only identify cells that have become degraded. Conventional impedance techniques cannot identify a healthy cell that is being subjected to a less than ideal (damaging) float charge (for its operating environment), or a cell that is suffering from unbalanced parasitic reaction problems despite being charged 'as recommended'. Because the consequences of the present float charge impact on (and eventually determine) battery life, the optimum float charge for the environmental and cell conditions should be applied so that maximum battery life is realised.

While traditional impedance measuring systems use a single frequency, more information about a battery can be extracted if the impedance spectrum over a range of frequencies is known. A system described by Scott[96] uses a bipolar, complex frequency, square wave, random current signal to determine component parameters for 'Randles' equivalent circuit. Assessment of these parameters is suggested to reveal information such as SOC and service life. A system described by Champlin et al[97 98 99], uses impedance measurements at two or more discrete frequencies (5 - 1000Hz) to construct an impedance model of the tested battery. The model is essentially a multi-

element impedance network in series with a DC voltage. With experimental data from n discrete frequencies, an impedance model with 2n elements is constructed to fit the data. When two test frequencies are chosen, the theoretical and experimental spectrums agree exactly at the tested frequencies, although away from these the agreement is poor. Using three discrete frequencies to calibrate a six-element model shows a significant improvement in the correlation of the modelled impedance spectrum and the continuously measured data. When a battery's impedance spectrum is monitored and modelled during various operational phases, such as charge and discharge, it is shown that components of the model continuously vary as functions of the battery's state. It is suggested[97] that parameters such as SOC, absolute charge, percent capacity, load current capability, internal temperature, and mono-block uniformity can be extracted from the values of model parameters. Attempts are made to relate model components to physical reactions occurring within a cell[99], and it is suggested that reactions at the positive electrode are orders of magnitude slower than those at the negative. This work largely focuses on the main discharge reaction, and associates capacitance 'C2' with the electrical overpotential, which is equal to the ionic double layer capacitance of the negative electrode's surface. This appears to deal only with operation below 100% SOC, and therefore excludes float charge operation. While the model is adapted to replicate a battery's impedance spectrum under differing operating conditions, a certain level of ambiguity is associated with a model that contains continuously changing parameters. Conventionally, a capacitor has a fixed value and the charge stored by the capacitor is varied. In the model described by Champlin, capacitor and conductance size vary as functions of the operating state. This requires an understanding of not only the model, but also of how the model changes with operating (charge) state.

The lowest frequency used in Champlin's impedance system (described above) is 5 Hz, however impedance analysis, using frequencies extending down to the milli- or micro-Hertz regions, may resolve information about electrochemical processes instead of the double layer processes detected by higher frequency measurements. Huet[100] has undertaken a review of the impedance of secondary batteries including low frequencies. Systems developed for low frequency analysis of lead acid batteries have recently been described by Karden et al[101] and Tenno et al[102].

The Electrochemical Impedance Spectroscopy (EIS) system described by Karden has a lower frequency limit, arbitrarily set to 30 μHz due to time restrictions. As this meter has a single channel, impedance measurements of each electrode are undertaken in separate experiments immediately after measuring the cell's impedance. The system restricts the amplitude of the

applied current signal to two-thirds of the (DC) float current. It is said "a better insight into the electrochemical processes, electrode properties, and transport characteristics is gained by extending the frequency range into the milli-Hertz or even micro-Hertz region". Because float charge may be regarded as being stationary for many weeks, this is the only operating phase for which there is no restriction on minimum frequency, due to the requirement of 'quasi-stationarity'. Flooded cell float impedance measurements are undertaken after several days of float charge at 2.23 V, with frequency ranging from 3 kHz - 38 μHz (measurement of $\underline{Z}$ at 38 μHz takes approximately 22 hours). It is shown that for only very low frequencies ($\sim < 0.5$ mHz) the impedance of the positive electrode can be observed in the overall cell's impedance. Above this frequency, the negative electrode's impedance masks that of the positive. Analysis of VRLA batteries on float charge at 2.15 V with test frequencies ranging from 6 kHz - 1 mHz reveals that impedances measured below 100 mHz are significantly higher (three - five times) in those cells operating in hydrogen evolving (polarised negative electrode) mode. Although this increase in low frequency impedance may be used to detect negative electrode polarisation, testing at multiple float voltages would be required to determine the point at which the negative begins to polarise. It is also suggested in this work that VRLA cells operating in recombinant mode do so with almost depolarised negative electrodes, however Teutsch's recent analysis[15] suggests that this only occurs in cells with unbalanced parasitic reactions.

Low frequency impedance analysis of VRLA batteries has also been undertaken by Tenno et al[102]. However, as this work utilises a presently unpublished 'model-based method' to perform the impedance analysis, the merits of this technique can not be assessed. This work's outcomes are therefore only briefly discussed in this thesis. The impedance analysis is divided into that of the faster double layer impedance involving capacitive current, and the slower electrochemical reaction impedance involving faradic current. The double layer impedances of the positive and negative electrodes are shown to have different frequency responses. The negative electrode has a peak in the phase angle at approximately 10 Hz, while the positive electrode's peak is at approximately 1 Hz (the double layer process is slower on the positive). It is shown that while the double layer impedance of both electrodes is strongly influenced by SOC (between 16 - 99% SOC), small inequalities between batteries cannot be detected by double layer capacitance. However, the significantly slower electrochemical impedance (measured in the milli- to micro-Hertz range) is shown to be a sensitive indicator to small inequalities, and can be used to distinguish between outwardly equal batteries with different back-up times.

As VRLA batteries are essentially sealed, access to the internal elements of cells is not practical. Impedance measurements applied through the terminals of a cell may allow an assessment of a cell's internal parameters to be made. To a degree, the selection of an appropriate testing frequency may allow some differentiation between reactions occurring at the positive and negative electrodes and the type of reaction (double layer or electrochemical). However, it has been said "It is clear that the impedance diagram of the cell does not enable separation of each electrode in a single way"[100]. The majority of commercially available lead acid battery analysis systems based on impedance techniques use test frequencies ranging from several Hertz up to kilo-Hertz. With these frequencies, the measurements provided by these systems are functions of double layer effects and internal resistance. Impedance analysis is largely comparison based, requiring the impedance of one cell or battery to be compared to another, or, more reliably, compared to historical impedance data of the cell under test. The abilities of impedance measurement systems to detect low capacity cells are commonly promoted by the manufacturers of such equipment. It has recently been shown that although these (Ohmic based) impedance techniques may perform satisfactorily when detecting cells of less than 60% capacity, the relationship between impedance and capacity becomes questionable above this level, and is practically non-existent above 80% capacity[103]. As measurement frequencies are extended down to milli- or micro-Hertz, internal parameters relating to electrochemical processes may be observed. However, as long time periods are generally required for such low frequency measurements, the requirements for both plant and temperature stability may restrict low frequency testing in practical telecommunication battery environments.

A measure of polarisation distribution between the positive and negative electrodes is necessary for float charge analysis and control. It has been suggested that at frequencies below 100 mHz, impedance measurements of a float charging battery increase significantly when the negative electrode is polarised[101]. However, there has been no indication that the magnitude of polarisation for either the positive or negative electrodes can be detected through appropriate impedance measurement. Almost universally, impedance measurements have been used for the detection of cells or batteries that have reduced capacity, and/or for estimations of a battery's remaining life.

2.4.3.3 Voltage Response

Assessment of lead acid batteries using impedance measurements generally relies on magnitude and phase measurements of voltage and current when a periodic signal is applied to the terminals of a battery. However, if a known perturbation (either voltage or current) is applied to the terminals, the corresponding response (in current or voltage) may be directly used to evaluate the state or condition of the battery. For ease of implementation, this testing typically involves applying a signal current (charge and/or discharge), and monitoring the battery's terminal voltage response. The perturbation applied to the battery may be intermittent or applied periodically. Generally, either the magnitude of the corresponding response or the existence or lack of a specific characteristic profile is analysed during the assessment. While the application of a known perturbation is normally required, SOH assessments on VRLA batteries using noise measurements[104] have also been suggested.

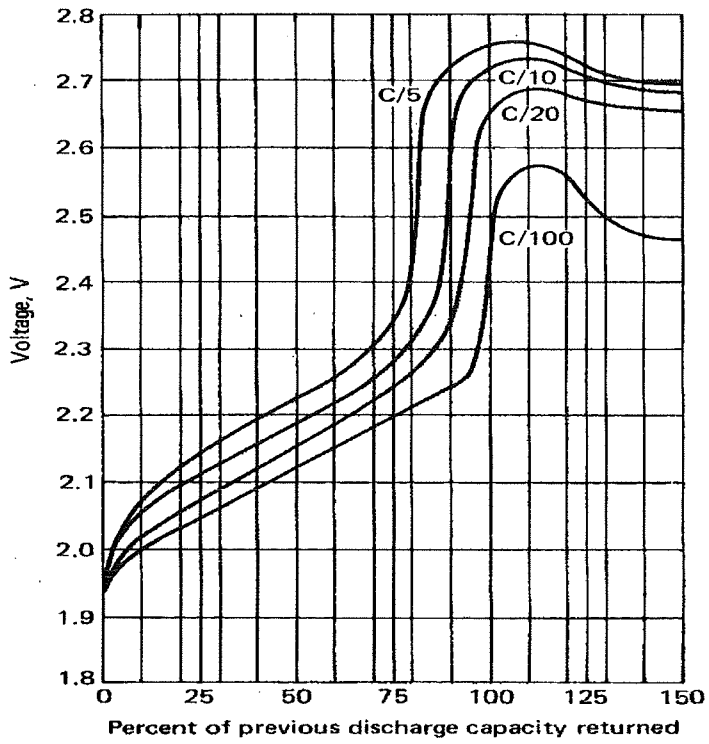

Figure 2.17 Cell Voltage Profiles with Constant Current Recharge[105]

Figure 2.17 shows the expected terminal response of sealed lead acid cells recharged at various constant current rates. As the cells approach their fully charged state, a rapid rise in terminal voltage is seen. This rapid increase occurs when the current supplied to the cell can no longer be

completely absorbed in the recharge reactions, and the excess current is consumed in the overcharge reactions. Due to kinetic limitations on reaction processes, the SOC at which this rapid rise in terminal voltage occurs is reduced as the rate of recharge is increased, or when the cell's temperature is reduced. As the current is maintained at a constant, the rapid rise in cell voltage suggests that the apparent internal resistance of the cell has increased. This voltage rise or increase in apparent internal resistance does not guarantee that a cell is fully charged. However, if the test current is of a similar magnitude to the expected float current and the cell is at a conventional operating temperature, a rapid increase in cell voltage or an increase in internal resistance may indicate that the cell is at or near its fully charged state. Some analysis systems detect this rapid increase in internal resistance by observing the magnitude of voltage response when a signal current is applied, while more complex systems assess the profile of the voltage response.

A system described by Gabriel et al[106] [107] applies a pulsed 1 A signal to a battery string or cell, and measures each cell's peak to peak voltage response to the applied charge pulses. The ratio of the peak to peak voltage response between fully charged and discharged cells can be as high as 22.7:1. For a given battery type, the measured peak to peak voltage response may be compared to a reference level calibrated for that battery. Cells with a peak to peak polarisation voltage above the reference level are considered to be fully charged. It is also suggested that the level of the measured polarisation voltage may be used as a control mechanism to ensure that each cell is fully charged. While it is suggested that the 'polarisation charger' system may eliminate the need for temperature compensation, equalise charge, and float voltage settings, and may also reduce corrosion, the system does not distinguish between, or identify the level of, polarisation on individual electrodes. Therefore, this system does not ensure that the float charge goals identified in Section 2.3 are achieved. Depending on the recharge rate, the increase in cell voltage towards the end of recharge does not guarantee that the cell is fully charged, as indicated by Figure 2.17.

The system described by Gabriel (above) applies a pulsed charge current signal to determine whether fully charged status or a particular level of polarisation has been achieved. Other systems that may appear similar apply pulsed discharge currents for analysis purposes[108]. Generally, these systems measure magnitudes of the voltage response to an applied discharge pulse. The relationship between applied current and voltage response is then used to determine

SOH or SOC with measurements relating to internal resistance. Because such systems are not typically used for float charge analysis, they are not covered in this work.

Analysis of the voltage response profile produced when a current perturbation is applied to a battery may reveal more information about a battery's state than simple magnitude measurements. A system described by Finger[109] uses a single 6 A current source commutated between the blocks that make up the battery system. The 6 A current source is shown to be connected to each 12 V block for a half-hour charge restoration period. During this time, the voltage response profile of the block receiving the charge current is monitored. At the end of the charge restoration period, the voltage profile is used to assess the battery's SOH. Figure 2.18 shows the window at the end of the half-hour charge restoration period that is used for the SOH assessment. The expected voltage within this window is compensated for by variables such as the number of discharge cycles and battery age. While this system targets VRLA batteries and is suggested to operate at a voltage designed to balance positive plate corrosion and negative plate self-discharge, it does not directly assess the polarisation of individual electrodes within each 2 V cell. The system is shown to operate on 12 V blocks, and the identification of a healthy state appears to target a window in the curves commonly accepted for constant current recharge of VRLA batteries, as shown in Figure 2.17. This does not ensure that each cell within a battery or each electrode within a cell is fully charged.

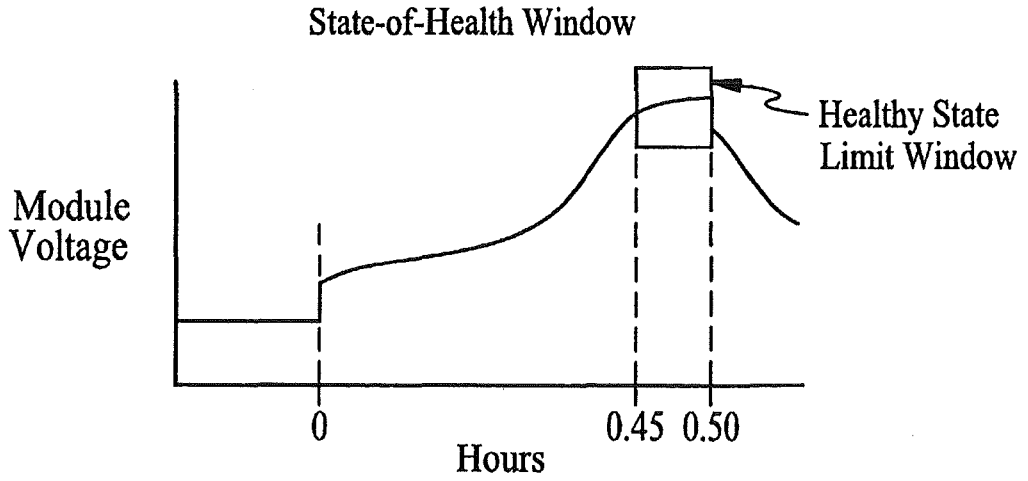

Figure 2.18 Battery Health Assessment using Voltage Response Profile[109]

Another system utilising the transient voltage produced in response to a current perturbation has been described by Cun et al[110]. This system utilises the voltage produced by battery blocks

during the charge phase of intermittent float charge. Figure 2.19 a) shows the response expected for a good block, while Figure 2.19 b) depicts the expected response of a defective block. The assessment is based on curve shape and rising and descending times. However, other than having been measured on known good and known defective batteries, no reasoning for these profiles is given.

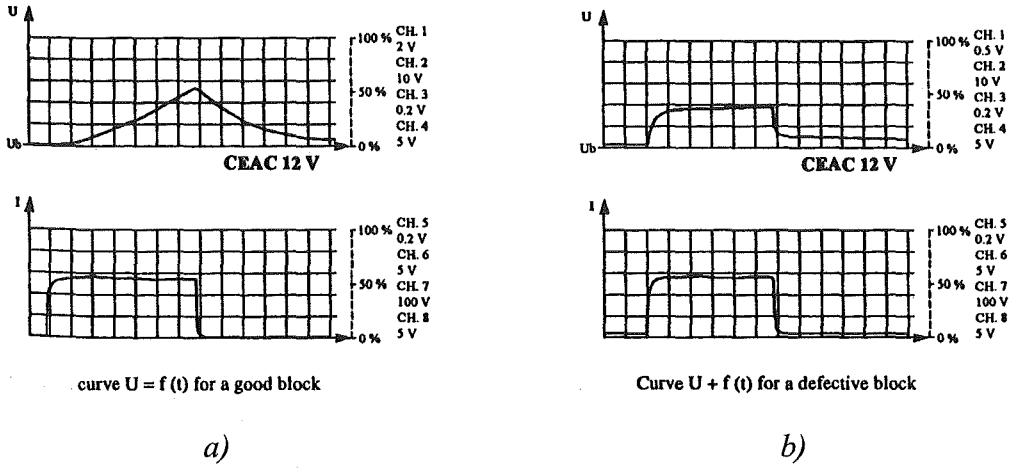

Figure 2.19 Detection of Faulty Battery Blocks using Transient Voltage Response[110]

A similar system described by Dupuis et al[111] compares the voltage response of cells or batteries to the average for the entire string when a known current pulse is applied. This system is intended to be used for checking lead acid storage batteries as they come off a production line. In a short test, cells or batteries are rejected depending on the polarity and absolute value of deviation from the average. The current pulses are either of constant intensity (5 A for 10 seconds), or increasing intensity over time (increasing at 1 A per second for 10 seconds). It is indicated that this system may detect internal shorts, reverse plate installation, reverse forming of cells, twisted plates, lack of electrolyte, and/or defective separators. As it is suggested that reference electrodes may be used with batteries that do not allow access to the terminals of every cell, it must therefore be assumed that this system targets flooded lead acid batteries. Measurements made with a reference electrode produce the voltage between the positive and negative electrodes of neighbouring cells, and may be analysed in a similar fashion to individual cell voltages. Although this system utilises a reference electrode, no analysis of the individual response of either the positive or the negative electrode within a cell is made.

2.5 Research Approach

There have been numerous attempts made to optimise float charge of lead acid or VRLA batteries. Section 2.4 of this thesis evaluates the ability of commonly used float charge techniques to meet the float charge goals that are identified in Section 2.3. These goals largely relate to polarisation of individual electrodes within a cell. Only a small number of these techniques directly target this critical electrode polarisation during float charge, and all of those that do, require the cell to be modified for the insertion of a reference electrode.

The key indicator for the success of the float charge is the polarisation distribution within a cell. Typical (recommended) float voltages apply a total polarisation of approximately 130 mV to a cell. To achieve maximum cell life, the positive electrode is required to support 40 - 80 mV of this polarisation, with the negative electrode supporting the remainder. At present, the only accurate way of determining the distribution of applied polarisation is through the use of some form of reference electrode. As reference electrodes are often fragile and require ongoing maintenance, their use is largely limited to testing carried out in a laboratory setting.

To facilitate this research specialised battery specific test equipment was required. Chapter 2 of this thesis has described many existing battery analysis techniques and test procedures, including Tafel plots, transient response, and impedance analysis. Chapter 3 of this thesis describes the test equipment and systems designed and constructed during the course of this research. The test systems developed allow existing techniques to be assessed and also provide a basis for further research.

There have been several suggestions in the literature that the impedance or response times differ for each electrode within a cell. This thesis investigates the ability of impedance and other similar frequency or time based measurement techniques to reveal additional information about a cell's internal operation.

In Chapters 4 and 5 of this research, an electrical equivalent model that replicates both the steady state and transient responses of each electrode within a VRLA cell is developed. This model is subsequently used in Chapter 6 to develop a test and analysis procedure that estimates how the polarisation, applied through the float charge, is distributed between the positive and negative

electrodes within a cell. This test may be applied to the terminals of a standard 2 V VRLA cell in field service, and requires no modification of the cell under test. Outcomes of this test and analysis procedure allow the identification of float charge imbalance problems, and may also be used as a basis for optimisation of the applied float voltage in order to maximise cell life.

2.6 References

[1] Hawker Energy Products (Oldham), *Standby Batteries – Lead Acid Recombination Cells ESPACE High Integerity HI Range,* Product brochure.

[2] D. Berndt, *Maintenance Free Batteries, Lead-Acid, Nickel/Cadmium, Nickel/Metal Hydride, A Handbook of Battery Technology,* Second Edition, Research Studies Press, 1997, p 99.

[3] David Linden (Editor in Chief), *Handbook of Batteries,* Second Edition, McGraw-Hill Inc, New York, 1994, s 25.2.

[4] David Linden (Editor in Chief), *Handbook of Batteries,* Second Edition, McGraw-Hill Inc, New York, 1994, *s* 24.2.1.

[5] David Linden (Editor in Chief), *Handbook of Batteries,* Second Edition, McGraw-Hill Inc, New York, 1994, *s* 25.1.

[6] *The Principle of the Gas-Recombination Battery,* Oldham ESPACE RG Series, Technical Handbook.

[7] S. S. Misra, T. M. Noveske, A. J. Williamson, *Catalyst Enhanced, Common Headspace VRLA Battery Designs,* Proceedings of INTELEC, 2000, 3-2, p 37.

[8] D. Berndt, *Maintenance Free Batteries, Lead-Acid, Nickel/Cadmium, Nickel/Metal Hydride, A Handbook of Battery Technology,* Second Edition, Research Studies Press, 1997, p 263.

[9] D. Berndt, *Maintenance Free Batteries, Lead-Acid, Nickel/Cadmium, Nickel/Metal Hydride, A Handbook of Battery Technology,* Second Edition, Research Studies Press, 1997, p 97.

[10] D. Berndt, *Maintenance Free Batteries, Lead-Acid, Nickel/Cadmium, Nickel/Metal Hydride, A Handbook of Battery Technology,* Second Edition, Research Studies Press, 1997, ss 2.3.3, 2.3.6.

[11] David Linden (Editor in Chief), *Handbook of Batteries,* Second Edition, McGraw – Hill Inc, New York, 1994, *s* 24.4.2.

[12] D. Berndt, *Maintenance Free Batteries, Lead-Acid, Nickel/Cadmium, Nickel/Metal Hydride, A Handbook of Battery Technology,* Second Edition, Research Studies Press, 1997, p 28.

[13] D. Berndt, *Maintenance Free Batteries, Lead-Acid, Nickel/Cadmium, Nickel/Metal Hydride, A Handbook of Battery Technology,* Second Edition, Research Studies Press, 1997, p 286.

[14] D. Berndt, *Maintenance Free Batteries, Lead-Acid, Nickel/Cadmium, Nickel/Metal Hydride, A Handbook of Battery Technology,* Second Edition, Research Studies Press, 1997, p 242.

[15] D. Berndt, U. Teutsch, *Float charging of Valve-Regulated Lead-Acid Batteries: A Balancing Act Between Secondary Reactions,* Journal of the Electrochemical Society, Vol. 143, No. 3, March 1996.

[16] D. Berndt, *Maintenance Free Batteries, Lead-Acid, Nickel/Cadmium, Nickel/Metal Hydride, A Handbook of Battery Technology,* Second Edition, Research Studies Press, 1997, p 287.

[17] S. S. Misra, A. J. Williamson, *On Temperature Compensation for Lead Acid Batteries in Float Service: Its Impact on Performance and Life,* Proceedings of INTELEC, 1996, 2-1.

[18] W. B. Brecht, J. A. Wertz, *Reference Electrode's use in the Analysis of Battery Performance and Operation,* Eleventh Annual Battery Conference on Applications and Advances, 1996.

[19] D. Berndt, U. Teutsch, *Float charging of Valve-Regulated Lead-Acid Batteries: A Balancing Act Between Secondary Reactions,* Journal of the Electrochemical Society, Vol. 143, No. 3, March 1996, p 792.

[20] D. Berndt, U. Teutsch, *Float charging of Valve-Regulated Lead-Acid Batteries: A Balancing Act Between Secondary Reactions,* Journal of the Electrochemical Society, Vol. 143, No. 3, March 1996, p 797.

[21] D. Berndt, *Maintenance Free Batteries, Lead-Acid, Nickel/Cadmium, Nickel/Metal Hydride, A Handbook of Battery Technology,* Second Edition, Research Studies Press, 1997, p 290.

[22] W. Cantor, *Field Experience with Reference Electrode Measurements,* Proceedings of INTELEC, 1996, 7-6, p 198.

[23] J. Jergl, B. Cole, & S. Purcell, *Real World Effects on VRLA Batteries in Float Applications,* Proceedings of INTELEC, 1996, 11-4.

[24] W.B. Brecht, D.O. Feder, J.M. McAndrews, A.J. Williamson, *The Effect of Positive Polarisation on Grid Growth, Cell Performance and Life "Willihnganz Revisited – 20 Years Later,* Proceedings of INTELEC, 1988, 5-7.

[25] D. Berndt, *Maintenance Free Batteries, Lead-Acid, Nickel/Cadmium, Nickel/Metal Hydride, A Handbook of Battery Technology,* Second Edition, Research Studies Press, 1997, s 7.2.3.2.

[26] Data source: F. J. Vaccaro, J. Rhoades, B. Le, *The Effects of Temperature on VRLA Reaction Rates and the Determination of Battery State of Charge Part 2-Fundamental Considerations,* Proceedings of INTELEC, 1997, 12-2, Table 3: 'Polarisations (Experimental)'.

[27] D. Berndt, *Maintenance Free Batteries, Lead-Acid, Nickel/Cadmium, Nickel/Metal Hydride, A Handbook of Battery Technology,* Second Edition, Research Studies Press, 1997, p 410.

[28] D. Berndt, *Maintenance Free Batteries, Lead-Acid, Nickel/Cadmium, Nickel/Metal Hydride, A Handbook of Battery Technology,* Second Edition, Research Studies Press, 1997, pp 295, 408.

[29] D. Berndt, *Maintenance Free Batteries, Lead-Acid, Nickel/Cadmium, Nickel/Metal Hydride, A Handbook of Battery Technology,* Second Edition, Research Studies Press, 1997, p 240.

[30] F. J. Vaccaro, J. Rhoades, B. Le, *The Effects of Temperature on VRLA Reaction Rates and the Determination of Battery State of Charge Part 2-Fundamental Considerations,* Proceedings of INTELEC, 1997, 12-2.

[31] D. Berndt, *Maintenance Free Batteries, Lead-Acid, Nickel/Cadmium, Nickel/Metal Hydride, A Handbook of Battery Technology,* Second Edition, Research Studies Press, 1997, p 295.

[32] J. J. Lander, *Silver, Cobolt and Positive-Grid Corrosion in the Lead Acid Battery,* Journal of the Electrochemical Society, Vol 105, No. 6, June 1958, Figure 2.

[33] W. E. M. Jones, *Quantifying Secondary Reactions in VRLA Batteries – What Purity Standards and Other Factors are Necessary to Prevent Negative Plate Discharge?* Proceedings of INTELEC, 2000, 23-3.

[34] D. Berndt, U. Teutsch, *Float charging of Valve-Regulated Lead-Acid Batteries: A Balancing Act Between Secondary Reactions,* Journal of the Electrochemical Society, Vol. 143, No. 3, March 1996, p 795.

[35] D. Berndt, *Maintenance Free Batteries, Lead-Acid, Nickel/Cadmium, Nickel/Metal Hydride, A Handbook of Battery Technology,* Second Edition, Research Studies Press, 1997, p 289.

[36] U. Teutsch, *A Mathematical Model for Float Operation of Valve-Regulated Lead-Acid Batteries,* Proceedings of The First Telecommunications Energy Special Conference (TELESCON 94), 1994, pp 89-96.

[37] D. Berndt, R. Brautigam, U. Teutsch, *Temperature Compensation of Float Voltage – The Special Situation of VRLA Batteries,* Proceedings of INTELEC, 1995, 1-1.

[38] Hawker Energy Products Inc, *Cyclon Selection Guide,* Third Edition, 1998, p 2.

[39] W. B. Brecht, J. A. Wertz, *Reference Electrodes Use in the Analysis of Battery Performance and Operation,* Eleventh Annual Battery Conference on Applications and Advances, 1996, p 264.

[40] W. E. Jones, D. O. Feder, *Behaviour of VRLA Cells on Long Term Float: Part 2 The effects of temperature, voltage and catalysis on gas evolution and consequent water loss,* Proceedings of INTELEC, 1996, 11-5.

[41] S. S. Misra, A. J. Williamson, *On Temperature Compensation for Lead Acid Batteries in Float Service: Its Impact on Performance and Life,* Proceedings of INTELEC, 1996, 2-1, pp 29, 31.

[42] J. Jergl, B. Cole, S. Purcell, *Real World Effects on VRLA Batteries in Float Applications,* Proceedings of INTELEC, 1996, 11-4, p 352.

[43] S. S. Misra, T. M. Noveske, S. L. Mraz, A. J. Williamson, *The Role of Gas Recombining Catalysts in VRLA Cells,* Proceedings of INTELEC, 1999, 3-2.

[44] F. Vaccaro, J. Rhoades, B. Le, J. Timmons, *A Catalyst in a VRLA Cell: The Affect on Life and Tafel Character,* Proceedings of INTELEC, 2001, 6-11.

[45] W. E. Jones, H. A. Vanasse, C. E. Sabotta, J. E. Clapper, E. F. Price, *Can VRLA Batteries Last 20 Years,* Proceedings of INTELEC, 1998, 19-4.

[46] W. E. Jones, D. O. Feder, *Correcting Inherent Imbalance and Consequent Failure of VRLA Cells by the Use of Catalysts,* Proceedings of TELESCON, 1997, p 302.

[47] W. E. Jones, D. O. Feder, *Behaviour of VRLA Cells on Long Term Float: Part 2 The effects of temperature, voltage and catalysis on gas evolution and consequent water loss,* Proceedings of INTELEC, 1996, 11-5, p 364.

[48] D. Berndt, *Maintenance Free Batteries, Lead-Acid, Nickel/Cadmium, Nickel/Metal Hydride, A Handbook of Battery Technology,* Second Edition, Research Studies Press, 1997, p 406.

[49] A. Lohner, E. Karden, R. W. DeDoncker, *Charge Equalising and Lifetime Increasing with a New Charging Method for VRLA Batteries.* Proceedings of INTELEC, 1997, 18-4.

[50] David Linden (Editor in Chief), *Handbook of Batteries,* Second Edition, McGraw-Hill Inc, New York, 1994, pp 25, 29.

[51] R. J. Kakalec, T. H. Kimsey, *A New Battery Plant Configuration that Eliminates Thermal Runaway in Valve Regulated Lead-Acid Batteries,* Proceedings of INTELEC, 2000, 16-1.

[52] S. S. Misra, A. J. Williamson, *On Temperature Compensation for Lead Acid Batteries in Float Service: Its Impact on Performance and Life,* Proceedings of INTELEC, 1996, 2-1.

[53] D. Berndt, *Maintenance Free Batteries, Lead-Acid, Nickel/Cadmium, Nickel/Metal Hydride, A Handbook of Battery Technology,* Second Edition, Research Studies Press, 1997, p 409.

[54] S. S. Misra, A. J. Williamson, *On Temperature Compensation for Lead Acid Batteries in Float Service: Its Impact on Performance and Life,* Proceedings of INTELEC, 1996, 2-1 p 30.

[55] G. Karlsson, *Recharge of Valve-Regulated Batteries at Elevated Temperaturers,* Proceedings of INTELEC, 2001, p 125.

[56] B. Culpin, P. L. WainWright, *An Investigation into the Effects of Abuse Charging and Thermal Runaway in VRLA Batteries,* Proceedings of INTELEC, 2001, pp 361-368.

[57] S. S. Misra, A. J. Williamson, *Thermal Runaway of VRLA Batteries: Published Test Methods versus Real Life Experience,* Proceedings of INTELEC, 1998, 22-3.

[58] D. Berndt, *Maintenance Free Batteries, Lead-Acid, Nickel/Cadmium, Nickel/Metal Hydride, A Handbook of Battery Technology,* Second Edition, Research Studies Press, 1997, p 410.

[59] J. Jergl, B. Cole, S. Purcell, *Real World Effects on VRLA Batteries in Float Applications,* Proceedings of INTELEC, 1996, 11-4, p 356.

[60] D. Berndt, *Maintenance Free Batteries, Lead-Acid, Nickel/Cadmium, Nickel/Metal Hydride, A Handbook of Battery Technology,* Second Edition, Research Studies Press, 1997, *s* 13.1.1.2.

[61] Institute of Electrical and Electronics Engineers, Inc., *IEEE Recommended Practices for Maintenance, Testing, and Replacement of Valve Regulated Lead Acid (VRLA) Batteries for Standby Application,* IEEE Std 1188-1996, p 14.

[62] S. S. Misra, A. J. Williamson, *On Temperature Compensation for Lead Acid Batteries in Float Service: Its Impact on Performance and Life,* Proceedings of INTELEC, 1996, 2-1, p 26.

[63] F. J. Vaccaro, J. Rhoades, B. Le, *The Effects of Temperature on VRLA Reaction Rates and the Determination of Battery State of Charge Part 2-Fundamental Considerations,* Proceedings of INTELEC, 1997, 12-2, p 236.

[64] H. Giess, *The Operation of VRLA MonoBlocks With an On/Off Float Charge Regime,* Proceedings of INTELEC, 2001, pp 116 – 120.

[65] R. J. Kakalec, T. H. Kimsey, *A New Battery Plant Configuration that Eliminates Thermal Runaway in Valve Regulated Lead-Acid Batteries,* Proceedings of INTELEC 2000, 16-1.

[66] X. Muneret, M. Coux, P. Lenain, *Analysis of the Partial Reactions within a Standby VRLA Battery Leading to an Understanding of Intermittent Charging Technique,* Proceedings of INTELEC, 2000, 2-1, p 295.

[67] D. P. Reid, I Glasa, *A New Concept: Intermittent Charging of Lead Acid Batteries In Telecommunication Systems,* Proceedings of INTELEC, 1984, pp 67-71.

[68] X. Muneret, M. Coux, P. Lenain, *Analysis of the Partial Reactions within a Standby VRLA Battery Leading to an Understanding of Intermittent Charging Technique,* Proceedings of INTELEC, 2000, 2-1, p 298.

[69] J-P.Cun, J-N. Fiorina, M. Fraisse, H. Mabboux, *Increased UPS Battery Life, Main Failure Modes, Charging and Monitoring,* Proceedings of INTELEC, 1997, 18-1.

[70] T. Sideris, S. Vasa-Sideris, E. K. Stefanakos, *Battery Ageing and the Case for Stopping Float Charging,* Proceedings of INTELEC, 1999, 6-3.

[71] P. Waltari, T. Suntio, A. Tenno, R. Tenno, *The Effects of Intermittent Charging on VRLA Battery Life Expectancy in Telecom Applications,* Proceedings of INTELEC, 2002, 8-2.

[72] D. O. Feder, T. G. Croda, K. S. Champlin, S. J. McShane, M. J. Hlavac, *Conductance testing compared to traditional methods of evaluating the capacity of Valve-regulated lead/acid batteries and predicting state of health,* Journal of Power Sources, 1992, Vol. 40, p 236.

[73] Institute of Electrical and Electronics Engineers, Inc., *IEEE Recommended Practice for Maintenance, Testing, and Replacement of Valve-Regulated Lead-acid (VRLA) Batteries for Stationary Applications,* IEEE Std 1188-1996, Annex A, p 11.

[74] K. D. Floyd, Z. Noworolski, J. M. Noworolski, W. Sokolski, *Assessment of Lead-Acid Battery State of Charge by Monitoring Float Current,* Proceedings of INTELEC, 1994, 20-2.

[75] W. R. Plow, B. B. Garrett, *Float Current Monitoring and Evaluation,* Proceedings of INTELEC, 2000, 19-1.

[76] L. Giuseppe, L. Bencivenni, *VRLA Batteries – Design, Manufacturing and Operation Overview,* Proceedings of INTELEC, 2000, 6-3, p 99.

[77] E. Boisvert, *Using Float Current Measurements to Prevent Thermal Runaway on VRLA Batteries,* Proceedings of INTELEC, 2001, pp 126-131.

[78] J. Frandfors, *Cell-Voltage Equalisers Series BMP 160,* Ericsson Review, 1992, No. 1-2.

[79] C. Pascual, P. T. Krein, *Switched Capacitor System for Automatic Battery Equalization,* United States Patent 5,710,504, January 20, 1998.

[80] G. L. Brainard, *Non-Dissipative Battery Charger-Equaliser,* United States Patent 5,479,082, December 26, 1995.

[81] W. E. Jones, D. O. Feder, *Behaviour of VRLA Cells on Long Term Float: Part 2 The effects of temperature, voltage and catalysis on gas evolution and consequent water loss,* Proceedings of INTELEC, 1996, 11-5, p 365.

[82] W. E. Jones, D. O. Feder, *Correcting Inherent Imbalance and Consequent Failure of VRLA Cells by the Use of Catalysts,* Proceedings of TELESCON, 1997, pp 295-302.

[83] S. S. Misra, T. M. Noveske, S. L. Mraz, A. J. Williamson, L. S. Holden, *The Role of Gas Recombining Catalysts in VRLA Cells,* Proceedings of INTELEC, 1999, 3-2.

[84] F. Vaccaro, J. Rhoades, B. Le, J. Timmons, *A Catalyst in a VRLA Cell: The Affect on Cell Life and Tafel Character,* Proceedings of INTELEC, 2001, pp 6-11.

[85] H. A. Vanasse, D. Jones, *Catalyst 101: The Basics of Using Catalysts in VRLA Cells,* Battcon 2002.

[86] H. A. Vanasse, F. J. Vaccaro, V. R. Nikolov, *Hydrogen Sulfide in VRLA Cells,* Proceedings of INTELEC, 2001, pp 245-251.

[87] E. A. Willihnganz, *Method and Apparatus for Measuring the State of Charge of a Battery Using a Reference Battery,* United States Patent 3,657,639, April 18, 1972.

[88] Y. M. Mistry, T. D. O'Sullivan, *Electrical Storage Cell Life Extender,* United States Patent 4,935,688, June 19, 1990.

[89] T. D. O'Sullivan, C. F. Leung, *Field Test of the Polarisation Controller on a Mixed Battery String,* Proceedings of INTELEC, 1992, 9-1.

[90] S. C. Chalasani, V. J. Thottuvelil, *Recharging Circuit and Method for Recharging a Battery Having a Reference Electrode,* United States Patent 6,137,266, October 24, 2000.

[91] D. Baert, *The Use of Analytical Models for Batteries,* Proceedings of INTELEC, 1999, 24.1.

[92] A. Tenno, R. Tenno, T. Suntio, *Soft Sensor Approach in Characterization of VRLA Batteries,* Proceedings of INTELEC, 2001, pp 554 –565.

[93] Z. Noworolski, U. Reskov, *Dynamic Properties of Lead Acid Batteries, Part 1: Initial Voltage Drop,* Proceedings of INTELEC, 1998, 10-3.

[94] P. Waltari, T. Suntio, A. Tenno, T. Tenno, *The Effects of Intermittent Charging on VRLA Battery Life Expectancy in Telecom Applications,* Proceedings of INTELEC, 2002, 8-2, p 126.

[95] G. Alber, *Ohmic Measurements: The History and the Facts,* Proceedings of Battcon, 2003, Paper 1.

[96] N. D. Scott, *A Single Integrated Circuit Approach to Real Capacity Estimation and Life Management of VRLA Batteries,* Proceedings of INTELEC, 2001, pp 307-312.

[97] K. S. Champlin, K, Bertness, *A Fundamentally New Approach to Battery Performance Analysis Using DFRA™/DFIS™ Technology,* Proceedings of INTELEC, 2000, 19-3.

[98] K. S. Champlin, *Method and Apparatus for Measuring Complex Impedance of Cell and Batteries,* United States Patent 6,002,238, Dec 14, 1999.

[99] K. S. Champlin, K. Bertness, *Results of Discrete Frequency Immittance Spectroscopy (DFIS) Measurements of Lead Acid Batteries,* Proceedings of INTELEC, 2001, pp 433-440.

[100] F. Huet, *A Review of Impedance Measurements for Determination of the State-of–Charge or State-of-Health of Secondary Batteries,* Journal of Power Sources, 1998, Vol. 70, pp 59-69.

[101] E. Karden, R.W. De Doncker, *The Non-Linear Low-Frequency Impedance of Lead/Acid Batteries During Discharge, Charge and Float Charge,* Proceedings of INTELEC, 2001, pp 65–72.

[102] A. Tenno, R. Tenno, T. Suntio, *Battery Impedance and its Relationship to Battery Characteristics,* Proceedings of INTELEC, 2002, 11-2, p 183.

[103] Z. Noworolski, U. Reskov, *Can a Battery Ohmic Tester Distinguish a Good Cell From the Pool of Better Ones?* Proceedings of INTELEC, 2002, 14-3.

[104] D. H. J. Baert, A. A. K. Vervaet, *Determination of the State-of-Health of VRLA Batteries by Noise Measurements,* Proceedings of INTELEC, 2001, pp 301-306.

[105] David Linden (Editor in Chief), *Handbook of Batteries,* Second Edition, McGraw-Hill Inc, New York, 1994, s 25.5.5.

[106] C. M. Gabriel, M. E. Burkum, *Apparatus and Method for Utilising Polarisation Voltage to Determine Charge State of a Battery,* United States Patent 5,314,385, May 25, 1993.

[107] C. M. Gabriel, M. L. Reed, C. E. Beck, *Concepts of Battery Charger Control Using Polarisation Voltage,* Proceedings of American Power Conference, 58th Annual Meeting, 1996.

[108] G. Alber, *Impedance Measurements: The History and The Facts,* Proceedings of Battcon, 2003, pp 1-1 – 7.

[109] E. P. Finger, *Method of Battery Charge Restoration Based on Estimated Battery Plate Deterioration and/or Based on Battery State of Health,* United States Patent 6,362,601, March 26, 2002.

[110] J-P. Cun, J-N. Fiorina, M. Fraisse, H. Mabboux, *Increasing UPS Battery Life, Mains Failure modes, Charging and Monitoring,* Proceedings of INTELEC, 1997, 18-1.

[111] J-M. Dupuis, P. L. Lasserre, *Method for Checking a Storage Battery,* United States Patent 4,044,300, August 27, 1977.

3 Test Equipment

In this Chapter a description of the test systems and test equipment constructed during the course of this project is given. The test systems developed allow existing battery analysis techniques, such as reference electrode testing (to produce Tafel plots), transient response, and impedance analysis, to be assessed. The developed test systems also provide the platform for further research. Steady state reference electrode testing is required to produce Tafel plots. While this testing typically requires milli-Amp and milli-Volt stability for time periods measured in hours, it is dependent on the capacity of the cell under test. Due to the thermal sensitivity of VRLA batteries, the temperature variation of the tested cell during this steady state testing should be less than 1°C. Transient response testing typically requires constant current charge and discharge facilities ranging from milli-Amps to Amps, and for single cell testing, voltage measurements with milli-Volt resolution over a 0-3 V range. Impedance measurements of VRLA storage batteries typically range from kilo-Hertz down to milli- and even micro-Hertz, with AC signals ranging from milli-Amps to several Amps. The voltage signals encountered during such impedance measurements typically range from milli-Volts to hundreds of milli-Volts. Current shunts used to measure the charge and discharge currents typical for storage batteries must be capable of passing several hundred Amps with minimal voltage drop (typically up to 50 mV). Due to the extremely low resistance of these shunts, their ability to resolve float current (typically 10s – 100s of milli-Amps) is not practical. To allow a single shunt to measure both float current and charge/discharge currents, a temperature-compensated precision shunt amplifier is also developed as part of this work.

This Chapter has been divided into two sections, the first of which describes the automated test system hardware and the MATLAB® based control software. The second section details electronic test hardware that was designed and constructed to allow this research to progress.

3.1 Test System

Three VRLA battery parameters, namely cell (or block) voltage, current, and temperature, are easily and therefore commonly measured. An additional parameter of ambient temperature is also useful when analysing results. The success of float charge relies heavily on the polarisation applied to the cell terminals being optimally distributed between the two (positive and negative) electrodes within the cell. Reference electrodes may be used for float analysis as they allow each electrode's operation to be individually assessed. A reference electrode is normally inserted through the cells' case so that it makes contact with the electrolyte within. This effectively gives the cell a third terminal, allowing the contributions of each electrode to the overall cell voltage to be directly measured.

As float charge typically involves maintaining a battery in a fully charged state for long periods of time, an automated test system is desirable to ensure that battery parameters may be accurately monitored during these extended time periods. There are many dedicated battery test systems commercially available, however these target either laboratory based analysis of chemical processes within a battery (used for cell design and verification), or end-user assessment of a battery installed in the field. As these test systems generally have predefined test procedures, their usefulness in exploratory research may be limited. In order to provide a test environment free of restrictions, an automated test system was constructed from programmable test equipment commonly found in electronics laboratories.

3.1.1 Hardware

Two separate test systems were constructed and used during this research. The system used for the majority of this work catered for both steady state and transient testing. A second test system was developed to allow both voltage and current controlled impedance testing.

3.1.1.1 Steady State and Transient Testing

Figure 3.1 shows the basic test system used throughout this project. The system is largely based around standard programmable test equipment commonly found in electronics laboratories. The equipment is programmed and controlled through a General Purpose Instrumentation Bus (GPIB

IEEE-488) from a desktop personal computer (PC). MATLAB was used to provide a common PC software environment for both automated testing and the subsequent analysis of the test data. MATLAB was chosen as the PC based software platform as it has simple unrestricted script-based programming for test set-up and control, and strong mathematical computation power for data analysis, and also due to its availability.

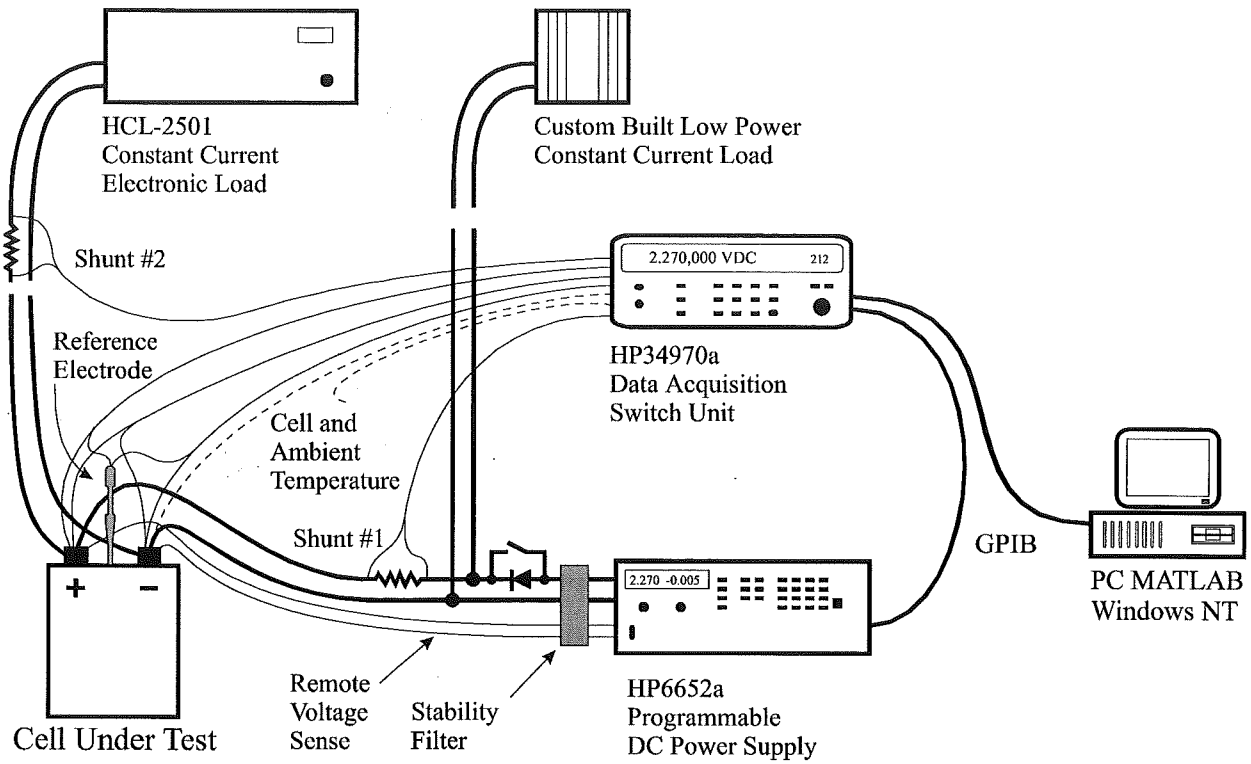

Figure 3.1 Automated Test System Set-up

The test system shown in Figure 3.1 contains two constant current loads. For discharge rates above 1 A, the HCL-2501 constant current load is used. Because this load is designed for discharge currents up to 500 A, its controllability and consistency at low currents is limited. In order to provide greater control at currents below 1 A, a low power constant current load was designed and constructed. Because each test is performed at a predetermined rate, no automated adjustment of the load was necessary, and the discharge rate was simply pre-set before initiating each test. Two current shunts are used to measure the battery current. Shunt #1 is a 1 Ω 100 W resistor, used to measure both the charge current and the low rate discharges. This is a relatively high value resistor for a current shunt, however it was chosen to simplify measurements of low discharge rates. Shunt #2 is a 200 mV 200 A (class 0.5) shunt manufactured by Compton, used to measure discharge rates greater than 1 A. During all discharge testing the power supply's

(HP6652a) voltage is set lower than the minimum battery voltage, thus allowing the series diode to become reverse biased. All measurements of voltage, current, and temperature were obtained with the HP34970a Data Acquisition / Switch Unit with an HP34901a 20 Channel Multiplexer.

An HP6652a programmable DC power supply is used for all charging. This supply has a programming accuracy of 10 mV and 25 mA. This power supply contains an over-voltage 'crowbar' protection circuit on its output. Because of this, a diode was placed in series with the positive supply line to prevent the tested cell from discharging should this be activated. As voltage stability of this supply is improved by eliminating the diode's voltage drop, the diode was shorted when voltage stability was critical and no discharging was required. To reduce steady state stabilisation times and ensure that the terminal voltage of the cell was consistent, the remote voltage sensing features of this power supply were also used. However, the combined effects of shunt resistance, cabling, and the diode introduced some low frequency noise. While the desired voltage on the terminals of the tested cell is held constant (within measurable limits), the current supplied to the battery and voltage on the output terminals of the power supply were found to contain low frequency (0.5 – 1 Hz) random noise. Simple LC filters in the remote sense lines reduced this noise. These filters directly coupled the high frequency response of the supply's output terminals with the remote sense input terminals, while still allowing the remote-sensed DC voltage to be applied to the sense inputs. Each filter consists of a 1200 μF capacitor and a 1.75 μH inductor. These are applied to both the positive and the negative sense leads.

For the test system shown in Figure 3.1, measurements of voltage, current, and temperature are taken by the HP34970a unit. K-type thermocouples are used for all temperature measurements, and current shunt voltages are appropriately scaled (using Mx+B features within the HP34970a unit) to provide true current readings. The HP34970a unit is a versatile piece of test equipment containing a single 22-bit (6½ digit) digital multimeter that can be over-sampled up to 26-bit resolution. For noise rejection, the integration time period for the analogue to digital conversion is set in multiples of the mains, with a maximum integration time of 200 PLCs. This single digital multimeter is switched between the desired input signals by mechanical relays on an armature card. Seven different armature cards are available to cover a range of applications from standard voltage, temperature, and current measurements, to matrix switching, RF multiplexing, digital input/output, and analogue outputs. The HP34970a meter has three bays into which any combination of armature cards may be inserted. For this application, an HP34901a 20 Channel Multiplexer card was used. This has the following key features: 20 differential channels of 300

V switching (both Hi and Lo switched), two channels for DC or AC current measurements (100 nA - 1A), a built-in thermocouple reference junction for temperature measurements, and switching speeds of up to 60 channels per second.

Dependant on the rate of discharge, one of two constant current electronic loads is used. For discharge rates up to and including 1 A, the purpose designed constant current load is used. Discharge testing above 1 A is performed with the HCL-2501 load. The low current load was designed and constructed as the result of difficulties experienced with the accuracy and consistency of the HCL-2501 at low currents. Further design detail of this low current load is given in Section 3.2.4. The HC Power Electronic Load (model HCL-2501-C001) is adjustable for constant current loads between 0 - 500 A, and voltages up to 80 V DC. This unit has a power limit of 2500 W that further limits the maximum discharge current limit above 5 V DC. The design of this load requires the DC supply (battery under test) to be raised above 1.5 V before an under-voltage lockout may be latched off. This causes problems when discharging 2 V lead acid cells. This under-voltage lockout is disabled when the unit's remote control is used, and for this reason the remote control is used to set the discharge rate. The remote control simply supplies a DC voltage between 0 - 5 V to select a load current between 0 - 500 A.

The PC used for test control and data storage is a Digital Venturis 5100, with 32MB of RAM and a 2GB hard disk. This has a National Instruments PCI-GPIB Card installed to enable communication with the test equipment. The PC's operating system is Microsoft Windows NT 4.00.1381, and all testing is controlled directly from MATLAB version 5.3.0.10183 (R11), as detailed in Section 3.1.2.1.

A Radiometer TR200 Mercury Mercurous-Sulphate reference electrode (see Appendix B) is used for all testing. To facilitate reference electrode testing, a sealed insertion adapter was designed and manufactured. This required a hole to be drilled and tapped (M8) in the battery container lid, with the O-ring sealed adapter screwed into this. A salt-bridge (K_2SO_4) was inserted through the adapter and aligned with its porous tip in contact with the cell's AGM separator. A second O-ring seal in the adapter was then tightened to seal and support the salt-bridge. The O-ring sealed adapter, salt-bridge, and reference electrode are shown in Figure 3.2.

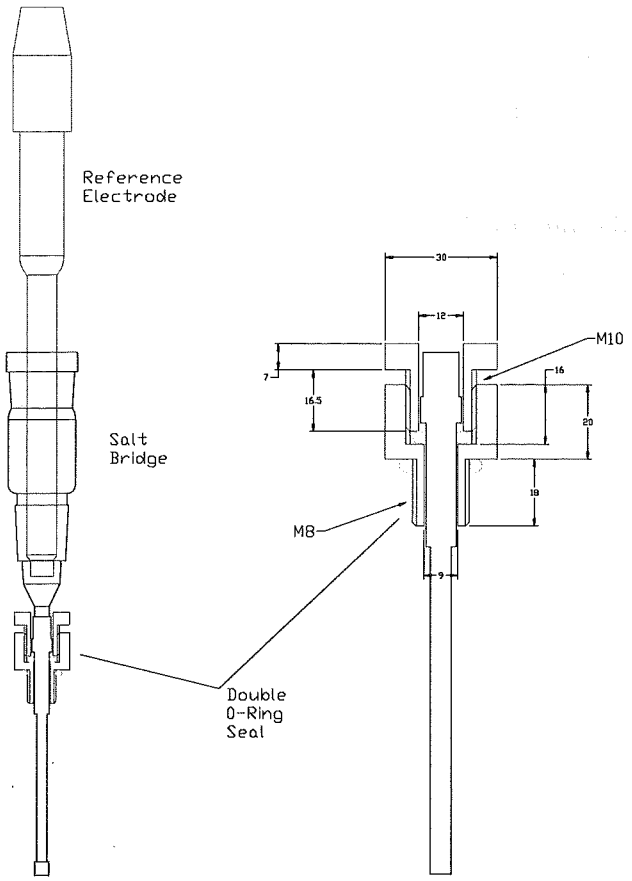

Figure 3.2 Reference Electrode, Salt-Bridge and Double O-Ring Seal

To verify expected reference electrode operation, the positive and negative electrode voltages (w.r.t the reference) are measured and the sum of these compared to the directly measured terminal voltage of the cell. Typically, the sum of the reference electrode measured voltages and the cell voltage agreed within 100 μV. If the tip of the salt-bridge loses contact with the AGM separator, or if the reference electrode is removed from the salt-bridge, the reference point is removed and the measurements do not agree. Ideally, simultaneous measurements are required to ensure that the working (positive and negative) electrode voltages sum to the total cell voltage. However, as the total measurement period of all channels is less than 1 second duration, and considering the cell's slow response during float charge, the slight delay between measurement of individual channels does not significantly influence results. Reference electrode testing of VRLA batteries can involve a number of difficulties, and is not common practice. Section 3.1.1.3 contains more detailed information on the use of the reference electrode.

3.1.1.2 Impedance Test System

The test system detailed above in Section 3.1.1.1 was used for all steady state (Tafel) and transient (charge and discharge) testing. The mechanical switching operation of the HP34970a unit restricts the frequency at which measurement channels may be scanned. The test system shown in Figure 3.3 was designed and constructed to provide the simultaneous high speed measurements of multiple data sources required for the investigation of cell impedance at frequencies ranging from DC up to several kilo-Hertz. The core of this test system was designed and constructed specifically for this project, again utilising conventional electronics laboratory test equipment to enable automation and control via GPIB interface. While preliminary impedance testing with this system identified a promising characteristic, analysis of this characteristic is simpler when conventional transient testing is used. For this reason, the impedance test system was never automated. The unit central to the impedance testing system provides an isolated interface between ground referenced laboratory test equipment and a VRLA cell that may either stand alone, or be situated anywhere in a battery string. A detailed description of this central unit is given in Section 3.2.1, and the key features of this impedance system are listed below.

Key features:

- Bi-directional optical signal isolation between ground referenced test equipment and tested cell.
- 4-wire cell interface, plus an additional reference electrode channel.
- Current or voltage control.
- DC coupled to allow low frequency or DC operation (frequency range DC – 2 kHz).
- Offset / DC bias generated separately (analogue output from HP34970a), and summed with AC signal (HP33120a) to provide set point (voltage or current).
- Bias subtraction from voltage signal and AC voltage gain of ten to simplify oscilloscope viewing.

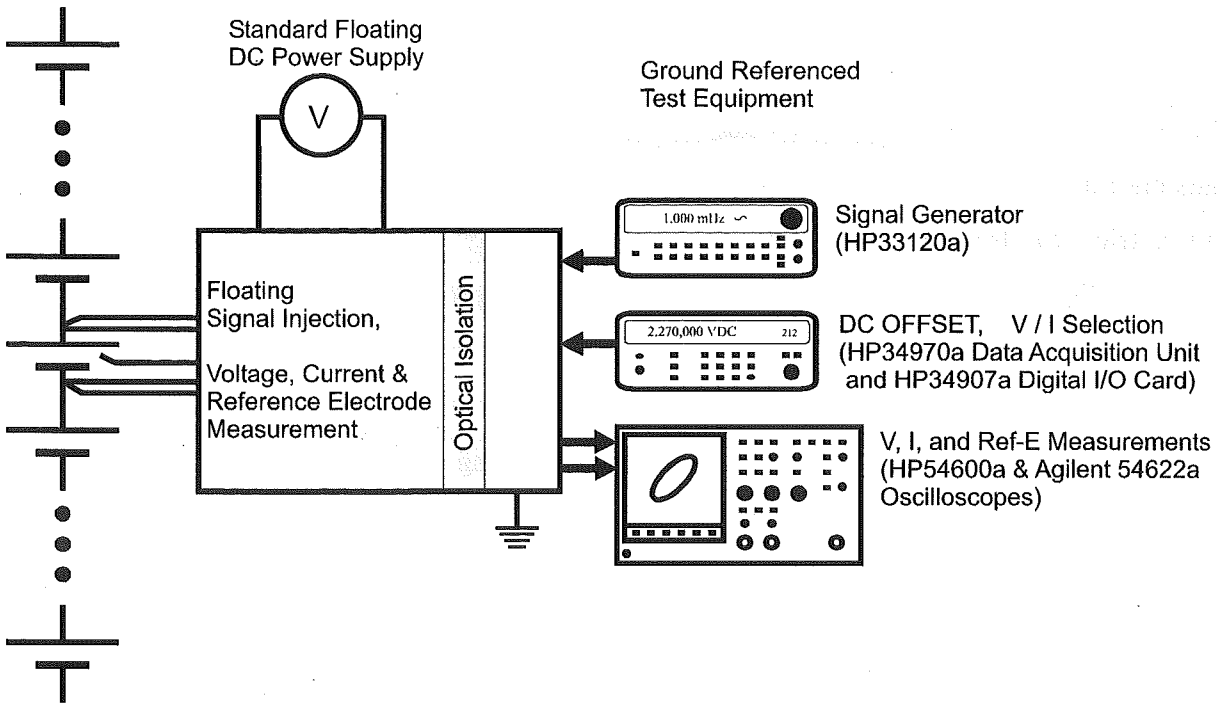

Figure 3.3 Impedance Measurement System

3.1.1.3 Reference Electrode Use in VRLA Cells

There are many difficulties involved with reference electrode testing of commercially available VRLA cells, and because of this they are not frequently used with VRLA cells[1]. As this type of testing is not common practice, documentation regarding the techniques involved is scarce. Being essentially sealed, the ability and ease of installing a reference electrode in a VRLA cell is reduced. To add a reference electrode to a VRLA cell, the cell's case must be punctured. This may alter its characteristic as the delicate gas balance in the cell's headspace may escape, and more importantly, puncturing the case will allow atmospheric oxygen to enter the cell. When atmospheric oxygen comes into contact with the negative electrode, its spontaneous reduction produces a depolarising effect, and gradually discharges the negative. For this reason, the installation and sealing of the electrode's salt-bridge was performed as quickly as possible. Following the installation, a boost charge was applied to the cell in an attempt to reverse any discharge the negative electrode may have incurred. The boost charge also promotes some gas venting in order to expel and rebalance headspace gases.

Apart from the problems associated with the addition of a reference electrode potentially modifying the cell's operation, the lack of available application information relating to the correct use of reference electrodes in VRLA cells results in many unknowns, which may lead to measurement error. Some of these potential problems include voltmeter input impedance, test duration, ageing of the reference electrode, junction diffusion, electrolyte/K_2SO_4 contamination, acid concentration compensation, and temperature correction. The data sheet supplied with the reference electrode has been included in Appendix B, however this provides little information in these areas.

Current drawn from or supplied through the reference electrode will charge junctions within the reference. This may result in measurement error, and possibly damage the reference electrode. Historical works attempt to alleviate this problem through the use of balance bridges, however advances in modern electronic instrumentation are believed to have eliminated this problem. In the voltage ranges suitable for single cell measurements, the HP34970a unit has the option of selecting either 10 MΩ or >10 GΩ input resistance. Although noise sensitivity is increased, the >10 GΩ voltmeter input resistance is used with all reference electrode measurements to prevent reference electrode damage or measurement error. In addition to this, as a result of the relay switching mechanism in the HP34970a, the reference electrode's measurement circuit is completed for only 21 ms while measurements are taken. For the remainder of the time, the reference electrode is essentially floating. Periodic comparisons between the sum of the positive and negative electrode voltages (measured w.r.t the reference electrode) and the terminal voltage of the cell verified satisfactory contact between the salt-bridge and the cell's electrolyte suspended in its separator.

Although it is suggested that mercury/mercurous sulphate reference electrodes are suitable for continuous measurement in VRLA batteries[2], ageing of the reference electrode is also a concern. It has been suggested that with correct maintenance, reference electrodes have a lifetime of approximately two years[3]. However, further correspondence with the manufacturer of the reference electrode suggested that this was conservative, and that reference electrodes will generally outlast the working electrodes (cell under test). As trends and relative responses are of greater significance than a precise measurement, slight accuracy degradation due to age is not seen to be detrimental.

Associated with reference electrode ageing and measurement accuracy, the test duration may also influence results through two separate mechanisms, namely wear-out of the reference electrode, and junction diffusion. Continuous long-term operation of reference electrodes may result in premature ageing, and it is recommended (Appendix B Data Sheet) that between measurements the reference electrode is stored in a protective tube filled with saturated K_2SO_4 solution. During continuous testing the tip of the reference electrode is submersed in the saturated K_2SO_4 solution of the salt-bridge, and between measurements the lead of the reference electrode is isolated from the metering equipment by the meter's switching relays. This situation replicates the state recommended for storage of the reference electrode, therefore no adverse effects should occur. The given conversion value (offset voltage) for the $Hg/Hg_2/K_2SO_4$ reference electrode to a standard hydrogen electrode (S.H.E.) assumes that an abrupt junction occurs at the interface of the saturated K_2SO_4 solution and the cell's sulphuric acid electrolyte. The permanent installation of the salt-bridge in the cell gives a possibility that a diffused junction and possibly even cross contamination may result over time. The tip of the salt-bridge utilises a porous ceramic plug that allows flow of ionic currents but largely prevents liquid flow. To alleviate the diffusion problem in an Hg/Hg_2SO_4 reference electrode (without a salt-bridge), a redesigned reference electrode that utilises gelled electrolyte has been suggested[4]. However, the design of the commercially available reference electrode and the lack of a suitable gelling agent prevented use of this technique in this research. Again, as relative response is more important than precise measurement, small voltage offsets generated through diffusion potentials should not significantly influence results. Repeated removal and installation of the salt-bridge and the associated ingestion of oxygen is considered to be more detrimental to cell operation than voltage offsets generated through diffusion potentials.

Mercury/mercurous sulphate reference electrodes are normally filled with dilute sulphuric acid with a density similar to that of the sulphuric acid electrolyte in the cell under test. As a lead acid cell is discharged, changes in its electrolyte density occur. If the acid density in the reference electrode and the cell differ, compensation of the reference electrode's potential to an S.H.E. is necessary. The Radiometer TR200 reference electrode used has a set acid density that cannot be altered. This research targets the fully charged region of operation, for which acid concentration within the cell under test does not change significantly. As relative response is more significant than precise measurement, no compensation of the reference electrode's potential is necessary. Similarly, temperature compensation of the reference's potential (w.r.t. S.H.E.) is also required. Typical compensation values have also been included in Appendix B,

however despite being supplied by the manufacturer of the used reference electrode, differences in the potentials at 25 °C are noted. Again, the relative response is more significant than precise measurement, and therefore no compensation of the reference electrode's potential is undertaken. All reference electrode based voltage measurements shown in this thesis have been converted to S.H.E using the +658 mV value stated by the data sheet supplied with the reference (Appendix B).

3.1.2 Software

The automated test system shown in Figure 3.1 is controlled directly from MATLAB run on a PC with a Windows NT operating system. The software used for control of the automated testing is divided into two functions, namely software used for communication with the test equipment (via GPIB), and application software which controls the test procedure. This application software is further divided into two functions, software used for continuous data logging of the transient testing, and software used to control Tafel testing.

3.1.2.1 Matlab – GPIB communications

A detailed description of the software and hardware used to enable MATLAB m-file scripts to control test equipment has been previously described[5], however for completeness, a brief description of this software and hardware interaction is provided in this Section.

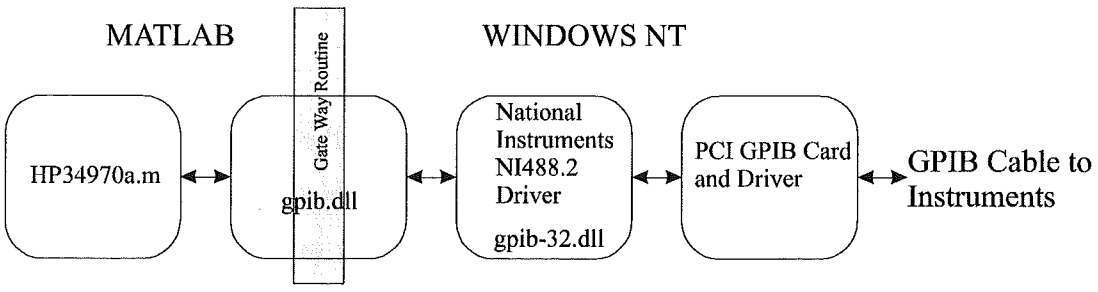

Figure 3.4 MATLAB – Programmable Test Equipment Communications

The Instrument Control Toolbox available with Version 6 (R12) of MATLAB provides a means of communication between MATLAB and programmable test equipment. However, this version of MATLAB was unavailable during the early stages of this research, and an alternative solution

was sought. The GPIB.DLL obtained from the Math Works website provided a mechanism for communication between programmable test equipment and MATLAB Version 5 (R11). This DLL (Dynamic Link Library) is not developed or supported by Math Works, however it is available through the MATLAB Central File Exchange[6]. The GPIB.DLL contains the MATLAB 'gate way'[7] routine, which provides a path from MATLAB's workspace out to the standard Windows operating system. Once in the Windows environment, calls to existing DLLs can be made. Figure 3.4 shows the communications path out of MATLAB to the programmable test equipment, such as the HP34970a unit. All equipment configuration and data acquisition is performed from within MATLAB via the GPIB connection shown in Figure 3.4.

To simplify the GPIB calls from application control code within MATLAB, instrument driver m-files are written for each piece of test equipment. These instrument driver m-files simply combine (wrap) the many GPIB calls required to perform a simple task. A simple call such as *'hp34970a 'scan''* produces the following sequence of GPIB calls:

```
gpib('wrt', ud, 'TRIG:SOURCE BUS')
gpib('wrt', ud, 'TRIG:COUNT 1')
gpib('wrt', ud, 'format:reading:time:typeABS')
gpib( 'wrt', ud, 'format:reading:time on')
gpib( 'wrt', ud, 'INIT')
gpib( 'wrt', ud, '*TRG')
gpib( 'wrt', ud, 'fetch?')
x = str2num(gpib( 'rd', ud ));
```

3.1.2.2 Continuous Data Logging

In comparison to the software used to perform Tafel testing, the software used for transient testing is straightforward and uncomplicated. Figure 3.5 shows the general layout and simplified functionality of the software modules used for continuous data logging during transient tests. The main file 'floatlog.m' is broken into three sections. The first section is modified according to the requirements of the test to be undertaken. This includes the name of the file to which test data will be saved, a configuration file that specifies the set-up of the data acquisition unit, cell voltage and current limits, and the time interval between successive measurements. The second section of the 'floatlog.m' file initialises and configures the programmable test equipment and the timer for data logging. The italic text indicates sub-functions within the instrument driver

and timer m-files. The third section of 'floatlog.m' continuously checks the timer, measures all configured channels of the data acquisition unit when a scan is due, and suitably formats and appends the results of this to the results data file. The name of the configuration file used to set-up the HP34970a unit is appended to the end of each line of the results file in order to maintain a record of instrumentation settings (filtering, integration time, scaling, etc). This configuration file name is preceded by a % (MATLAB comment) symbol to avoid problems when loading this numeric data into MATLAB. A sample of the saved data file format is shown in Figure 3.6. The first six numbers of each line correspond to the time of the scan (year, month, day, hour, minute, second). The next three numbers indicate the ambient and cell temperatures (°C), and battery current (A). The last three numbers are the cell's voltage and the voltage of the negative and positive electrodes measured with a Hg/Hg_2SO_4 reference.

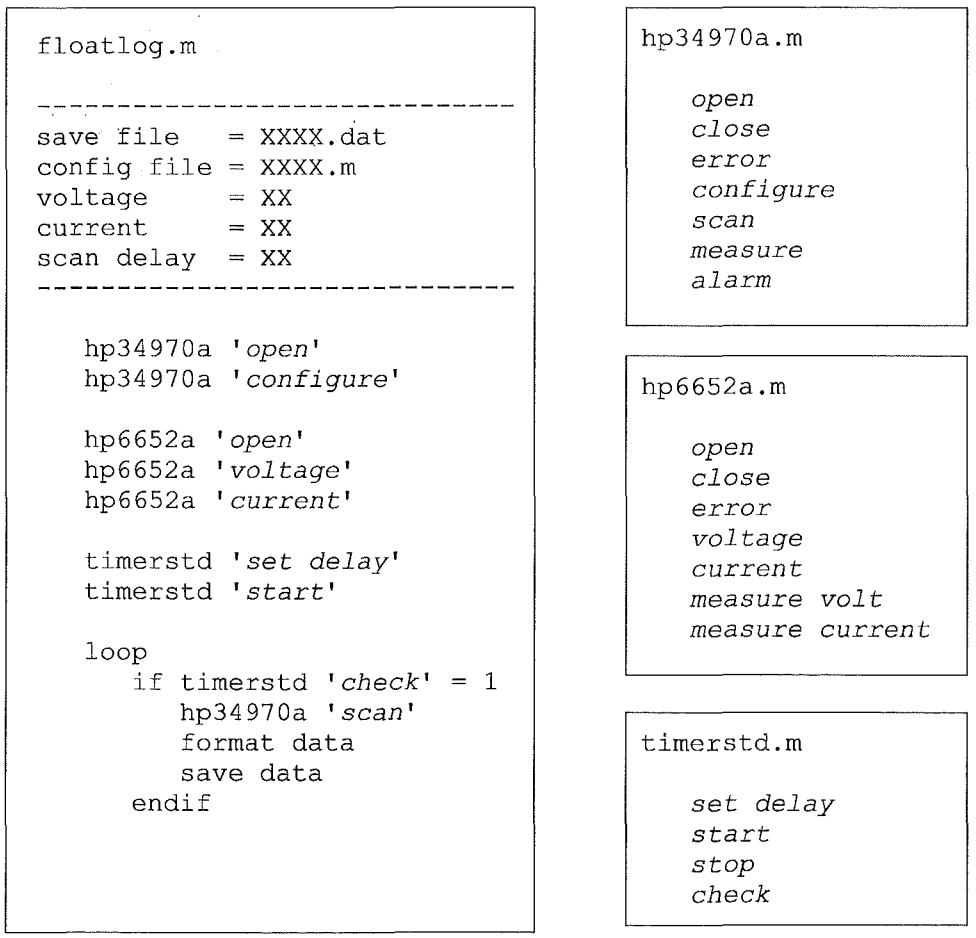

Figure 3.5 Software Modules used for Continuous Data Logging

```
2003 1 17 7 26 13.607 20.7800 25.2530 -2.5098 2.3469 1.1452 1.2017  % floatconfig2.m
2003 1 17 7 26 23.600 20.8080 25.2310 -2.4893 2.3469 1.1404 1.2065  % floatconfig2.m
2003 1 17 7 26 33.615 20.7350 25.2400 -2.4708 2.3469 1.1359 1.2110  % floatconfig2.m
2003 1 17 7 26 43.597 20.7630 25.2460 -2.4541 2.3469 1.1327 1.2142  % floatconfig2.m
2003 1 17 7 26 53.611 20.7380 25.2360 -2.4390 2.3469 1.1296 1.2173  % floatconfig2.m
2003 1 17 7 27 3.635  20.7870 25.2360 -2.4253 2.3469 1.1269 1.2200  % floatconfig2.m
2003 1 17 7 27 13.605 20.7670 25.2560 -2.4130 2.3469 1.1246 1.2223  % floatconfig2.m
2003 1 17 7 27 23.624 20.7590 25.2320 -2.4017 2.3469 1.1226 1.2243  % floatconfig2.m
2003 1 17 7 27 33.616 20.8000 25.2430 -2.3916 2.3469 1.1209 1.2260  % floatconfig2.m
```

Figure 3.6 Saved Data File Format

3.1.2.3 Tafel Testing

The Tafel testing software uses modules and data storage formats similar to those used for transient testing and shown in Figure 3.5 and Figure 3.6. However, as the measurements must be analysed for stability before the test stage can be incremented, the main control file is considerably more complicated. Figure 3.7 shows a simplified flow diagram of the procedure used to perform Tafel testing. This testing is performed by maintaining a constant float voltage, and waiting for the current and both the positive and negative electrode's voltages to stabilise before the float voltage is incremented and the procedure repeated.

The mechanical relays used in the HP34970a unit have a finite life, and rapid measurements of multiple channels will prematurely age the switching matrix card. To prevent this, after the cell test voltage has been set only the current channel is monitored until the current is seen to be stable. Whilst only a single channel is monitored, no switching is necessary and excessive ageing is avoided. To reduce measurement error, current stability is determined by performing linear least squares regression of data sampled every 2 seconds over a 5 minute period. Current stability is assumed when the slope of the regression line indicating current change is less than 10 μA over a 1 hour period. After the current has been determined to be stable, the meter is reconfigured for voltage and current measurements. These are logged at 1 minute intervals, and linear least squares regression is performed over a 1 hour period to ensure stability. The absolute slope of the voltage regression line is used to determine stability, with less than 50 μV change in a 1 hour period indicating steady state. When steady state is determined, the Tafel points (cell and electrode voltages, float current, and temperature) are recorded before the float voltage is

incremented and the process is repeated. To maintain a log of the cell's transient behaviour throughout Tafel testing, the meter is configured for both voltage and current measurements and the state of the battery recorded every 10 minutes. Figure 3.8 plots the transient response of the cell during Tafel testing, and relates to the 25 °C Tafel plot shown in Figure 4.25.

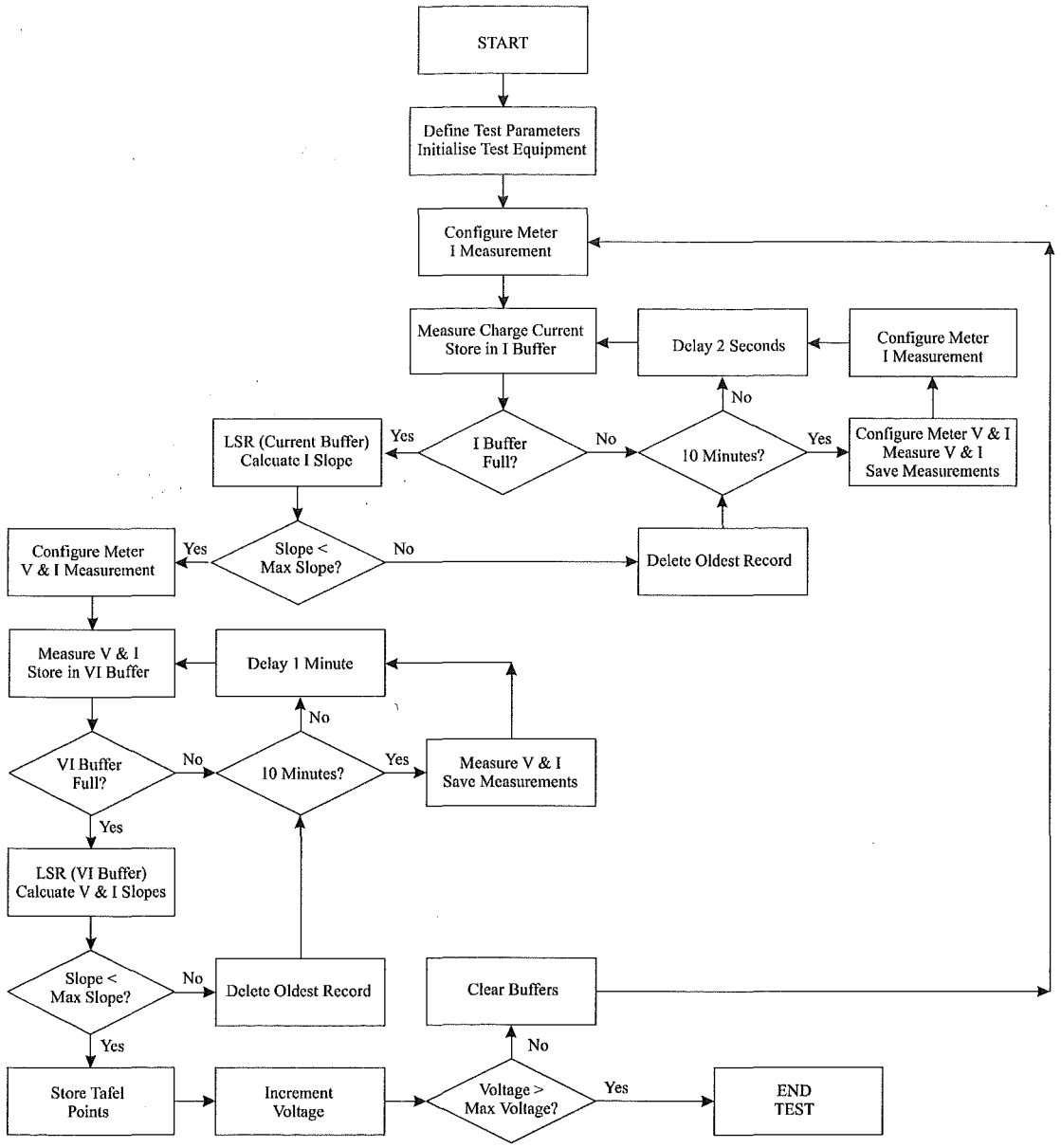

Figure 3.7 Flow Diagram of Tafel Testing Software

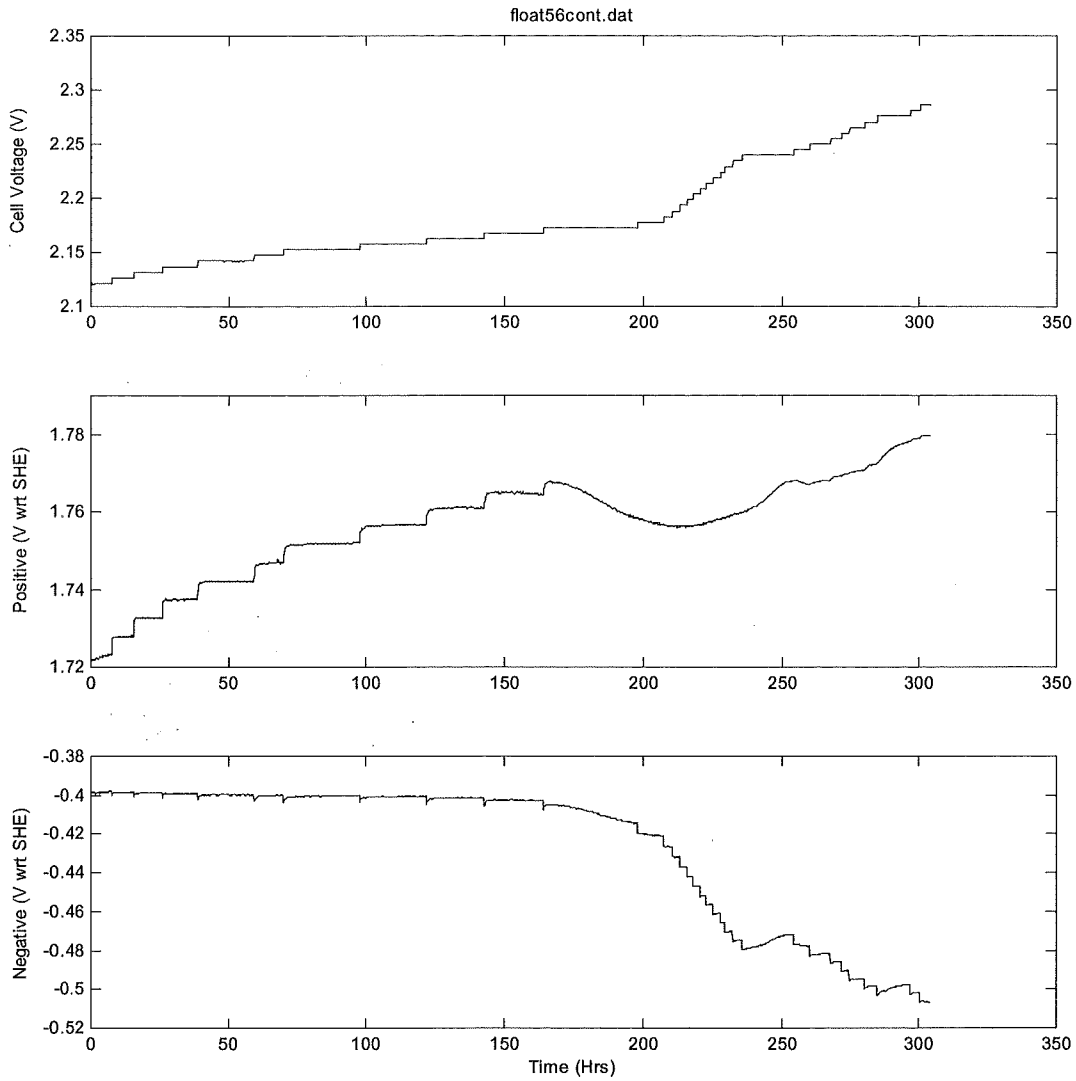

Figure 3.8 Transient Profile during Tafel Testing

The basis of Tafel analysis is to maintain a constant voltage (or current) on the cell under test, and wait until the current (or voltage) has stabilised to a steady state value. These values are recorded, the supply is set to a new value, and the process is repeated. While the concept of detecting steady state (no change in the measured current or voltage) is simple, mathematically this is not practical and finite minimum slopes must be detected. Linear least squares regression of the sampled data points over a specified time period provides noise rejection and a simple method of determining the rate of change (slope) of the data. The regression period was chosen as a trade off between noise reduction and test duration.

Few guidelines on Tafel testing have been found in the literature. The Tafel testing procedure described in this Chapter is the end result of continuous refinement and improvement over many tests. A Tafel test method described by Misra et al[8] uses constant current steps while waiting for the cell and plate voltages to stabilise before data is recorded. Data gathering from high to low currents is their preferred mode, however at very low currents, the opposite steps were used in order to gain stability in that region. It is also stated that it may take weeks for a particular current value to stabilise.. Other work suggests that Tafel points should be approached from both directions and averaged, or that the extrapolations should be averaged[9], although no reasoning is given for this practice. Unless there is hysteresis in lead acid cells, the approach path taken to the steady state Tafel point should not affect the steady state value. Approaching each Tafel point from both directions may provide a reduction in test duration as a true steady state condition may not required, although this technique will significantly complicate the test procedure. Stepped voltage Tafel testing is predominantly used during this research, as it provides greater resolution than stepped current.

3.2 Custom Hardware Designed

During the course of this research the design and construction of several electronic circuits was found to be necessary in order for the project to proceed. In this Section, a description of these circuits is given. Appendix D contains the circuit schematics, and Printed Circuit Board (PCB) layouts (top and bottom copper layers, and the component overlays). While these circuits were considered necessary for continued progress, the design is not critical to the outcomes of this research. For this reason only a brief description and key features of these circuits are given.

3.2.1 Isolated Impedance Measurement

The isolated impedance acquisition circuit combines the signals received from the HP33120a signal generator and the analogue output of the HP34970a unit into one signal. This is then optocoupled to a high power buffer, which injects the signal into the cell under test. The 4-wire connection to the cell under test utilises separate voltage sense and signal (current) injection connections for each terminal of the cell. The selection of either voltage or current feedback allows the demand signal to be interpreted or realised as battery current or terminal voltage.

Both the cell's terminal voltage and supplied charge current are optocoupled back to a ground referenced oscilloscope for subsequent analysis. A third reference electrode signal may also be optocoupled from the cell under test to the ground referenced test equipment. Because small forced changes in the cell's terminal voltage can require large signal currents, several options for assessing the cell's voltage are provided. These options include a direct 1:1 DC voltage output, the ability to subtract either the supplied DC bias or an arbitrary DC voltage before amplifying the remaining AC signal by ten. This allows the relatively small AC component of the signal to be assessed independently of the DC operating point. All signals are DC coupled and have no theoretical minimum frequency limit.

A single floating DC supply (5 V 3 A) is used to power this impedance circuit. This supply provides battery charge current (when necessary), and also powers electronics for signal transfer between the ground referenced test equipment and the potential at which the battery is situated. Two matched ± 5V isolated supplies are derived from the single floating DC supply through a basic push-pull switch mode DC/DC converter. The electrically isolated signal transfer is achieved using HNCR200 analogue optocouplers. These devices contain one Light Emitting Diode (LED) source, and two closely matched photodiodes. One of these photodiodes is used to monitor and stabilise the output of the LED at the transmitting end. At the receiving end, the second photodiode responds to the stabilised LED output to reproduce the signal. The use of this feedback technique virtually eliminates the non-linearity and drift normally associated with analogue operation of optocouplers.

Only one prototype of this impedance acquisition system has been constructed and debugged (as far as the PCB layout would allow). While several minor problems exist with the circuit design and layout, this prototype worked sufficiently well to perform an initial investigation of impedance analysis. This initial investigation identified the large signal characteristic as being significant to float charge and polarisation detection. As large signal assessment can also be performed using simple transient testing, further development and refinement of the impedance acquisition circuit was not undertaken.

High frequency noise originating from the switch-mode supply is the most significant problem in the impedance circuit, and is always present in the battery measurement signals. Small amounts of averaging applied to the signals viewed on the oscilloscope removes much of this noise, however it would be preferable to eliminate the source of the noise. Noise reductions may be

achieved by increasing the gap between the switching supply and the analogue signal paths, and shielding the signal circuitry and/or power supply. Noise conducted through the power supply rails may be reduced by adding shields between transformer windings, or by increasing the filtering of unregulated DC output.

Precise matching of the ± 5V isolated supplies is required for the signal optocouplers to function correctly. Although a degree of adjustment and calibration is provided, the low cost regulators drift with time. Similarly, difficulties are encountered with offset and gain calibration of the many optocouplers. This is believed to be due to resistor tolerances, as precision operational amplifiers with favourable specifications (10 μV typical offset voltage, 40 pA bias and offset current, and extremely low thermal drift) are used. Single 0 V reference points and discrete (star) returns for each signal channel are implemented where possible to avoid cross-talk between measurement signals. Further improvements may be realised if this star technique is applied to the 5 V rails used in the optocouple circuits.

While the minor problems associated with this prototype circuit make the use of the impedance measurement system more difficult than necessary, overall the system functions as expected and produces adequate results.

3.2.2 Precision Current Shunt Amplifier

The magnitude of float current is extremely small when compared to discharge and recharge currents. Because of this, measurement of float current is not normally possible using the standard current shunts that measure discharge and recharge currents. Section 2.4.1.6 details how monitoring of float current may provide additional information regarding a battery string's SOC or SOH. A shunt typically used to monitor current in a telecommunication battery string will produce a 55 mV signal when a current of 500 A is passed through it. When combined with a suitable calibration resistance network, such a shunt produces 10 mV per 100 A. Manganin current shunts are commonly used for thermal resistance stability. To monitor the float current (typically hundreds of milli-Amps) passing through a conventional low resistance current shunt, a high gain amplifier is required to measure the voltage produced across the shunt. When a manganin shunt is connected to copper PCB track, two thermocouple junctions exist in the voltage measurement circuit. If the temperature of these junctions is identical, the thermal

voltages developed will cancel. In typical installations however, one end of the shunt is connected to a bus-bar carrying the load current, and the other end is connected to cables leading to the battery. With differing terminations, significant temperature differences between the ends of the shunt can be experienced. The manganin/copper thermal voltage is approximately 1.5 μV/°C, which is similar to the voltage developed by the shunt at the current resolutions typically required for telecommunication battery float charge.

To allow a microprocessor based VRLA Battery Intelligent Node[10] to accurately assess the float current passing through a typical telecommunication battery shunt, a precision high gain amplifier was developed. A temperature measurement of both copper/manganin junctions allows the temperature difference to be calculated. Using this information, the measured shunt voltage can be appropriately compensated. Figure 3.9 shows a diagram of the current shunt/PCB thermocouple junctions, the high gain amplifier, and analogue to digital input of the microprocessor. Temperature measurement of the thermocouple junctions is achieved using temperature dependant resistors and additional analogue to digital inputs of the microprocessor.

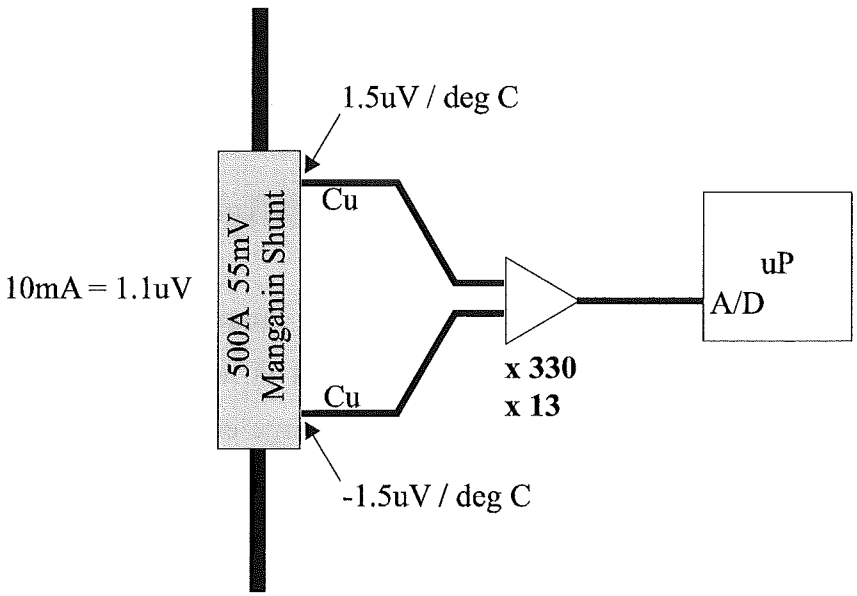

Figure 3.9 Current Shunt Amplifier Thermocouple Junctions

The microprocessor used for the intelligent node is a Texas Instrument MSP430F149. This contains a 12-bit analogue to digital converter, with a selectable 1.5 or 2.5 V input range. The circuit diagram, PCB component layout, and top and bottom copper layers of the developed amplifier are shown in Appendix D. To cover the wide range of current encountered during

normal battery operation, two amplifiers are used. An amplifier with a gain of 13 covers the entire ±500 A range of the shunt, at a resolution of approximately 250 mA. A second amplifier with a gain of 330, and a range of ±20 A with a resolution of approximately 10 mA is used for float current measurements. Chopper stabilised operational amplifiers are used to minimise input offset errors and drift, and precision (0.1 %) resistors are used in signal paths.

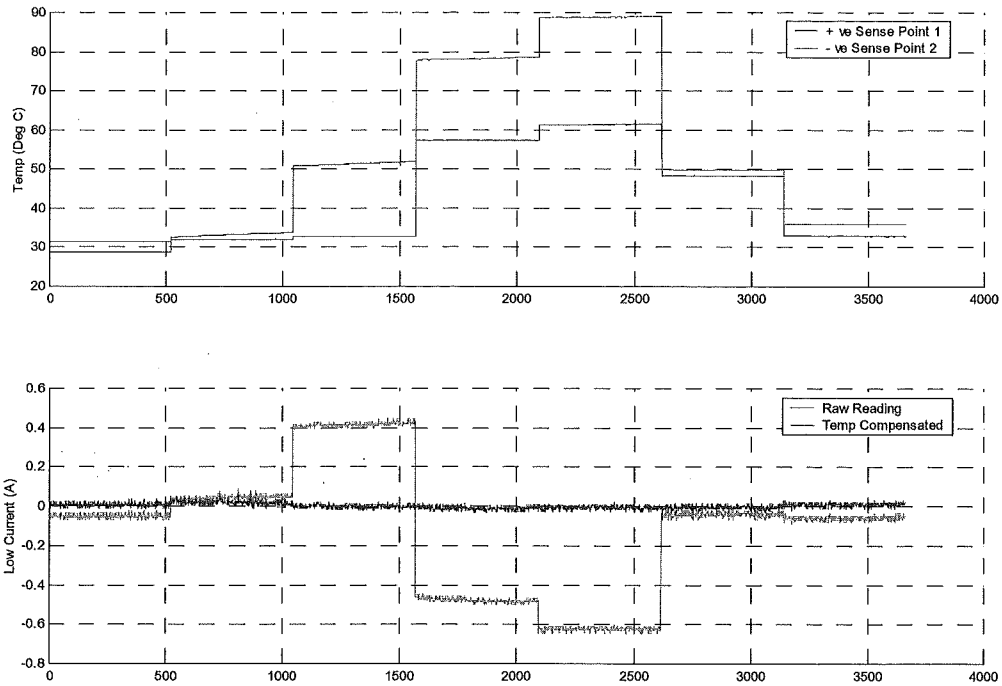

Figure 3.10 Temperature Compensated Shunt Performance at Zero Current

The developed circuit board also contains an isolated switch mode supply, allowing the monitored battery to power the shunt and intelligent node circuitry. No problems were experienced with the analogue amplifier circuitry, however a second prototype of the switch mode supply has been prototyped to improve the surface mount chip transformer's (Philips IIC10) inter-winding coupling, and to reduce its leakage inductance. While significant improvements have been made to this supply circuit, the core appears to run relatively hot considering the minimal power requirements of the transformer. Noise from the switch mode supply does not have a large impact on the signal measurements. The temperature measurements contain only 1 bit of noise, while the signal out of the high gain amplifier typically contains 3 – 4 bits of noise. This noise may easily be filtered by software within the microprocessor. Figure 3.10 shows microprocessor measurements from the shunt with no float current. The temperature

at either end of the shunt has been artificially raised in order to show the effects of temperature imbalances on float current measurement. Measurement of and compensation for the temperature difference produces the expected zero current reading.

3.2.3 Temperature Controller

As the procedure for performing Tafel tests was refined and improved, the influence of ambient temperature became more notable. The majority of early testing was undertaken in an air-conditioned room, where a cyclic fluctuation of the ambient temperature was noted (approximately 2 °C over a 20-30 minute period). This was considered too rapid to affect the cell temperature. During the course of this research several physical relocations of the test system were imposed. The final relocation was to a room that was air-conditioned, although this was automatically switched off at night and during weekends. The resulting variation in the uncontrolled ambient temperature during these times was noted to have an effect on measurement results. A temperature controlled water bath was developed to maintain a consistent battery temperature, regardless of the room temperature. An insulated picnic hamper was used as the basis for the bath, and contained the water. The sides of the hamper were extended (above the water line) with polystyrene, allowing the lid to be fitted above the cell under test when a reference electrode was inserted. A 34 V 600 W water-cooled element was used to provide the necessary heating. Water in the bath was circulated with a submersible 4.5 W garden pond pump.

A simple temperature sensing and control circuit was developed to regulate water temperature. LM335 temperature sensing integrated circuits were sealed with pre-glued heat-shrink tubing, and submersed in the circulated water. The temperature dependent voltage produced by the LM335 is compared to a set reference point, and the result of this comparison is used to activate the heating element as required. Due to the volume of water in the bath and the effective insulation, it was found that 12 V applied to the heating element provided a suitably slow water temperature increase to allow the circulated water to be maintained at a uniform temperature. A minimum amount of hysteresis was applied to the comparator circuit, ensuring that the element is either switched hard on or off, thus avoiding excessive heat dissipation in the MOSFET switch. The developed temperature controller regulated the cell temperature to within 0.2 °C. An LM10 (operational amplifier with a built in reference) was used to produce the set reference

point, and thermally induced drift of this reference again resulted in a very slight dependence on the ambient temperature. This variance was typically less than 0.3 °C, and does not significantly influence test results. For safety, an additional over-temperature cut-out circuit is also included. This operates in a similar manner to the main temperature control, but the reference point is set approximately 10 °C higher than the desired controlled temperature. If a fault in the main control system causes the second higher temperature to be exceeded, or the safety temperature sensor becomes disconnected, power to the entire temperature control system will be cut. Power can only be reapplied manually. A schematic diagram of the temperature controller and associated PCB has been included in Appendix D.

3.2.4 Constant Current Load

The available HCL-2501 constant current load was designed for discharge rates up to 500 A. Because of this, resolution and noise problems are experienced when discharging at rates below 1 A. To overcome these problems, a low rate constant current load was developed. The circuit diagram and PCB for the designed load have been included in Appendix D. This relatively simple circuit compares voltage developed across a current sensing resistor in the discharge path to a pre-set reference value. The result of this comparison is used to control the on state of a transistor, in order to ensure that voltage across the sense resistor matches the desired current (reference voltage). As the transistor is essentially used as a variable resistor to ensure that the desired current is drawn from the battery, suitable heat sinking is required. The circuit is designed to be powered from the cell under test, thus avoiding the need for any additional power supplies. This constant current load is also designed to terminate the discharge should an adjustable end voltage be reached. This feature allows the load to be used for unsupervised capacity testing of small batteries. To measure the duration of a discharge to the defined end voltage, a connection that supplies power to a small analogue travel clock (replacing its battery) is used. When the end voltage of the battery under test is reached, the load is disconnected along with the supply to the travel clock. The discharge duration can be determined from the elapsed time on the clock. An adjustable voltage divider ladder is also provided to allow testing of batteries with differing numbers of cells. A minimum voltage of approximately 1.6 V is required to produce the reference voltage, and therefore the constant current discharge unit requires at least two 1.5 V (Nickel/Cadmium or Nickel/Metal Hydride) cells, or a single 2 V lead acid cell for operation. Either of two current ranges may be selected by shorting a jumper that alters the

current sense resistor. The low current range allows discharge currents between 0 – 1.5 A, while the high range allows discharge currents up to approximately 15 A.

3.3 References

[1] H. A. Vanasse, D. Jones, *Catalyst 101: The Basics of Using Catalysts in VRLA Cells,* Proceeding of Battcon, 2002, p15-4.

[2] D. Berndt, *Maintenance Free Batteries, Lead-Acid, Nickel/Cadmium, Nickel/Metal Hydride, A Handbook of Battery Technology,* Second Edition, Research Studies Press, 1997, p 18.

[3] Radiometer Analytical, *Guide to Reliable pH, Ion and Conductivity Measurements,* Product Brochure, p 9.

[4] F. Vaccaro, J. Rhoades, B. Le, J. Timmons, *A Catalyst in a VRLA Cell: The Affect on Cell Life and Tafel Character,* Proceedings of INTELEC, 2001, p 7.

[5] P. M. Hunter, *Advanced Battery Management and Control* Masters of Engineering Thesis, University of Canterbury, 1999, s 6.1.1.

[6] http://www.mathworks.com/matlabcentral/fileexchange/loadFile.do?objectId=216

[7] The Math Works Inc, *MATLAB Application Programming interface Guide,* 1998, Version 5, *s* 3.

[8] S. S. Misra, A. J. Williamson, *On Temperature Compensation for Lead Acid Batteries in Float Service: Its Impact on Performance and Life,* Proceedings of INTELEC, 1996, 2-1, p 27.

[9] Bellcore, *Generic Requirements for Accelerated Life Testing of Valve regulated Lead Acid Batteries at High Temperature,* Technical Reference TR-NWT-001200, January 1992, Issue 1, pp 2-7.

[10] A. H. Anbuky, P. Hunter, T. Johnson, D. Lim, *VRLA Battery Intelligent Node,* Proceedings of INTELEC, 2002, 11-1.

4 Float Charge Model

It is commonly accepted that there is little correlation between the exact float voltage and SOC, similarly the precise float current is not a true indication of SOC. However it is generally accepted that at the end of a recharge, when the change in charge current is less than 10% over a three-hour period, the battery is considered fully charged[1]. While this is commonly accepted, it has been shown in Chapter 2 that although the battery may appear to be on a float charge, a cells design and construction materials may actually result in one of the electrodes within the cell being gradually discharged.

While excessive deviation between cell voltages may indicate a possible problem, it is commonly expected that there will be a distribution in the steady state float voltages of individual cells that are charged in a series-connected string from a common supply. Detailed trend analysis of discharge performance and float voltage variations over the life of the battery may reveal some information on the status of individual cells within the battery. Spot measurements of variance between cells are unlikely to uncover subtle problems.

Challenged with determining optimal float charge control, the following goals have been identified:

1. Each cell is maintained in a fully charged state indefinitely.
   >> Both electrodes within each cell must be polarised above their open circuit potential.
2. Maximise cell life.
   >> Positive Plate Polarisation maintained at specified value (minimum corrosion rate).
   >> Gassing must be maintained within acceptable levels.

With steady state voltages and currents not providing a definitive indicator of the actual charge status of VRLA cells in continuous float service, some form of active test procedure may be required. A test such as impedance or response to voltage and current perturbations may reveal more information about the actual charge status of the cell or its internal operation.

Ideally, a practical indicator is required to provide a spot assessment of the charge status of individual cells. A measure of the polarisation of each electrode within a cell will provide

sufficient information to allow both float charge goals to be achieved. Ensuring both electrodes are polarised will satisfy the first goal, while ensuring the polarisation of the positive electrode is maintained near an optimal value will satisfy the second.

Over recent years there has been increasing support for the use of impedance based techniques to assess the condition of VRLA batteries (Section 2.4.3.2). However the majority of these appear to deal with assessing remaining capacity during discharge, SOH, or life predictions rather than charge status and charge control optimisation. While a timely indication of battery or cell failure is essential to guarantee continuous power supply, impedance based methods may not identify charge control problems until damage has been done and the life of a cell has been reduced.

4.1 Preliminary Float Behavioural Testing

With steady state float voltage and current showing little correlation to actual charge status, it was necessary to find an indicator that would provide sufficient information to diagnose float charge problems or allow float charge optimisation. There have been several suggestions (see Section 2.4.3) that the frequency response of the positive and negative electrodes differ significantly. This suggests that impedance or perturbation testing may reveal the necessary information on the inner workings of a cell. An investigation was undertaken in an attempt to identify a characteristic that would allow the charge status of each electrode within a cell to be determined using only the two terminals of the cell. This investigation was broken into several key phases.

The first phase was familiarisation with reference electrodes and their use in Tafel plots. Battery designers and chemists rely on Tafel plots to analyse float charge behaviour and determine appropriate float voltages. It was essential to become familiar with Tafel analysis, as the envisaged outcome of this research was a simplified, field-useable alternative to Tafel analysis. Results of this research will ultimately be compared to or judged against conventional Tafel plots and analysis. Once familiar with reference electrodes, the second phase of testing involved assessing the possibilities of using impedance to reveal 'hidden' information on the inner operation of a cell. Results of this lead to an analysis of the cell's transient voltage profile in the third phase, from which a suitable means of identifying covert polarisation information was found. An in-depth exploration of the phenomenon was then undertaken. This involved a test

plan to cover common operational variables and allow the phenomenon to be appropriately modelled.

4.1.1 Tafel Plots

Tafel testing and Tafel plots form the basis of float operation analysis for many types of batteries. These are extensively used to analyse the float charge characteristics of lead-acid and sealed-lead-acid batteries. Typically, when the steady state values of voltage and current are plotted on a linear/log graph, a Tafel plot produces a series of straight lines. The technique was named after its discoverer, J. Tafel, who in 1905 was the first to describe the over-voltage/current relationship[2]. Tafel analysis is based around steady state measurements and requires well-controlled conditions. It is therefore normally confined to laboratory testing only, as the technique and required equipment do not lend themselves to automated field use. The ultimate aim of this research was to identify a practical field useable alternative to Tafel testing. For the outcomes of the research to be valid, familiarity with these testing techniques was essential, as Tafel testing is the benchmark by which any alternative technique will be judged.

Although the concept behind Tafel testing is relatively simple, there appears to be little information recently published on modern standards, methods, and practices. There are numerous publications on early test and measurement systems involving equipment such as balance bridges and chart recorders, however with the advances in modern automated digital test and measurement systems, there appear to be few guidelines detailing modern test practices. This may be because test practices are common knowledge to those in the industry, or it may be that the details have become unimportant now that specifically designed testing units may be purchased[3], where all the operator is required to do is connect the battery and reference electrode.

The primary reasons for the first series of tests were to become familiar with reference electrode testing, and to refine the test system and automation software. The aim of these tests was to reproduce the Tafel plots commonly seen in the literature for float charge analysis. This first series of tests should answer questions including: should the test be voltage or current controlled? and, should this be increasing or decreasing? Also of interest is the effect puncturing the cell's case to add a reference electrode has on cell characteristics.

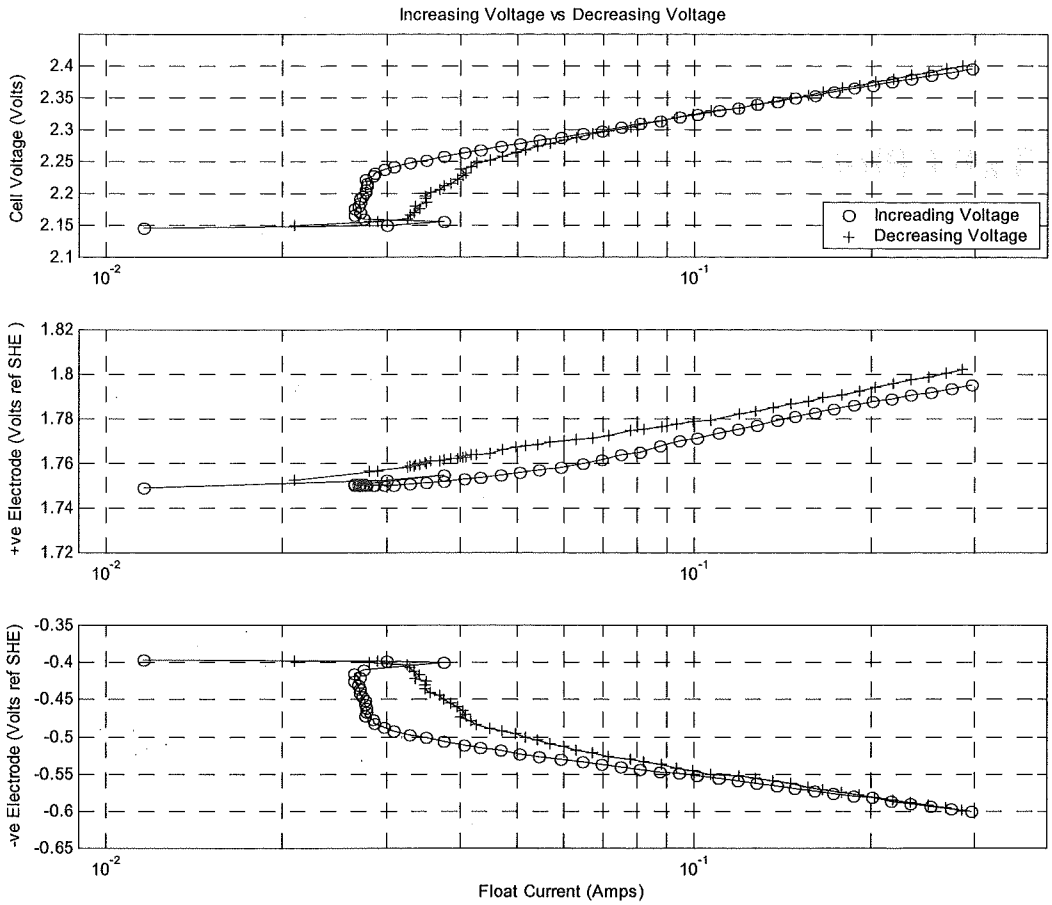

Figure 4.1 Voltage Control Increasing vs Decreasing

Figure 4.1 shows Tafel plots generated by setting the voltage and allowing the current to stabilise before measurements are taken and a new voltage is set. As the measurements are steady state, it is thought that the approach path should not be important unless there is some form of hysteresis. Figure 4.1 shows the differences between increasing or decreasing the voltage after each steady state point. This is not believed to be related to premature steady-state-detection, as at a given voltage the current of the increasing plot is lower than that of the decreasing plot. A voltage increase would produce a current spike that decays down to the steady state value, while decreasing voltage would initially draw little current and gradually rise to the steady state value. This may suggest that there is some form of hysteresis present that warrants further investigation. If hysteresis is found, and is seen to be repetitive and predictable, it may be taken advantage of in order to optimise float charge and control.

While few guidelines on Tafel testing have been found, there are suggestions that Tafel points should be approached from both directions and averaged, or that the extrapolations should be averaged[4], although no reasoning is given for this practice. A description of Tafel test methods used by Misra et al[5] describes using constant current steps and waiting for the cell and plate voltages to stabilise before data is recorded. Data gathering from high to low currents is their preferred mode, however at very low currents the opposite steps were used in order to get better stable values in that region. It is also stated that it may take weeks for a particular current value to stabilise. While apparent approach related differences have been noted, the size of these is relatively small (10-15 mA current difference at low float voltages, producing a 10-20 mV shift in plate polarisations – for a given float voltage). The reason for the difference is unknown, and further detailed investigation is necessary. Possible causes may include test history, a shift in battery characteristics due to testing, experimental variance, or possible hysteresis. While an understanding of the cause of the variance is desirable, the variance is not large enough to hinder further work.

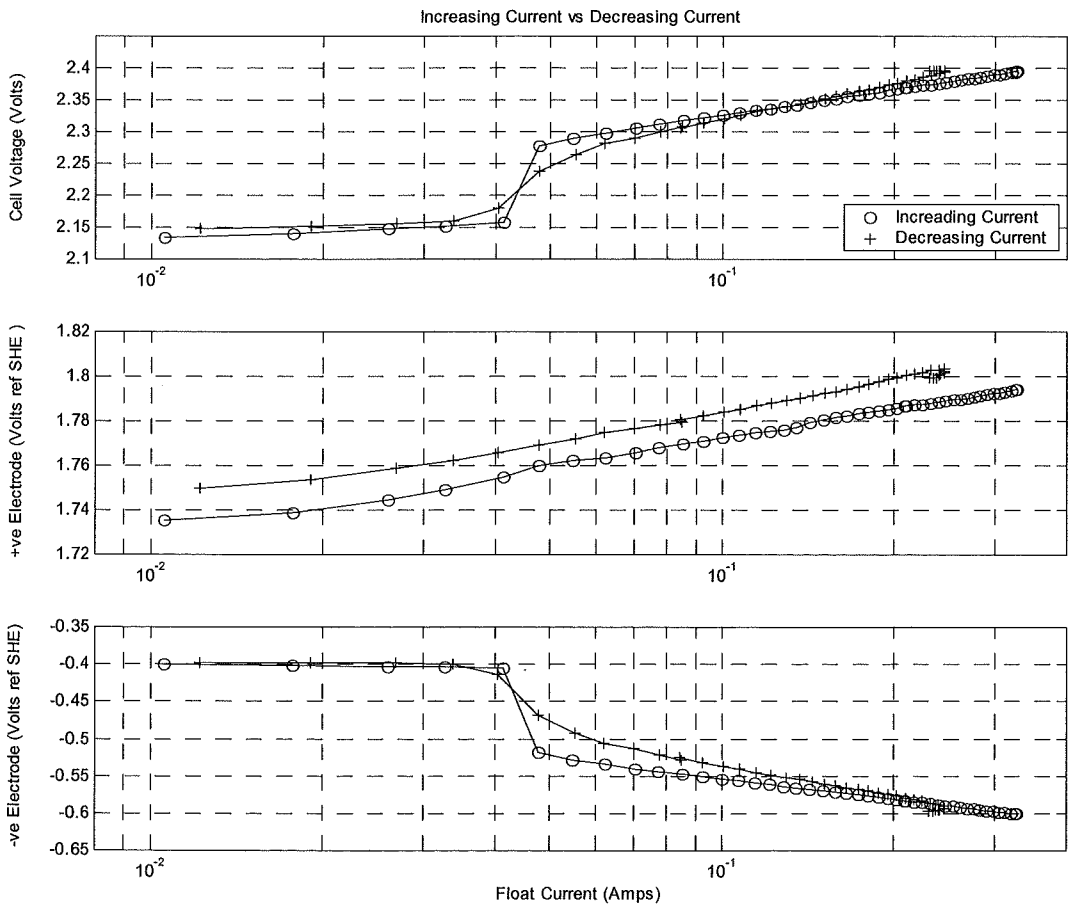

Figure 4.2 Current Control Increasing vs Decreasing

Figure 4.2 shows a similar plot to Figure 4.1, however the plots have been generated by fixing the current, and allowing the cell voltage to stabilise before measurements are taken and a new current is set. The decreasing current-plot has an upper voltage limit of 2.4 V, causing the cluster of results around this point. Again it can be seen that there is an offset in the polarisation of the positive electrode from the increasing plot to the decreasing plot. It is also noted that there is a small variance in the Tafel slope of the negative electrode. This may be due to gassing or dryout caused by the amount of time spent at the higher voltage during the initial part of the test, or experimental variation.

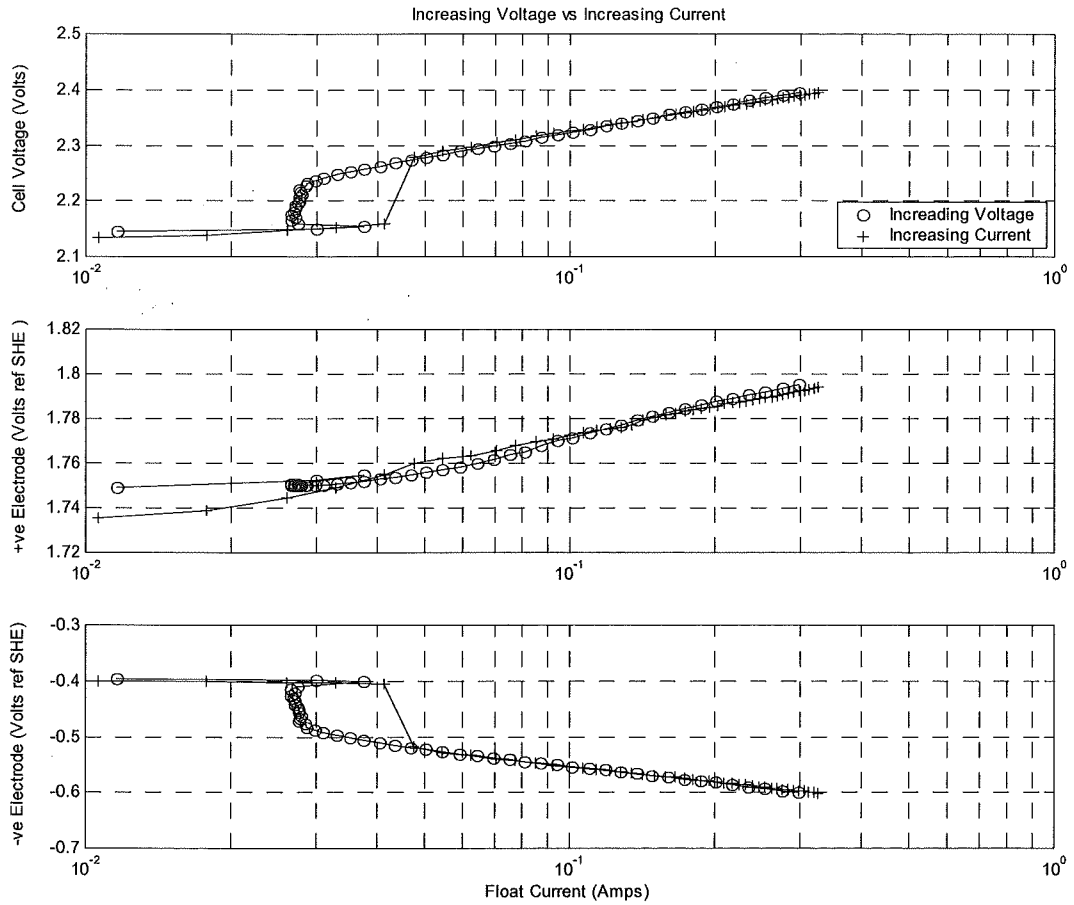

Figure 4.3 Voltage Increments vs Current Increments

Figure 4.3 compares the difference between current and voltage controlled testing. Very similar plots are produced with no polarisations, and high polarisations, however significant information is 'missed' with current controlled testing due to the drop in current as the negative electrode

begins to polarise. Current is a function of voltage, but voltage is not a function of current. For this reason, it was decided that future testing would be voltage controlled.

To perform reference electrode testing on a VRLA cell, a hole must be drilled in the case of the cell to allow insertion of the reference electrode. The greatest problem associated with the addition of the reference electrode the inability to sufficiently seal the insertion point and avoid the formation of gas leaks. It is well documented that oxygen entering the cell through case leaks may have a depolarising effect on the negative electrode. The above test plots show that the current at which the negative electrode begins to polarise is similar to that at which the positive begins to polarise. This suggests that the cell is functioning as intended, although at the manufacturer's recommended float voltage of 2.27 V, about 20 – 30 mV of positive electrode polarisation is evident. Ideally, this should be between 40 - 80 mV. With low positive polarisation, excess polarisation exists on the negative electrode, however this suggests that the reference electrode insertion point is appropriately sealed, and that no leaks are present.

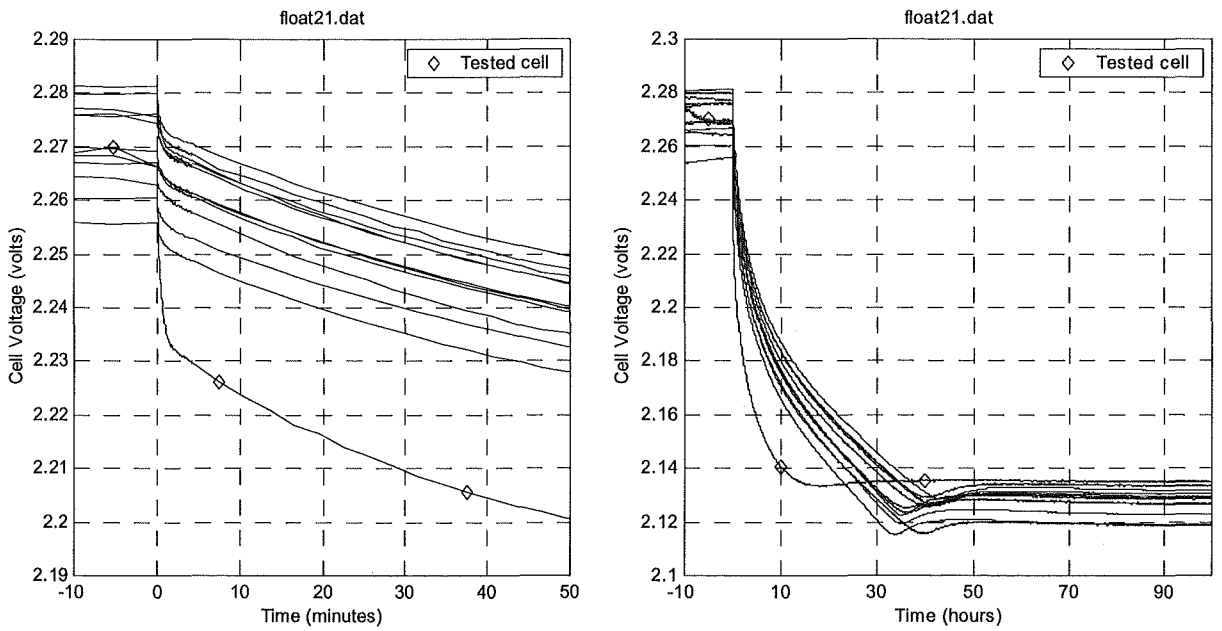

a) b)

Figure 4.4 Open Circuit Characteristics of Tested and Untested Cells.

After the testing was completed, the reference electrode insertion-hole in the tested cell was plugged. The cell was then returned to its original string, where it was placed on float charge for 24 hours. The charger was then removed and the string left to decay to its open circuit state.

Figure 4.4 compares the untested cells with the tested cell. It is clear that the tested cell has a larger initial drop and faster decay to open circuit, however the open circuit voltage is similar to that of the untested cells. The reason for this difference is unknown, however it is suspected that it may be related to the temporary addition of the reference electrode, or due to the differences in recent charge and discharge history of the tested and untested cells.

4.1.2 Impedance

With VRLA batteries, physical measurement parameters are limited to voltage, current, and temperature. Resolution in temperature sensing is relatively inexpensive, however the high cost required to accurately measure individual cell temperatures (sensor accuracy and physical connection) so that comparisons can be made between cells is unjustified. The only practical measurements available for analysis are cell voltage and string current. It is commonly accepted that minor differences in float-voltage between cells, and the exact value of float current for a string are not definitive indicators of cell health or SOC, however excessive differences may indicate potential problems. The limited measurement possibilities of a VRLA battery combined with a poor or non-existent correlation with desirable identifiers, such as SOC or SOH, has forced alternative measurement techniques such as impedance to be investigated.

There are a number of commercial units in the marketplace that use measurements of conductance, impedance, resistance, or dynamic response of a pulsed voltage/current to analyse the state of VRLA batteries. Generally, these instruments inject a voltage or current signal and measure the responding current or voltage waveform. The amplitude and phase shift of the response are typically used to calculate the impedance at the test frequency. Many commercial test instruments attempt to correlate measured or derived parameters at specific frequencies with physical parameters such as grid or electrolyte resistance. This information, or more importantly, any differences in measurements between similar cells or changes in a single cell when tracked over time, highlights potential problems. While there are many claims of analysis advantages with the use of impedance testing, generally all solutions rely on some form of ohmic-based measurement comparison, as little is gained from a single measurement unless the cell under test is severely degraded.

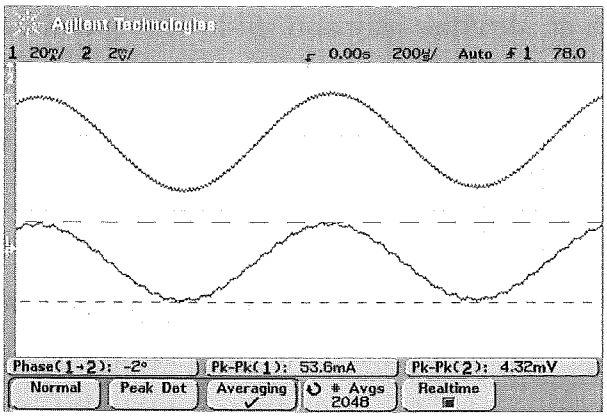

a) 1000 Hz

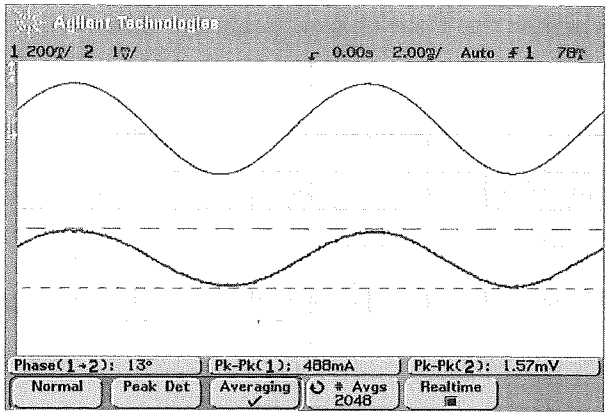

b) 100 Hz

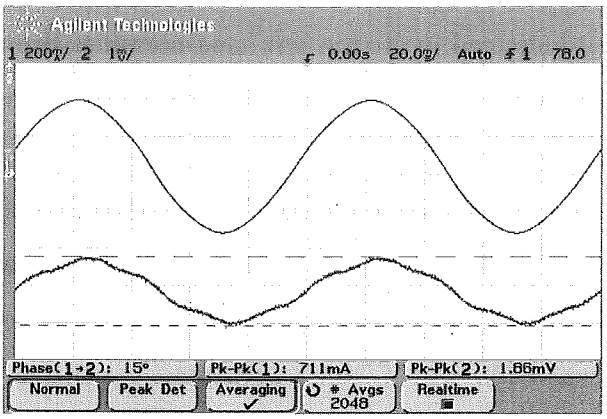

c) 10 Hz

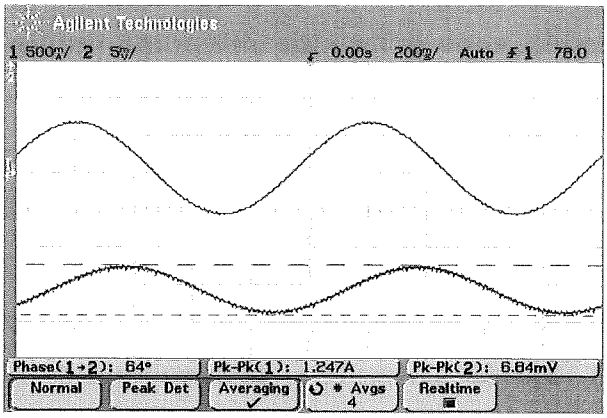

d) 1 Hz

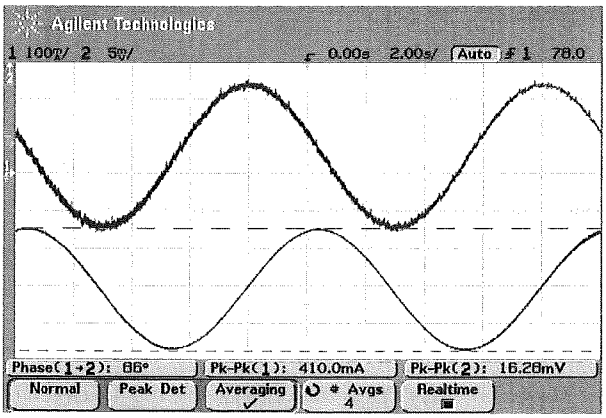

e) 0.1 Hz

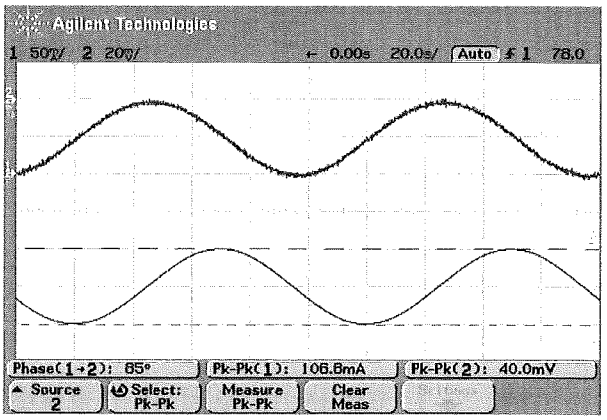

f) 0.01 Hz

Figure 4.5 Applied Voltage and Current at Various Frequencies

Using the impedance acquisition hardware described in Chapter 3.2.1, initial testing was undertaken to assess the potential use of impedance based measurements for charge analysis and control. With suggestions in literature that the frequency responses of the positive and negative electrodes within a cell are different, impedance appeared a logical technique to investigate. It was envisaged that an impedance signature or identifier might be found that would indicate

whether the float charge goals are achieved. Such an identifier may also aid in setting a more appropriate float voltage. If impedance or differences in impedance could be used to separate the response from each electrode within a cell, it may be possible to detect conditions such as a fully charged state, or negative plate discharge.

Figure 4.5 shows the current required to maintain a sine-wave voltage (centred about 2.27 V) on the terminals of a 275 Ah VRLA cell on float charge. The plots show the terminal voltage of the cell and the applied current waveforms at frequencies ranging from 0.01 Hz to 1 kHz. Due to offsets introduced through level shifting, the DC level (referenced to the indicated ground) is not correct, however the scale (mV or mA per division) indicated in the top left hand corner of each plot is true. In all plots, the top trace is the applied current and the bottom trace is the signal voltage on the cell's terminals. Using the peak to peak voltage and current, and the phase difference from the plots, the resistance, reactance, and equivalent capacitance at each test frequency have been calculated and shown in Table 4.1. It can be seen in Table 4.1 that as the test frequency increases the apparent capacitance decreases, and even becomes slightly inductive at 1000 Hz. Compared to the large variance in reactance (X_C and X_L) with frequency, the change in resistance is relatively small. It is expected that unless there is a change in the electrolyte concentration, there should not be any significant change in cell resistance over a short period of time.

Frequency	**Voltage (VPP)**	**Current (IPP)**	**|Z| (Ω)**	**Phase (degrees)**	**R (Ω)**	**X_c X_L (Ω)**	**C (Farads) *L (Henries)***
1000	0.0043	0.0536	0.0806	-2	0.0805	*0.0028*	*445.6E-9*
100	0.0016	0.4880	0.0032	13	0.0031	0.0007	2.199
10	0.0019	0.7110	0.0026	15	0.0025	0.0007	23.506
1	0.0068	1.2470	0.0055	64	0.0024	0.0049	32.283
0.1	0.0163	0.4100	0.0397	86	0.0028	0.0396	40.180
0.01	0.0400	0.1068	0.3745	85	0.0326	0.3731	42.657

Table 4.1 Impedance Test Results on Float (2.27 V)

The test plots in Figure 4.5 and the analysis in Table 4.1 are all undertaken at discrete frequencies about a given float voltage. Ideally, these measurements should be repeated for other float voltages and compared with data obtained with a reference electrode. Due to

difficulties in selecting a test signal amplitude sufficiently large to minimise the influence of noise, while still ensuring that the test voltage and current remained sinusoidal, the measuring process could not be easily automated, and therefore only limited testing was undertaken. Compounding the impedance measurement problems are the time base and storage limitations of available test equipment. The plots shown in Figure 4.5 were recorded using an Agilent 54622A Digital Storage Oscilloscope (DSO). This instrument has a time base that extends to 50 seconds per division, which makes it possible to compare the phase of two signals down to frequencies of several milli-Hertz. Initial testing was undertaken with a Hewlett Packard 54600A DSO, which has a maximum time base of five seconds per division, and limits phase measurements to a lowest frequency of approximately 25 mHz. At frequencies lower than this, the oscilloscope's X vs. Y mode (with storage) was used. When the cell's voltage is plotted on the Y-axis and the supplied current is plotted on the X-axis, the displayed trace can be used to determine the phase difference between the two signals, provided both inputs (voltage and current) are sinusoidal. By combining peak to peak current and voltage measurements and the phase difference between them, the resistance and reactance at the test frequency may be calculated. As no time base is required, this technique may be used at any frequency.

Figure 4.6 shows the type of plot expected with voltage input recorded on the y-axes and current input on the X-axes. The phase angle between the measured voltage and current sine waves is a simple calculation of $sin\theta = A/B$ *or* C/D. The peak to peak values of voltage and current can be directly measured from the maximum swing (span) in the Y and X directions. To determine the sign of the angle (current leading or lagging the voltage) the waveforms must be compared in the time domain.

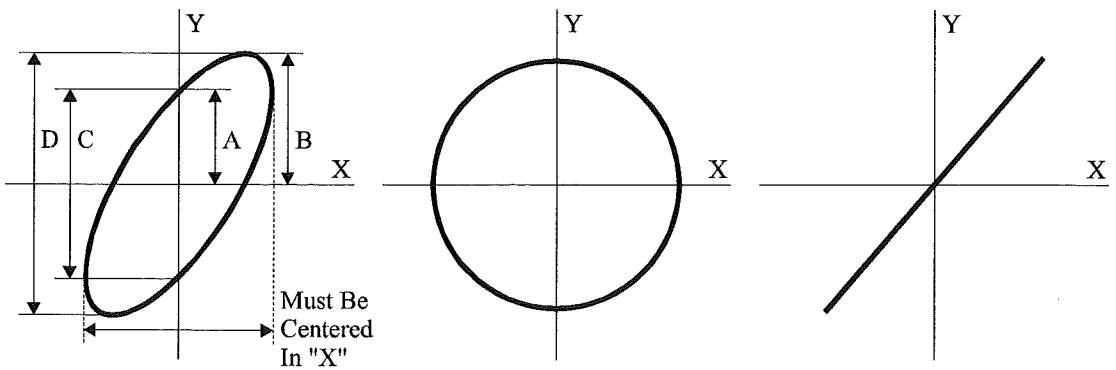

a) Measurements b) 90° Out of Phase c) In Phase (resistive)

Figure 4.6 Sine Wave Phase Measurements

The phase measurements and calculation above rely on both waveforms being sinusoidal, with the resulting plot being a symmetrical circle, ellipse, or straight line. If the impedance of the cell under test is not constant, the resulting plot may not be symmetrical and will appear distorted. This was noted when the appropriate amplitude of the applied voltage signal for the test frequency was not selected.

Similar to the testing above, if a triangle voltage is applied to the cell terminals, the resulting voltage-current plot may be analysed to determine the impedance of the cell under test. Using a triangle voltage waveform can greatly simplify analysis if the Device Under Test (DUT) has a capacitive or resistive nature. The basic formula $I = C\ dV / dt$, suggests for a constant rate of change of voltage (dV / dt), as occurs in a triangle waveform, a capacitive device will produce two parallel vertical lines as shown in Figure 4.7 a). The (current) separation of these lines is proportional to the rate of change of the voltage and the size of the capacitance. If the DUT is purely resistive, Ohms law holds, and a single straight line is produced as shown in Figure 4.7 b). The slope of the line is proportional to the size of the resistance. If the DUT has both resistive and capacitive components, the results are combined as shown in Figure 4.7c).

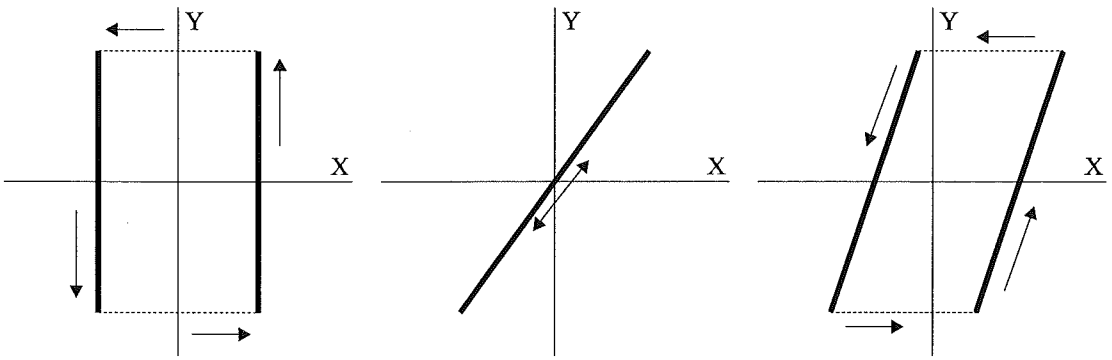

a) Pure Capacitance b) Pure Resistance c) RC Combination

Figure 4.7 Triangle Voltage and Current Waveforms

An interesting characteristic becomes apparent when applying a triangle voltage waveform with reduced frequency or increased amplitude of the test signal. Figure 4.8 shows the XY plot for applying a 278 mV peak to peak triangle voltage to the terminal of a 275 Ah VRLA cell on float charge. In this plot, the units per division indicated in the top left corner are appropriately scaled, and DC offsets have been corrected. It is interesting to note that near the nominal float voltage, the cell appears almost entirely capacitive, however as the voltage is raised above this

point, it maintains the same capacitance. The progressive introduction of a resistive component is indicated by a tilt to the right at higher voltages. Below the nominal float voltage the plot is seen to flare out, indicating an increase in capacitance. The variance from the ideal waveforms (for constant resistance and capacitance) shown in Figure 4.7 suggests that the impedance of a cell may change considerably within the float region. Great care must be taken in selecting signal amplitudes and frequencies if valid measurements are to be obtained.

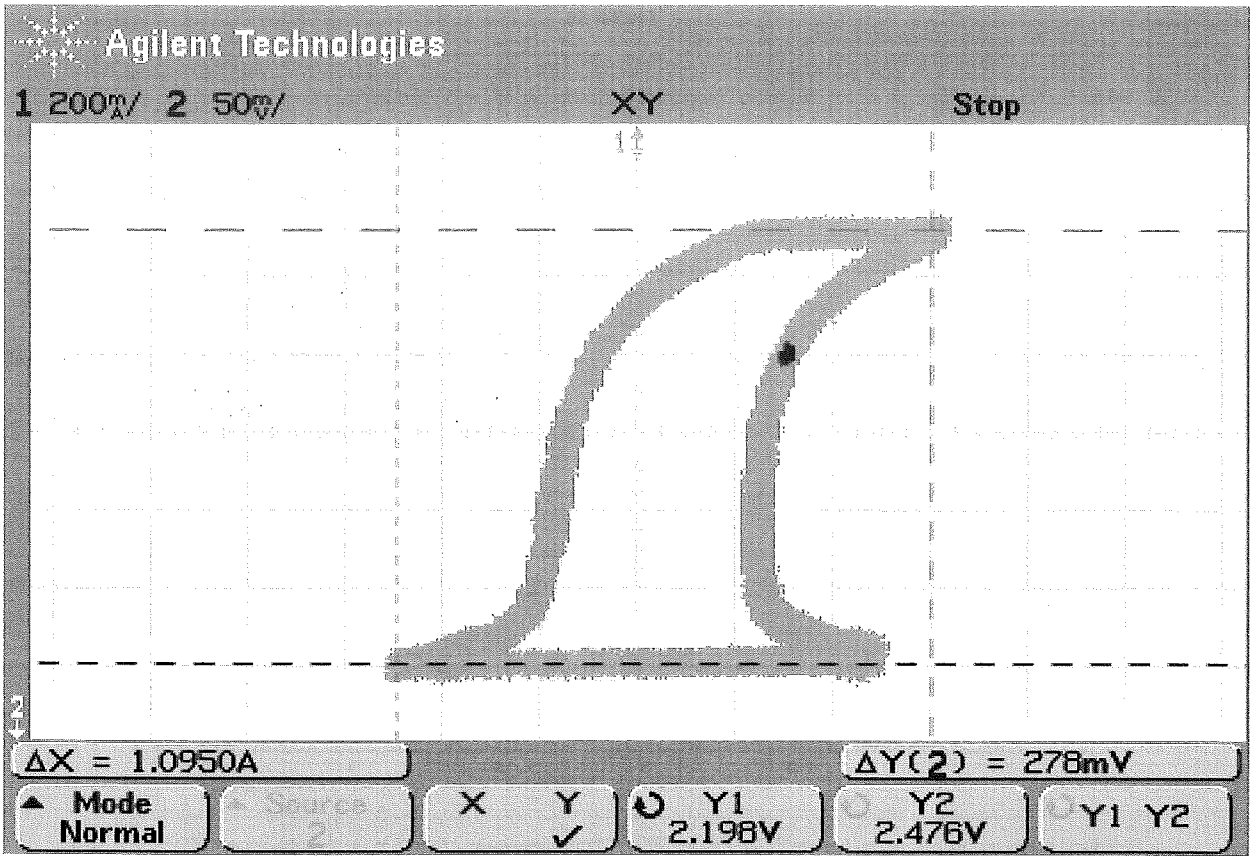

Figure 4.8 Current Required (X axis) to Force a Triangle Voltage (278 mVPP at 10 mHz) (Y axis) on a Cell's Terminals

Conversely, if a constant current square-wave signal is injected into a cell on float charge, from the above analysis it is expected that the change in cell voltage will not be linear, as would be the case if the impedance were constant. As the test frequency is reduced or the injected test-current is increased, a non-linear response indicating changing impedance is expected. Figure 4.9 shows the voltage profiles of a 275 Ah cell that has been subjected to ± 1 A current injection whilst part of a 12 cell string on float at 2.27 VPC. The float current for the string was approximately 190 mA. As expected, it can be seen that the impedance is not constant. It is also seen in Figure 4.9

that when a current perturbation is applied to a fully charged cell on float charge, the voltage response at the terminal of the battery is almost entirely produced from the response of the negative electrode. In this case there was a change of approximately 250mV in the negative electrode, and a 10mV change in the positive electrode over this time. The negative electrode changes between two voltage limits, while the positive electrode has a relatively constant slope during both the charge and discharge phases.

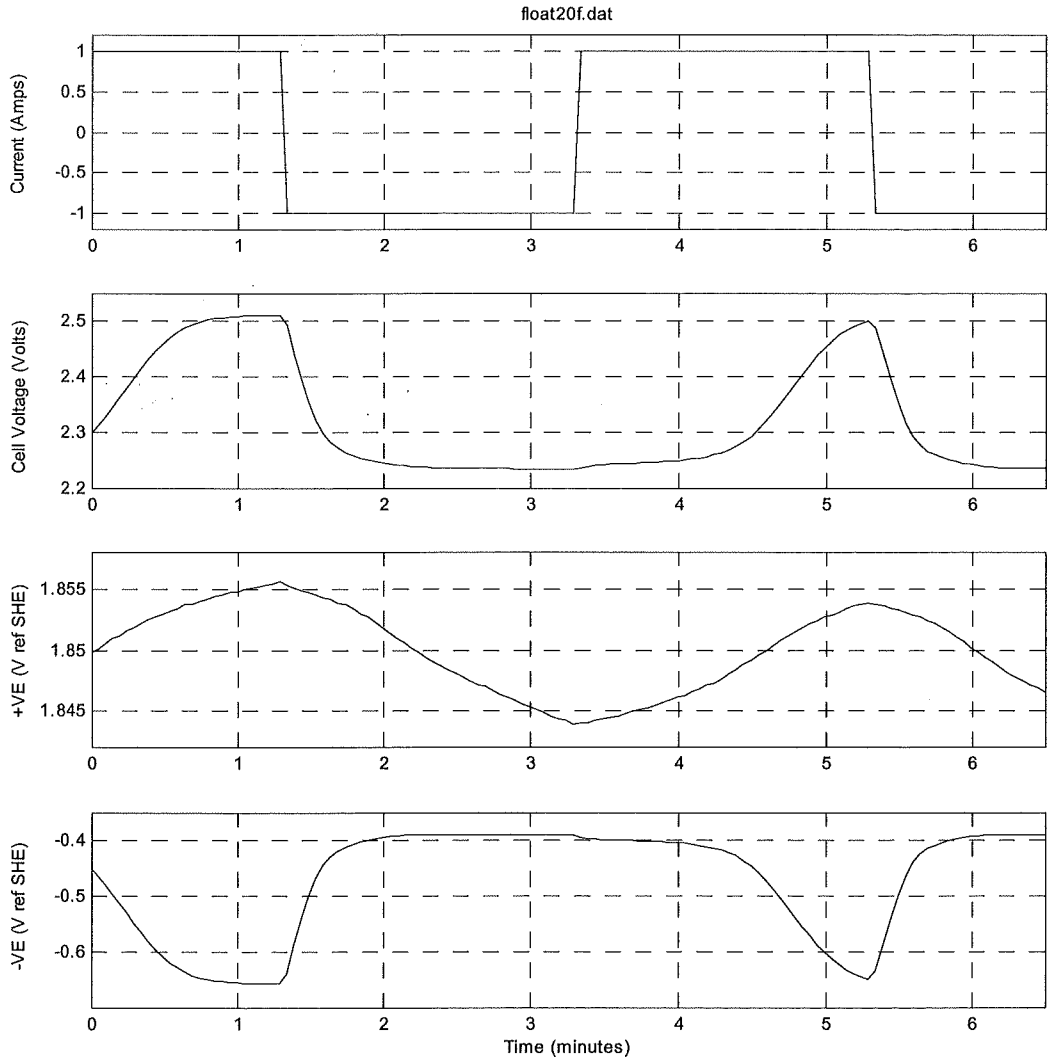

Figure 4.9 Voltage Response ± 1 A Current Manipulation

With prior knowledge of the cell's impedance/float voltage profile, an appropriately selected 'small signal' impedance measurement may be able to determine the cell's operating region. However there is a band in the normal float region that appears to have little change in

impedance. As optimal float charge requires the positive electrode's polarisation to be maintained at a specific value, a single impedance measurement (and impedance/float voltage profile knowledge) will only determine which region the cell is in. Combining impedance measurements and a slight charge or discharge (to change the float voltage) may determine where the impedance boundaries are. With this information it is possible electrode polarisations may be estimated, however impedance measurements alone do not provide sufficient information for float charge optimisation.

Impedance measurements, and in particular tracking the resistance component trend over time, may be of benefit in estimating remaining life, as the resistance of the continually corroding grid ultimately determines the end of life. Impedance measurements alone do not have the ability to determine whether the presently applied float charge is maintaining the corrosion rate at minimum levels. Tracked impedance measurements can only determine when the cell has been degraded, or damage to the cell has occurred.

4.1.3 Transient

It has been shown in the previous Section that there is an abrupt change in the impedance (apparent capacitance) of a cell as the negative electrode makes the transition from recharge to overcharge, or vice-versa. However, simply detecting this transition does not ensure optimal float charge has been achieved. The primary float charge goal requires both electrodes to be raised above their open circuit potentials, while the second float charge goal requires an appropriate distribution of polarisation between both the positive and negative electrodes.

While it may be possible to detect this change in impedance (as the negative electrode becomes fully charged) with dedicated impedance testing equipment, determining an appropriate universal test frequency and signal levels for all batteries may be difficult. Determining the present operating point through impedance measurement would require knowledge of the impedance around this region, and the use of an additional discharge/charge supply to manipulate the cell's charge through this transition point.

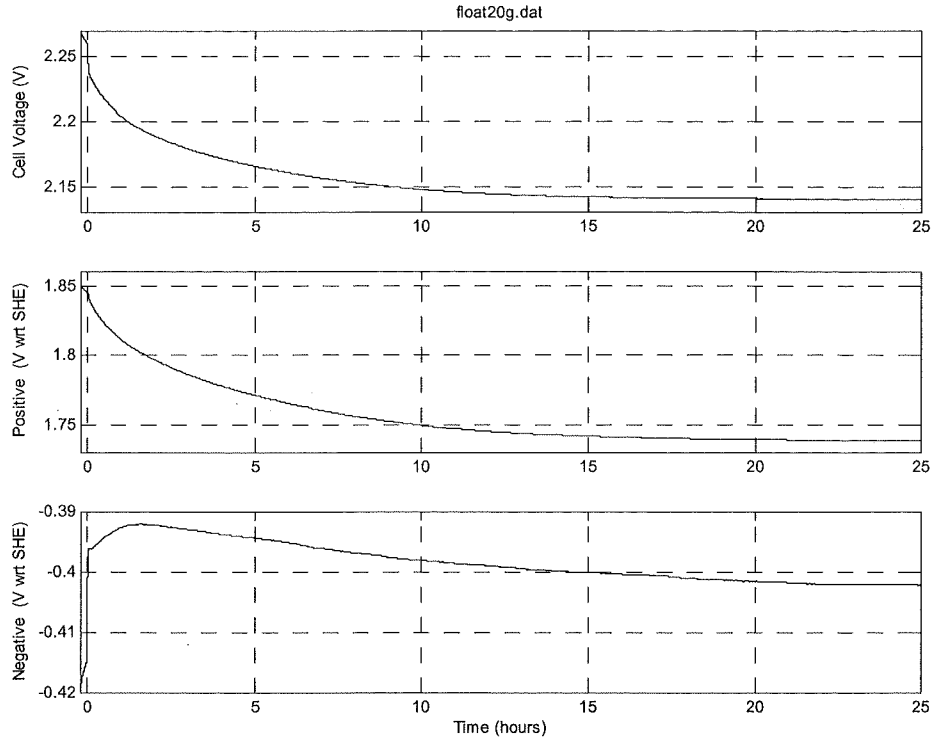

a) 25 Hours

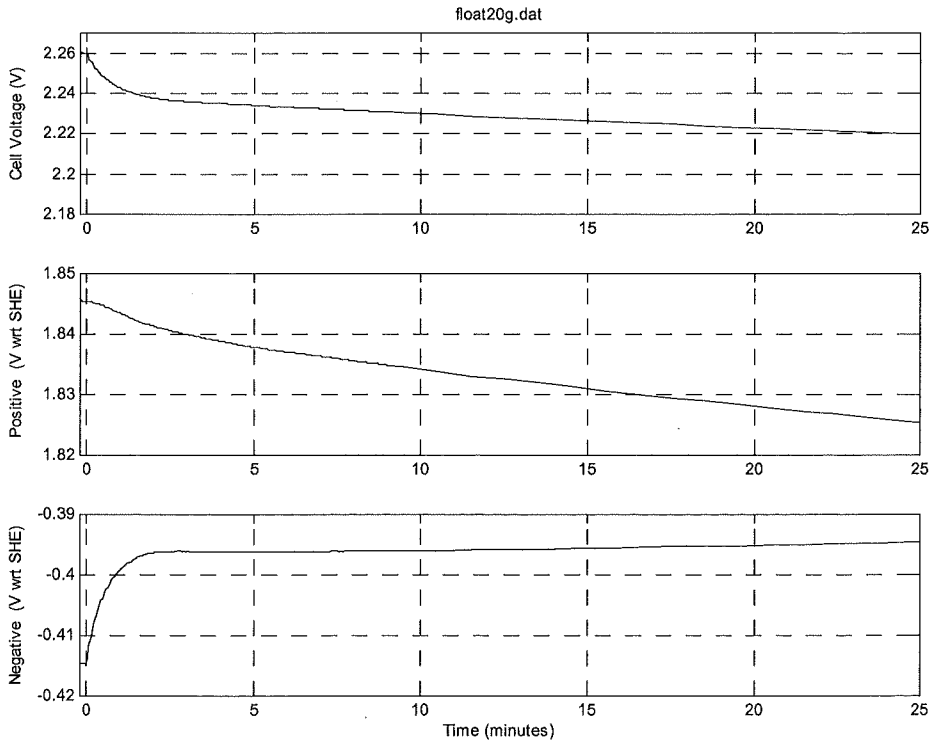

b) 25 Minutes

Figure 4.10 Open Circuit 'Discharge'

Drawing a constant current from the cell under test and detecting any changes in the slope or discharge curve is a far simpler concept to implement. This approach does not require history or knowledge of the cell, except for an appropriate discharge rate. It is commonly accepted, and shown in most constant current recharge plots, that an increase in the rate of voltage rise occurs as the cell nears a full SOC. Similarly, it is accepted that before open circuit voltage measurements can be made (for specific gravity and SOC estimations) the cell must stand disconnected from the charge supply for a minimum of 24 - 48 hours. Figure 4.10 shows the voltage decay as the charging supply is removed from a VRLA cell on float charge. It can be clearly seen in the 1 A discharge plots of Figure 4.9, and the open circuit decay plots of Figure 4.10 that the time response of the negative electrode is significantly quicker than that of the positive electrode. In the short-term (minutes), the overall terminal response of a cell is a function of the changes in the negative electrode while the positive electrode voltage remains virtually constant. When the negative electrode has decayed to its fully charged open circuit value, the positive electrode dominates the terminal response of the cell (over a significantly longer period).

On closer inspection of the negative electrode in Figure 4.10 b), it can be seen that there is approximately an 18mV drop in the first three minutes. A further 5mV decay to the electrode's minimum is evident in Figure 4.10 a) after approximately 1.5 hours. A small voltage recovery (increase) of approximately 10 mV is seen on the negative electrode over the remainder of the 24 hour period shown. It is understood that the gas recombination process at the negative electrode has a depolarising effect. When the float charge supply is removed, there is an initial rapid decay of the voltage on the negative electrode. After this initial negative decay, the positive electrode supports the remaining polarisation. It is speculated that as there is still polarisation on the positive electrode, hydrogen and oxygen continue to be produced. As expected, this migrates to the negative electrode, where it recombines and further depolarises the negative. As the over-voltage of the positive electrode decays to its open circuit value, the amount of overcharge-gas produced reduces, in turn reducing the amount of gas recombining at the negative. It is speculated that this may be a possible reason for the slight (10 mV) recovery of the negative as the positive electrode discharges.

A significant difference in the time constants associated with the overcharge polarisation decay of the positive and negative electrodes has been identified. This difference is seen as a possible mechanism to allow the polarisation distribution within a single cell to be assessed without the

use of a reference electrode. Requiring only a simple current perturbation test, the procedure may be automated and applied to cells in float service in the field. This test has the potential to identify whether a cell is fully charged, as well as to give an indication of the positive plate polarisation, which is related to grid corrosion rates and life estimations. Such a current perturbation test should have the ability to regularly assess the status of cells in field service. This should provide a guide for float charge optimisation so that the float charge goals may be achieved.

4.2 Conceptual Float Model

The key requirement for optimal VRLA battery float management requires the polarisation of both the positive and negative electrodes within each cell to be maintained at specific values. For a given lead-acid battery chemistry, the fully charged open circuit voltage should be known. Subtracting this open circuit voltage from the float voltage gives the total polarisation for the cell. Determining how this polarisation is distributed between the positive and negative electrodes will indicate if the float charge goals have been fulfilled, and aid in selecting a more appropriate float voltage if required. Preliminary testing with the aid of a reference electrode has identified significant differences in the transient-response of the positive and negative electrodes' polarisation. If each electrode within a cell is modelled appropriately, it should be possible to use the model to decompose the terminal response (to a predefined test) into the contributions from each electrode within the cell. In doing so, it should be possible to estimate the internal status of a cell without the aid of a reference electrode.

The model developed below is aimed specifically at the float charge region of VRLA cell operation, and should reproduce both the steady state and transient responses of a cell on float charge. As the model is targeting the float phase of battery life, the representation of the main discharge and recharge reactions is basic and unrefined. Existing cell models derived from impedance, step, or transient responses attempt to predict available capacity or remaining life. As the aim of this model is to provide a tool for the assessment and optimisation of float charge, the model is not intended to be used for available capacity estimation or SOH assessment. However, the model should potentially identify float health problems such as positive or negative plate discharge.

Figure 4.11 shows the response of a 275Ah cell on float charge (approximately 200mA) that has been supplied with an additional ±1A current injection. It can be seen that the basic response of both the positive and negative electrodes can be approximated by a series of straight lines. Over the test period shown, two straight lines represent the positive electrode. The slope of these lines is dependent on the polarity of the injected current. As the test signal consisted of an alternating constant current, the linear response suggests a single capacitor may be a suitable model. Over the same test period the response of the negative electrode is more complex, and consists of a series of lines linked with suitable transition functions. With a positive current injection (charging) three distinct lines are shown, while for the negative injection current (discharging) two distinct lines are seen.

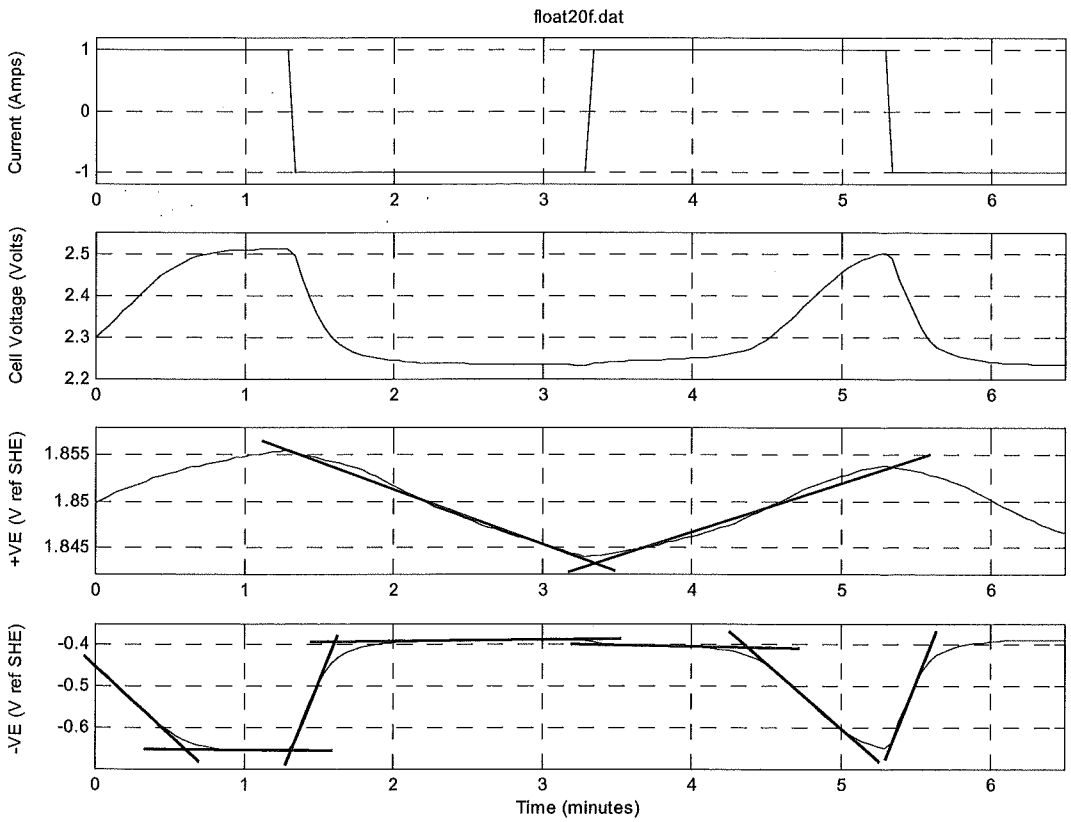

Figure 4.11 Capacitor Model I = C dV / dt Approximation

Starting from the transition of negative to positive current injection, a very gradual (near-zero) slope is seen. After approximately one minute on charge, a transition occurs and a faster linear rise is seen before it returns to a near-zero slope. When a negative current commences, there is an initial rapid drop in electrode voltage, followed by a brief transition to a line with almost no

slope. Again, as the injected signal was a constant current, the response can be approximated by straight lines, and several capacitors may be used to model the response. The size of the capacitors can be determined through the basic formula $I = C\ dV / dt$. If it is found that the lines previously described as near-zero slopes are in fact horizontal, appropriate sized resistors may be used in the model.

It is important to note the voltage scale of the positive and negative electrodes in Figure 4.11. During the period where there is approximately 200 mV change in the negative electrode, there is less than 5mV change in the positive electrode. As both electrodes are subjected to identical current, the relative difference in the effective capacitance of each electrode during this time must be significant. Figure 4.12 shows a continuation of the 1 A discharge in Figure 4.11. On this time scale, it can be seen that the positive polarisation discharge by a 1 A load (275Ah cell) can be approximated as a linear decay. Slight voltage recoveries, similar in nature to that of the Coup de Fouet, can be seen at both the positive and negative electrodes. To avoid complicating the model, and to minimise the number of required calibration parameters, no attempt has been made to model these small recoveries. Typically, at the very low discharge rates used, these recoveries have been less than 10 mV. In relation to the total polarisation and the optimal polarisation window, these recoveries are considered small and should not significantly influence the results.

Figure 4.10 showed the open circuit voltage decay when a cell was removed from float charge. It can be seen that the ratio of time responses for the polarisation decays of both the positive and negative electrodes is similar to the 1 A discharge shown in Figure 4.12, however the shapes of the decays differ. It has been shown that a constant rate of voltage decrease results from a 1 A constant current discharge, suggesting that a capacitor model is appropriate. At low discharge currents such as open circuit self-discharge, the exponential decay suggests a resistor (self-discharge) in parallel with a capacitor is a suitable model. As the rate of the self-discharge is small when compared to the 1 A discharge, the addition of a self-discharge resistor should not alter the constant voltage decay when a 1 A discharge is modelled.

A parallel resistor capacitor model may be suitable for the transient response of a VRLA cell on float charge, but the model must also reproduce the steady state characteristics. Excluding parasitic reactions such as hydrogen evolution at the negative electrode and grid corrosion of the positive electrode, there is no net charging or discharging of the cell when it has stabilised to a

steady state. As virtually all the energy supplied to the cell during steady state float charge is consumed in the internal oxygen cycle and eventually dissipated as heat, steady state is best modelled through appropriate resistance values. The steady state characteristics of lead acid batteries are often shown in the form of Tafel plots, such as Figure 4.1. When steady state voltage current pairs are plotted on linear/log axes, straight lines are produced. Each electrode has a slope measured in milli-volts per decade, and a minimum current (start or break point) at which polarisation begins. As the voltage is proportional to the log of the current, a non-linear resistor is required to reproduce this characteristic.

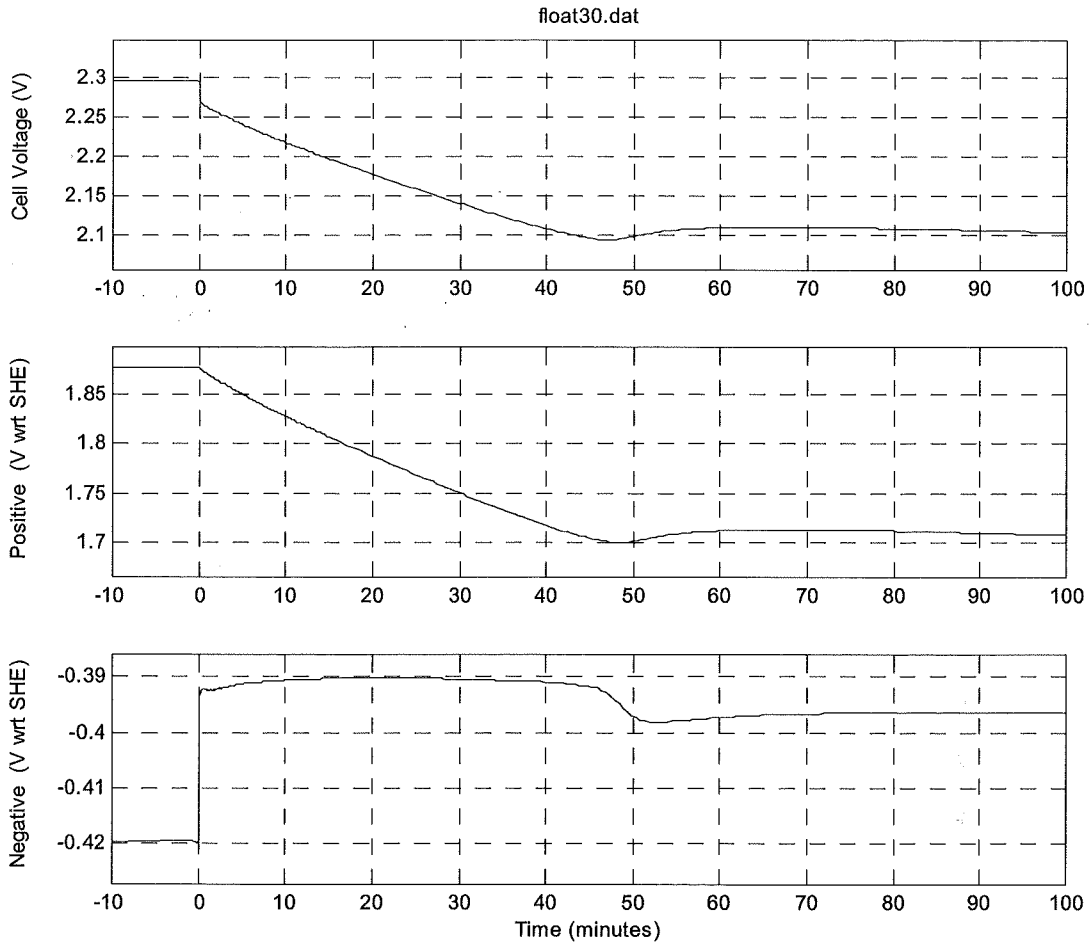

Figure 4.12 Complete Polarisation Discharge at 1 A

Figure 4.13 shows how a simplified cross section of a VRLA cell is used to produce the general structure of the cell model. While the basic physical characteristics of cell components have been used, no attempt has been made to model the electrochemical reactions occurring within the cell. The model is an electrical circuit that will mimic the response of each electrode and the

entire cell under both steady state and transient conditions. The aim of the model is to aid the understanding of what is occurring within a cell at individual electrode level, based on information derived from the terminal response of the cell. While it may be possible to speculate about the chemical processes or reactions occurring within the cell, the model's elements are not developed to recreate the chemical reactions or processes occurring within a VRLA cell.

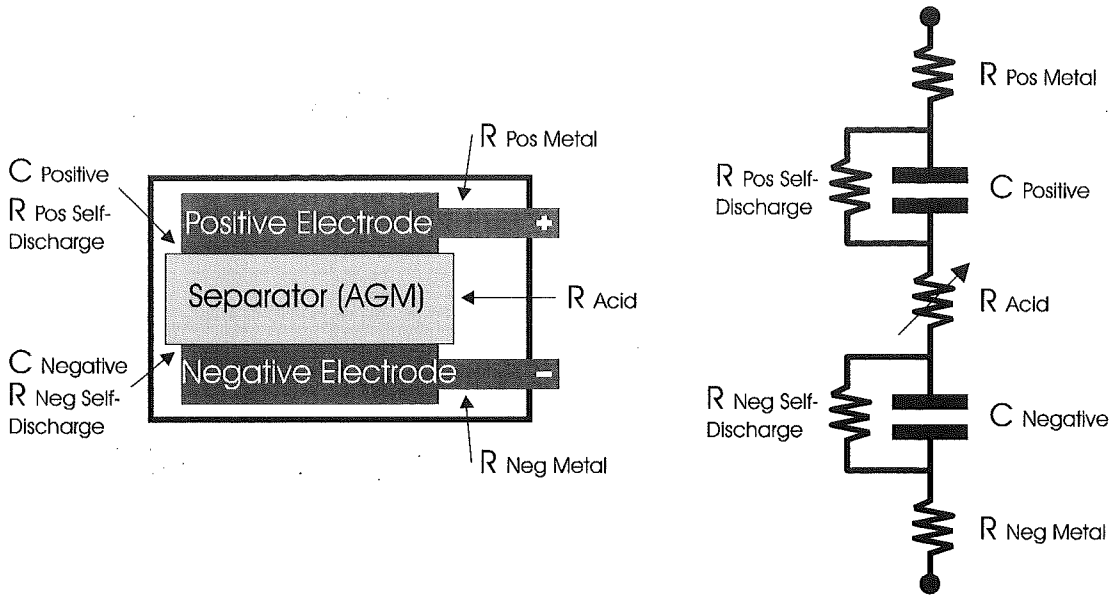

Figure 4.13 Basic Cell Model Architecture Development

It can be seen in Figure 4.13 b) that the distributed metallic resistance of the grid has been lumped into a single resistor for each electrode in the model. Metallic resistance has traditionally been an important aspect of cell models, as it is often used to indicate the amount of grid corrosion and remaining life. However, as this model is intended for float charge analysis, the influence of metallic resistance (or changes in resistance) is very small, and does not greatly affect the result due to the very low currents associated with float charge and float testing. The model also greatly simplifies the energy storage. It is assumed in the developed model that charge is stored and a potential produced at the junction between the electrode and the acid absorbed in the separator. Conventional reaction based modelling elements such as mass transport to the reaction site, kinetic limitations, and available surface area, etc. are not used in this model. Charge storage for each electrode is modelled with an appropriately sized conventional capacitor. A resistor placed in parallel with these storage capacitors is used to

simulate the self-discharge of the cell. The acid is modelled with a variable resistor, varying from a high resistance when the cell is discharged, to a very small resistance when fully charged. However for the purposes of float modelling, the variable resistor may be replaced with a single fixed (float) value. Again, as the currents associated with float charge and testing are small, the generally low value of acid resistance suggests that resistance changes with time, caused by increasing concentration with dryout, should not greatly influence the analysis.

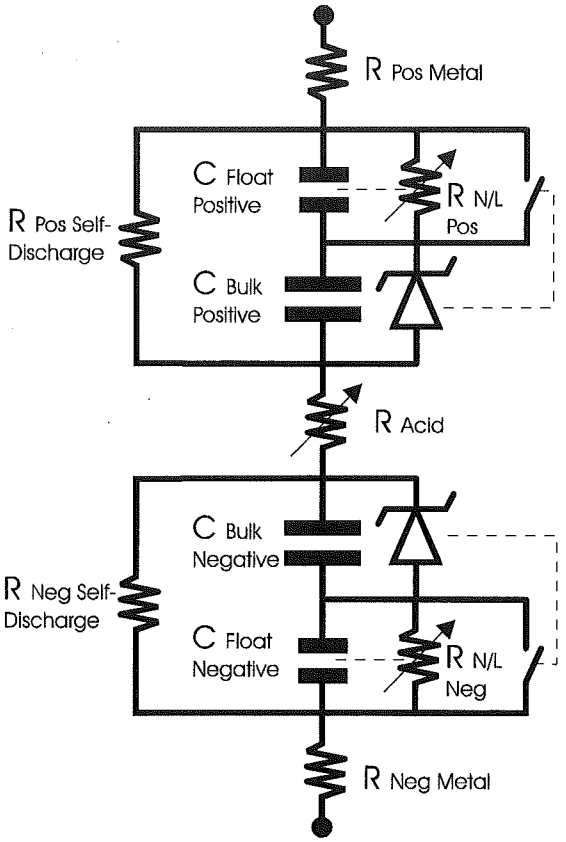

Figure 4.14 VRLA Float Charge Model

Figure 4.14 shows how the basic model of Figure 4.13 b) is adapted to produce the overcharge response identified in Sections 4.1.1 and 4.1.3. The bulk capacitors cater for the main charge/discharge region of cell operation, while the float capacitor and non-linear resistor are used to model the float region of cell operation. In parallel with the bulk capacitor is a zener diode, which is used to limit the maximum voltage able to be supported by the capacitor. The zener voltage of this diode has a value equal to that of the fully charged open circuit voltage of the electrode. The switch shorting (eliminating from the circuit) the float charge capacitor and non-linear resistor is closed when the float charge capacitor's voltage has discharged to zero.

When the voltage on the bulk capacitor increases (due to charge current) to the zener voltage, the diode starts conducting and the float switch opens. This then requires the charge current to pass through the parallel non-linear resistor / float capacitor combination causing the float capacitor to charge. The capacitor will continue to charge until the supplied charge current is passed completely by the non-linear resistor, i.e.: $V_{Cap\_float} = I_{Supply} \times R_{Non\text{-}Linear}$. The value of the non-linear resistor is a function of the voltage on the float charge capacitor.

It is evident in the above model that the structures of both the positive and negative electrodes are similar, however the time constants associated with the electrodes' float components are considerably different. It is believed that these differences, when combined with a current perturbation test, may be used to determine the contribution each electrode makes to the total polarisation of a cell.

4.3 Structured Float Testing and Results

Section 4.1 detailed the initial testing which identified a transient feature with the potential to reveal information on a cell's response to the supplied float charge. It appears feasible that the individual electrode polarisations may be estimated from the cell's terminal voltage response to a change in the applied float current. Section 4.2 detailed the general structure of an equivalent electrical model that has the ability to replicate both the steady state and transient responses of a VRLA cell on float charge. Through the use of an appropriate test procedure and model, it should be possible to first analyse how individual cells in field service are responding to the applied float charge, and secondly to provide a reference to assess the effectiveness of attempts to correct cell problems.

Discharge I \ Float V	2.3 V	2.1 V	2.2V	2.35 V
	26 *Tafel plot*			
Open Circuit	27	32	37	44
10 mA	28	33	38	45
100 mA	29	34	39	46
1 A	30	35	40	47
10 A	31	36	41	48
			42 *test failed*	49 *pre-Tafel*
			43 *Tafel plot*	50 *Tafel plot*

Table 4.2 Discharge Test Plan

To verify and characterise the model shown in Figure 4.14, a series of tests was planned and undertaken. This testing involved charging a single cell with a fixed float voltage until the current stabilises, then removing the charge supply and discharging the cell with a constant current, while the voltage profiles of each electrode and the cell are monitored. Testing was undertaken for four float voltages and five discharge rates, including open circuit. Float voltages both above and below the fully charged open circuit voltage were used. All testing was performed with the aid of a reference electrode to separate the contributions of each electrode. Table 4.2 shows the test number (26 - 50) and associated data file of the raw test data, e.g. 27 relates to test data file float27.dat. This file contains the open circuit decay for a cell that had previously been on a float charge at 2.3 V. All of the testing shown in Table 4.2 was performed at approximately 22 °C. At the conclusion of this testing a further series of tests was undertaken at temperatures between 25 and 45 °C.

The planned testing was largely aimed at assessing the transient response of a cell when discharged from various float voltages at various discharge rates. To track changes in the cell as testing proceeded, Tafel plots were also performed at the beginning, during, and at the end of the planned testing.

4.3.1 Tafel Plots

Tafel plots are conventionally used to evaluate how a cell responds to an applied float voltage. It is envisaged that the outcome of this research will be a field useable test or procedure that will determine a slice of a Tafel plot (detailing electrode polarisations) at the present float voltage. Therefore, to evaluate the accuracy of any developed test or procedure, a conventional Tafel plot is required so that comparisons and assessments may be made.

Figure 4.15 compares Tafel plots of the test cell at the beginning, middle, and end of the testing detailed in Table 4.2. It can be seen that throughout the testing there are changes in the polarisation characteristics of the cell. The response of the positive electrode remains reasonably consistent, with the majority of the characteristic changes being associated with the negative electrode.

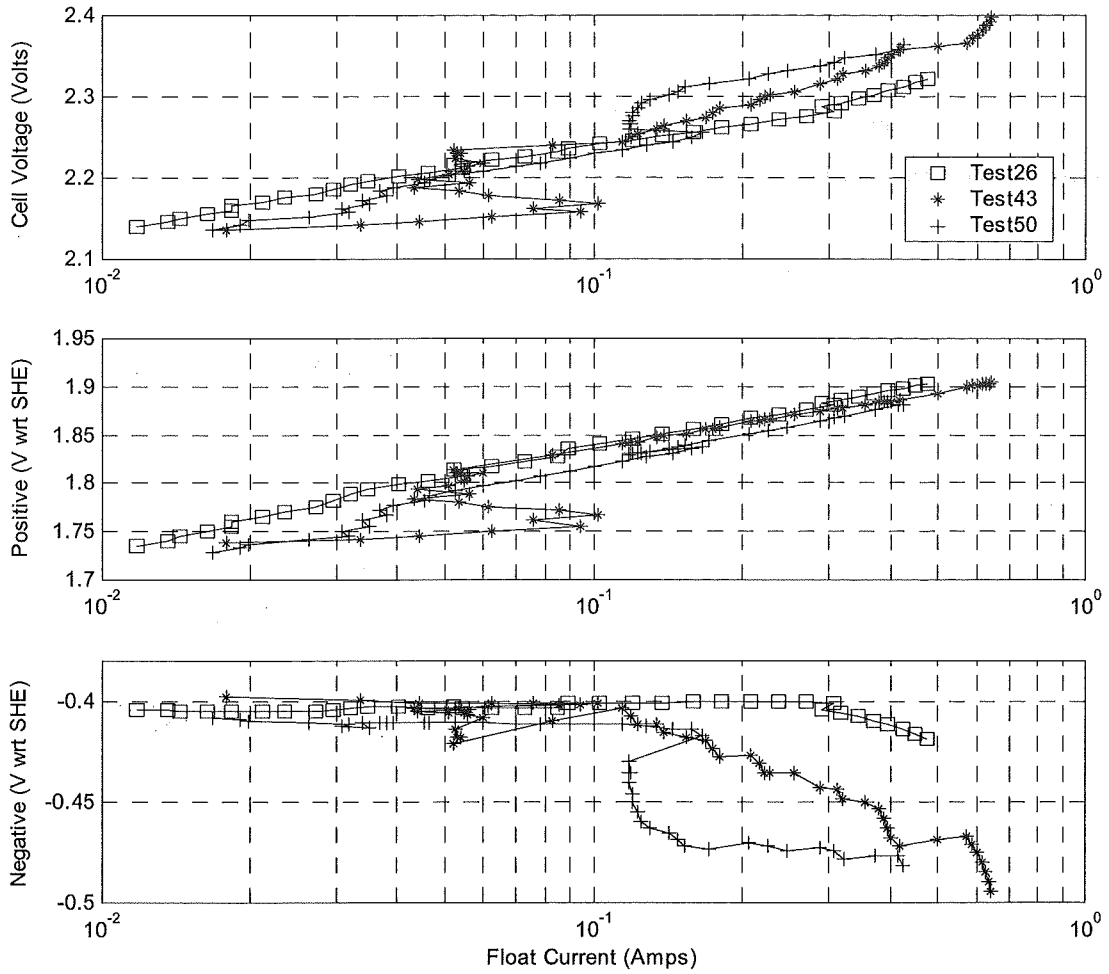

Figure 4.15 Cell Variation Throughout Testing

From the day a VRLA cell is manufactured, unavoidable reactions within the cell cause it to gradually wear out. While it is expected that there will be some changes in the cell as it ages, the testing duration is relatively short when compared to the expected life of the cell. It is thought the changes noted above do not result directly from the accepted wear-out process of a VRLA cell.

The first Tafel plot (Test 26) shows that the negative electrode does not begin to polarise until the float current has risen to approximately 300 mA. As the positive electrode begins to polarise at approximately 20 mA, the 300 mA required to polarise the negative electrode appears excessive. While the reasoning for this large difference must be related to the cell's chemistry and is beyond the scope of this work, it is possible that the test set-up or process contributed to

this unbalanced effect. It is understood that atmospheric oxygen entering the cell through leaks in the cell case can have a depolarising effect on the negative electrode. It is possible that a poor seal around the reference electrode insertion point may allow unwanted oxygen from the atmosphere to enter the cell. However with the aid of soapy water around the pressure relief valve, it was noted at the higher voltages encountered during the latter stages of the Tafel testing that gas was occasionally released from the pressure relief valve. It is unlikely gas would vent through the pressure relief valve rather than via a poor seal around the reference electrode entry point. Another possible reason for the large unbalanced effects seen in the first Tafel plot may be that atmospheric oxygen entered the cell when it was initially punctured to allow insertion of the reference electrode. However, after the electrode was added, care was taken to 'work' the cell and vent some gas in an effort to rebalance internal gases.

The tests detailed in Table 4.2 were undertaken in several series, with each test within a series being performed at the same float voltage. The first series of tests was performed at 2.3 V, which is a reasonably high voltage, but remains within the allowed voltage range for the cell, and should not significantly alter the cell's characteristics. The second series of tests used a float voltage of 2.1 V, which is below the fully charged open circuit voltage ($\approx$ 2.14 V) and no polarisation was expected. The third series of tests was performed at 2.2 V, slightly above the fully charged open circuit voltage. During this third series of tests, indications suggested that the polarisation response had changed from the first test and the proceeding Tafel plot. At the end of the third series another Tafel test was undertaken. It can be seen in Figure 4.15 that the Test 43 plot has a negative polarisation intercept or break point, just slightly greater than 100 mA. This is a significant reduction from the 300 mA recorded in Test 26. Again, the reason for the changes in the cell's characteristics has not been investigated, but is likely to be related to the testing history. The period of time spent 'float charging' the cell below its fully charged open circuit voltage may have changed the overcharge characteristic, or this change may have resulted from the time spent testing at 2.3 V. This voltage may have been high enough to cause gas venting leading to dryout or further elimination of atmospheric oxygen ingested during the addition of the reference electrode.

The Tafel plot (Test 50) performed at the end of the planned testing shows further changes to the characteristic of the negative electrode. While the negative polarisation break point is at a similar current to the previous Tafel plot (Test 43), the characteristic has changed. In Test 43,

the overall negative polarisation formed a straight 'Tafel' line on a linear/log graph. In the final Tafel plot (Test 50), the negative electrode's characteristic has changed to a rapid increase after the polarisation break point. This rapid increase then settles to an almost constant polarisation as the float current is further increased.

It is accepted that the VRLA cell is a complex living electrochemical system, and the impacts of any active testing may therefore influence or alter the future characteristics of the cell. As passive testing is not possible, it is accepted that changes in the tested cells' characteristics may occur as the tests proceed. Normal cell ageing, test history, and set-up and stabilisation times all have an impact on a cell's characteristics. The production of a single Tafel plot, as shown in Figure 4.15, requires several days set-up time (open circuit stabilisation), followed by approximately two weeks of testing. With only a single test system and a finite research time, it is accepted that some variance over the duration of the testing may be experienced. It is neither economic nor feasible to endlessly repeat tests in attempts to eliminate or reduce changes in the characteristic. A compromise between set-up times, stabilisation times, test duration, and characteristic drift is needed. It must be accepted that there may be some changes in the characteristics over the duration of the testing. It is important to be aware of any changes, and monitor these as they occur throughout the testing period.

4.3.2 Transient Test

The initial testing identified the use of differences in the transient response of the positive and negative electrodes' polarisation as a means of estimating the polarisation of each electrode. To further investigate the possibility of using transient response as an analysis tool, and to examine how variations in operating conditions affect the transient response, the tests detailed in Table 4.2 were performed. The analysis of the testing has been undertaken to isolate the effects of applied float voltage and discharge rate. All analysis in this Section assumes the cell temperature to remain between 22 and 23 °C.

4.3.2.1 Constant Voltage, Variable Discharge Rate

Figure 4.16 shows the effects of discharging a cell that has been float charged at a voltage that is too low. It is hypothesised that when a cell is not fully charged, the dual-slope rapid decay

associated with the discharging of the polarisation capacitance would not be present. Instead, the response of the cell is expected to be a simple, steady decay associated with the discharge of the main storage reaction.

To be sure that the cell under test was not fully charged, it was first discharged to approximately 80% SOC (this should settle to an open circuit voltage of approximately 2.09 V) and then charged with a supply set to 2.1 V. As the fully charged open circuit voltage for this cell is approximately 2.14 V, a charge voltage of 2.1 V should result in the cell being 'float charged' at only 85% SOC. The cell was charged at 2.1 V until steady state (no change in charge current) was achieved before the discharge testing plotted in Figure 4.16 was initiated. The terminal voltage was maintained in a tight group at approximately 2.1 V prior to the discharge. With the exception of the 10 A discharge, there appears to be a drift of the electrode potentials with each successive test. It is seen that the potential of the positive electrode increases with each test. The reason for the 10 A discharge not following the trend is due to the testing order. As virtually no decay was seen in the first (open circuit) test, the 10 A test was bought forward to the second test performed so that it could be determined whether a measurable response would be obtained. Having verified a measurable response, the remainder of the testing at 2.1 V was performed in the planned order (10 mA, 100 mA, and 1 A). While care was taken to visually ensure the achievement of steady state conditions before initiating the next test, time limitations resulted in finite settling times. Reasoning for the drift in electrode potential below open circuit is not essential to the outcomes of this research, and therefore the cause has not been investigated. However, it is speculated that the drift may be related either to the finite settling time, or to differences between discharge and recharge efficiency of each electrode at this operating point.

As expected, it can be seen in Figure 4.16 that at low currents (open circuit to 100 mA) there is virtually no change in the cell's terminal voltage when the charge is removed and the discharge commenced. As the discharge current is increased, an increased rate of voltage decay for the cell and each electrode can be seen. This is a combination of increased voltage drops due to resistive components, and an increased rate of cell discharge. The response of the negative electrode to higher discharge rates shows an initial drop followed by a constant voltage, suggesting a large capacitor and series resistor may be used as a model. When compared to the negative, the response of the positive electrode at high rates has a significantly slower and larger initial drop, followed by a slow continuous decrease in electrode voltage. This suggests that a similar series resistor-capacitor model would require a slightly smaller capacitor and a larger resistor. The

modelled positive resistance may also require a small capacitor in parallel with the resistor to give the slower response of the initial drop. While a complete battery operational model will require a detailed model of the bulk discharge, to avoid excessive calibration parameters the bulk capacitors, positive metal, negative metal, and acid resistances detailed in Figure 4.14 are sufficient for a model targeting the float (overcharge) region of VRLA battery operation.

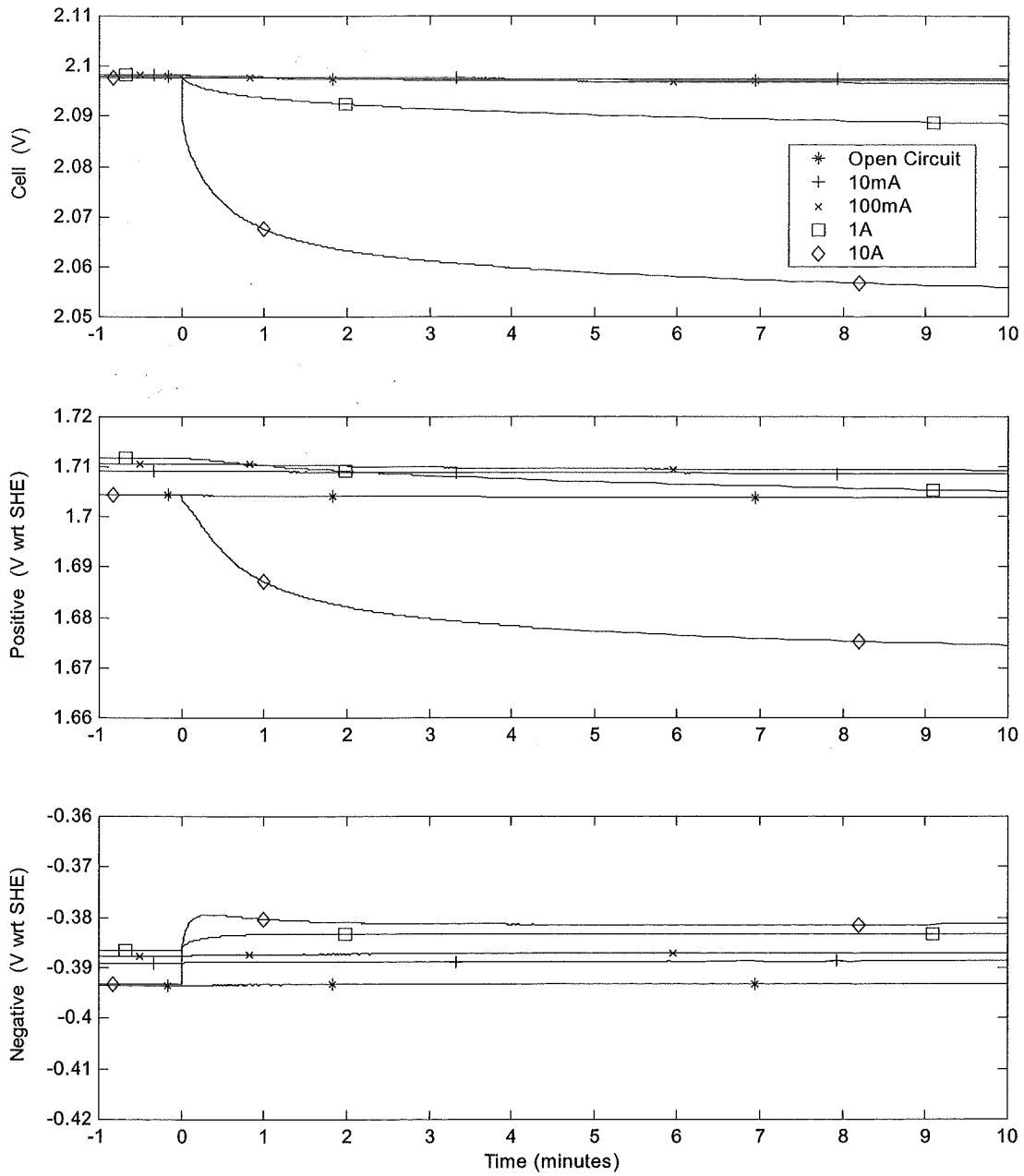

Figure 4.16 Variable Discharge Rate from a 2.1 V Float Charge.

It can be seen in Figure 4.16 that almost no change in the terminal voltage occurs with discharge rates lower than 1 A. This is desirable, and in keeping with the proposed model. If the bulk charge capacitors are orders of magnitude bigger than the overcharge capacitors, it is expected that when there is no polarisation, the change in terminal voltage from low rate discharges will be very slow. Test currents of a magnitude similar to or lower than the float current are preferred, as resistive drops are seen to have very little influence on the response voltage. No terminal voltage response is seen when no polarisation exists.

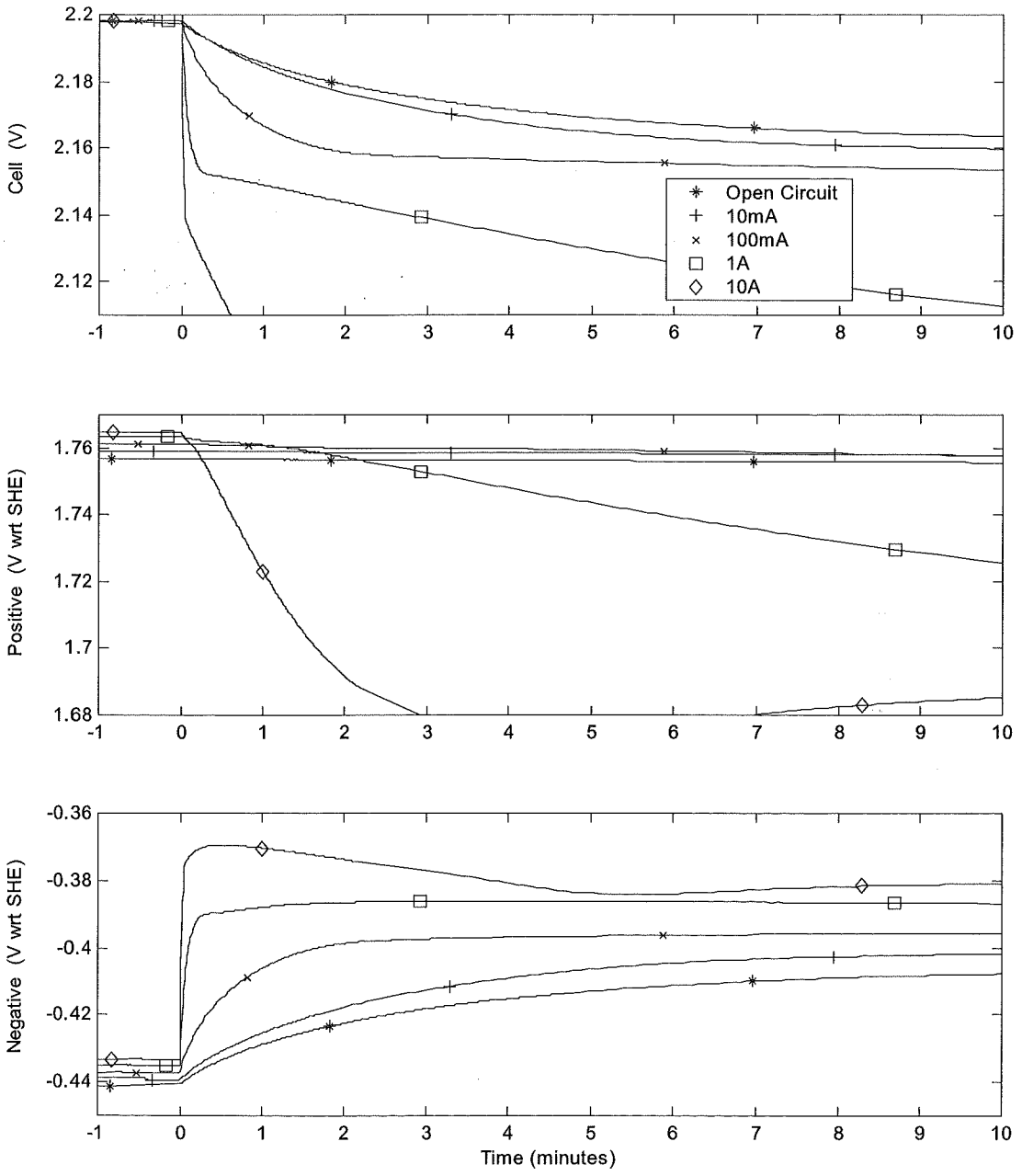

Figure 4.17 Variable Discharge Rate from a 2.2 V Float Charge

Figure 4.17 shows the response of various discharge rates for a cell that has been float charged at approximately 2.2 V. The fully charged open circuit voltage for this cell is 2.140 V at 20°C. When measured against a Standard Hydrogen Electrode (SHE) the positive electrode has a fully charged open circuit potential of 1.738 V, and the negative electrode has a potential of 0.402 V.

During the series of tests conducted at a float voltage of 2.2 V, it was noted that the potentials of each electrode prior to the discharge did not correspond to the first Tafel plot (Test 26 in Figure 4.15). It can be seen in Figure 4.17 that prior to the discharge, the positive electrode has a potential of approximately 1.76 V with respect to (wrt) SHE, and the negative electrode's potential is -0.438 V wrt SHE. Tafel Test 26 in Figure 4.15 suggests that at this test voltage, the positive electrode should have a potential of approximately 1.8 V, and the negative 0.4 V wrt SHE. As a significant amount of negative electrode polarisation is seen prior to the discharge in Figure 4.17, it was suspected that the battery characteristics might have changed as a result of testing. At the end of this series of tests another Tafel plot (Test 43, Figure 4.15) was conducted. While this plot does show a small peak of approximately –425 mV in the negative electrode potential at a cell voltage of 2.2 V, there is still a discrepancy of 15 mV between the Tafel and transient tests. It is suspected that this may be related to settling time limitations in the Tafel plots. Electrode potential plots in Figure 4.17 typically took three to four days to settle to steady state (prior to the discharge), however the current used for steady state detection in Figure 4.15 stabilised much faster.

It can be seen in Figure 4.17 that the response of the positive and negative electrodes is as expected. At the low discharge rates (open circuit to 100 mA) the negative electrode is seen to decay to the fully charged open circuit potential, while there is very little response from the positive electrode. At the 1 A and 10 A discharge rates, a decrease in the positive electrode potential is seen, however when compared to the near instantaneous drop of the negative at these rates, the transient response of the positive electrode is significantly slower. Also evident at the higher discharge rates is a small 10 – 20 mV recovery on the negative electrode following the initial voltage. This recovery appears to coincide with the point in time at which the positive electrode polarisation is discharged.

The negative electrode's fully charged open circuit voltage for the cell tested in Figure 4.17 is approximately –400 mV. As the discharge rate is increased, the negative electrode is seen to

decay to lower voltages. It is believed that the potential differences are due to resistive effects. At discharge rates of a similar magnitude to the float current, the influence of these resistive volt-drops is negligible. Again, similar to the plots shown in Figure 4.16, it is evident in Figure 4.17 that each successive test has a small drift in electrode potential prior to the discharge. This drift increases the potential of the positive electrode at the expense of the negative.

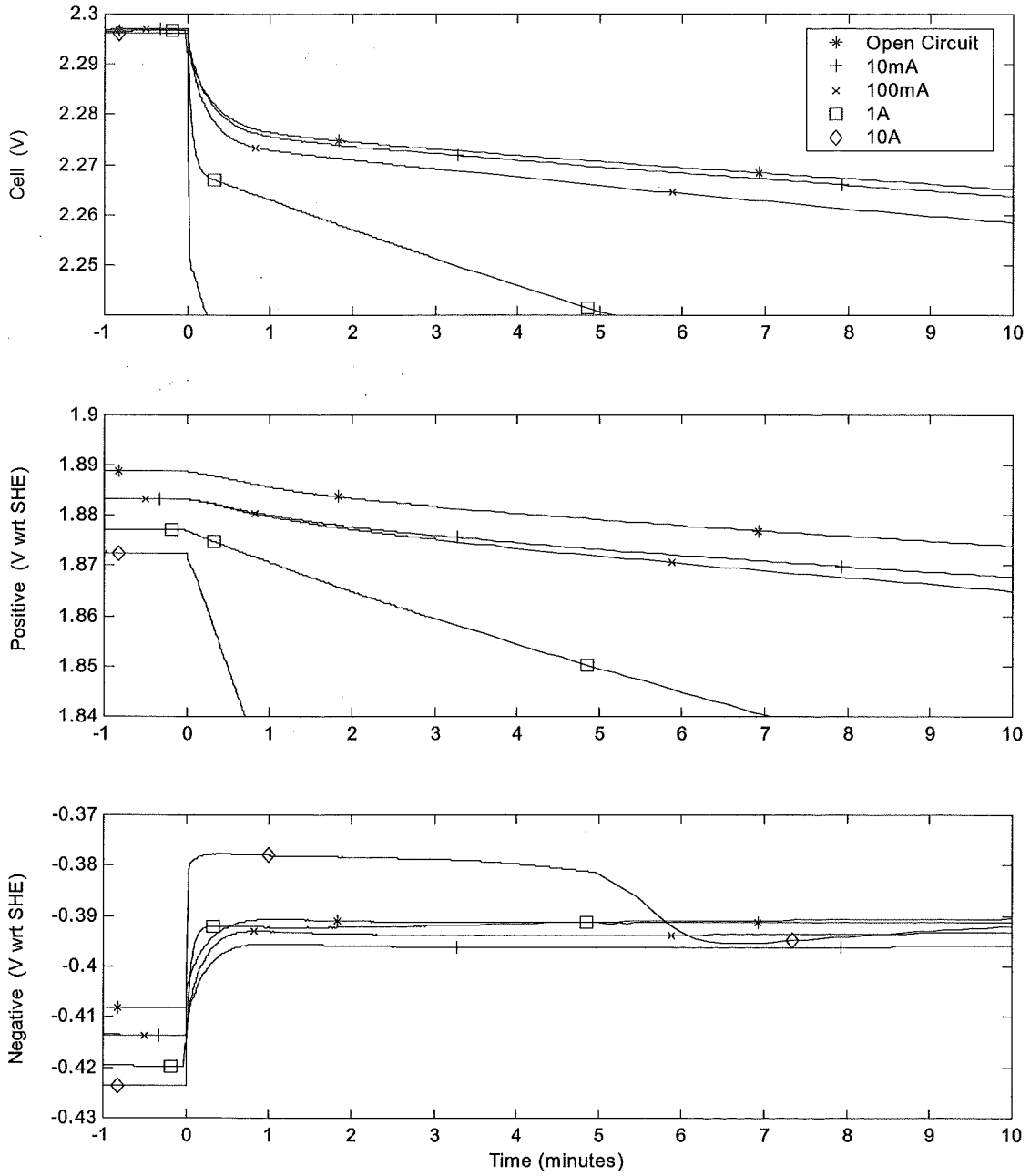

Figure 4.18 Variable Discharge Rate from a 2.3 V Float Charge

Figure 4.18 shows the previously tested cell discharged from a float voltage of approximately 2.3 V. As the 2.3 V series of tests was the first to be conducted, it is appropriate to compare these tests to the first Tafel plot (Test 26) shown in Figure 4.15. The Tafel plot shows that at a cell voltage of approximately 2.3 V the negative electrode is just beginning to polarise, and has a potential of approximately –410 mV. This correlates well with the open circuit plot in Figure 4.18. Similarly, the Tafel plot (Test 26) shows a positive electrode potential of approximately 1.89 V, which again correlates well with the positive electrode's potential seen prior to the open circuit plot (Figure 4.18). However, as the testing progresses, a shift in the electrode potentials can be seen prior to the discharge. The change in potential of the negative electrode is seen to increase as opposed to the positive increasing in the previous two plots (Figure 4.16 and Figure 4.17). While the reason for this change is unknown, it may be related to the repeated shallow discharging during testing. The trend of increasing negative electrode potential with testing is supported by later Tafel plots (Tests 43 and 50).

Prior to the discharge testing, the difference between the float voltages in Figure 4.16 and Figure 4.17 is approximately 100 mV. With a fully charged open circuit voltage of approximately 2.14 V, the 2.2 V tests have a total polarisation of 60 mV, while the 2.3 V tests have a total polarisation of 160 mV. For float charge optimisation, it is important to know how this total polarisation is distributed between the positive and negative electrodes at the operated float voltage. It can be seen that as the float voltage is increased, there is an increase in the potential of the positive electrode, and a decrease in the potential of the negative. Comparison at a similar discharge rate, for example 100 mA, shows that the potential of the positive electrode increases by 123 mV, from 1.760 V at a cell float voltage of 2.2 V, to 1.883 V at a float voltage of 2.3 V. Similarly, it can be seen that the potential difference (wrt SHE) of the negative electrode has decreased by 24 mV, from –438 mV at a float voltage of 2.2 V, to –414 mV at a float voltage of 2.3 V. As the fully charged open circuit potential of the negative electrode is approximately -400mV, there is about 14mV of negative polarisation at a cell float voltage of 2.3 V, and 38 mV at a float voltage of 2.2 V. The fully charged open circuit potential of the positive electrode is approximately 1.74 V. At a float voltage of 2.2 V the positive electrode has approximately 20 mV of polarisation, while at a float voltage of 2.3 V this is 143 mV. As the optimal positive electrode polarisation for minimal grid corrosion is accepted to be between 40 - 80 mV, a float voltage should be found between these two operating conditions to produce the desired result.

On comparison of the cell voltage discharge profiles in Figure 4.17 and Figure 4.18, it can be seen that although the discharge rates are similar, the rate of voltage decay is faster in Figure 4.18. As the initial response in both plots is almost entirely from the negative, it would be expected that with more negative polarisation, the rate of decay in Figure 4.17 would be faster. It is, however, seen to be slower. Dependant on the discharge rate, the decay of the negative electrode's polarisation takes up to take up to ten minutes in Figure 4.17, while in Figure 4.18 this is seen to be less than one minute at all discharge rates. While the reason for this feature is related to the cell's chemistry and is not subject to investigation in this research, it is speculated that the increased rate of decay in Figure 4.18 may be due to a greater depolarising effect from oxygen recombination. As Figure 4.18 has significantly more polarisation, it is expected that there will be more production and corresponding recombination of overcharge gas. As oxygen recombination is said to have a depolarising (slight discharging) effect on the negative electrode, the increased positive polarisation may explain the increased rate of negative polarisation voltage decay in Figure 4.18. While small differences in the rate of the negative electrode polarisation decay have been noted, these are not significant when compared to the rate of polarisation decay of the positive electrode. Furthermore, these slight variations do not affect the ability to use the transient response to externally determine the polarisation distribution within the cell.

Excluding the high rate (10 A) discharge, Figure 4.18 shows a rapid (less than one minute) decay of the negative electrode to within 10 mV of its fully charged open circuit potential. An overshoot (settling period) and recovery is seen on the 10 A discharge, with the recovery appearing to coincide with the time at which the positive electrode reaches its fully charged open circuit potential. While the overshoot and recovery is visible on the 10 A discharge, it is also present to a lesser extent on the lower rate discharges. However, as the magnitude of the overshoot appears to be proportional to the discharge rate, the overshoot is not obvious at low discharge rates, and the recovery occurs outside the plotted region. Over the period of this negative electrode decay there is less than 10 mV change in the potential of the positive electrode.

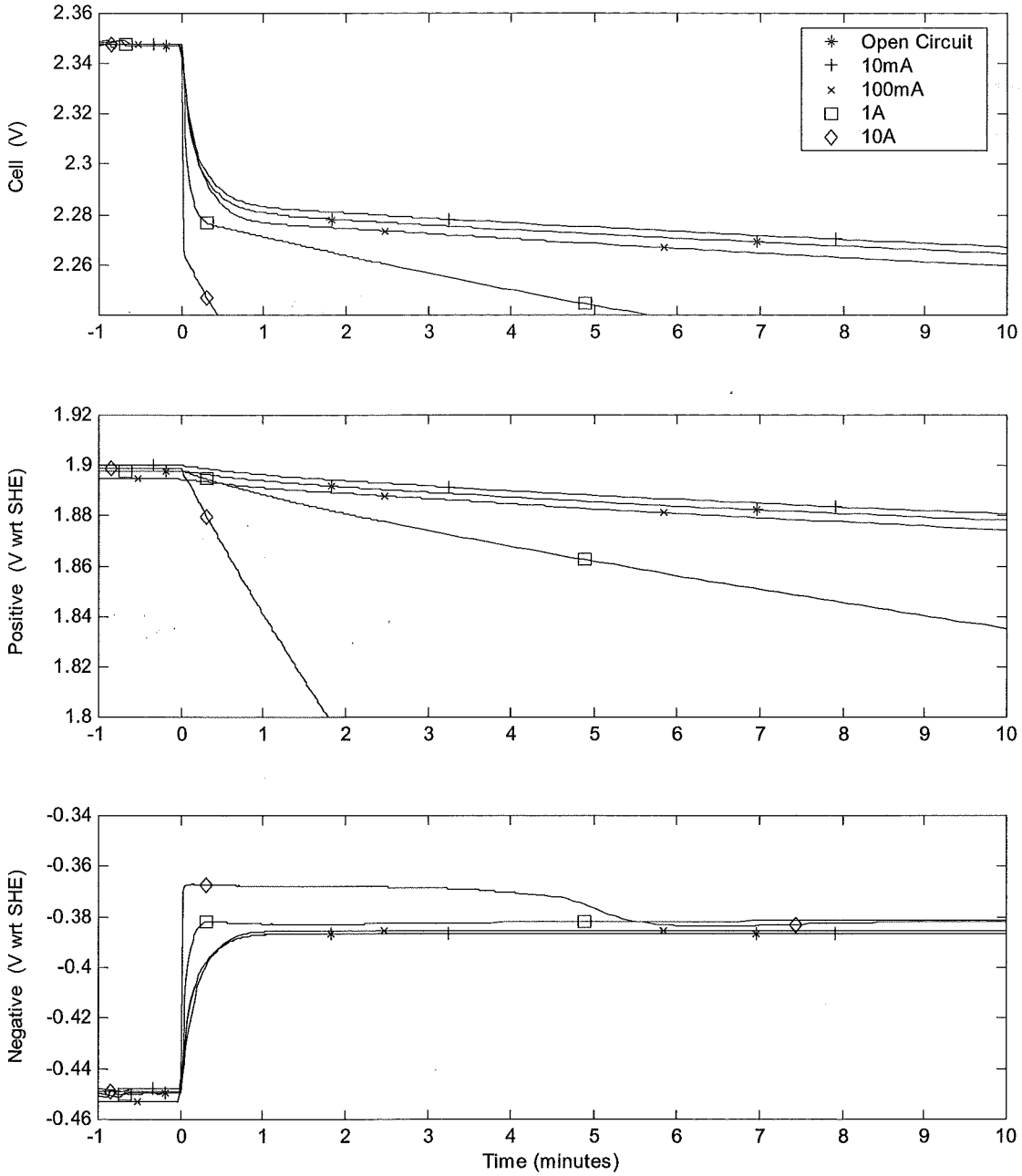

Figure 4.19 Variable Discharge Rate from a 2.35 V Float Charge

Figure 4.19 shows the cell and each electrode's responses to various discharge rates after being float charged at 2.35 V. In keeping with previous analysis, the discharge response of the negative electrode is still significantly quicker than the positive. Less than one minute is required for the negative electrode's polarisation to decay, and during this time there is virtually no change in the positive electrode's potential. It can again be seen that the negative electrode

temporarily overshoots to a slightly lower potential than the fully charged open circuit value before a recovery is made. The magnitude of this overshoot is again dependent on discharge rate, with an overshoot of approximately 16mV for a 100 mA discharge rate. It is noted that the amount of overshoot has increased slightly from that evident in the series of tests conducted at a float voltage of 2.3 V. The electrode potentials prior to the discharge in Figure 4.19 are in reasonable agreement with Tafel Tests 43 and 50, shown in Figure 4.15.

Assuming that the fully charged open circuit voltages of the positive and negative electrodes are 1.74 V and 0.4 V respectively, it can be seen that at a float voltage of 2.35 V there is about 160 mV of positive polarisation, and 50 mV of negative polarisation. With the prior knowledge that the fully charged open circuit terminal voltage is approximately 2.14 V, the 2.35 V float charge suggests that there is 210 mV of polarisation. By simply measuring the initial terminal voltage drop at the beginning of a light discharge, it is possible to estimate that there were 60 - 70mV of negative polarisation, and that the remaining polarisation (140 – 150 mV) is associated with the positive electrode. While there is a slight 10 - 20 mV underestimate of the positive electrode's polarisation, it is clear that the polarisation is well outside the desirable 40 – 80 mV window. If polarisation estimations were to take into account negative overshoot, tighter polarisation estimations may be achieved.

4.3.2.2 Constant Discharge Rate, Variable Float Voltage

Figure 4.20 through Figure 4.24 show the effects float voltage has on the polarisation discharge response. In a given figure, all plots have the same discharge rate. Prior to the discharge the test cell had reached steady state at the indicated float voltage. In all plots the 2.1 V float charge is intentionally below the fully charged open circuit voltage, in order to differentiate the responses of a fully charged cell and a cell not fully charged due to a low float setting. As the 2.1 V float charge plots are not fully charged, polarisation does not exist, and these should therefore not be used for comparison of transient polarisation decay trends.

Figure 4.20 shows the open circuit decay when the float charge is removed. It can be seen that for the plots starting from 2.2, 2.3, and 2.35 V, the negative electrode eventually settles to an open circuit potential of approximately –400 mV after 24 hours. However, in the short-term (10 - 20 minutes) up to 20 mV difference in the negative's potential is evident. This stems from a 10

mV overestimate caused by an overshoot in the trace with strong positive polarisation, and a 10 mV underestimate from the trace with minimal positive polarisation. Similarly, the negative electrode's polarisation decays much faster in the plots demonstrating significant positive polarisation.

If an initial drop in terminal voltage when the float charge is removed is used as an estimate of the negative electrode's polarisation, the accuracy of this estimate is seen to be ±10 mV. This drop should be obvious well within the first hour following the removal of the float charger. If no significant drop is seen and the cell voltage is above the fully charged open circuit voltage (often given in battery specification manual), it may be assumed that the cell is suffering from negative plate discharge. If the terminal voltage decays to the fully charged open circuit voltage within the first hour, it may be assumed that the cell is suffering from positive plate discharge.

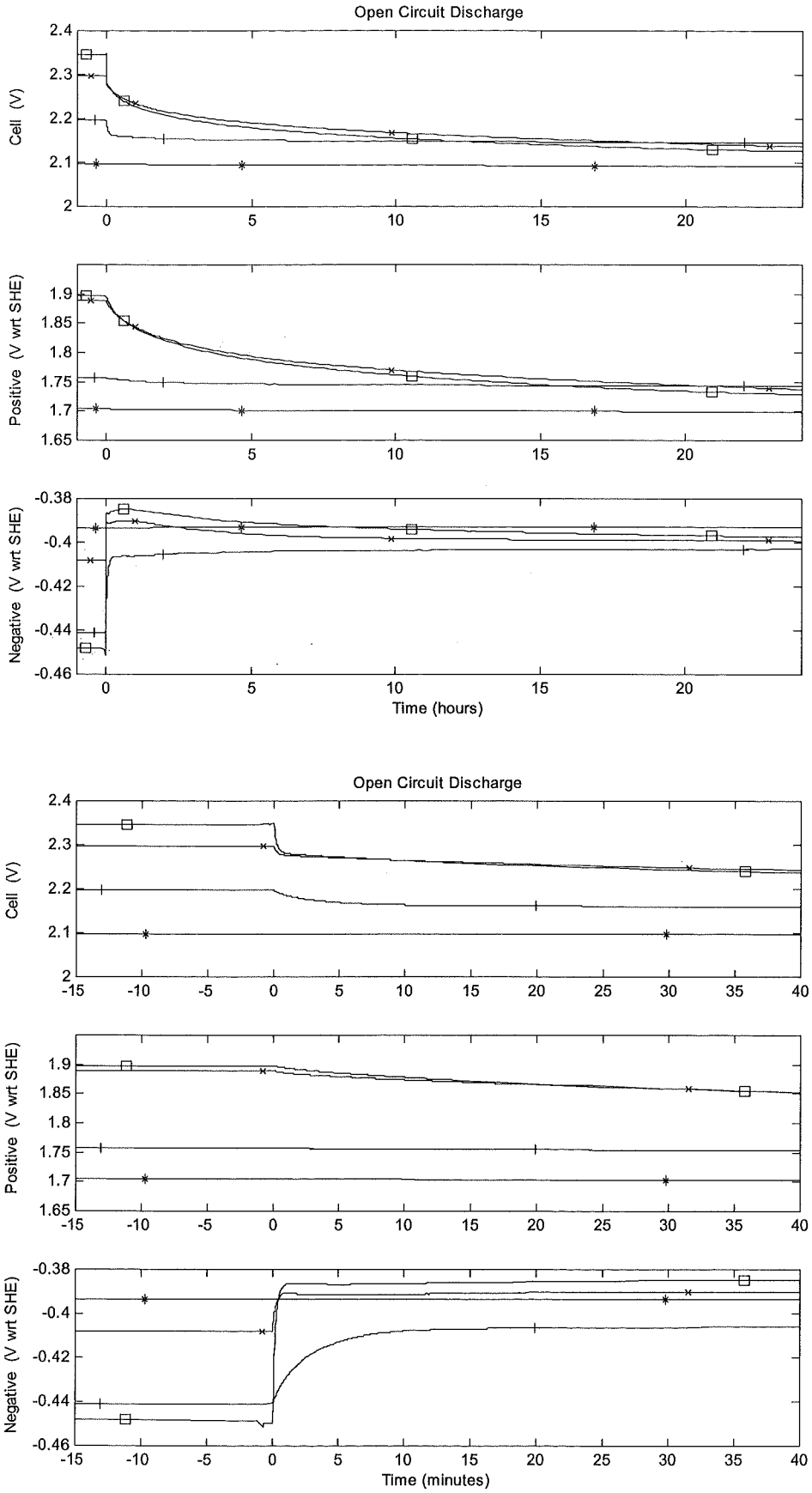

Figure 4.20 Open Circuit Decay from Various Float Voltages (Bottom: magnified time scale)

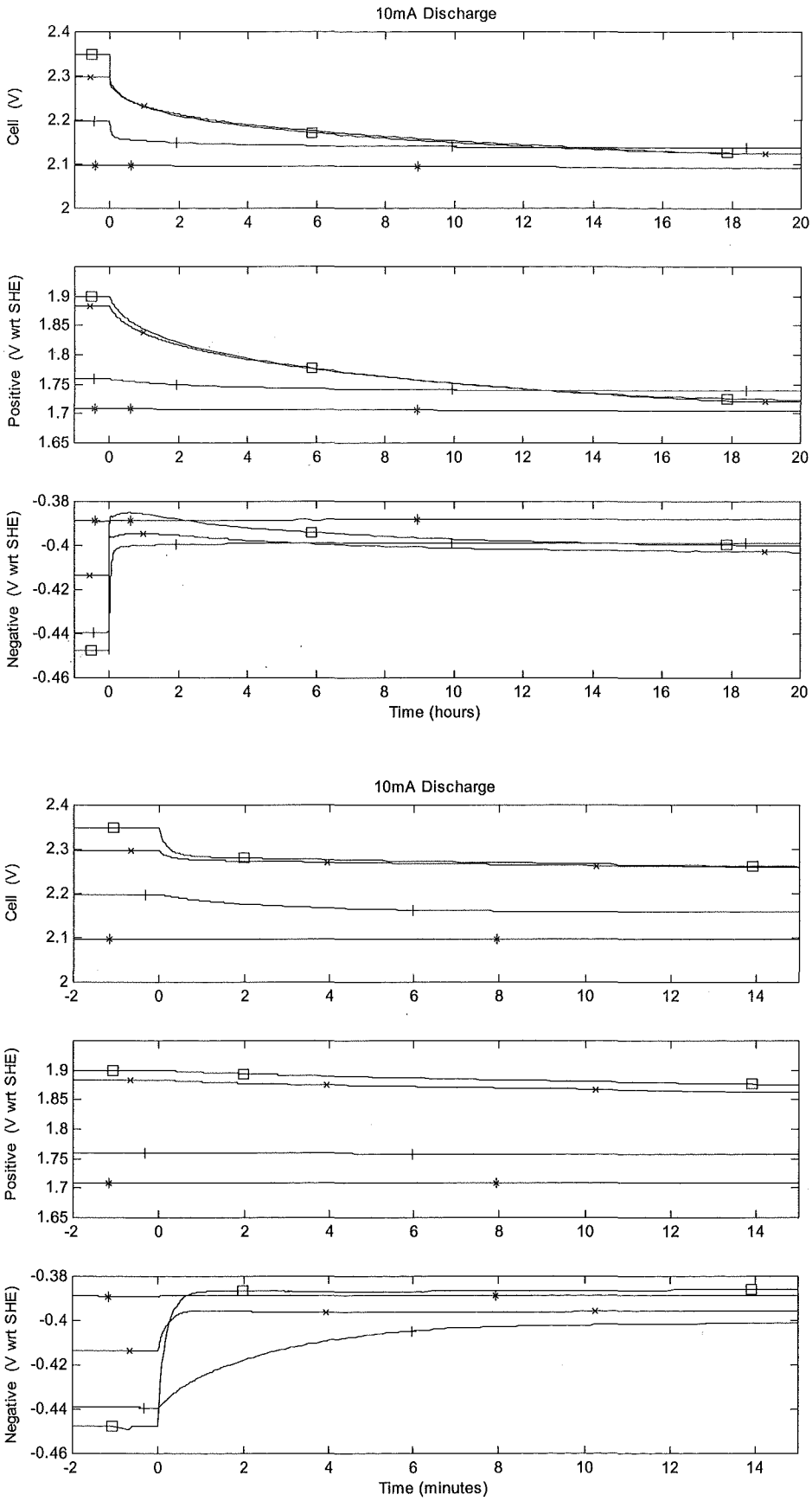

Figure 4.21 10mA Discharge from Various Float Voltages (Bottom: magnified time scale)

The plots in Figure 4.21 show the effects that float voltage variations have on the voltage response of a 275 Ah (C_{20}) cell when a 10 mA discharge is applied. Excluding the plot beginning at 2.1 V, after approximately 20 hours the negative electrode potentials form a relatively tight group around –400 mV. After the same period there is slightly more separation in the potential of the positive electrode, ranging from 1.72 - 1.738 mV. However the lower two traces, starting at float voltages of 2.3 and 2.35 V, do show a gradual Coup de Fouet-like voltage recovery past the plotted region. On a much shorter time scale, it can be seen that the negative electrode of the 2.2 V float charge takes approximately 13 minutes to decay to its fully charged open circuit potential. The negative electrodes of the plots starting at float voltages of 2.3 and 2.35 V show a significantly quicker decay of approximately one minute, and some overshoot. The maximum negative overshoot is seen to be 13 mV, associated with the plot starting from the highest (2.35 V) float charge. Again, it is speculated that the increased rate of negative polarisation discharge and overshoot are due to the level of positive polarisation.

For the higher float voltages it takes approximately 20 hours to discharge the positive polarisation at the 10 mA rate. This is significantly longer than the period of time (up to 15 minutes dependant on associated positive polarisation) taken to discharge the negative polarisation capacitance. With such a vast difference in discharge times it is a relatively simple task to associate the shape and characteristic of the terminal response to that of each electrode. Virtually no change in the potential of either electrode (or the combined terminal response) is seen when a 10 mA discharge is applied to a cell that is not fully charged. The plot with a 2.1 V float charge is estimated to have a SOC of approximately 85%, with no significant change in cell voltage even after 20 hours of 10 mA discharge.

The plot in Figure 4.22 is similar to the previous two plots, however in this plot the test cell is subject to a constant discharge current of 100 mA. Very similar trends are seen, however the time scale is reduced due to the increased discharge rate. It can be seen that the negative electrode still rapidly decays and slightly overshoots its fully charged open circuit potential. The worst case of overshoot is approximately 15 mV, and is similar to that seen in the previous plot. The duration of the polarisation decay of both electrodes has decreased with the increased discharge current. The shortest (worst case) positive polarisation decay takes two to three hours, while the longest time taken for the negative polarisation to decay is four to five minutes. Virtually no change in the positive electrode's potential is seen over this short negative polarisation decay period. It is therefore obvious that separating the responses of each electrode is still possible.

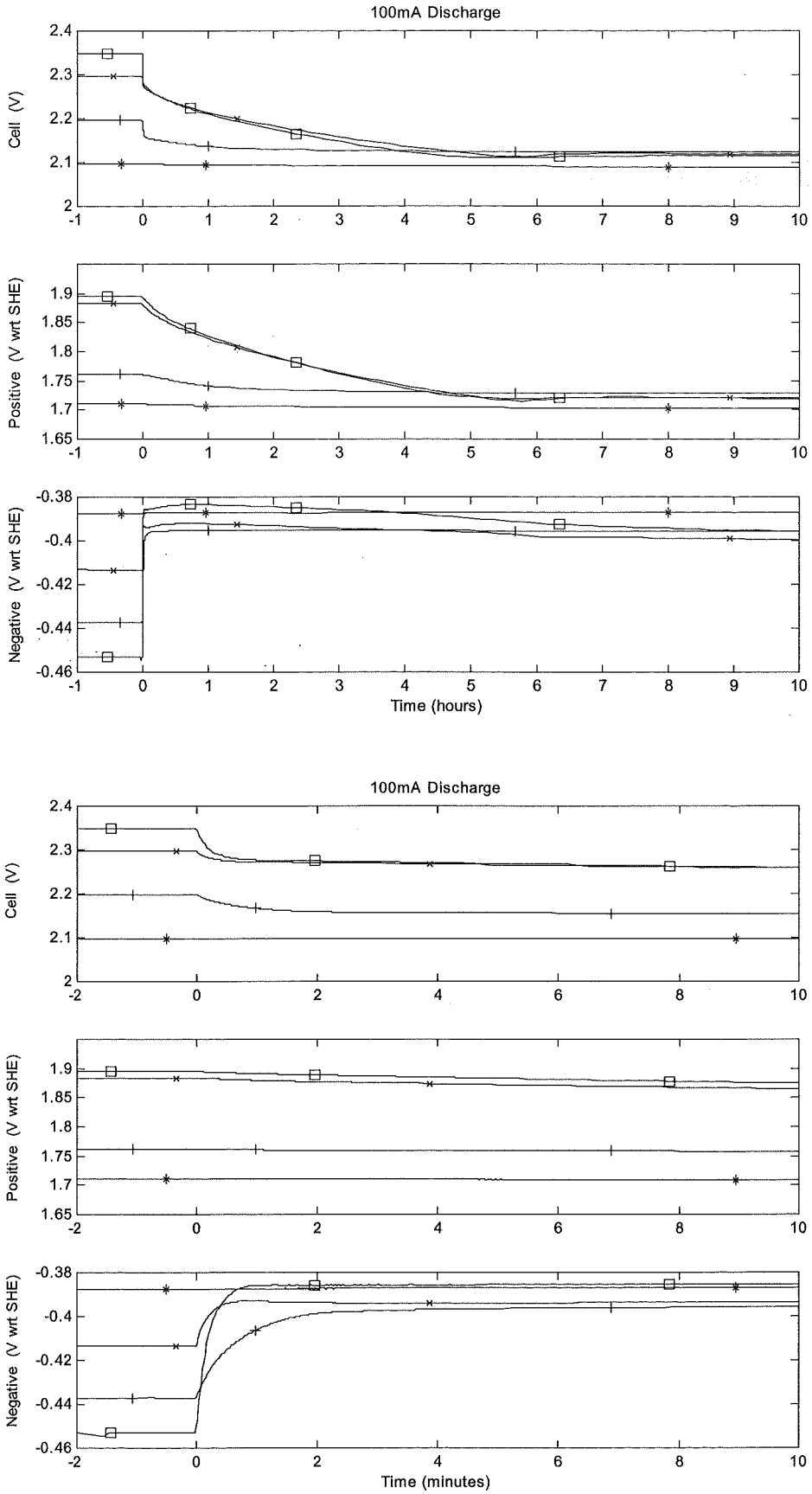

Figure 4.22 100mA Discharge from Various Float Voltages (Bottom: magnified time scale)

As expected, the 1 A constant current discharge plots detailed in Figure 4.23 show significantly reduced polarisation decay times. Dependant on the level of polarisation at the start of the discharge, the positive electrode's polarisation decay ranges from 30 - 45 minutes, and the negative electrode ranges from 18 - 30 seconds. At the 1 A discharge rate, the amount by which the negative electrode temporarily overshoots its open circuit potential is seen to increase. At this rate, overshoot is seen in all plots and has a magnitude ranging from 8 – 18 mV. Overshoot is visible in plots showing low amounts of positive polarisation. The increased level of overshoot is suspected to be due to increased resistive-volt-drops associated with increased discharge current. Due to the increased discharge rate, the overshoot recovery is more obvious, and reasonably well aligned with the end of the positive polarisation decay. A very small response of less than 8 mV is seen in the cell that is not fully charged. This is also believed to be largely due to resistive effects and should not affect the analysis. Using the significant time differences, the terminal response may be separated into that of each electrode, however the increased current causes resistive volt drops to cloud the measured response.

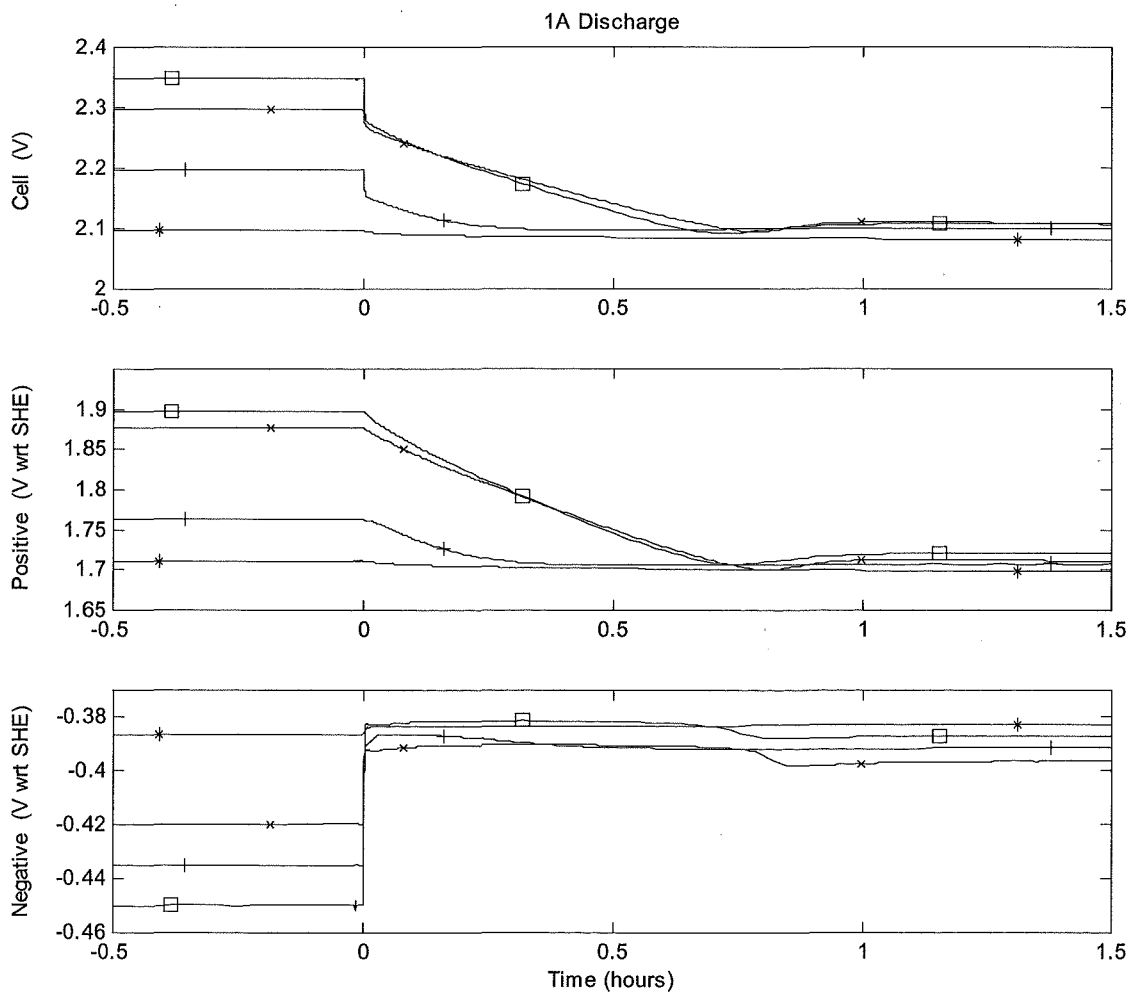

Figure 4.23 1 A Discharge from Various Float Voltages

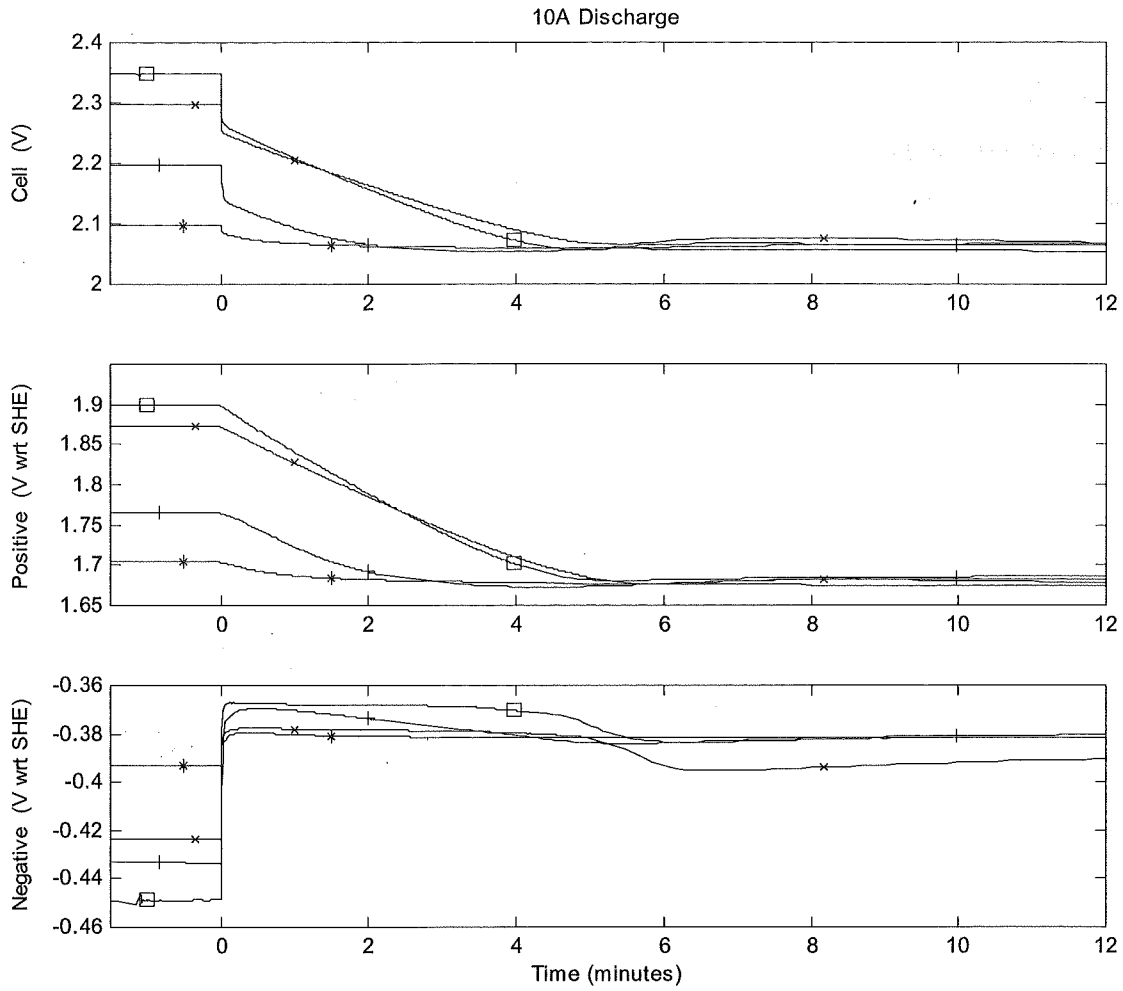

Figure 4.24 10 A Discharge from Various Float Voltages

Figure 4.24 shows the discharge profiles from several float voltages for a cell that is discharged at a constant 10 A rate. As expected, the relatively high discharge rate reduces the time required for the polarisation to decay, with the positive electrode taking three to six minutes, and the negative taking only three to nine seconds. The amount of negative electrode overshoot also increases at this discharge rate, ranging from 20 - 33 mV. However the recovery of the negative electrode still corresponds to the point at which the positive polarisation has become discharged. The increased negative electrode overshoot is believed to be due to resistive volt-drop increases associated with the increased current. This effect is also seen in the plot of the cell that is not fully charged. The plot starting at 2.1 V shows a 30 mV decay after one minute. This is significantly more than the slope expected for the main discharge reaction at a 10 A discharge rate. When the high rate discharge profiles are compared to those of the lower rates (or open circuit), the exponential decays seen at low rates appear to become linear. Assuming the

capacitor model shown in Figure 4.14 is employed, the change in the discharge profile suggests that the high rate constant current discharge is significantly greater than the self-discharge current. Similar characteristics in electrode discharge profiles are present at both high and low rates, however the effect of resistive elements and associated voltage offsets make estimation of the electrode polarisation and distribution more difficult at high discharge rates. There are significant time advantages when using a high rate discharge polarisation estimation test, as the test may be performed in a matter of seconds, rather than tens of minutes as required for the open circuit decay.

4.3.2.3 Transient Test Summary

Through the use of reference electrode testing, it has been shown that the polarisation of both the positive and negative electrodes has a characteristic similar to that of a parallel resistor–capacitor combination. Although capacitors associated with polarisation are very small, when compared to an equivalent capacitance for the main charge-discharge reaction, polarisation capacitance is significant and may be used to analyse the float charge operation of a cell. It has also been shown that there is a significant difference in the capacitance associated with the polarisation of the positive and negative electrodes. The differences between the capacitance of the positive polarisation, negative polarisation, and bulk charge storage may be exploited to determine the polarisation of each electrode within a cell without the use of a reference electrode.

When a cell is discharged, both electrodes within the cell are subject to an identical current. Differences in the effective polarisation-capacitance result in dissimilar discharge duration for each electrode. It has been shown that the duration of the positive electrode's polarisation discharge is typically about 100 times longer than that of the negative. However, this has been seen to range from about 30 to 1400 times. Even at the lowest end of this range, when the negative electrode's polarisation has become discharged, there is negligible change in the potential of the positive electrode.

With analysis of the polarisation discharge profile, it is possible to determine the contribution each electrode makes to the total polarisation. It has been shown that the initial fast transient is almost entirely due to the polarisation decay of the negative electrode. The positive electrode is responsible for the remaining slower polarisation decay to the fully charged open circuit voltage.

If the voltage drop associated with the negative polarisation decay is subtracted from the total polarisation, the amount of positive polarisation may be estimated without further discharging the cell, and more importantly, without significantly altering its state. The total polarisation is a simple calculation of subtracting the settled fully charged open circuit voltage from the float voltage.

Significant reductions may be made to the required test duration by increasing the discharge current. At high discharge rates, the influence of resistive elements within the cell produces current dependent voltage offsets in the measured transient response. At discharge rates up to a similar magnitude to that of the normal float current (approximately C/1000), the effects of these resistive elements are seen to be negligible. At a discharge rate of C/1000, the test duration should typically be less than ten minutes and require less than 0.02% of the cell's capacity to be discharged.

Under certain conditions the rapid response of the negative electrode is seen to overshoot its fully charged open circuit potential. This is normally followed with a slight recovery back to the open circuit potential as the positive electrode's polarisation becomes discharged. While it may be possible to explain the reason of this overshoot and recovery through cell chemistry and reactions, this is beyond the scope of this investigation. It is speculated that as the amount of overshoot appears to increase with positive polarisation, the overshoot is related to the depolarising effect oxygen recombination has on the negative electrode, because less oxygen is produced with lower positive polarisation values. The discharge rate also appears to influence the magnitude of the overshoot, with the amount of overshoot being seen to increase with increased discharge rates. When using recommended float voltages and discharge rates less than C/1000, the amount of negative overshoot is typically seen to be less than 10 mV. Considering the window of optimal positive polarisation is 40 mV wide (40 – 80 mV), a 10 mV offset in the estimate should not severely degrade the test result.

It has been shown that the discharge duration associated with the polarisation of the positive and negative electrodes differs considerably. As the amount of capacitance associated with polarisation is extremely small when compared to the total stored energy, very low discharge rates (or even natural open circuit decay) are required to properly view the profile. Low rate discharge testing also reduces the effects of resistance-based current dependent voltage offsets in the measured response. Analysis of the polarisation discharge profile, between the float voltage

and the stabilised open circuit voltage, allows the polarisation voltage of each electrode to be assessed. Primarily, this may be used to ensure that both electrodes within a cell are fully charged. A secondary function of this is that the positive electrode's polarisation may be used to determine the cell's most appropriate float voltage, thus minimising positive grid corrosion. The hardware needed to perform the analysis requires only an extremely low rate discharge unit, and voltage measurement. This test may be automated and performed on any VRLA cell in field service that has access to the cell's terminals. Due to the low power requirements, both test hardware and installation costs should be minimal.

4.3.3 Temperature Testing

All of the analysis and testing performed in the previous Section was undertaken at a room temperature of approximately 22 °C. It is a commonly accepted guideline that for every 8 - 10 °C increase in battery temperature, the reaction rates within the battery are doubled. It is expected that the overall polarisation decay may vary as the battery temperature is varied, however the response time ratios of the positive and negative should remain similar.

Figure 4.25 compares the steady state (Tafel) characteristic of a cell at temperatures of 25, 35, and 45 °C. It keeping with the above guideline, it can be seen that for a given float voltage, e.g. 2.25 V, the float current approximately doubles with each 10 °C increment in temperature. The drop in current at approximately 2.15 V indicates a slight reduction in the cell potential at which the negative electrode begins to polarise, however overall steady state characteristics remain reasonably consistent as the temperature is varied.

Taking into account the expected variations caused by temperature changes, a comparison of Figure 4.25 and Figure 4.15 shows the plots in Figure 4.25 to be more consistent. After the final planned Tafel plot (Test 50), in an effort to improve test consistency, Tests 51, 52, and 53 were used to make improvements to the Tafel testing control code. Tests 54, 56, and 58 relate to the 45, 25, and 35 °C plots in Figure 4.25. These were performed under identical settling times and maximum slope values. The modifications to the test code included lengthening settling times, more stringent slope requirements, and the addition of an absolute value current slope detection condition. This was necessary as under certain conditions, the current drawn by the cell following a step increase in voltage does not always decay to the steady state value as expected.

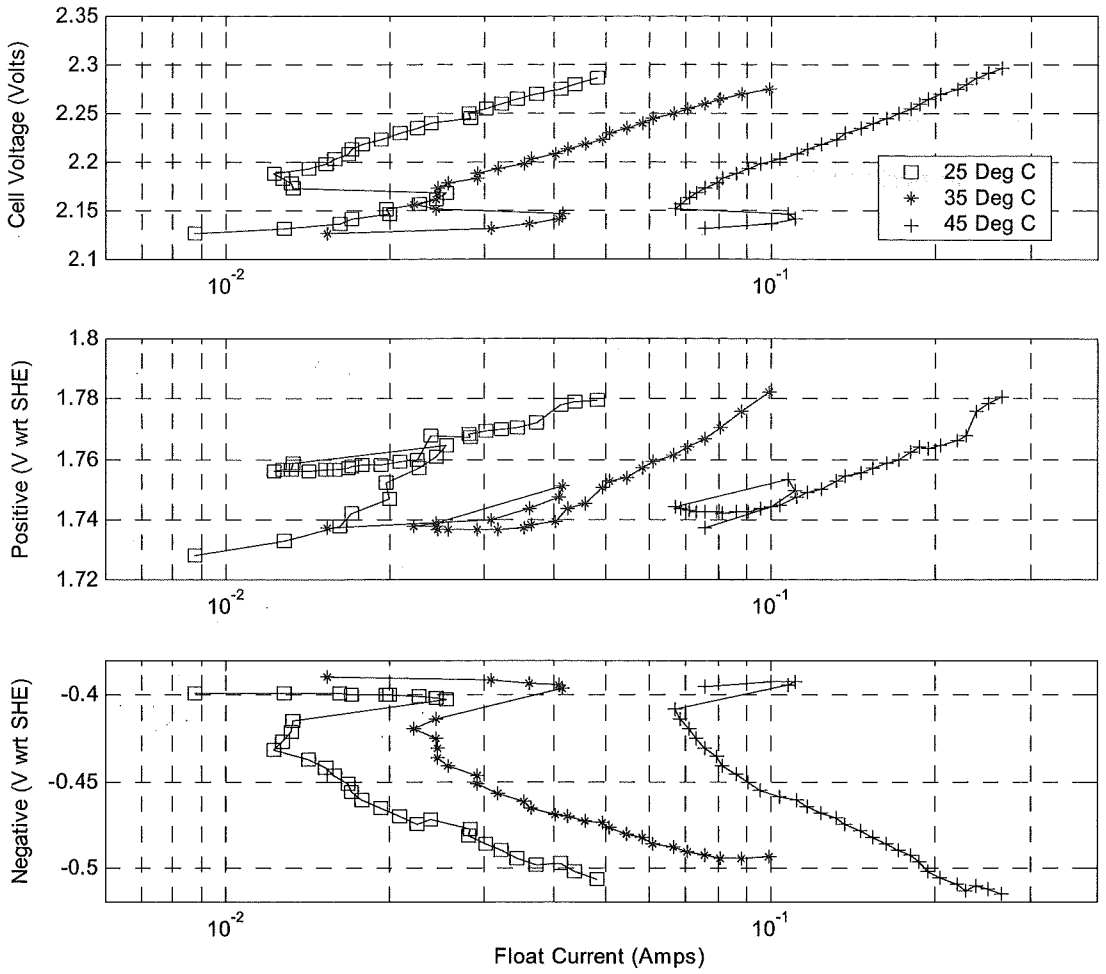

Figure 4.25 Tafel Variations with Temperature

Before the negative electrode begins to polarise, a step increase in cell voltage instantaneously increases the current drawn by the cell. This increased current gradually decays to the steady state value. However, when the negative electrode begins to polarise, the current characteristic changes. A step increase in cell voltage is accounted for almost entirely by polarisation of the negative electrode, while there is only a small increase in the current drawn by the cell. As the cell stabilises to the new float voltage, there is a redistribution of the polarisation gained by the negative. The positive electrode gradually increases its polarisation, with a corresponding decrease in the negative. As the polarisation gained by the negative electrode partially redistributes and stabilises to an increased polarisation on the positive electrode, there is a slight increase in the current drawn by the cell at that float voltage. As an increasing current (+mA/Hr) is greater than the minimum negative slope (-10 μA/Hr) used to detect stable current, an

increasing current would result in premature detection of current stabilisation. In order to resolve this problem, the detection criterion was changed to ensure the absolute value of current slope is less than the stable detection limit.

Although premature detection of a stable current will change the results significantly, the effects should not be noticed due to the two-stage steady state detection used. The first stage of steady state detection requires the current drawn by the cell to be stable, while the second ensures that the electrode potentials are stable. If both current and voltage measurements are stable, all voltage, current, and temperature measurements are made and stored before the float voltage is incremented. Proper (absolute) current stabilisation detection does however significantly reduce the required relay switching in the HP34970a data acquisition unit. This should extend the test acquisition unit's life.

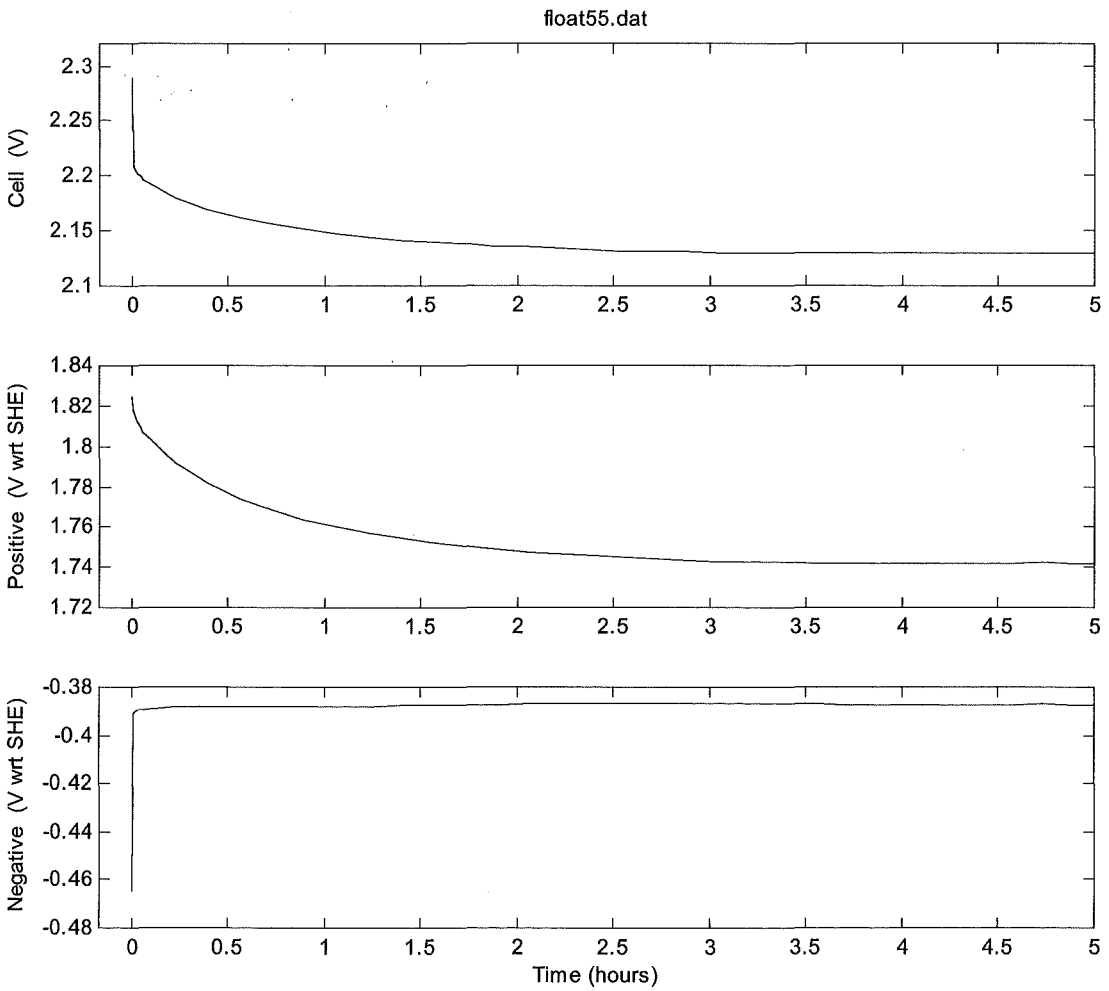

Figure 4.26 Open Circuit Decay from 2.29 V at 45 °C

Figure 4.25 shows how the steady state float characteristics of a cell change with temperature. It can be seen that as the temperature is increased, as expected the characteristic remains largely unchanged apart from an increase in current. Figure 4.26 shows an open circuit decay of a cell at 45°C. It can be seen that from the float voltage of approximately 2.29 V, there is a rapid and almost instantaneous decay of the negative electrode's polarisation to its fully charged open circuit potential. The positive electrode is seen to take approximately four hours to decay to its fully charged open circuit potential. During the short period required for the negative electrode's polarisation to discharge, there is virtually no change in the potential of the positive electrode. While the increased temperature has significantly reduced the time required for the polarisation to discharge in comparison with the plots at 22 °C in Section 4.3.2, the large difference in discharge duration of each electrode is still present. Transient analysis of a cell's terminal voltage profile during a low rate (or open circuit) discharge is still able to resolve the response of each electrode within the cell, and determine their polarisation. Cell temperature may alter the overall duration of the transient test, however the relative response differences of each electrode still exist.

4.4 References

[1] Institute of Electrical and Electronics Engineers, Inc., *IEEE Recommended Practice for Maintenance, Testing, and Replacement of Valve-Regulated Lead-acid (VRLA) Batteries for Stationary Applications,* IEEE Std 1188-1996, Annex A, p 11.

[2] J. Tafel, Z phys. Chemie, 50 (1905), p 641, as cited by: D. Berndt, *Maintenance Free Batteries, Lead-Acid, Nickel/Cadmium, Nickel/Metal Hydride, A Handbook of Battery Technology,* Second Edition, Research Studies Press, 1997, p 65.

[3] Radiometer Analytical, *Complete Systems for Electrochemical Research,* Product Brochure, www.radiometer-analytical.com.

[4] Bellcore, *Generic Requirements for Accelerated Life Testing of Valve regulated Lead Acid Batteries at High Temperature,* Technical Reference TR-NWT-001200, January 1992, Issue 1, pp 2-7.

[5] S. S. Misra, A. J. Williamson, *On Temperature Compensation for Lead Acid Batteries in Float Service: Its Impact on Performance and Life*, Proceedings of INTELEC, 1996, 2-1, p 27.

5 Model Implementation

The float charge model shown in Figure 4.14 was developed to allow steady state and transient float charge features of both electrodes to be modelled. While the components and their layout have been selected to reproduce the overcharge response and to aid understanding of float charge voltage distributions, simulation of this model is complicated by the two switches that short (eliminate) the overcharge components. With two switches, four (2^2) separate simulation circuits are required so that all combinations of switch states are represented. On-Off switches do not allow smooth transitions to be made from one operating state to the next. Replacing the switches with variable resistors that change from a short (0 Ω) to open circuit (MΩ) may provide smooth transitions. However 0 Ω resistors pose computation problems (divide-by-zero errors), as circuit nodes have effectively been eliminated. While the model functions similarly to the circuit in Figure 4.14, for simulation simplicity it has been simplified to that shown in Figure 5.1. The dual capacitors representing the bulk and overcharge capacitance of each electrode in Figure 4.14 are combined into a single variable capacitor which 'switches' between the bulk and overcharge capacitance values. A smoothly transitioned 'switch' may be achieved through the implementation of an appropriate mathematical function.

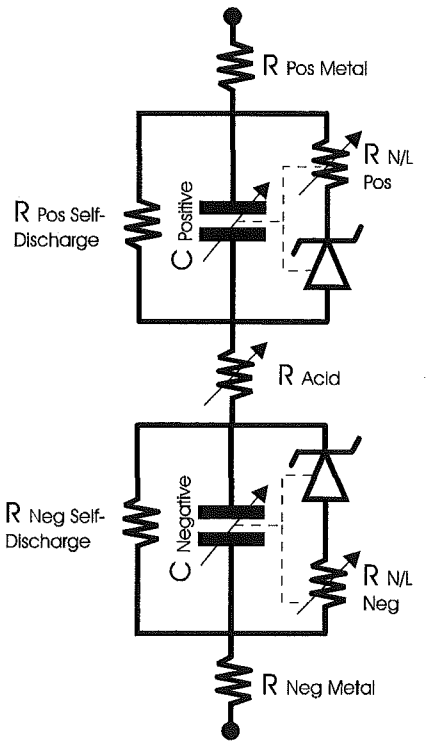

Figure 5.1 Implemented VRLA Battery Float Charge Simulation Model

5.1 Model Components

Matlab and the Matlab Ordinary Differential Equation (ODE) solver were chosen as the environment for the development and simulation of the VRLA battery float charge model shown in Figure 5.1. While it should be possible to simulate the cell model in any electrical circuit simulation package, modelling of non-standard components such as the non-linear (logarithmic) overcharge resistors and the dual value capacitors may be difficult to implement in some of these packages. Matlab provides an environment that does not have any limitations on how components are specified. Component values may be specified as functions of other components, or as functions of the present state (voltage-across or current-through) of other components in the circuit. Similarly, piece-wise modelling can be implemented through the use of 'if - then' statements. This is useful for implementing components such as zener diodes.

Section 5.2 details the Matlab based software that was developed to model the float charge region of VRLA battery operation. The software is broken into three components: component sizing, model equations, and simulation control. In the remainder of Section 5.1 the individual components of the model are described, along with how appropriate values were selected. Section 5.2 describes the 'run time' simulation software, which allows the supplied voltage and current to be adjusted throughout the simulation, so that different or altered operating conditions can be shown. Section 5.3 details the underlying differential equations that allow the model to be simulated.

5.1.1 Non-Linear and Self-Discharge Resistors

Section 2.2.1 detailed how Tafel plots are often used to describe the steady state float operation of a VRLA cell. As a Tafel plot represents the steady state characteristic, no net charging or discharging of the cell exists. Virtually all of the energy supplied to the cell through the float charge is consumed in the internal gas cycle. Eventually, this energy must either be dissipated to the atmosphere as heat, or lost through gas venting. As there is no net change in stored energy during steady state float, resistance is the obvious choice of model component. However, the straight lines of a Tafel plot are produced only when a linear/log graph is used to plot polarisation against float current. This suggests that a single or constant value resistor is not appropriate. The resistance value required to replicate Tafel characteristics must be a function of

either the electrodes' polarisation, or the applied float current. The top left plot of Figure 5.2 shows a single Tafel line that has a slope of 100 mV per decade, and a polarisation of 250 mV at a float current of 1 A. In the lower plot of Figure 5.2, the variation in resistance required to produce the Tafel line is shown as a function of float current, while in the right hand plot of Figure 5.2 the required resistance is plotted as a function of the electrodes' polarisation.

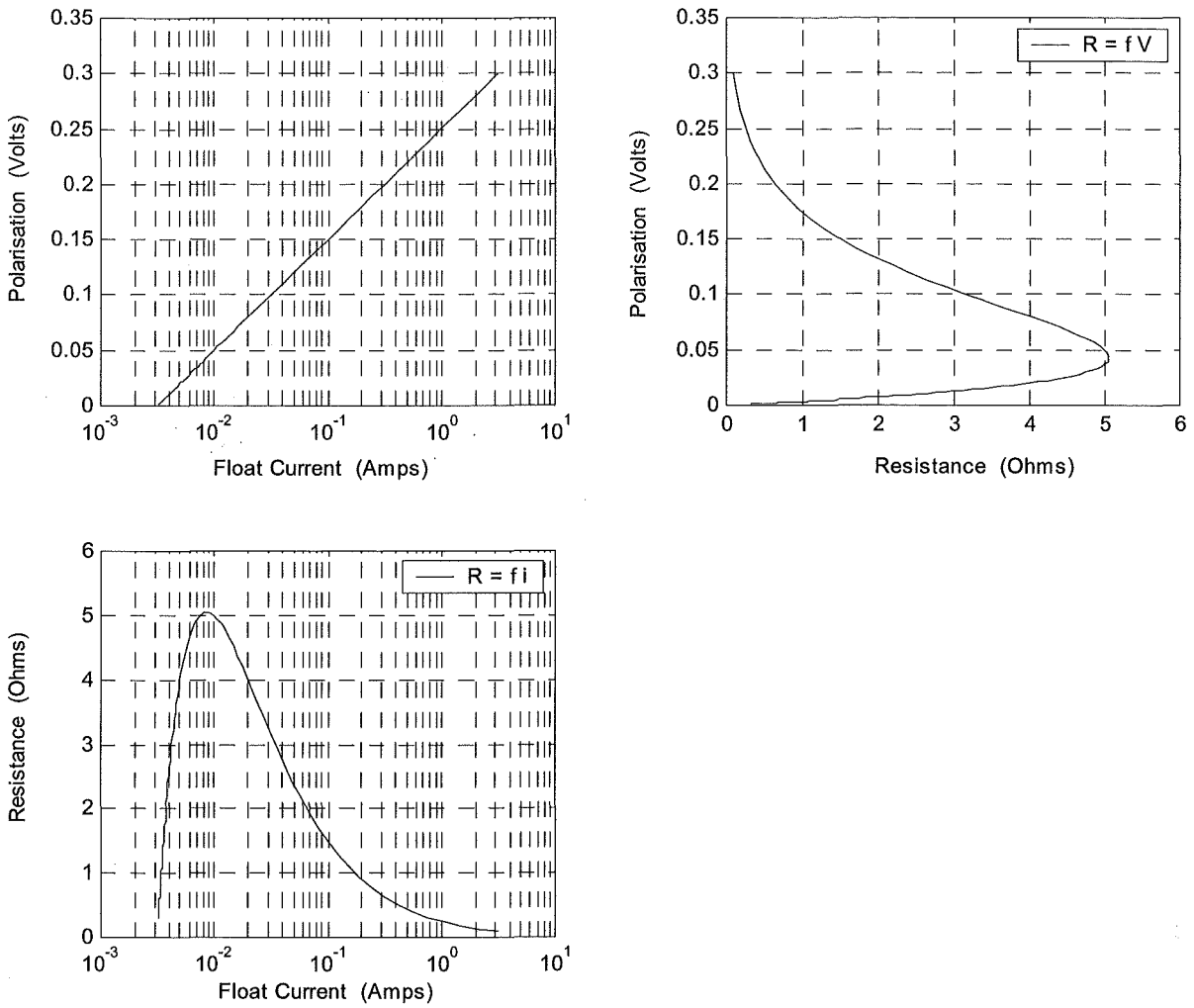

Figure 5.2 Equivalent Overcharge Resistance as a Function of Float Current or Polarisation

A Tafel line may be specified through any two of the following: 1) Tafel intercept (current at zero polarisation); 2) Tafel slope; or 3) Polarisation at a point (e.g. 1 A). The relationships between these points are graphically shown in Figure 5.3. The component value selection program vrla_part_size.m uses the specified float voltage, the float current, the polarisation of the positive electrode at the float voltage, the open circuit voltage, and each electrode's Tafel

slope to calculate the polarisations of each electrode at 1 A. By doing this, the location of the positive Tafel line is directly defined by the specified operating point. The location of the negative Tafel line is used to balance the equations concerning the total polarisation supplied to the cell at the float voltage. Figure 5.3 shows the relationship between the possible variables used to describe a Tafel line and how the required simulation parameters are obtained by the software vrla_part_size.m. The simulation model required the parameters shown in **bold** (Tafel slope and polarisation at 1 A), while the characterisation (specifying) parameters are shown in *italics*. Experience has shown that the location of the positive Tafel line is reasonably stable over time, however the location of the negative Tafel line has been seen to drift considerably. The Tafel slopes of each electrode have also been seen to remain reasonably consistent over time.

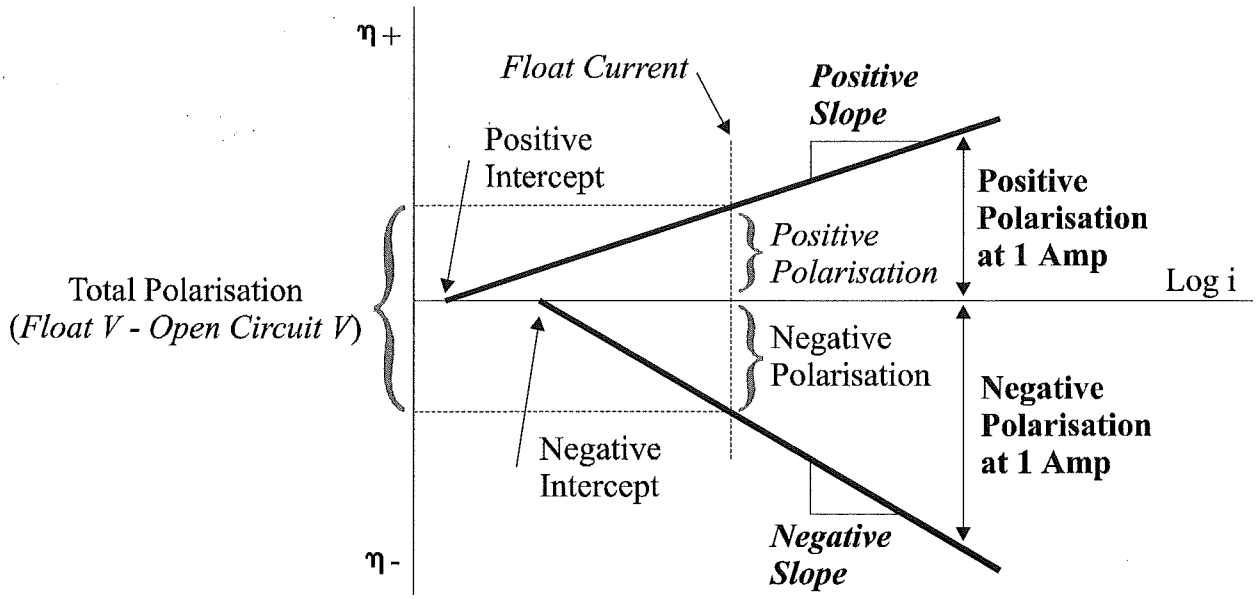

Figure 5.3 Model Specification of the Overcharge Tafel Characteristic

Equation 29) shows how the non-linear overcharge resistance is calculated as a function of the polarisation voltage (difference between the capacitor and zener voltages) and the model parameters (polarisation at 1 A and Tafel slope). This function may be easily scaled to represent any desired Tafel line, and was used to produce the polarisation versus resistance curve shown in Figure 5.2. Experimental polarisation data may show a slight deviation from a straight Tafel line, especially at low polarisation values. While for most purposes a straight Tafel approximation is satisfactory, if a more precise simulation is necessary Equation 29) may be modified as required.

$$r = \frac{p}{10^{\left(\frac{p-p1}{s}\right)}} \qquad 29)$$

where: r = resistance
p = polarisation (volts)
$p1$ = polarisation at 1 A (volts)
s = Slope (volts / decade)

The value of the self-discharge resistor is selected so that the minimum current required for polarisation (Tafel intercept) is drawn at the point when polarisation begins, i.e.:

$$R_{\text{Self-discharge}} = \text{zener\_voltage} / \text{Tafel\_intercept\_current} \qquad 30)$$

Subtracting the capacitor voltage from the diode's zener voltage produces the electrode's polarisation. Ohms law is then used to calculate the current flowing through the non-linear (overcharge) resistor based on the polarisation and the resistance value. Similarly, the capacitor voltage and the self-discharge resistance are used to calculate the self-discharge current. Figure 5.1 shows the self-discharge resistor in parallel with the series connected overcharge resistor and zener diode combination. This is not entirely correct, as the self-discharge resistor should be in parallel with the zener diode. It has been implemented as shown in Figure 5.1 however, in order to avoid computation problems. At and below the fully charged open circuit voltage, the non-linear overcharge resistor must have no resistance, however this introduces divide-by-zero computation problems. To compensate for the current through the self-discharge resistor during overcharge, this self-discharge current is subtracted from the overcharge resistor current before the differential equations are solved.

5.1.1.1 Minimum Grid Corrosion Point – An Observation:

In Figure 5.2 a voltage- or current-dependant equivalent resistance that replicates Tafel characteristics is shown. While the computation of this equivalent resistance may be achieved with a simple Ohms law calculation at each steady state operating point (voltage-current pair), plotting this equivalent resistance against current or voltage reveals an interesting characteristic. It can be seen in the top right plot of Figure 5.2 that there is a peak in resistance at approximately 43 mV. The corresponding Tafel line has a slope of 100 mV per decade and 250 mV of

polarisation at 1 A. Interestingly, the peak in resistance occurs within the accepted window (40 - 80 mV) for minimum grid corrosion. While this is purely an observation derived from a mathematical phenomenon, it does entice further investigation.

Figure 5.4 shows the corrosion current versus electrode potential for several lead alloys by several experimenters. While it is acknowledged that the various tests were performed under differing conditions with different techniques, and that direct comparisons can therefore not be made, general trends can be identified. For reference, a Tafel slope of 80 mV per decade has also been shown for oxygen evolution. It can be seen that the Tafel slopes for the corrosion of lead and lead alloys vary from 170 mV per decade (Rogatchev (1983) 10.6%) to 255 mV per decade (Willihnganz).

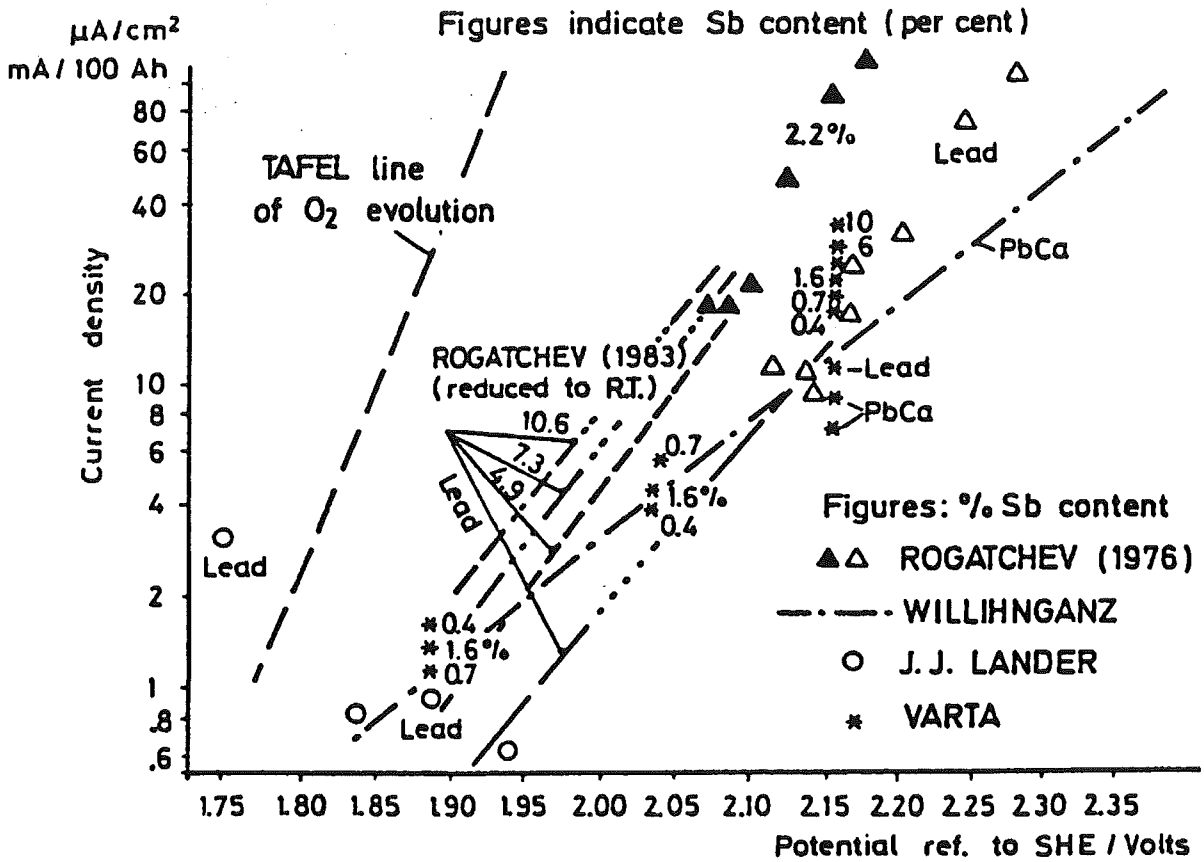

Figure 5.4 Corrosion Rate of Lead and Lead Alloys at Constant Potential[1]

Corrosion is a complex reaction, influenced by external parameters such as temperature, electrode potential, and acid concentration, as well as by internal parameters including the

composition of the corroding alloy, metal-lographic structure, and local distribution of alloying additives. Corrosion rate measurement must be based on a number of general rules combined with empirical experience, as exact evaluation may not be possible[1]. However the observation detailed below, based on the characteristic of the electrode as a whole, displays some interesting features and similarities to experimental data.

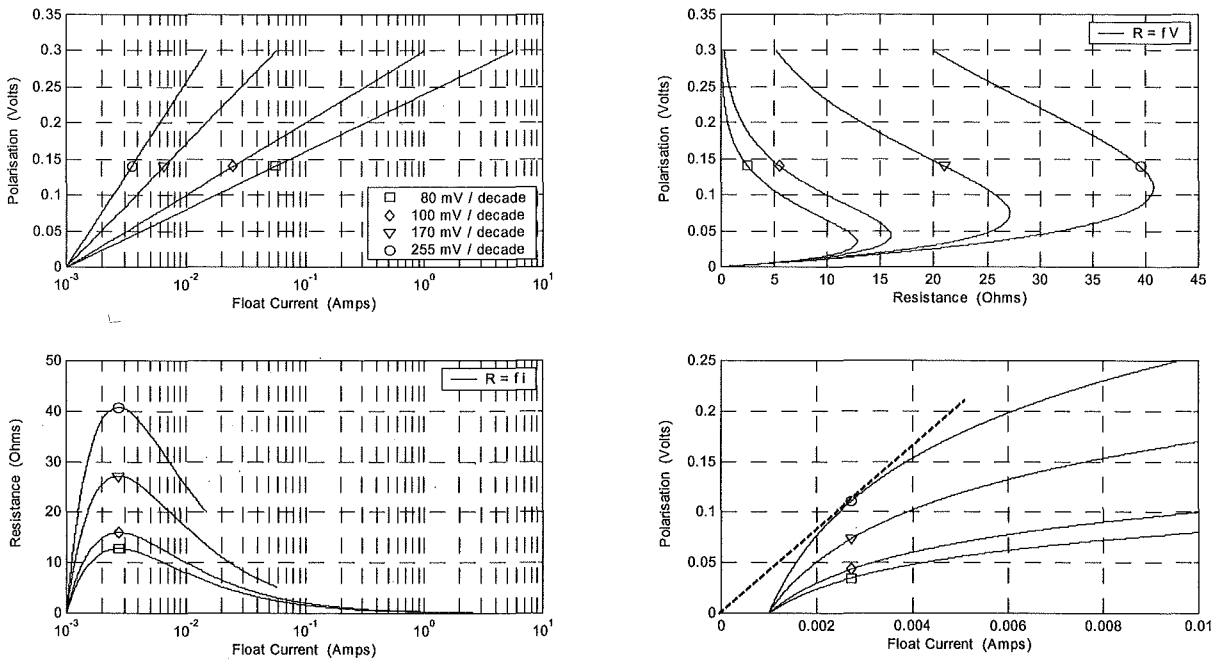

Figure 5.5 Variation in Equivalent Resistance with Tafel Slope

Figure 5.5 compares the Tafel slopes for oxygen evolution and the corrosion rates of several lead alloys shown in Figure 5.4. The Tafel lines have all been normalised to have a zero polarisation intercept point at 1 mA. The equivalent resistances required to replicate the Tafel lines have been calculated and plotted against polarisation (top right), and float current (bottom left). The equivalent resistance versus float current plot shows that the current associated with the peak in equivalent resistance remains constant regardless of the Tafel slope. However the polarisation at which the equivalent resistance peak occurs increases with the Tafel slope.

When a linear axis is used to plot the polarisation-voltage/float-current data, the reason for the occurrence of the peak in the equivalent resistance becomes apparent. The same polarisation versus float-current data shown in the top left plot of Figure 5.5 has been re-plotted in the lower right plot on a linear axis. With a conventional fixed value resistor, current is a direct function of

the applied voltage, and a voltage-current plot of such a resistor will pass through the origin. The bold line in the lower right plot of Figure 5.5 shows that the point at which a line starting at the origin forms a tangent with the polarisation-current curve corresponds to the peak in the equivalent resistance. At polarisations lower than this tangent point, the curve has a steeper slope, indicating increased resistance, while at polarisations above this tangent point, decreased resistance is indicated by a gradient lower than the fixed resistance.

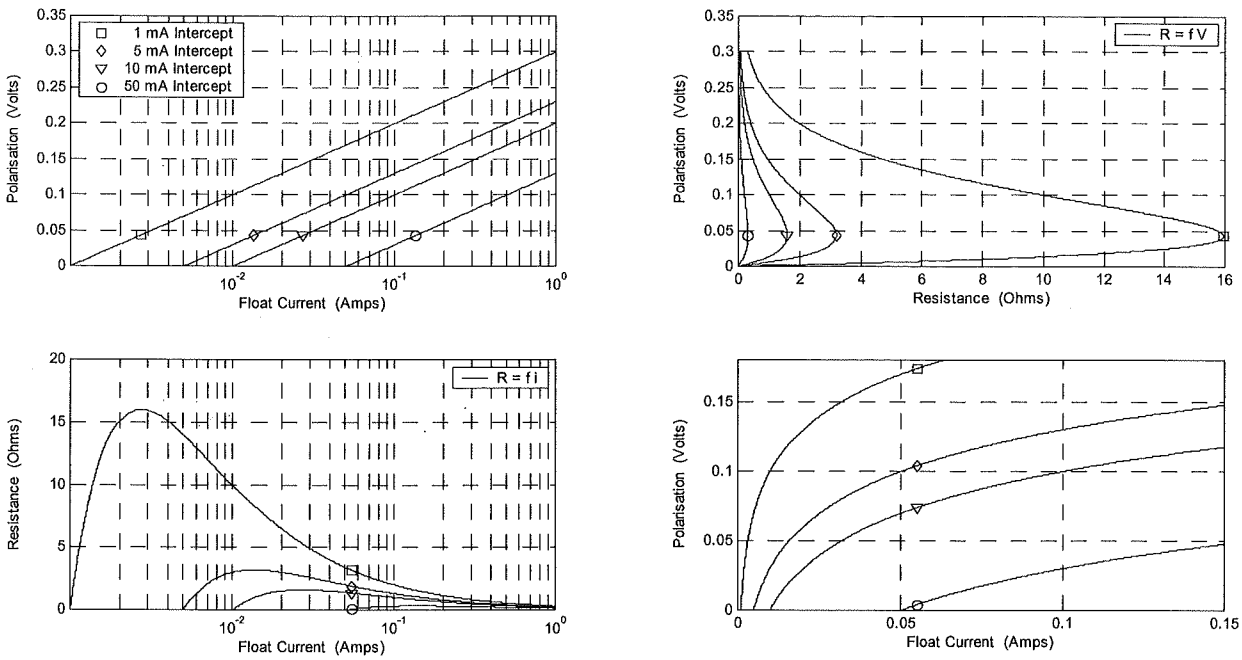

Figure 5.6 Variation in Equivalent Resistance with Intercept Point

Figure 5.6 shows four Tafel lines with an identical slope of 100 mV per decade, separated by differences in the zero polarisation intercept point. It can be seen in the plot of equivalent resistance versus polarisation that despite the differing Tafel intercept point, the polarisation at which the peak in resistance occurs remains constant. The plot of the float current versus equivalent resistance shows that the float current at which the peak resistance occurs increases in association with the zero polarisation intercept point.

The Tafel slope determines the polarisation at which the peak in equivalent resistance occurs. The current of this peak is determined by the current at which the zero-polarisation intercept point occurs. In batteries of differing capacities, the float current is expected to increase proportional to the capacity. A Tafel plot of the positive electrode's polarisation would however

have the same slope regardless of the cell's capacity. As the Tafel slope remains constant, the polarisation at which the peak in the equivalent resistance occurs would also remain constant.

As the lowest Tafel slope (i.e.: oxygen evolution) dominates the polarisation of the electrode by consuming the most current to support the reaction, the significance of the Tafel plots relating purely to the rates of grid corrosion is reduced. The overall polarisation of the electrode is set through the dominant reaction of oxygen evolution. The current consumed through grid corrosion is determined by the polarisation on the electrode rather than by the current flowing through it. Therefore, as the float current is increased, the change in current consumed through grid corrosion is significantly reduced from that expected by the corrosion Tafel line, despite the grid corrosion Tafel plots having a greater slope.

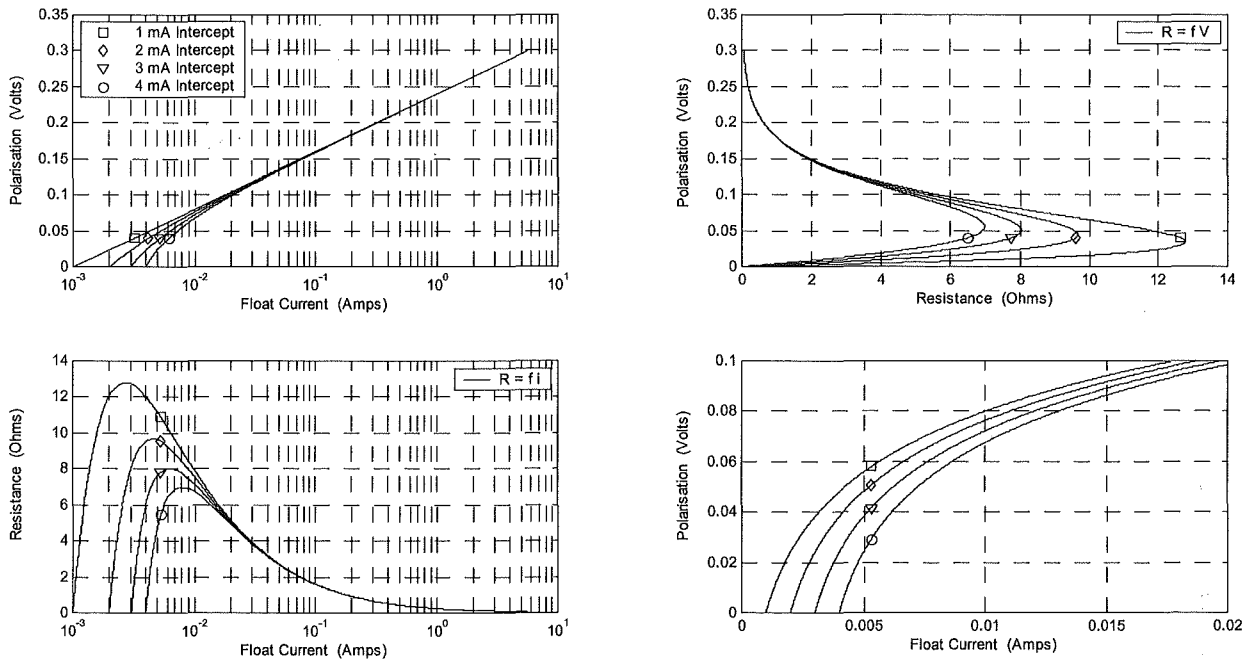

Figure 5.7 Variation in Equivalent resistance with Grid Corrosion Correction

Figure 5.7 shows the effects of adding grid corrosion currents of 1, 2, and 3 mA to an 80 mV per decade, 1 mA intercept, Tafel line representing the evolution of oxygen. The introduction of a slight curve can be seen at low polarisations, as the corrosion current becomes significant in comparison with the oxygen evolution current. The increase in corrosion current required to produce an increase in polarisation is insignificant when compared to that associated with

oxygen evolution. For this reason, Tafel plots are often simplified to a straight line associated with oxygen evolution, rather than the slight curve seen at low polarisations.

The curved traces in the top left plot of Figure 5.7 are characteristic of that expected for the positive electrode (combining oxygen evolution and grid corrosion) in a VRLA battery. Interestingly, the equivalent resistance versus polarisation plot, seen in the top right of Figure 5.7, has resistance peaks occurring between 35 and 56 mV. The oxygen evolution Tafel slope used to generate these plots was 80 mV per decade, however 90 mV per decade has also been commonly stated[2 3]. When the same corrosion current levels used in Figure 5.7 are added to an oxygen evolution slope of 90 mV per decade, the polarisation range associated with the peak equivalent resistance is shifted slightly, and is seen to be 39 - 63 mV. While this range appears very similar to the general range accepted by battery chemists to have minimum corrosion, no associated verification has been undertaken. Any attempt to verify a correlation between the polarisation at which the peak in equivalent resistance occurs, and the polarisation producing minimum corrosion, would require significant electrochemical testing which is beyond the scope of this thesis. At this stage, the occurrence and similarities of this phenomenon must be considered purely coincidental. However, the similarities have been noted, and the influences producing the peak in equivalent resistance, and its location, have been explained.

No verification or proof has been undertaken to correlate the mathematical phenomenon of the peak equivalent resistance point with the minimum grid corrosion point. However, the often debated point or range of positive polarisations associated with minimum grid corrosion appears almost identical to the values obtained with a little mathematical manipulation of commonly found experimental data. This may warrant further experimental investigation and analysis. If a correlation between the mathematical peak in equivalent resistance and the corrosion minimum were experimentally proven, a chemistry free method of assessing the optimal positive polarisation for maximum life would be facilitated.

5.1.2 Energy Storage Capacitors, Bulk and Overcharge

Section 5.1.1 described the model components required to reproduce the steady state overcharge characteristics of a VRLA cell. This Section will describe the energy storage elements required to replicate the transient response of a VRLA cell as it moves from one steady state operating

point to another. Section 4.2 showed how a relatively high rate of constant current discharge (as compared to the natural self-discharge) produced a linear decay in the polarisation of each electrode. As some form of energy storage is required to slow the transition from one steady state operating point to the next, and due to the linear voltage decay produced when a constant current is drawn from a cell, capacitors are the obvious choice of model component. The model in Figure 5.1 employs a single variable capacitor for each electrode. Effectively, each of these capacitors has two values, one value for the bulk energy storage mechanism associated with the main charge-discharge reaction, and a second value associated with the polarisation transient response, which is significantly smaller. Although it may appear that energy is not conserved while the capacitor's value at each electrode is varied from the large bulk storage value to the smaller overcharge value, energy contained in the bulk storage capacitor is not lost. Rather, it is made unavailable during overcharge. When the float charge is removed and the overcharge voltage decays, the variable capacitor's value returns to that of the bulk storage, and its stored energy becomes available again.

The size of the total (positive plus negative) bulk storage capacitance is calculated from the voltage difference between the fully charged rest voltage and the discharged rest voltage, the discharge current, and the discharge time ($C = i \bullet dt / dV$). Assuming that the fully charged and discharged rest voltages are 2.14 and 1.9 V, the equivalent capacitance required to represent the bulk storage is approximately 15,000 Farads/Ah. Alone, this capacitor representation will produce an uncharacteristic linear voltage decay when a constant current discharge is applied. While this is significantly different to a typical constant current discharge curve, the model is targeted at the overcharge region of VRLA battery operation, and only a basic representation of the bulk storage is required. However, the discharge profile is significantly improved if the variation in the electrolyte resistance is modelled during the discharge, as will be shown in Section 5.1.4. Furthermore, as only a single capacitor is used to model the bulk storage of each electrode, the reduction in apparent available capacity with increased discharge rate is not modelled. Similarly, the bulk recharge characteristics are not accurately modelled. By applying a current-limited constant voltage recharge, it is expected that the current limit will be exercised until the cell voltage has risen to the charger voltage, and that this voltage will then be maintained as the charge current exponentially decays to the float value. As the bulk storage of each electrode is modelled by a single capacitor, when the float voltage is reached, the current drops directly to that required for float charge. If improved modelling of the bulk discharge and

recharge characteristics is required, a distributed capacitor–resistor ladder type circuit may be necessary. This may be optimised to replicate the apparent reduction in available capacity seen in high rate discharges, and also to provide the exponential decay in recharge current when recharging with constant voltage. A distributed capacitor-resistor ladder type circuit should attempt to replicate the mass transport and kinetic limitations within a cell. However, as the developed model is intended for float charge analysis, the basic single capacitor representation of bulk storage at each electrode is sufficient, and requires minimal calibration.

The total capacitance used to model the main charge-discharge reactions must be distributed between the two electrodes. The software vrla_part_size.m, used to calculate the component values for the simulation model, contains a parameter 'pos_bulk_percent' to allow the total bulk capacitance to be split as desired between the positive and negative electrodes. This allows each electrode's voltage-change ratio and the voltage supported on each electrode to be defined. For example, if the 'pos_bulk_percent' were set to 60, the positive electrode would provide 60% of the cell's voltage, and 60% of the change in the terminal voltage during discharge would be attributed to the positive electrode. As series connection decreases the total capacitance, the distribution of the total bulk-storage capacitor must be such that each electrode produces the desired voltage-change during discharge, and that the series combination of the two capacitors still equals the required total. While the theory of sizing the capacitance of each electrode to produce a desired voltage-change during discharge is valid, the dominant reason for the characteristic shape of the discharge profile is due to an increasing electrolyte resistance. Voltage drops associated with electrolyte resistance overshadow the differences in each electrode's voltage decay. At high discharge rates, the apparent distribution of discharge voltage-change is more heavily influenced by the simulated location of the reference electrode (division of acid resistance) than the actual voltage-change on each electrode. The component value selection software also calculates a voltage offset (to be added to the model's centre, or reference, point). This offset voltage is the difference between the model's centre point voltage (centre of acid resistance) and the voltage that would be produced when a $Hg/Hg_2SO_4/K_2SO_4$ reference electrode is used on a cell in the same charge state. The offset voltage effectively normalises the voltage obtained by the simulated reference electrode as the 'pos_bulk_percent' is altered. The simulated reference-electrode does not reveal the actual voltage supported on each electrode's capacitor. A 'pos_bulk_percent' value of 75% was found to be the most suitable and has been used for all simulations.

Having calculated the total required bulk storage capacitance and an appropriate distribution for each electrode, the capacitors required to produce the overcharge transient response must also be calculated. Due to variance between batteries, no precise method of determining the overcharge capacitor size for each electrode has been established. However, it has been found that 0.3% of the total bulk storage capacitance is suitable as an initial value for the overcharge capacitance of the positive electrode, and that 0.005% is suitable for the overcharge capacitance associated with the negative. Having calculated these initial values, simulation results can be compared with experimental data, and the overcharge capacitance values fine-tuned so that simulation results replicate experimental data.

Figure 5.8 shows the transition between the bulk storage capacitance and the overcharge capacitance of each electrode. It can be seen that as the electrode voltage rises above the zener voltage, there is a rapid decrease in the capacitance to the overcharge value. To provide a smooth change between the two capacitance values, a transition region has been defined. Below the zener voltage for each electrode, the capacitor has the value calculated for the bulk storage of that electrode. Inside the transition region, the capacitance is a function of the electrode voltage as shown by Equation 31), while above the transition region, the capacitance has the value calculated for overcharge. Suitable transition regions have been found to be 40 mV for the negative electrode, and 10 mV for the positive.

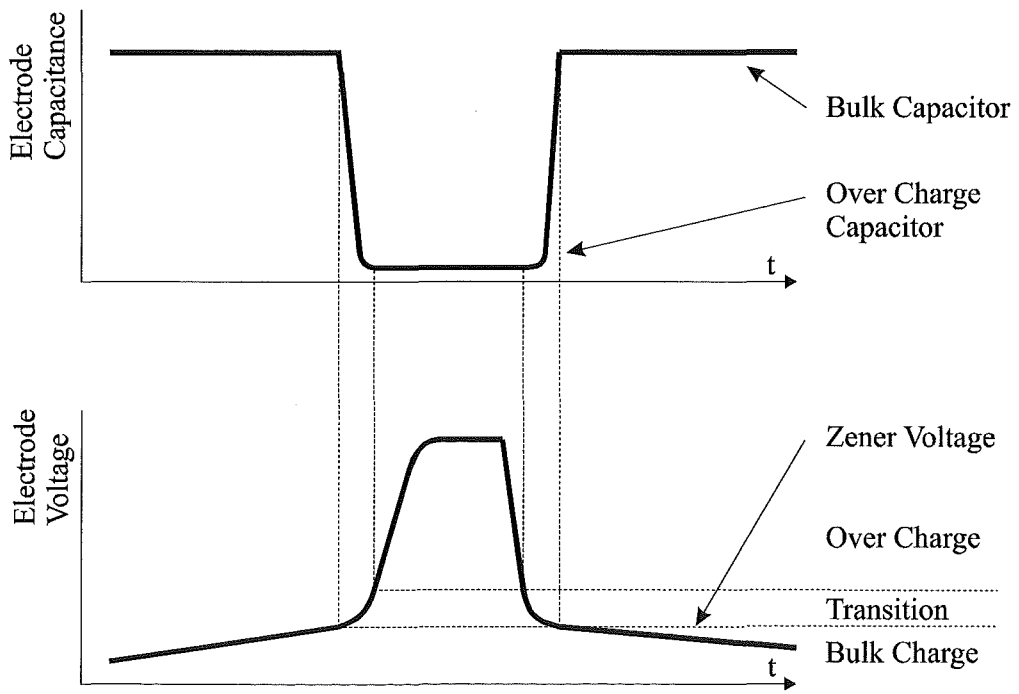

Figure 5.8 Transition of Bulk Storage and Overcharge Capacitance Values

$$C_{trans} = C_{ochg} - 1 + \left(C_{bulk} - C_{ochg} + 1\right)^{\left(1 - \left(\frac{V_{cap} - V_{zen}}{V_{trans}}\right)\right)^{S}} \quad 31)$$

where, C_{trans} = Capacitance during transition
C_{ochg} = Overcharge Capacitor Value
C_{bulk} = Bulk-Charge Capacitor Value
V_{cap} = Capacitor Voltage
V_{zen} = Zener Voltage
V_{trans} = Transition Voltage-Range
S = Shaping Term (5 was used)

5.1.3 Zener Diodes

The zener diodes in the model are ideal, as when the capacitor voltage is below the zener voltage no reverse current flows through the diode. When the capacitor voltage is above the zener voltage, the current through the diode is determined by the value of the non-linear overcharge resistor, and the voltage across the same resistor. The voltage at which the zener diode begins to conduct is determined by the relative sizing of the bulk storage capacitors for each electrode. This is determined through the 'pos_bulk_percent' variable in the component value selection software vrla_part_size.m previously described in Section 5.1.2.

5.1.4 Acid Resistance

As the electrolyte specific gravity, and hence resistance, does not change considerably in the float charge region of VRLA battery operation, a fixed value of acid resistance is sufficient for float modelling. However, by attempting to provide a more realistic voltage profile during the bulk discharge, the effects of the change in electrolyte resistance during discharge have been modelled. While the model of acid resistance effectively changes the overall resistance, it is still a single element model, and does not attempt to model time dependant quantities such as mass transport, electrolyte gradients, or kinetic properties.

The variation in electrolyte resistance is largely modelled on the long-standing guideline that the specific gravity of an open circuit cell is the voltage of the cell minus 0.85. As the sum of the

voltage on the positive and negative electrodes' bulk-storage capacitors is equivalent to the open circuit voltage, this may be used to determine the specific gravity of the simulated electrolyte. A function is then used to calculate the specific conductance based on specific gravity. This specific conductance is then converted to resistance, and scaled so that the specified fully charged acid resistance is produced at the point at which the cell is fully charged and overcharge begins. As the cell model enters the overcharge region, the electrolyte resistance is held constant at the value specified for the fully charged state.

Equation 32) shows the function used to calculate the specific conductance of the electrolyte based on the calculated specific gravity. Figure 5.9 shows a plot of the function in Equation 32), along with some values of specific conductance at 20°C found in the literature[4]. It can be seen that above a specific gravity of 1.3, the function has some deviation from the literature values, however the specific gravity of the electrolyte used in VRLA cells is typically less than 1.3.

$$SC = SC_{PK} \times \left(\frac{\left| SG - C_{PKSG} \right|^{Shape}}{-1 \times \left| 1 - C_{PKSG} \right|^{Shape}} + 1 \right) \qquad 32)$$

where: SC = Specific Conductance
SC_{PK} = Value of Conductance Peak ~0.76
SG = Specific gravity
C_{PKSG} = SG at the Conductance Peak ~1.235
$Shape$ = Curve Fitting Variable ~ 2.15

The required value of the fully charged electrolyte resistance must be determined from experience or battery manufacturers' data. However, as this parameter has very little influence on float analysis, a default value of 1 milli-ohm may be used. Generally speaking, the electrolyte resistance will be inversely proportional to cell capacity.

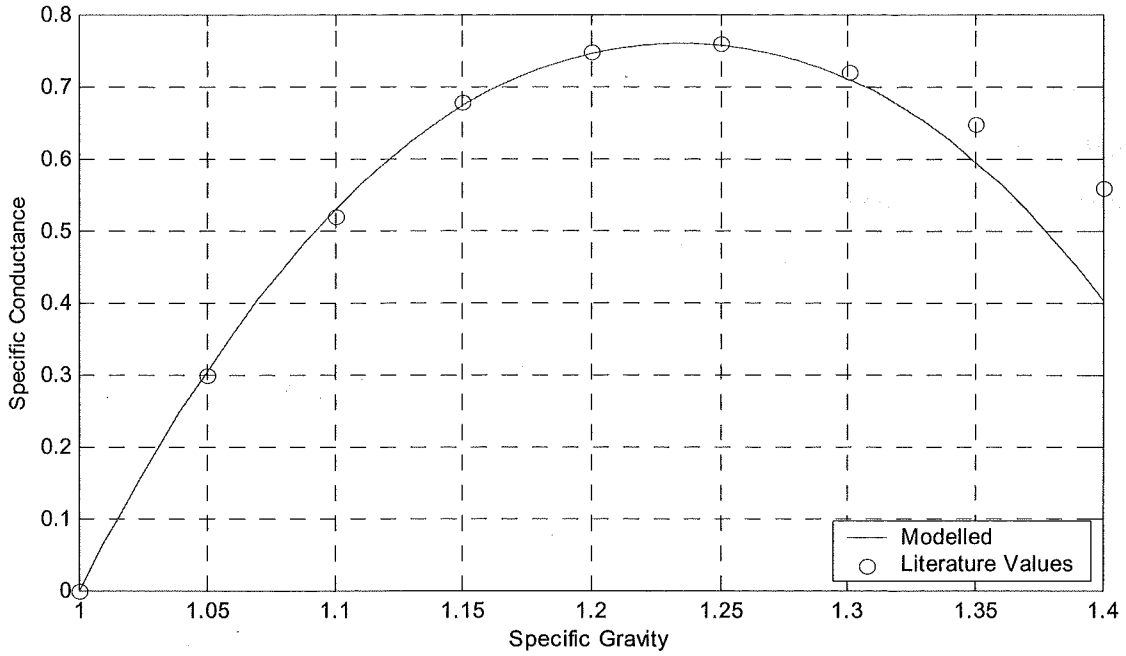

Figure 5.9 Electrolyte Specific Conductance as a Function of Specific Gravity

5.1.5 Metallic Resistance

Similar to the electrolyte (acid) resistance, the metallic resistance has very little influence on the float characteristics of a cell. However, for completeness, a single lumped-resistor simulating the effects of the current conducting path (grid) of each electrode has been included in the model. Again, no method of determining the value of the metallic resistors has been investigated, and default values of 10 micro-ohms have been used for all simulations. The sum of the acid resistance and the two metallic resistors should equal the internal resistance of the cell.

5.2 Simulation Software Interaction

The Matlab based VRLA battery simulation software is broken into three separate modules: component value selection, modelling (differential equations), and simulation. The general functionality and interaction of these modules is shown in Figure 5.10. Of these three modules only the component value selection module (vrla_part_size.m), and the simulation control module (vrla_float_sim.m) require user interaction. While the differential equation module

(diff_vrla.m) is the simulation workhorse, it performs all of the simulation calculations in the background, with no direct user interaction required.

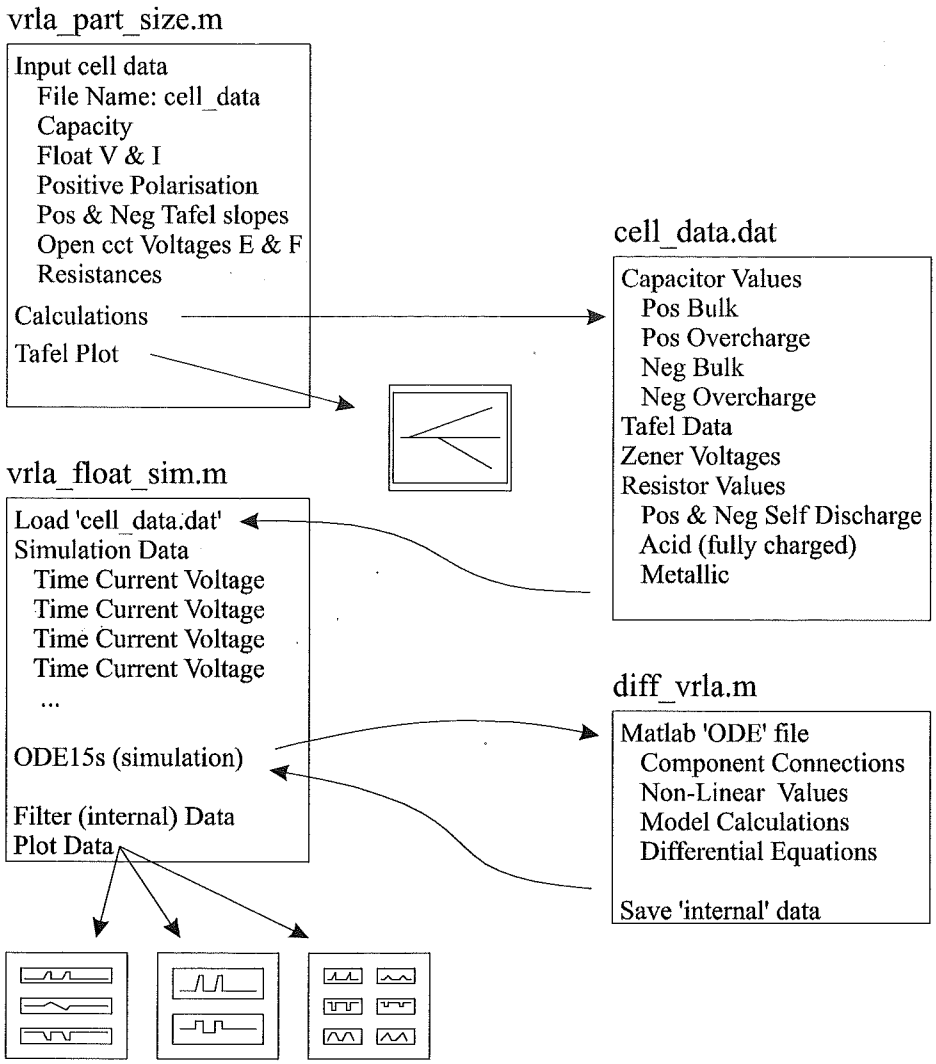

Figure 5.10 VRLA Battery Float Charge Simulation Software Module Interaction

The 'vrla_part_size.m' m-file provides a simplified method for converting easily found or measured battery data into the component values required for the simulation model. Values that are not commonly found or easily measured are positive polarisation at the float voltage, the Tafel slopes, and the acid and metallic resistances. As the resistance values are not critical to the float model, default values may be used if more appropriate values are not available. The positive polarisation may be set in the optimal (40 – 80 mV) range, or it may be set to model imbalance problems. Alternatively, the described polarisation estimation test (Section 4.3.2.3) may be used to estimate the positive polarisation for the float conditions. If the Tafel slopes of

each electrode are not available, default values may be successfully used due to the generally limited variation in Tafel slopes. The part-sizing module has two outputs: a Tafel plot of the supplied cell data, and a data file (cell_data.dat) which contains the cell specific parameters required for the simulation. The Tafel plot allows viewing and verification of the steady state characteristics of the supplied cell data, and if necessary, correction of problems with the simulation model. The cell specific output data file contains a listing of key input parameters used to generate the data file, along with the model's component values that have been calculated by the part-size program. If required, the output data file may be directly edited or modified.

The 'diff_vrla.m' module is the heart of the simulation, and contains the equations required to model the cell. The cell model is essentially a Matlab ODE file, containing differential equations of the 'state variables' (capacitors), along with the model's other component relations, dependencies, and calculations. As the 'diff_vrla.m' module is the simulation core, Section 5.3 details this more thoroughly. This file does not require any direct user interaction.

The 'vrla_float_sim.m' Matlab-m file is used to control the 'run-time' variables throughout the simulation. To do this, a matrix is defined that contains the operating conditions, such as the power supply voltage and current, and the duration for which the supply is maintained in that state. The matrix has three columns: time (in seconds), current, and voltage. Each row in the matrix represents a new set of operating conditions. For a given row, the defined voltage and current are maintained from a specified time until the commencement time of the next set of operating conditions. Essentially, the total simulation performed by the 'vrla_float_sim.m' file, is a concatenation of many short simulations with differing conditions. The voltage and current settings are similar to a conventional bench top power supply, and either current or voltage regulation may be selected. If voltage control is desired, the current is set greater than that drawn by the battery at the set voltage. If current control is required, the current is set at the desired level, and a high voltage is selected so that the current drawn by the battery at that voltage is greater than the desired current. If a discharge is required, a negative current value is set.

Effectively, through the use of the simulation matrix many short simulations are cascaded together so that any range of operating conditions may be analysed. For the simulation period, the differential equation file (diff_vrla.m), power supply voltage and current settings, simulation

options, and cell specific parameters (obtained from the 'cell_data.dat' file) are passed to the Matlab ODE solver. Matlab has seven different ODE solvers, each targeting a different type of problem. These solvers are divided into two groups for stiff and non-stiff equations. For a stiff problem, solutions can change on a very short time scale compared to that of the interval of integration, but the solution of interest changes on a much longer time scale[5]. As the VRLA battery simulation undergoes rapid change as the cell model enters its overcharge state, stiff ODE solvers were found to work more reliably. Of the stiff ODE solvers, the ode15s solver was found to be the fastest and least prone to failure. This solver has been used for all simulations.

An ODE solver normally returns only times and values of state variables (in this case, capacitor voltages) during the simulation period. However, as the developed cell model contains components with values that change according to the state of the circuit, it is advantageous to know how these component values change as the simulation progresses. At the end of the simulation equation file, component values and operational data such as individual component voltages and currents, are appended to the end of an 'internals' matrix. In doing so, a complete record of the simulation is produced.

As the ODE solver varies the time step according to the rate of solution change, there is a certain amount of 'hunting', where the time step used is too large and the solution is outside the allowed tolerance. When this occurs, the ODE solver reduces the time step and recalculates the solution. As this variable time step 'hunting' produces many incorrect results in the 'internals' matrix, these are removed when the simulation is complete by filtering the saved 'internals' matrix to hone in on the solution. The filtered 'internals' simulation results are then plotted as required to allow the complete simulation to be viewed.

5.3 Float Simulation (ODE) File - diff_vrla.m

As the characteristics of VRLA float charge have been modelled using electrical components, any analogue circuit simulation package should be able to simulate the developed model, provided the simulation environment allows sufficient freedom to specify dependant components such as the non-linear overcharge resistors and the dual value capacitors. Through the use of the ODE solver in Matlab, analogue circuits may be simulated as shown by Attia[6]. When compared to dedicated analogue circuit simulation packages, the Matlab ODE environment may not

initially appear as simple, or provide rapid simulation development or modification. It was chosen as the simulation environment as there are no restrictions placed on components or their models.

The simulation of analogue circuits with the ODE solver is based around expressing the circuit (in an ODE file) in terms of its state variables. State variables are the currents associated with inductors, and the voltages associated with capacitors. Currents or voltages associated with resistors do not specify independent state variables. Through nodal or loop analysis, the differential equations specifying the dependencies of the state variable must be extracted from the circuit to be simulated. These equations are then rearranged and processed with the initial conditions, so that the rate of change (derivative) of the state variables is determined. The ODE file passes the derivatives of the state variable back to the ODE solver for evaluation. If the solution is outside the acceptable or defined tolerance, the calculations are rejected, the time step is reduced, and the ODE file processed again based on the reduced time step. If the solution is within the accepted tolerance, the solution is kept, the time is incremented, and the ODE file processes again for the new time step and new initial conditions. This process is repeated from the defined initial conditions to the final time specified for the simulation. While the complete code for the diff_vrla.m ODE file is given in Appendix A, a brief description of the functionality calculations and flow of the ODE is given in the remainder of this Section.

Based on the capacitor voltages supplied to the ODE file through the initial condition values, the amount of polarisation on each electrode is calculated. From these polarisation values, the values of the non-linear overcharge resistors are calculated, along with the size of the dual-value capacitors used for energy storage at each electrode. The initial conditions of the capacitor voltages are also used to calculate the effective resistance of the electrolyte, as described in Section 5.1.4. Once the value for the acid resistance has been obtained, the present cell state is compared to the simulation charger voltage and current settings in order to determine whether the charge (or discharge) is current or voltage controlled, as detailed in Equation 33).

The currents through the self-discharge and non-linear overcharge resistors at each electrode are also calculated based on the voltages across the resistors and the value of the resistance for the present state of the cell. If the current through the non-linear overcharge resistor is seen to be negative (due to negative polarisation), the current through this resistor is set to zero to create the diode's 'zener' action. Using the supply current determined through Equation 33), the voltages

produced by the metallic and acid resistances are also calculated. Finally, with the currents and voltages associated with all the resistive elements in the circuit known, the rates of change of the capacitor voltages can be calculated.

if $V_{Charger\_set} - V_{IC\_Cpos} - V_{IC\_Cneg} < I_{Charger\_set} \times (R_{P\_metal} + R_{N\_metal} + R_{Acid})$

$i_{supply} = (V_{Charger} - V_{IC\_Cpos} - V_{IC\_Cneg}) / (R_{P\_metal} + R_{N\_metal} + R_{Acid})$ // voltage controlled

else

$i_{supply} = i_{Charger\_set}$ // current controlled

endif 33)

As the simulation circuit shown in Figure 5.1 contains two capacitors, there are two state variables. The current through these capacitors and the value of the capacitors determines the voltage rate of change on these capacitors. Applying Kirchhoff current law to nodes where the capacitors are connected into the model (i.e.: acid - capacitor junction), the current flowing through the capacitors at the present operating point is established. This in turn allows the derivatives (rates of change) of the capacitor voltages to be calculated. These derivatives are eventually passed back to the ODE solver for calculation of the solution and next time increment. Before the diff_vrla.m file is exited, the required internal values from this pass through the ODE file, and are appended to the bottom of a 'global' matrix so that the values are not lost when the m-file is terminated.

5.4 Model Limitations and Boundaries

The model described previously in this Section was developed to replicate both the steady state and transient responses of a cell's positive and negative electrodes while on float charge. When the responses of each electrode are combined, the overall terminal response of a cell is reproduced. For a given float voltage, the model will draw the same float current as the cell it was modelled on, and for a given float current, the model will produce the same terminal voltage. This is true not only for the steady state levels, but also the transient response, as the model is moved from one steady state operating point to another. As the model was developed for the analysis of a cell's operational state, it is not based on cell chemistry, or intended to directly explain this. However, it may be possible for certain features of the model to be interpreted from a chemistry perspective.

While the model was developed to replicate both the steady state and transient responses, only the most significant transient features overall have been modelled. Small features, such as the Coup de Fouet-like voltage overshoot and recoveries detailed in Section 4.3.2, have not been modelled for either electrode. These overshoot and recoveries are seen as the electrodes enter the bulk charge region after spending time in the overcharge float region. However, as these features typically have small magnitudes (5 - 10 mV), and appear to lack magnitude and duration consistency, no attempts have been made to model these features.

As the model targets the float charge phase of VRLA battery life, only a very basic implementation of the main charge-discharge reaction has been modelled. The voltage change at the modelled cell terminals for a full discharge will be similar to that for a full discharge of a cell at the rate specified with the cell's nominal capacity. As implemented, the model will deliver the same (rated) capacity, regardless of the discharge rate. Cell kinetics limits the transport of the reacting species to and from the reaction site, and is largely responsible for the reduction in available capacity as the discharge rate is increased. As the model was not intended for analysis of the bulk charge and discharge regions of operation, no attempt has been made to replicate kinetic limitations within the bulk energy storage in order to reduce calibration requirements. For similar reasons, the model does not reproduce the exponential current decay seen when a cell is recharged with a voltage limit. While the model will reproduce the response of a cell at any temperature provided appropriate calibration data is supplied, the model will not replicate changes for a single set of cell calibration data in these operating characteristics due to temperature variation.

By modelling both electrodes within a cell separately, the terminal response of the cell may be decomposed into the response produced by each electrode without the aid of an additional reference electrode. While this would imply that a well-calibrated model is required, the electrodes' transient responses have been found to be sufficiently different that the model (and associated calibration) is not necessary for certain analyses, such as polarisation distribution estimation.

5.5 Developed Model Results

During the testing required for the development of this model, it was noted that the characteristics of the tested cell appeared to be changing. Tafel tests were completed periodically to verify these changes. Figure 4.15 shows the variations in the Tafel characteristics at the start, middle, and end of testing. It can be seen that the changes are almost entirely caused by variations in the characteristics of the negative electrode, while the positive remains relatively consistent. The changes in the cell's characteristics may be due to the cyclic nature of the testing, the addition of the reference electrode, or natural ageing of the cell. For verification of the developed float charge model, the use of a single set of cell specifying calibration data would be preferable. However, given the changes that occurred within the cell throughout testing, a single set of cell calibration data can not be used to compare the developed model with the experimental data.

Figure 5.11 shows the Tafel points for the experimental data (Tests 27 - 48) prior to discharge testing. It is evident that although a single Tafel line can be used to represent the positive electrode for all testing, such a line can not be used to encapsulate the range of points covered by the negative electrode. The model has been validated using three sets of cell specifying calibration data, which differ only by the position of the negative electrode's Tafel intercept. This allows a negative electrode to be specified to match the experimental data at a particular stage of testing. The data points marked with a '+' symbol are below the fully charged open circuit potential, where Tafel characteristics are not expected. The dashed lines in the lower plot indicate the three positions of the negative electrode's Tafel line. The slope of the line is held constant at 131 mV per decade, a measurement obtained from Figure 4.25. For clarity, the calibration data file and associated Tafel plot produced by the cell characterising software have been provided with the set of simulated responses for each test voltage.

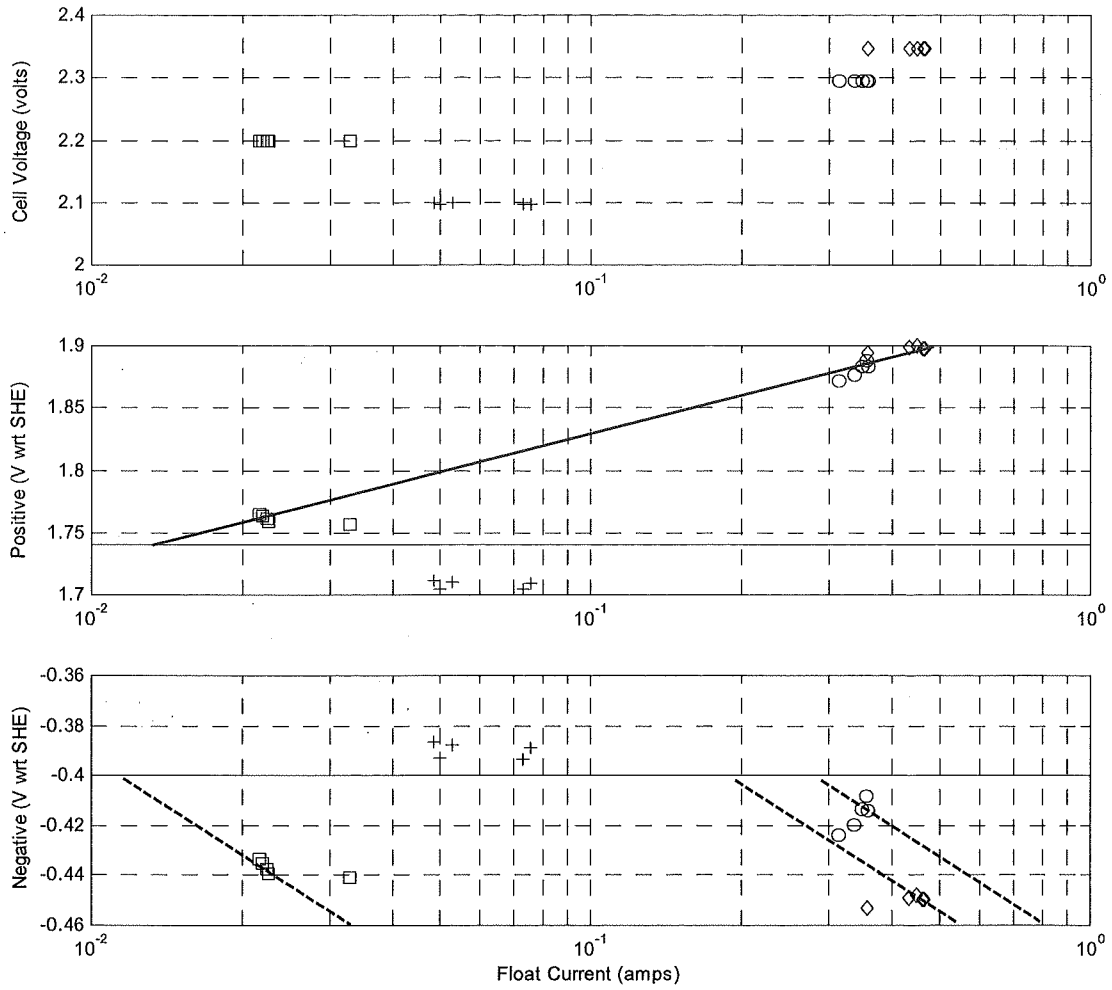

Figure 5.11 Variation in Negative Tafel Characteristics with Testing

5.5.1 Open Circuit Decay

Figure 5.12 shows the simulated open circuit decay of a 275 Ah VRLA cell from a float voltage of 2.26 V. The cell model for the 2.2 V test conditions described in Table 5.1 and Figure 5.14 has been used for this simulation. At a float voltage of 2.26 V, this cell model has approximately 50 mV of positive polarisation, and 70 mV of negative. With this ideal polarisation distribution, maximum float life should be realised and the cell should remain fully charged indefinitely. This simulation may be compared with similar experimental data shown in Figure 4.10.

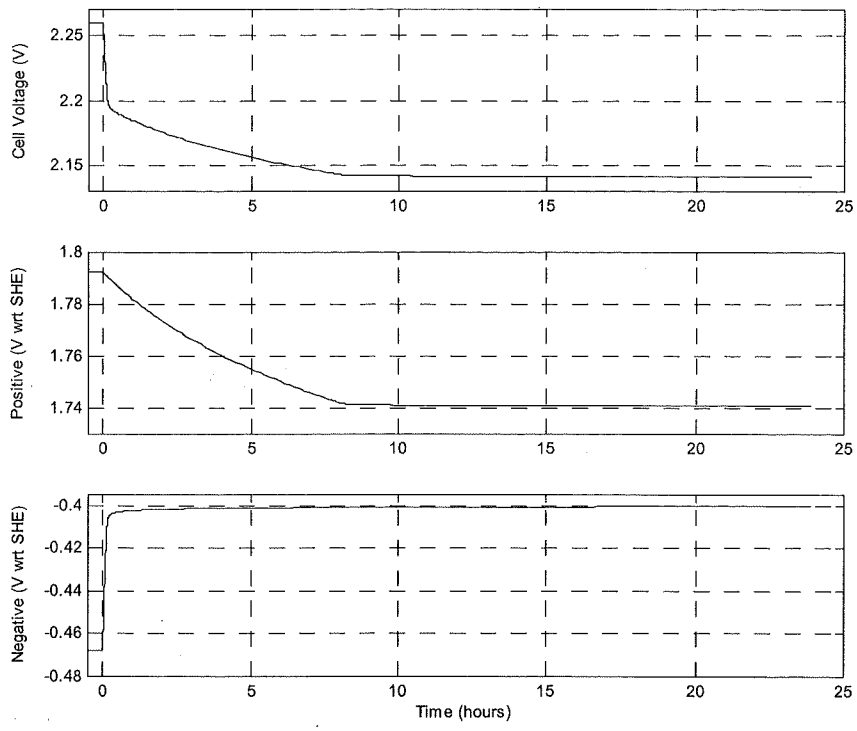

a) 24 Hours

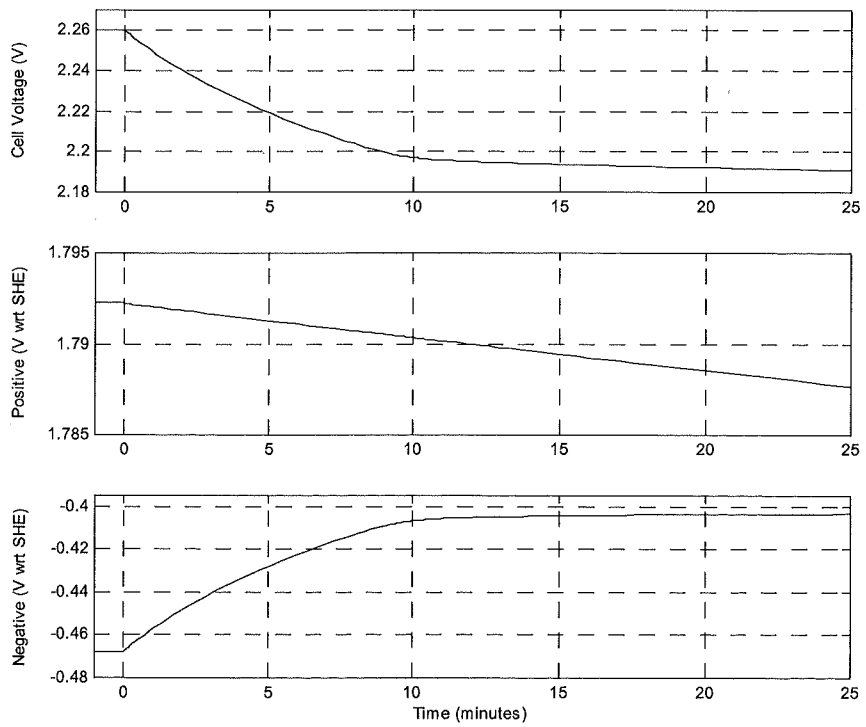

b) 25 Minutes

Figure 5.12 Simulated Open Circuit Discharge (From Float at 2.26 V)

When the measured open circuit decay (Figure 4.10) is compared to the simulated response, the overall trends and time responses are reproduced. However, prior to the charger being removed, there are differences between the polarisation distributions of the simulation and the experimental data. These differences result from the model's steady state (Tafel) characteristics not matching the cell's characteristics. As the simulation has more negative electrode polarisation than the experimental data, it is expected (and seen) that the simulated polarisation decay of the negative electrode will have a longer duration. Similarly, as the simulation has less positive electrode polarisation, it is expected (and seen) that the positive polarisation decay in the simulation will be shorter than that in the measured data. Although there are slight differences in the duration of the polarisation decay due to variance in the initial starting polarisation, the slopes and relative duration of the polarisation decay are reproduced accurately by the model. The simulated polarisation on both electrodes naturally decays to the fully charged open circuit rest potential as required. As stated earlier, no attempt has been made to model the Coup de Fouet-like overshoot and recovery of the negative (or positive) electrode seen in Figure 4.10. This effect is less than 10 mV in the experimental data.

5.5.2 Constant Current Discharge

Section 5.5.1 detailed a simulation of natural open circuit voltage decay due to the presence of the fixed value self-discharge and non-linear overcharge resistors. In this Section, simulations of forced constant current discharges are given for a range of discharge rates and starting float voltages. As explained in Section 5.5, in order to match cell variations seen in the experimental data, separate cell models must be used for each set of tests at the differing float voltages.

When a cell is operated below its fully charged open circuit rest potential, only a small terminal voltage response to very low rate discharges is expected. Figure 5.13 shows the discharge response of the developed model after being float charged at 2.1 V. Given that for this model the fully charged open circuit rest potential is 2.14 V, it is estimated that at 2.1 V the model has a SOC of approximately 83%. As this is well into the bulk charge region of cell operation, it is expected that low rate discharges will have little effect on the voltage profile for each electrode, or on the cell as a whole. For this simulation, the cell calibration data file for the 2.2 V tests has been used. The simulated discharges from a float voltage of 2.1 V, shown in Figure 5.13, and the experimental results shown in Figure 4.16 have been plotted on the same voltage and time

axes so that they may be easily compared. The experimental data appears to show some variation in the polarisation distribution prior to discharge. However, when each trace is closely analysed, it is seen that discharge related voltage changes occur only with the higher rate discharges of 1 and 10 A. As all of the simulation traces start with identical polarisations, this small spread in results is not replicated in the simulation. Similarly to the experimental results, offset voltages are only apparent with the higher rate discharges. While these offsets are not appropriately scaled, the metallic and acid resistances in the model may be tuned to provide better representation of high rate discharge voltage offsets. As the model was not targeting the main charge-discharge region of operation, only default values of these components have been used.

As expected, when a cell is not fully charged, a low rate discharge will not produce a measurable change in the voltage on either electrode, or on the cell as a whole. This effect has been shown in both experimental results (Figure 4.16) and simulations using the developed model (Figure 5.13).

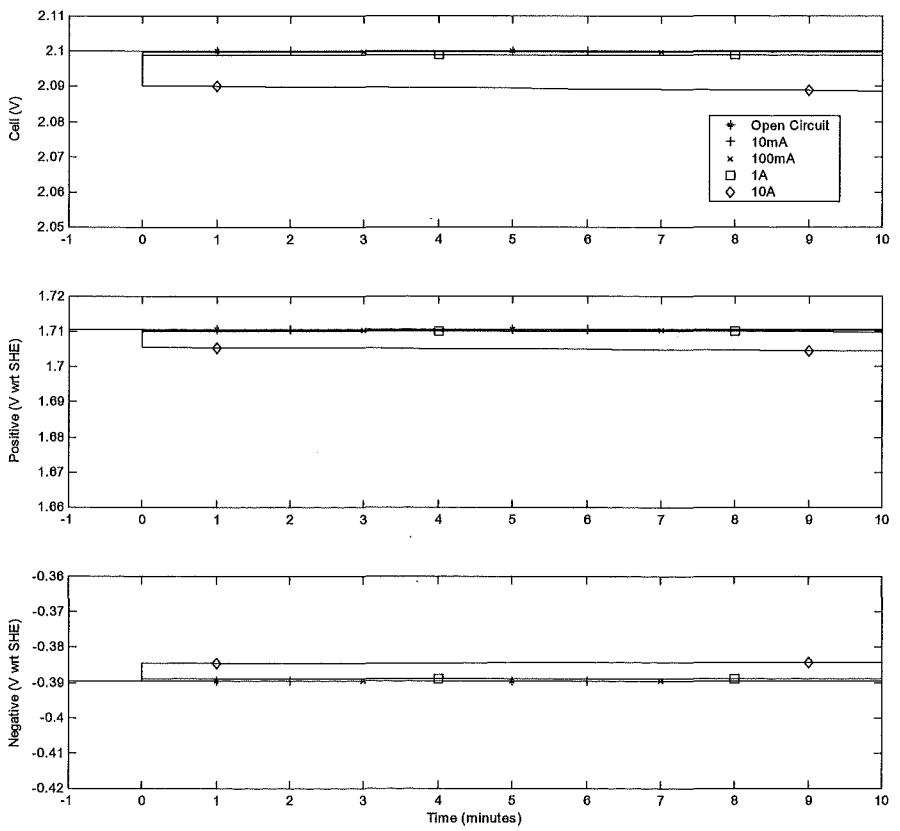

Figure 5.13 Simulated Discharges from 2.1 V (Below Fully Charged Open Circuit Voltage)

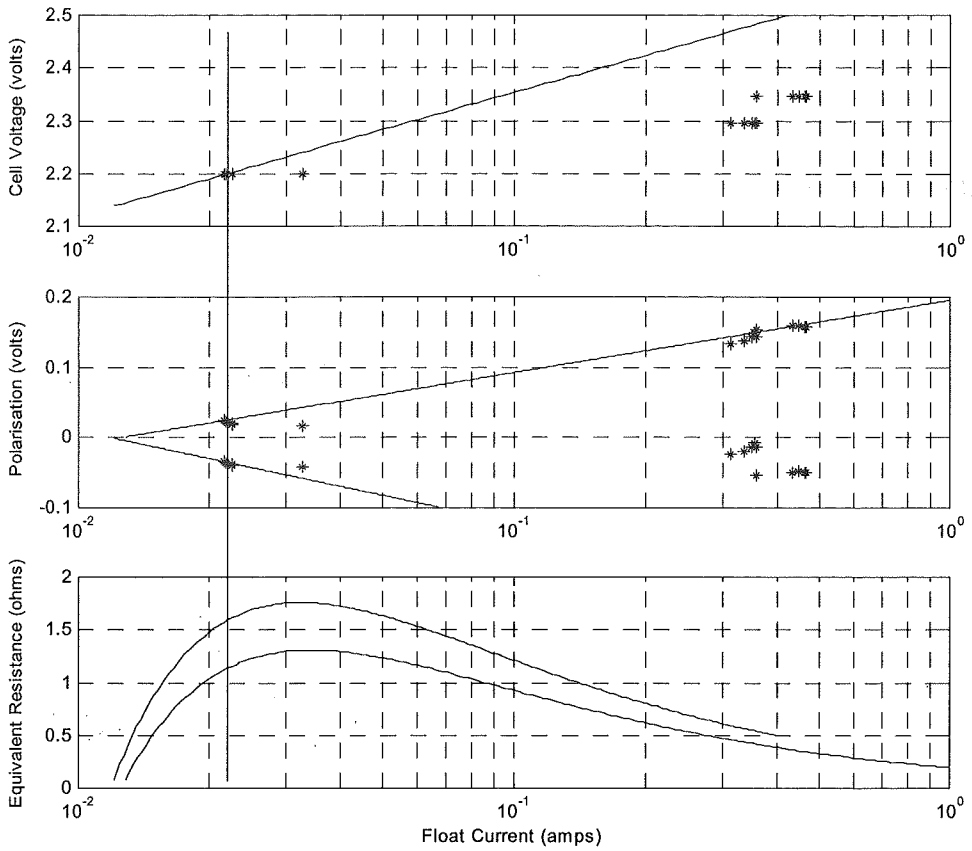

Figure 5.14 Tafel Plot and Equivalent Tafel Resistances for Cell Model at 2.2 V

```
2hi_275_2v2.dat

      275.000000  % cell_capacity

       10.000000  % discharge_time -not reqd
        2.200000  % float_voltage -not reqd
        0.022000  % float_current -not reqd
        0.025000  % pos_polarisation @float -not reqd
        1.900000  % empty_open_cct_rest_volt -not reqd
        2.140000  % full_open_cct_rest_volt -not reqd
       75.000000  % pos_bulk_percent -not reqd

        0.522160  % hg_hg2so4_offset_voltage wrt center
        1.605000  % volt_ochg_start_pos
        0.535000  % volt_ochg_start_neg

  5500000.000000  % c_bulk_p
 16500000.000000  % c_bulk_n
    12375.000000  % c_ochg_p
      206.250000  % c_ochg_n

        0.103000  % pos_ochg_slope
        0.012581  % pos_ochg_int -not reqd
        0.195730  % pos_ochg_1a
        0.131000  % neg_ochg_slope
        0.011892  % neg_ochg_int -not reqd
        0.252143  % neg_ochg_1a

        0.001000  % full_chg_acid_res
        0.000010  % pos_metal_res
        0.000010  % neg_metal_res
      127.576535  % pos_self_dischg_res
       44.989035  % neg_self_dischg_res
```

Table 5.1 Data File for the Cell Model at 2.2 V

Figure 5.15 shows the model's simulation of several discharge rates from a float voltage of 2.2 V. The cell calibration parameters used for this simulation are given in Table 5.1, and the corresponding Tafel plot of the steady state characteristics of the model is shown in Figure 5.14. This simulation may be compared to similar experimental tests shown in Figure 4.17. It can be seen in both the simulation and experimental plots that at this float voltage both electrodes have low values of polarisation. The negative electrode has approximately 35 mV of polarisation, while the positive electrode has about 25 mV. The cell will remain fully charged as both electrodes are polarised, however the positive electrode is well below the 40 - 80 mV window specified for minimum grid corrosion. Therefore, at this float voltage the life of the cell will be reduced through increased grid corrosion.

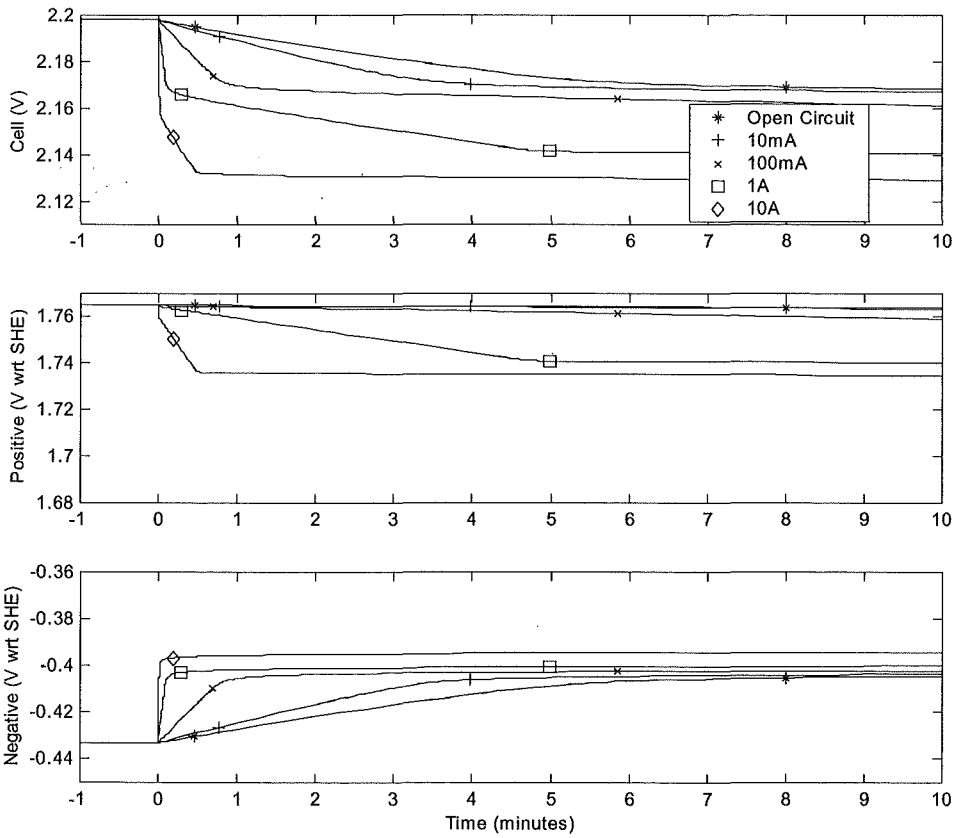

Figure 5.15 Simulated Discharge from a 2.2 V Float Charge

On the displayed time scale, both the experimental and simulated plots indicate that from a float voltage of 2.2 V, the voltage response on the cell's terminals due to low discharge rates (< 1 A) is almost entirely due to the change in the potential of the negative electrode. Over the ten

minute period shown, there is virtually no change in the potential of the positive electrode with discharge rates up to 100 mA. However, over the same period the potential of the negative electrode decays completely to its open circuit rest potential. If the cell's fully charged open circuit rest potential is known, the total polarisation may be easily calculated for a given float voltage. The difference in the polarisation decay of each electrode may be used to assess the polarisation distribution within a cell, using only the cell's terminal voltage profile.

For the 1 and 10 A discharge traces in the experimental data (Figure 4.17), the cell's terminal voltage drops significantly below the open circuit rest voltage of 2.14 V. This voltage drop is due to a combination of resistive volt-drops and Coup de Fouet-like voltage overshoots (and recoveries) often seen during the initial stages of lead acid battery discharge. As the magnitude of these voltage overshoots and recoveries reduces with the discharge rate, no attempt has been made to model these features. However, resistive voltage drops seen at high discharge rates are modelled in the simulation. When the polarisation decays at the start of the 10 A discharge in Figure 5.15, the potential to which each electrode settles is seen to be below their fully charged rest potentials. This is due to the metallic and acid resistances within the cell model.

When the float voltage used during testing was raised to 2.3 V, the characteristics of the cell appeared to change significantly, as previously explained in this Section, and did not follow the expected Tafel behaviour. To allow the model to replicate the cell's characteristics at 2.3 V, a new cell model is required. The cell calibration data file used for the 2.3 V simulations is shown in Table 5.2, and the corresponding Tafel plot of the simulation steady state characteristics is shown in Figure 5.16. From this Tafel plot it can be seen that below a float voltage of approximately 2.28 V, the negative electrode is not polarised, and for this reason the cell will not be maintained in a fully charged state indefinitely. It is also interesting to note that at a float voltage of 2.3 V, a total of 160 mV of polarisation is supplied to the cell. Of this, approximately 10 mV is supported on the negative electrode, with the remaining 150 mV supported by the positive. As the positive polarisation is significantly greater than the optimal 40 - 80 mV, excessive grid corrosion will occur and the rate of gas production will increase. If the gas production rate is greater than that which can be re-combined within the cell, gas venting will occur and the cell may fail prematurely due to electrolyte loss.

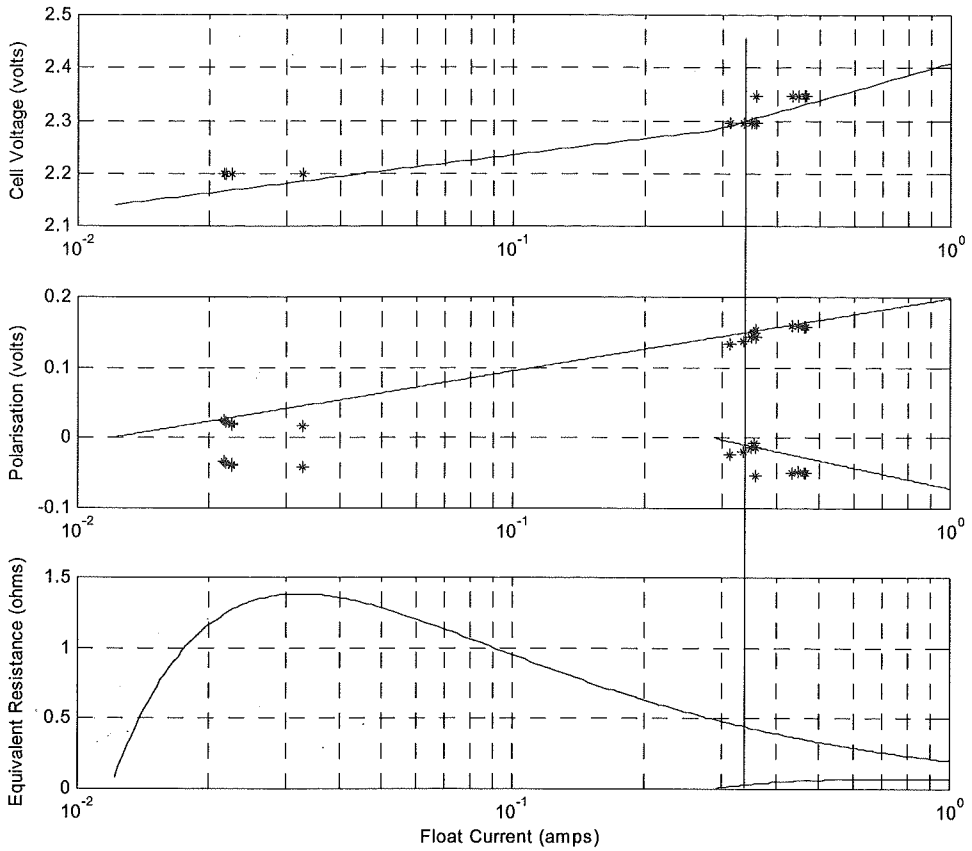

Figure 5.16 Tafel Plot and Equivalent Tafel Resistances for Cell Model at 2.3 V

```
2hi_275_2v3.dat

275.000000  % cell_capacity

       10.000000  % discharge_time -not reqd
        2.300000  % float_voltage -not reqd
        0.340000  % float_current -not reqd
        0.150000  % pos_polarisation @float -not reqd
        1.900000  % empty_open_cct_rest_volt -not reqd
        2.140000  % full_open_cct_rest_volt -not reqd
       75.000000  % pos_bulk_percent -not reqd

        0.522160  % hg_hg2so4_offset_voltage wrt center
        1.605000  % volt_ochg_start_pos
        0.535000  % volt_ochg_start_neg

  5500000.000000  % c_bulk_p
 16500000.000000  % c_bulk_n
    12375.000000  % c_ochg_p
      206.250000  % c_ochg_n

        0.103000  % pos_ochg_slope
        0.011890  % pos_ochg_int -not reqd
        0.198258  % pos_ochg_1a
        0.131000  % neg_ochg_slope
        0.285196  % neg_ochg_int -not reqd
        0.071376  % neg_ochg_1a

        0.001000  % full_chg_acid_res
        0.000010  % pos_metal_res
        0.000010  % neg_metal_res
      134.991617  % pos_self_dischg_res
        1.875905  % neg_self_dischg_res
```

Table 5.2 Data File for the Cell Model at 2.3 V

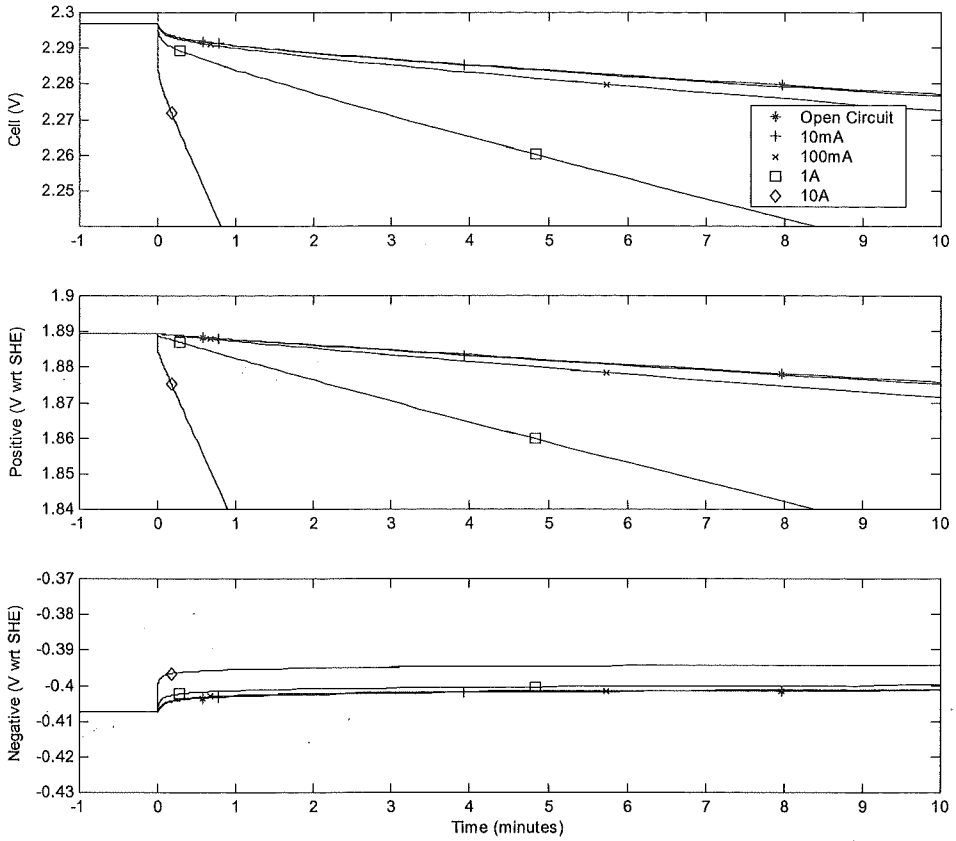

Figure 5.17 Simulated Discharge from a 2.3 V Float Charge

Figure 5.17 shows the developed model's simulation of various discharge rates from a float voltage of approximately 2.3 V. This simulation may be compared to the experimental test results shown in Figure 4.18. In both the simulation and experimental test results, it can be seen that as predicted in the Tafel plot (Figure 5.16), the positive electrode supports the majority of the applied polarisation. While the negative electrode has a small amount of polarisation, it should remain fully charged. However, considering the level of total polarisation applied to the cell, it is obvious that the cell is not operating in the manner necessary for its maximum life to be realised. Within a couple of minutes of the discharge commencing, the negative electrode has decayed (approximately 8 mV) to its fully charged rest potential. During this time, at the low discharge rates there is virtually no change in the potential of the positive electrode. Again, due to resistance elements within the cell and the model, for the higher rate discharges the negative electrode is seen to settle to a potential below its fully charged rest potential.

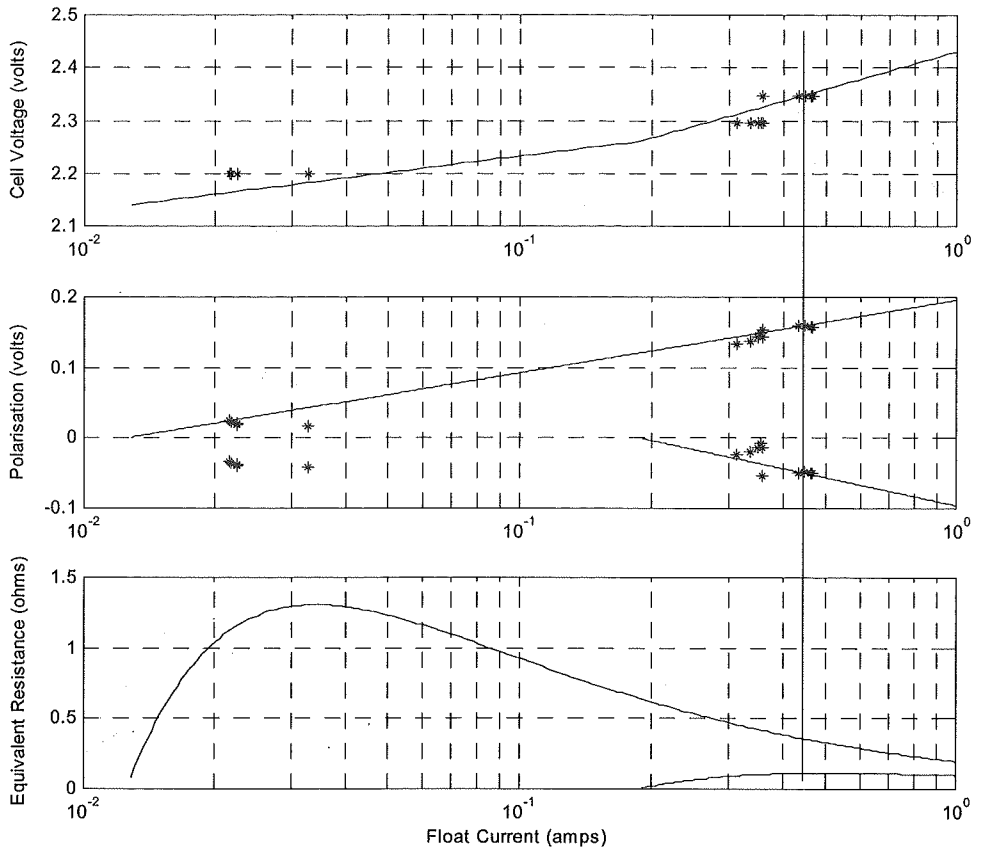

Figure 5.18 Tafel Plot and Equivalent Tafel Resistances for Cell Model at 2.35 V

```
2hi_275_2v35.dat

        275.000000  % cell_capacity

         10.000000  % discharge_time -not reqd
          2.350000  % float_voltage -not reqd
          0.450000  % float_current -not reqd
          0.160000  % pos_polarisation @float -not reqd
          1.900000  % empty_open_cct_rest_volt -not reqd
          2.140000  % full_open_cct_rest_volt -not reqd
         75.000000  % pos_bulk_percent -not reqd

          0.522160  % hg_hg2so4_offset_voltage wrt center
          1.605000  % volt_ochg_start_pos
          0.535000  % volt_ochg_start_neg

    5500000.000000  % c_bulk_p
   16500000.000000  % c_bulk_n
      12375.000000  % c_ochg_p
        206.250000  % c_ochg_n

          0.103000  % pos_ochg_slope
          0.012584  % pos_ochg_int -not reqd
          0.195719  % pos_ochg_1a
          0.131000  % neg_ochg_slope
          0.186867  % neg_ochg_int -not reqd
          0.095429  % neg_ochg_1a

          0.001000  % full_chg_acid_res
          0.000010  % pos_metal_res
          0.000010  % neg_metal_res
        127.544161  % pos_self_dischg_res
          2.862995  % neg_self_dischg_res
```

Table 5.3 Data File for the Cell Model at 2.35 V

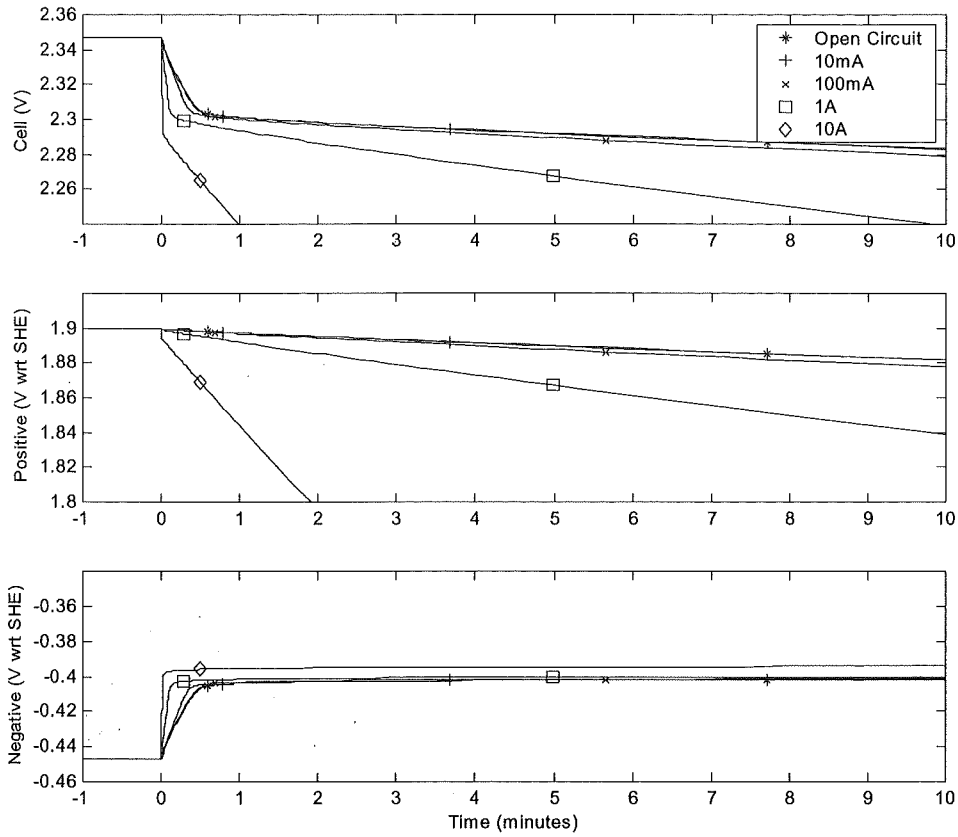

Figure 5.19 Simulated Discharge from a 2.35 V Float Charge

Figure 5.19 shows simulated discharge profiles produced by the model for a cell that has been float charged at 2.35 V. Again, due to the cell's characteristics not following the expected Tafel profile, a new model of the cell at this operating point is required. Table 5.3 shows the model characterisation data used in the simulations and Figure 5.18 shows the model's Tafel characteristics at this operating point. This simulation may be compared to similar experimental test results shown in Figure 4.19.

When the simulation is compared with experimental data, the features and time responses of the various discharge rates again show a very close likeness. The only difference is a slight offset in the level to which the negative electrode settles. The low rate discharge plots of the negative electrode's potential in Figure 4.19 are seen to settle at a potential approximately 13 mV below its fully charged rest potential. This is due to the previously described Coup de Fouet-like overshoot, and would be seen to recover if the plotted duration were increased. On the displayed

time scale, this recovery is only visible on the 10 A trace, although this trace does not make a full recovery due to the current induced resistive voltage drops. The magnitude of these voltage offsets appears to increase with both positive polarisation and the discharge rate. For low discharge rates and recommended float voltages, these offsets are typically less than 10 mV. As these overshoot offsets are small compared to the total polarisation supplied to a cell, and to the 30 mV positive polarisation window for minimum grid corrosion, no attempt has been made to model the Coup de Fouet-like voltage overshoots.

5.5.3 Bulk Discharge and Recharge

The developed model targets the float charge region of operation, however to allow the differences between the overcharge region and the main energy storage regions of cell operation to be identified, a basic representation of the bulk energy storage is necessary. As detailed in Section 5.1.2, this bulk energy storage has been achieved through the use of appropriately sized capacitors. While this representation alone will produce an uncharacteristic linear discharge profile, when combined with a basic representation of electrolyte resistance during discharge, a more realistic profile of the main discharge reaction is produced.

Figure 5.20 shows simulated discharges of the bulk storage elements within the developed VRLA battery float charge model. The discharge currents shown relate to open circuit, 20, 10, 5, and 2 hour discharge rates. While the simulated discharge curves do not show the transient Coup-de-Fouet feature often seen during the initial stages of lead acid battery discharge, the fan of discharge curves produced by the model has a realistic profile at the various discharge rates. For the time scale shown in this figure, the overcharge polarisation decay can only be seen on the open circuit trace. It is seen that the positive electrode's polarisation takes a little over eight hours to decay to its open circuit rest potential of 1.74 V. The open circuit decay of the negative electrode's polarisation is only just visible on this time scale. The cell model used for this series of simulations was the 2.2 V cell previously described and detailed in Table 5.1. This cell model has optimal, well-balanced float charge characteristics, enabling maximum cell life to be realised.

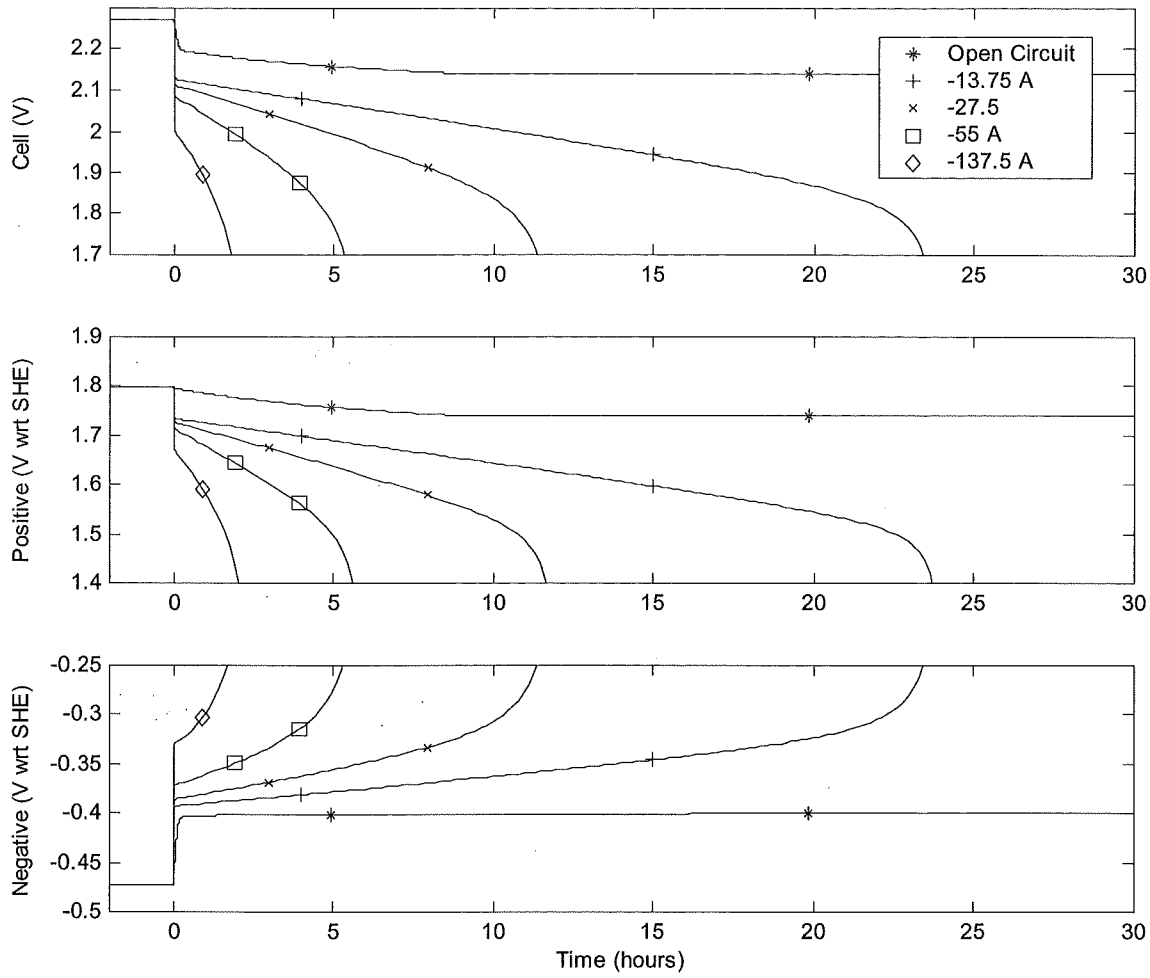

Figure 5.20 Simulated Discharge of a 275 Ah VRLA Cell

Figure 5.21 magnifies the first 30 seconds of the high rate discharges shown in Figure 5.20. It can be seen that while polarisation decay of both electrodes is still present at high discharge rates, it becomes difficult to resolve the decay of the negative electrode unless a very high sampling rate is used. As voltage offsets associated with internal resistance increase with the discharge rate, the significance of information gained by associating features and levels of a cell's voltage profile is reduced as the discharge rate is increased. Ideally, for polarisation distribution assessment, the natural open circuit self-discharge profile is preferred. However, it has been found that at discharge rates up to C/1000, the current induced resistive voltage drops are acceptably small.

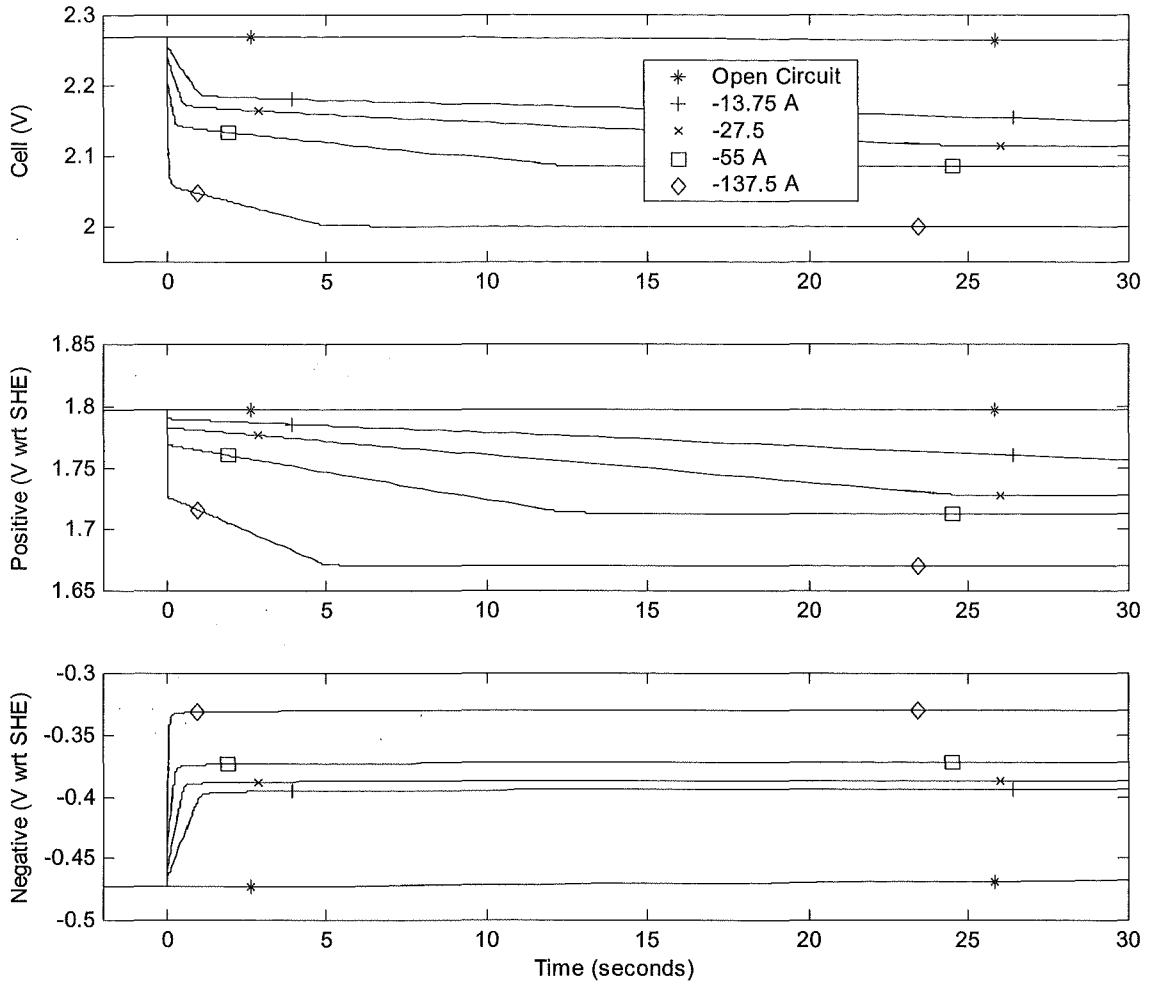

Figure 5.21 Simulated Start of Discharge (275 Ah VRLA Cell)

While a basic representation of the bulk storage of a VRLA cell has been provided, some important characteristics of this region have not been modelled. These characteristics include the apparent reduction in available capacity as the discharge rate is increased, and the exponential decay in charge current seen when a cell is charged from a constant voltage supply.

5.5.4 Current Perturbation Testing

Figure 5.22 shows the developed float charge model's response to a ±1 A current signal. Again, the cell data file used to calibrate the model is that specified to replicate the cell characteristics for the 2.2 V series of tests. This calibration file is detailed in Table 5.1. The model's simulated

response to this current injection may be compared with similar experimental test results shown in Figure 4.9. It can be seen that overall, the plots of the simulated voltage response on each electrode and on the cell compare well with the experimental data.

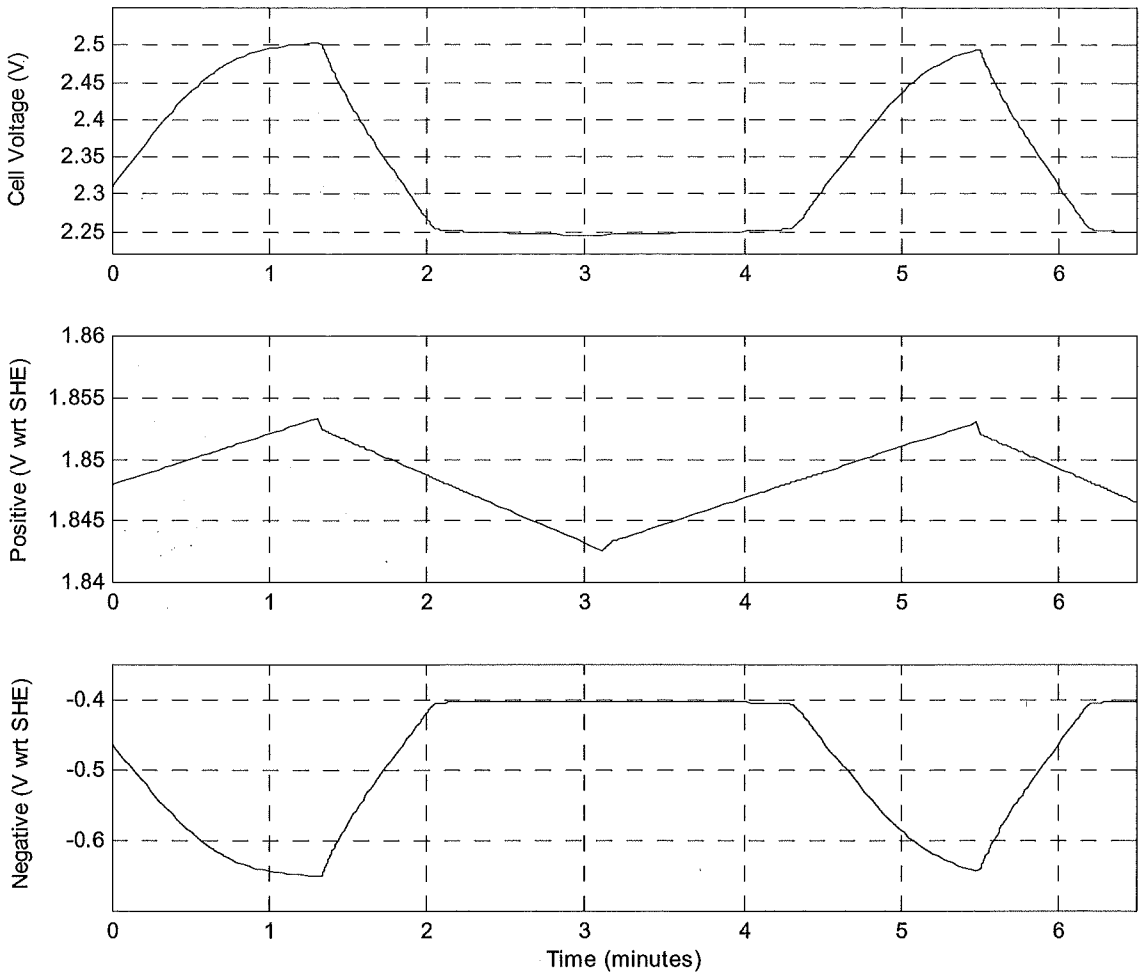

Figure 5.22 Simulated Response to ± 1 A Current Manipulation

The simulated voltage levels and rates of change of each electrode (and the cell) are very similar to that shown in the experimental plots. It can be seen that the cell's terminal characteristic is almost entirely due to the response of the negative electrode. During the displayed period, there is only 10 mV of change in the potential of the positive electrode, while over the same period there is almost 250 mV of change in the potential of the negative. As the decay of the negative electrode ceases near its fully charged rest potential, the first decay of a cell's terminal voltage may be associated with the polarisation of the negative electrode. Knowledge of the cell's fully

charged rest voltage, float voltage, and negative polarisation allows the positive polarisation to be easily calculated.

The plot of the positive electrode in Figure 5.22 contains small steps as the cell changes from charge to discharge. These steps are due to the resistive elements in the model, with electrolyte (acid) resistance being the major contributor. As these steps are not present in the experimental data, it would be preferable to eliminate these from the simulation. Buffering the electrolyte resistance with a small capacitor may achieve this. However, as the magnitude of these resistive steps is small (< 1 mV), they do not significantly affect the simulation.

The transition of the negative electrode between the overcharge and bulk charge regions of operation is more abrupt in the model than in the experimental results. While significant time has been spent attempting to develop a transition function for merging these two regions of operation, the vast difference in capacitance between the overcharge and bulk charge makes development of a suitable function difficult. As implemented, within the transition region the value of capacitance is a function of the capacitor's voltage. This effectively produces positive feedback, i.e.: when supplied with a constant current, as the voltage on the capacitor increases, its value decreases, causing it to charge faster. The power term in Equation 31) and the transition window can be varied to change the profile within this transition region.

5.5.5 Model Results Summary

The developed model reproduces the underlying steady state and transient characteristics of a VRLA cell in, or near, the float charge region of operation. The model requires only a minimum set of cell specific calibration data, and may be easily calibrated or adapted to any desired cell. A software module has been provided to allow the majority of this cell specific calibration data to be extracted from easily measured or commonly available cell parameters. To limit the calibration requirements only a basic representation of the bulk charge region of operation has been provided. If a complete cell model is required, the bulk charge region of cell operation requires further development, however in the present state this does not affect the float charge analysis. The calibration data may be varied to identify the responses associated with a healthy (optimal polarisation distribution) float charging cell, or a cell suffering float charge polarisation imbalance problems that must ultimately reduce the life of the cell. Float charge imbalance

problems can produce a gradual discharging of an individual electrode (either positive or negative) while 'float charging'. Float charge imbalance can also increase the rate of grid corrosion, and the production of overcharge gas, which, if vented, may result in premature cell failure through dryout.

The developed model will estimate the polarisation distribution within a conventional (float charging) 2 V VRLA cell, through the use of a simple test applied to the cell's terminals. No modification to the cell is necessary, and no reference electrode is required. The estimated polarisation distribution can reveal whether the cell is operating as desired, or whether it is suffering from polarisation imbalance problems. Furthermore, the estimated polarisation distribution may be used as a basis for optimisation of the float charge voltage. From the test results presented in this Section, it is obvious that the tested cell did not display consistent (textbook) Tafel characteristics over a range of operating points for the duration of this testing. The large shift in the zero polarisation Tafel intercept point of the negative electrode highlighted problems with this cell.

5.6 References

[1] D. Berndt, *Maintenance Free Batteries, Lead-Acid, Nickel/Cadmium, Nickel/Metal Hydride, A Handbook of Battery Technology,* Second Edition, Research Studies Press Ltd., 1997, p 161.

[2] D. Berndt, U. Teutsch, *Float Charging of Valve-Regulated Lead-Acid Batteries: A Balancing Act Between Secondary Reactions,* Journal of the Electrochemical Society, Vol. 143, No 3, March 1996.

[3] H. Bode, Translated by R. J. Brodd & K. V. Kordesch, *Lead-Acid Batteries,* The Electrochemical Society Series, Wiley-Interscience (a division of John Wiley & Sons), New York, 1977, p 315.

[4] D. Berndt, *Maintenance-Free Batteries Lead-Acid, Nickel/Cadmium, Nickel/Metal Hydride A Handbook of Battery Technology Second Edition,* Research Studies Press Ltd., 1997, Figure 4.20, p 144.

[5] The Math Works Inc, *Using MATLAB Version 5*, The Math Works Inc, January 1998, p 8-8.

[6] J. O. Attia, *Electronics and Circuit Analysis Using MATLAB,* CRC Press, 1999, s 5.4.

6 Analysis and Applications

In the previous two Chapters the cell testing used for the development and verification of the model was almost entirely undertaken with a reference electrode inserted in the cell. As a VRLA cell essentially functions as a sealed unit, puncturing the case of the cell to add a reference electrode may modify the characteristics of the cell. The purpose of this Chapter is to ensure that the trends and characteristics identified and modelled in the previous Chapters are present in a cell that has not been modified through the addition of a reference electrode. This Chapter also aims to verify that the previously identified trends and characteristics are not specific to a particular VRLA cell type or construction.

A demonstration of the developed technique for assessing the polarisation distribution within a standard 2 V VRLA cell is provided within this Chapter. This test is applied to the terminals of an unmodified cell in order to estimate the polarisation of each electrode. A reference electrode is then inserted into the same cell, and the estimated polarisation on each electrode is verified through direct measurement.

6.1 Different Cell Tests

All previously described testing was undertaken with a single cell that had been modified to allow the use of a reference electrode. The tested cell was a Hawker Energy ESPACE 2-HI275, with a nominal capacity of 275 Ah (C_{10} to 1.8 V at 20 °C). Manufactured by Hawker Energy in France, this cell design has a flat, cast, lead-calcium grid with a high tin content.

To verify that the identified and modelled characteristics for the assessment of polarisation distribution are not cell specific, a second series of tests using a different cell type was planned and undertaken. The cell selected for this series of tests was chosen to be as dissimilar as possible from the previously tested cell. The cell selected and used for testing was a Hawker Energy (formally Gates Energy Products) CYCLON 2 V 25 Ah BC Cell. While it would have been preferable to use a cell from a different manufacturer, the CYCLON cell was chosen due to availability. Although both cells tested are manufactured by Hawker Energy, they are manufactured at different sites using extremely different construction techniques. The ESPACE

cells are manufactured at facilities in Arras, France, while the CYCLON cells are manufactured in Warrensburg, U.S.A. The CYCLON cell tested has a nominal capacity of 25 Ah (C_{10} to 1.85 V at 25 °C), and has a high purity (lead purity > 99.99%) lead-tin grid that has been punched from a lead sheet. Rather than a conventional flat stack, the grids in a CYCLON cell are spirally wound to produce a cylindrical cell.

As a VRLA cell is an active electrochemical system with a finite life, the influence of any testing may modify the characteristics of the cell. It is impossible to verify directly that characteristics identified with the aid of a reference electrode are present and consistent in cells that have not been modified for reference electrode testing. It was decided that comparison of the voltage response on a cell's terminals for a given test, both before and after adding a reference electrode, was the only practical method of assessing whether the addition of the reference electrode significantly modifies a cell's characteristics. The verification testing using the CYCLON cell was divided into two halves. In the first half, the cell was used unmodified. This testing involved discharging and recharging the cell at various rates, and from several float voltages. These tests were then repeated during the second phase of testing, for which a reference electrode was added to the cell. The testing undertaken is detailed in Table 6.1.

No Reference Electrode			Reference Electrode Added	
Test File	Description		Test File	Description
			float68.dat	Added reference electrode Recharged 100mA 1.5Hrs Recharged 300mA 2.35V 45Hrs Float 45Hrs at 2.27
float60.dat	3Hr discharge at 7.5A to 1.75V Recharge at 7.5A to 2.45V Float 150hrs at 2.27V		float69.dat	3Hr discharge at 7.5A to 1.75V Recharge at 7.5A to 2.45V Float 150hrs at 2.27V
float61.dat	45Hr open cct decay from 2.27V recharge7.5mA 50 Hrs – float 2.27V		float70.dat	45Hr open cct decay from 2.27V recharge7.5mA 70 Hrs – float 2.27V
float62.dat	Discharge at 10mA from 2.27V Recharge7.5mA to 2.27V – float		float71.dat	Discharge at 10mA from 2.27V Recharge7.5mA to 2.27V – float
float63.dat	Discharge at 85mA from 2.27V Recharge 100mA to 2.27V Float		float72.dat	Discharge at 85mA from 2.27V Recharge 100mA to 2.27V Float
float64.dat	Discharge at 800mA from 2.27V Recharge 1A to 2.27V Float at 2.31		float73.dat	Discharge at 490mA from 2.27V Recharge 1A to 2.31V Float at 2.31
float65.dat	Discharge at 10mA from 2.31V Recharge 10mA to 2.31V – float		float74.dat	Discharge at 10mA from 2.31V Recharge 10mA to 2.31V – float
float66.dat	±14mA current perturbation test Float at 2.31 V		float75.dat	±11mA current perturbation test Float 10mA for 3.5Hrs ~2.4 V 11mA discharge 190Hrs
float67.dat	100Hr open cct decay from 2.31V recharge7.5mA 50 Hrs – float		float76.dat	Recharge / float 2.35V for 195Hrs Open cct Decay 10 weeks

Table 6.1 Verification Testing with a 25 Ah CYCLON Cell

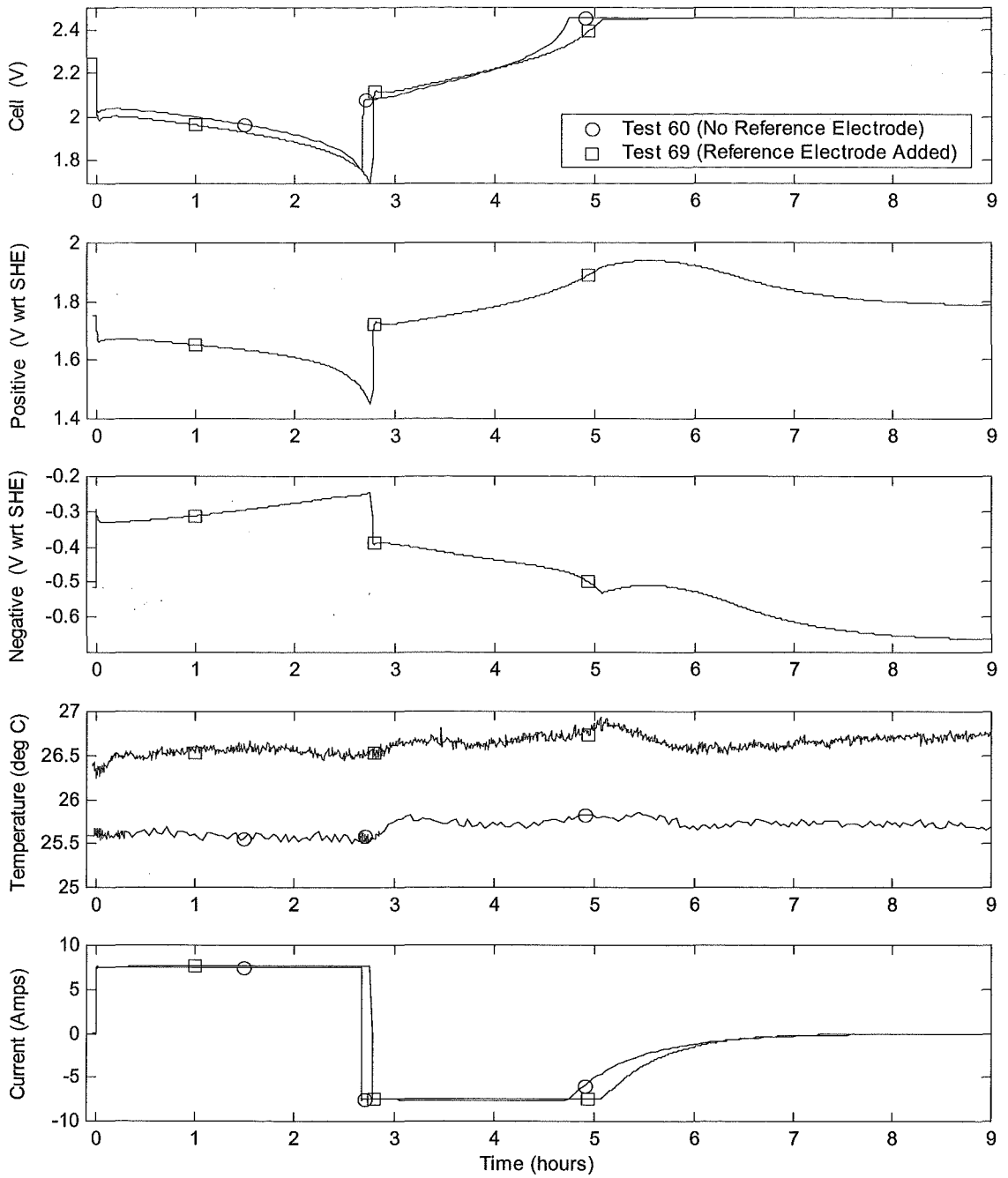

Figure 6.1 Discharge and Recharge (7.5 A) - Before and After Reference Electrode Addition

Figure 6.1 shows the discharge and recharge profiles of the CYCLON cell both before and after the addition of the reference electrode. Between Tests 60 and 69, the cell had undergone approximately six weeks of testing in an unmodified state (Tests 61 – 67). It was therefore expected that the profiles of each discharge plot might not be identical. However, this test was

expected to determine whether the overall capacity of the cell had been affected by the addition of the reference electrode. It can be seen that the terminal voltage of the cell with the reference electrode has a slightly lower profile (-35 mV) for the majority of the discharge. While the discharge test with the reference electrode had a slightly greater discharge current (+50 mA), this small increase in rate should not significantly affect the cell's terminal voltage.

The discharge tests shown in Figure 6.1 were performed at a three-hour rate to an end voltage of 1.75 V. It is interesting to note that while the test with the reference electrode had a slightly lower terminal voltage for the majority of the discharge, at the end voltage of 1.75 V, both traces pass through the same point. This indicates that the cell's capacity has not been changed significantly by the addition of the reference electrode, or by weeks of testing. Following a discharge duration of two hours and 41 minutes, the cell has approximately 89% of its nominal capacity. It is apparent through plots of the reference electrode's potentials that the cell is positive-limited. This is seen at the end of the discharge, where the positive electrode's potential begins to decay rapidly, while the trajectory of the negative electrode remains constant. This suggests that either there is less active material on the positive electrode, or the electrode was not fully charged.

Figure 6.2 shows the profile of the open circuit voltage decay for the test cell before and after addition of the reference electrode. It can be seen that the voltage profiles on the cell's terminals have the same characteristics with and without the reference electrode, however a small offset in the potential to which the cell's voltage settles is evident. The test performed with the reference electrode in situ is seen to settle to a potential approximately 6 mV lower than that seen before the reference electrode was added. At this stage it is unclear whether this difference is due to the addition of the reference electrode, or due to the amount of cell testing undertaken between the two series of tests.

While there is an offset in the potentials to which the cell's terminal voltages settle, when the profiles of the individual electrodes are assessed with the aid of the reference electrode, it is seen that there is only a minimal change (< 3 mV) in the potential of the positive electrode. Over the same period there is approximately 110 mV change in the potential of the negative electrode. As the voltage profiles on the terminals of the cell have the same general characteristics with and without the reference electrode, it is reasonable to expect that the voltage profiles on each electrode remain similar both before and after insertion of the reference electrode. Assuming

that for the period displayed in Figure 6.2, prior to addition of the reference electrode (Test 61), the profile of the positive electrode is similar to that measured after adding the reference electrode, there are two possible causes for the voltage offset. Either, the negative electrode settles to a lower potential, or the potential of the positive electrode is reduced. It is not possible with the available information to determine the true cause or location (which electrode) of this small voltage offset. However, as the magnitude is only 6 mV, the existence of this change does not significantly degrade the analysis or assessment.

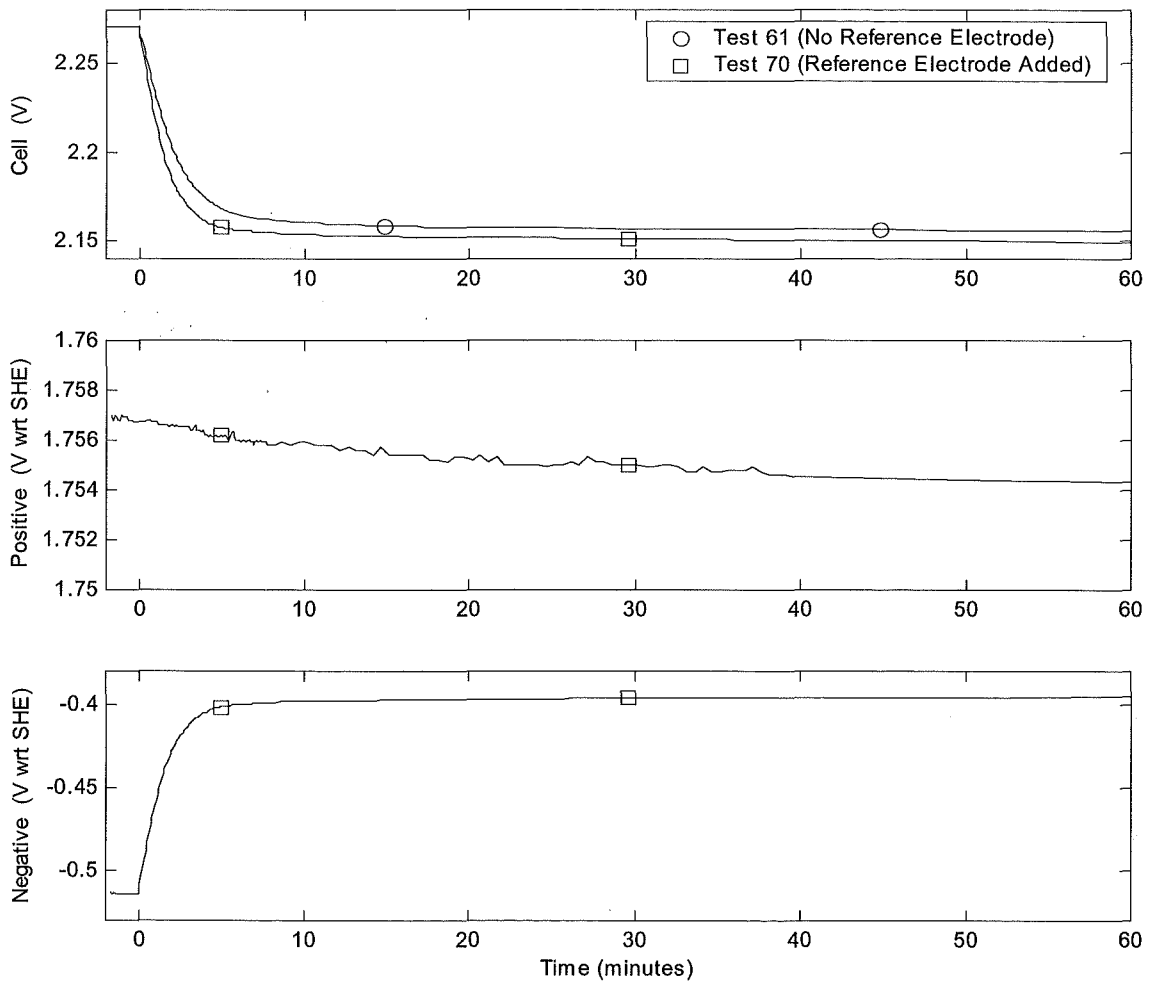

Figure 6.2 Open Circuit Decay - Before and After Reference Electrode Addition

Figure 6.3 shows the same test data as is plotted in Figure 6.2, but with a significantly extended time axis. Approximately 45 hours of open circuit discharge is shown, followed by 50 hours of constant current recharge. The current limit for this recharge was set to 7.5 mA, and an

unattainable voltage was set to ensure the current limit is maintained throughout the recharge. To highlight the differences in the response of each electrode, the plots of the positive and negative electrodes have been displayed with an identical voltage axis scale. It can be seen over the entire displayed region that the terminal response of the cell is almost entirely due to the response of the negative electrode. There is no significant change in the potential of the positive electrode over this period.

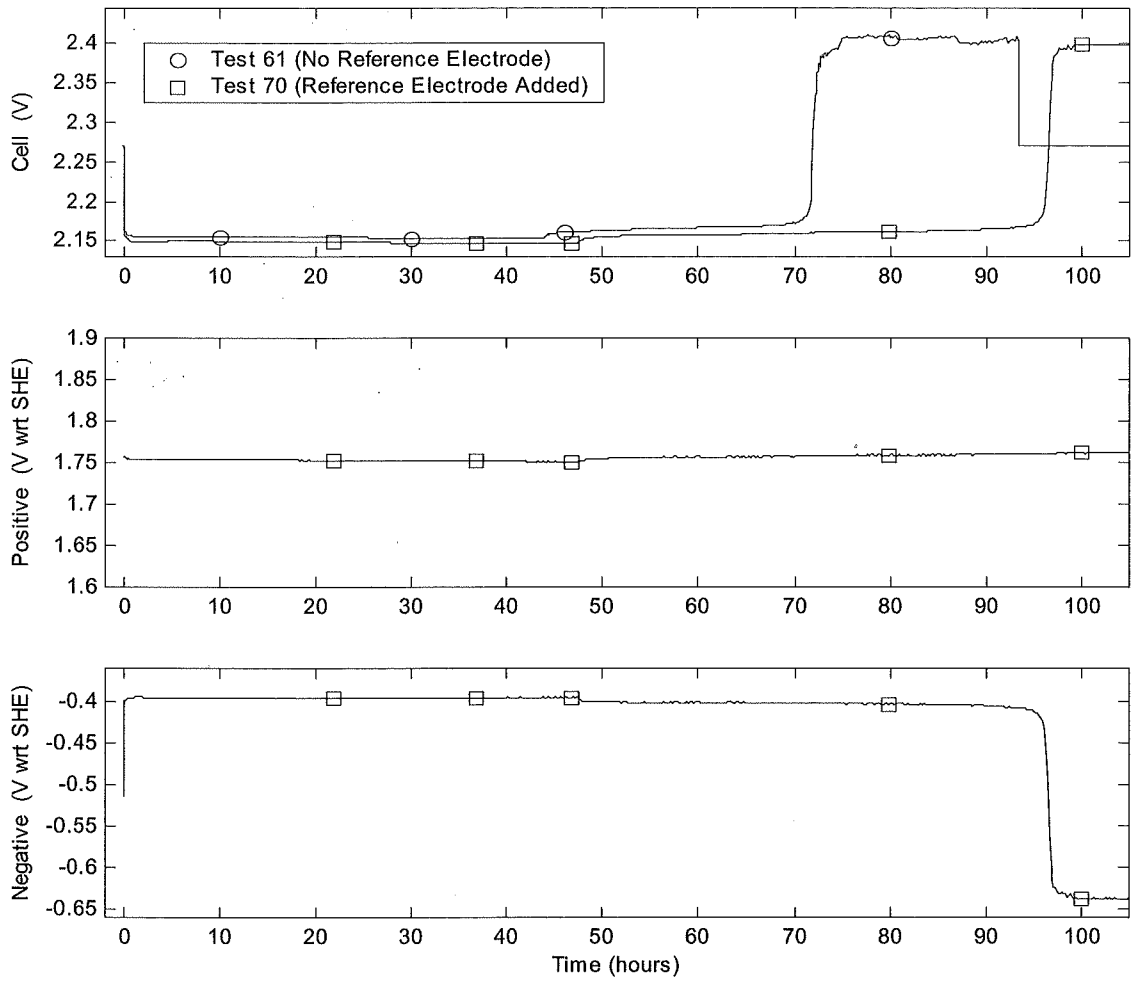

Figure 6.3 Open Circuit Decay and 7.5 mA Recharge, - Before and After Reference Electrode Addition

During the constant current recharge shown in Figure 6.3, a distinct rapid-rise of 230 mV is seen after approximately 71 and 96 hours for Tests 61 and 70 respectively. Information from the test equipped with a reference electrode (Test 70) reveals that this rapid rise in terminal voltage is

due to the polarisation of the negative electrode. It can be seen in Figure 6.3 that the duration of the open circuit decay for Test 70 is approximately 3.5 hours longer than that of Test 61, without the reference. Despite both tests having similar recharge currents, Test 70 takes approximately 24 hours longer to reach the point where the negative electrode begins to polarise. This indicates that either the rate of self-discharge has increased slightly, or the recharge efficiency has decreased. As the duration of both recharges in Figure 6.1 are similar, it is assumed that the delayed polarisation of the negative electrode in Test 70 (Figure 6.3) is due to a slight increase in the self-discharge rate following the addition of the reference electrode. While there is a difference in the times at which this rapid-rise occurs, with strong similarities in the characteristic shape and voltage levels of the two traces, it must be concluded that the electrode responsible for the characteristic is the same in both cases. As the cell voltage settles at approximately 2.4 V, a small amount of noise is seen in the traces of the cell voltage. This is due to current regulation noise, highlighted through the cell's increased sensitivity to float current in this region of operation. The average recharge current was maintained at approximately 7.5 mA, however a low level of noise was present.

It can also be seen in Figure 6.3 that the previously mentioned offset in terminal voltage is present during both the open circuit decay and the recharge phases of the plot. Despite the large change in the cell's terminal voltage over the open circuit decay and recharge process, the terminal voltage offset remains consistent. In the latter stages of the constant current recharge, the voltage settles to approximately 2.4 V. Even after the rapid voltage change to this operating point, the voltage on the cell with the reference electrode is still approximately 6 mV low. It was shown in Chapters 1 and 5 that within the first few minutes of removal of the float charger, the potential of the negative electrode decays to its fully charged rest potential. In certain situations, a Coup de Fouet-like slight overshoot of this settling potential (typically < 10 mV) has been seen. Such an overshoot is normally followed by recovery back to the negative rest potential when the positive electrode has decayed to its fully charged rest potential. No significant Coup de Fouet-like voltage overshoot or recovery is seen for either cell trace in Figure 6.3. As no obvious overshoot and recovery is evident, it is assumed that within the first few minutes following the removal of the float charger, the negative electrode settles to its fully charged rest potential. Given this, and the consistent offset (lowering) of the cell's voltage profile after the addition of the reference electrode, it is concluded that either the reference electrode's addition or the previous six weeks of cell testing has caused a slight (6 mV) lowering of the positive electrode's potential.

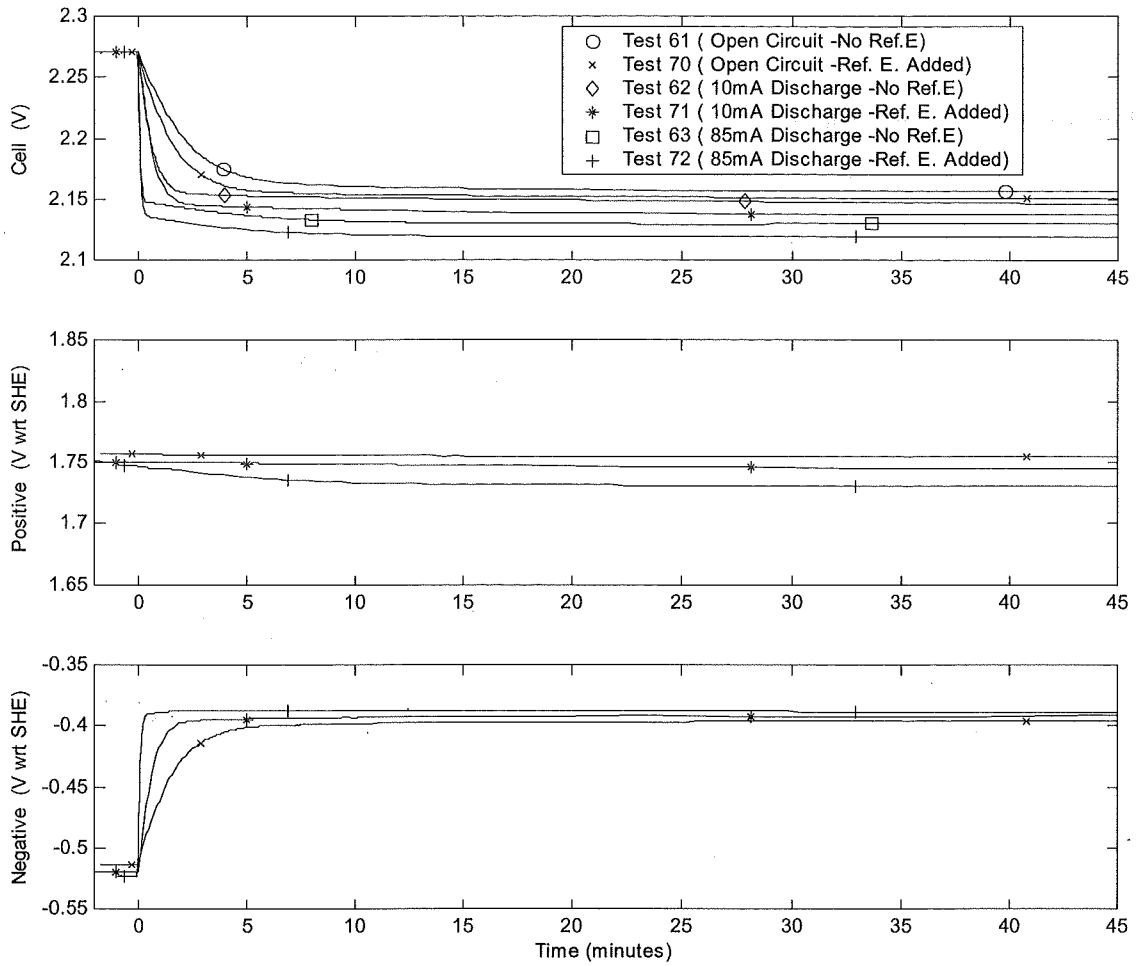

Figure 6.4 Discharge Profiles - Before and After Reference Electrode Addition

Figure 6.4 displays the effects that discharge rate variations have on the voltage profile of a cell, both before and after insertion of a reference electrode. For each discharge rate, comparison of the cell's voltage profiles reveals similar characteristics and responses before and after the addition of the reference electrode. In each case however, the previously described voltage offset following the addition of the reference electrode is evident. As the discharge rate is increased, this offset voltage is also seen to increase, from approximately 6 - 11 mV. However, for the tests utilising a reference electrode, up to 10 mV variations in the potentials of each electrode are seen prior to the removal of the charger. Although several days of stabilisation were allowed between subsequent tests in order to reduce any influences from previous tests, the variance in the potential of each electrode may be an unavoidable consequence or side effect of the previous testing.

The characteristics and response times of the various discharge rates are similar both before and after the addition of the reference electrode. Therefore, it is assumed that the same mechanism or electrode, identified with the aid of the reference electrode, was responsible for the characteristic occurring before the reference electrode was added to the cell. The addition of the reference electrode is not seen to significantly alter the characteristics or behaviour of the cell.

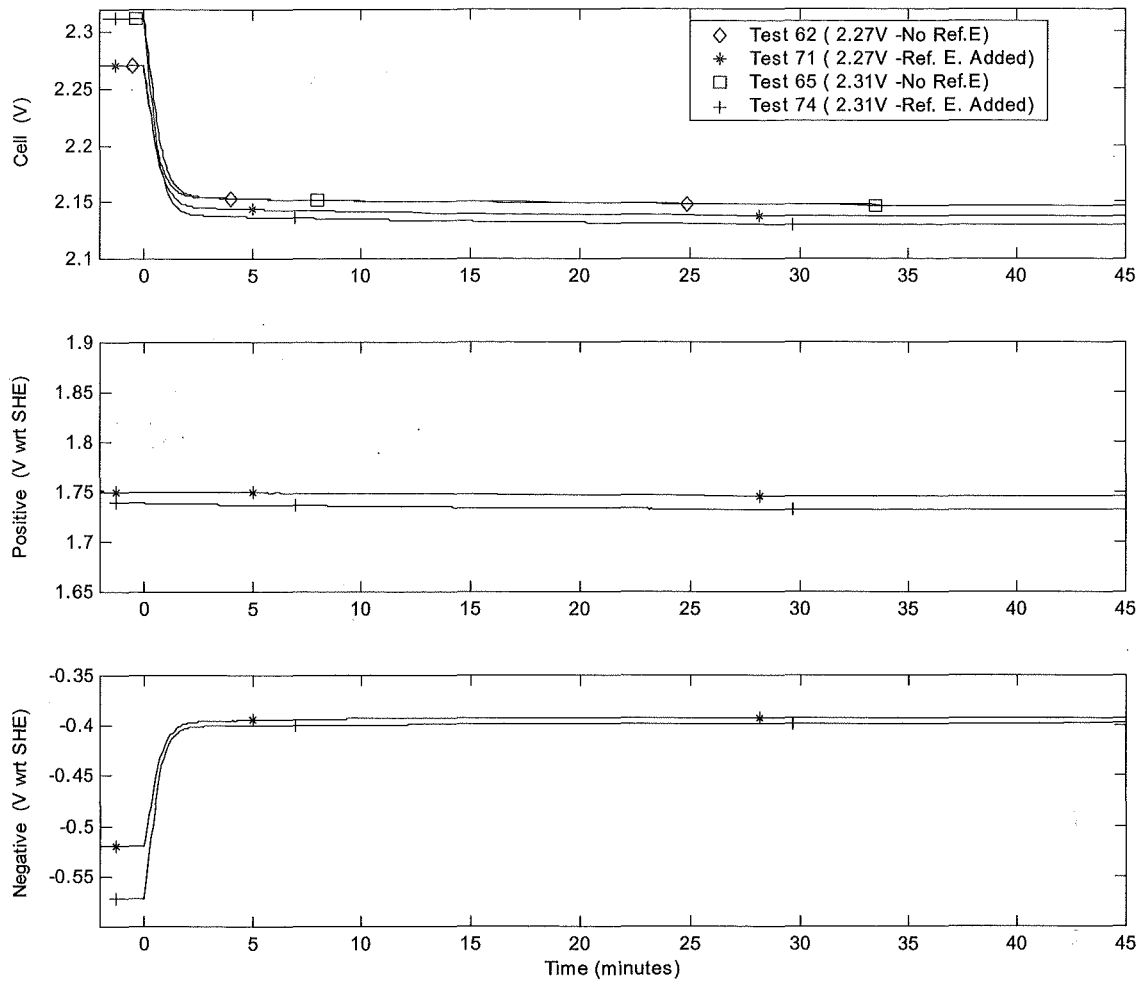

Figure 6.5 Change in Polarisation with Float Voltage – Before and After Reference Electrode Addition

Figure 6.5 shows the effects of float voltage variations and the influence these have on the cell's voltage profile during a constant current (10 mA) discharge. Again, with the exception of the small offset in the settling voltage, the characteristics seen on the terminals of the cell both before and after the reference electrode has been added have a very similar appearance. It is

reasonable to assume that as the voltage profiles on the cell's terminals are similar with and without the reference electrode, the origin of the characteristics is the same before and after it is added. From the results of the tests performed with a reference electrode, it is clear that over the displayed period, the characteristics seen on the terminals of the cell are solely due to the response of the negative electrode.

It can be seen that the cell voltages in Tests 62 and 65 settle to an identical potential. If it is accepted that within the first few minutes of the discharge, the negative electrode decays to its open circuit rest potential (which remains consistent), Tests 62 and 65 must have identical positive polarisations, despite Test 65 having a 40 mV higher float voltage. From the initial voltage drop, it is evident that the additional 40 mV of polarisation supplied to the cell through the increased float voltage has been consumed entirely by the negative electrode. There has been no increase or decrease in the polarisation of the positive electrode as a result of the additional increase in float voltage. This differs from the plots utilising the reference electrode, where it can be seen that for the higher float voltage (Test 74) the cell voltage settles to a lower potential than in the test with the lower float voltage (Test 71). Again assuming that the negative electrode decays to its open circuit rest potential, the lower settled terminal voltage implies reduced polarisation on the positive electrode. This is verified through the reference electrode's measurements of the positive's potential. For the plots with the reference electrode, an unexpected increase in the float voltage, based on expected textbook Tafel characteristics, resulted in the potential of the positive electrode reducing slightly.

An interesting trend seen throughout this series of reference electrode testing is the continual decline in the potential of the positive electrode. While lengthy float charge stabilisation times (two to seven days) were used between successive tests, prior to each discharge test the measured potential of the positive electrode was seen to be reducing. Prior to the discharge of Test 70, the positive electrode had a potential of 1.757 V wrt SHE. Despite the increased float voltage applied in Test 74 prior to the discharge, this test had a positive electrode potential of 1.739 V. While it is not possible to determine whether this reduction in positive electrode potential is due to the addition of the reference electrode or the repeated testing, a significant change has been noted. If this change was solely due to the repeated testing, it is plausible that a similar reduction was occurring during testing, before the reference electrode was added. This may account for the small voltage offset seen on comparison of the tests performed before and after the reference electrode was added.

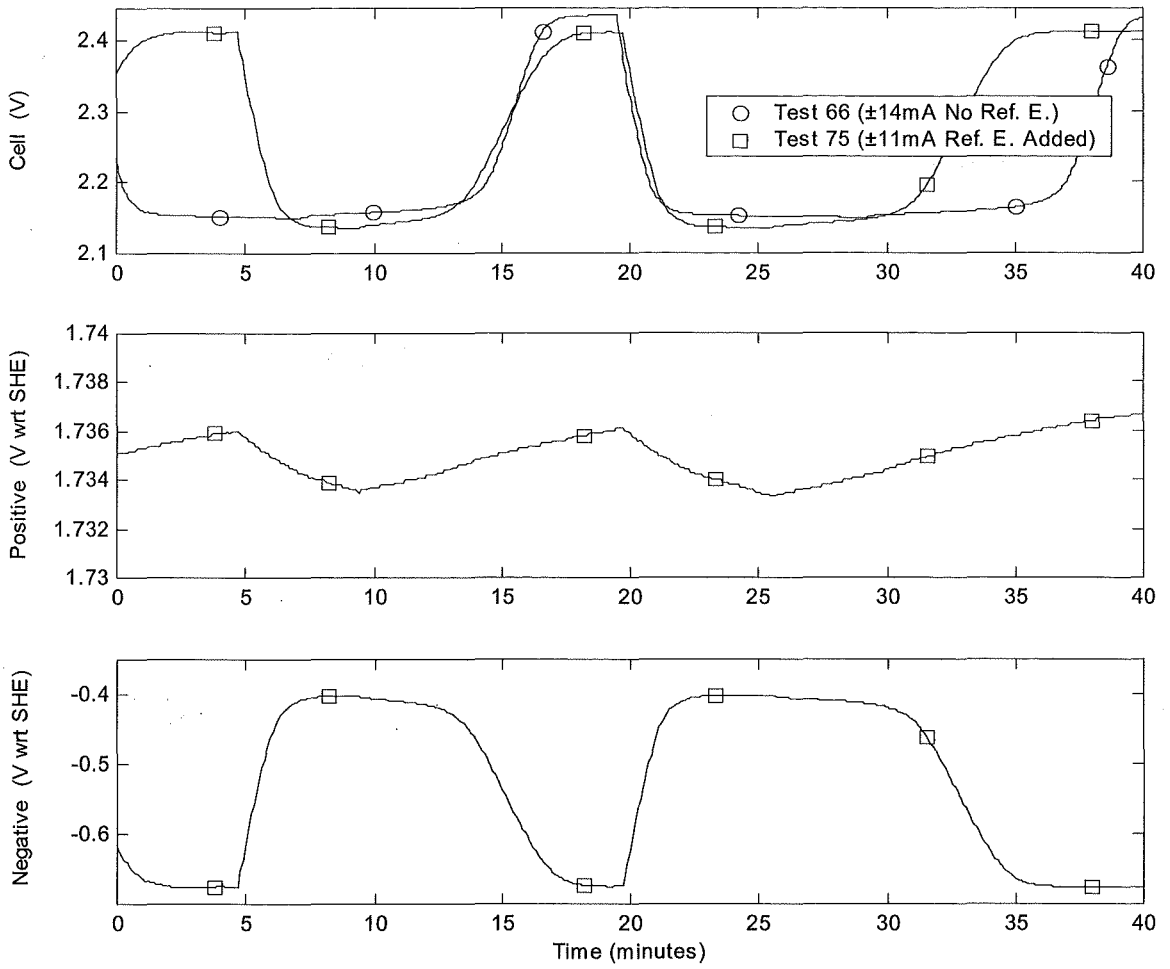

Figure 6.6 Current Perturbation - Before and After Reference Electrode Addition

Figure 6.6 shows the effects of a continuous charge/discharge signal being applied to the terminals of the cell. While a similar test signal was applied before and after the addition of the reference electrode, the level and period of the injected signal differ between the two tests. When the cell voltage profile for each test is compared, the same general response is seen, however the voltage levels and rates of change differ slightly. Overall, the test with the reference electrode (Test 75) has a slightly lower cell voltage profile, and is also seen to have a slightly slower rate of voltage rise when charge current is supplied to the cell. The lower cell voltage profile can be attributed to a decreased potential on the positive electrode as previously discussed, while the reduced rate of voltage rise may be caused by the combination of reduced signal and a slightly increased rate of self-discharge.

As the signals applied in these tests were not identical, the resulting responses of the cell were not expected to be identical either. The underlying characteristic profiles are similar in both plots however. As the cell's terminal voltage characteristics before and after the addition of the reference electrode are similar, it is expected that the individual electrode producing these characteristics was not significantly altered through the addition of the reference electrode. The association of individual electrode contributions with the characteristic response of a cell's terminal voltage profile using a reference electrode must still be valid when no reference electrode is present. Through measurement with a reference electrode, it can be seen in Test 75 that the variation in the positive electrode's potential over the displayed period is less than 3 mV, while for the same period the change in the negative is more than 150 mV. The negative electrode is responsible for virtually the entire terminal response of the cell in Test 75. Due to this, and to the similarities in the cell's terminal characteristics in Tests 66 and 75, it must be assumed that the negative electrode is largely responsible for the cell's terminal characteristics in Test 66.

In this Chapter, the transient features of a cell's terminal voltage response to an applied current signal have been shown to be largely unchanged by the addition of a reference electrode. When a cell's terminal characteristics are decomposed into the responses of the positive or negative electrodes by using a reference electrode, characteristic features of the terminal response may be linked to characteristic features of individual electrodes. As the terminal characteristics of a cell have been shown to remain consistent with the addition of a reference electrode, it must be assumed that the characteristics of each electrode producing the terminal response also remain consistent. With this assumption, characteristic features identified in the terminal response of a cell may be associated with characteristic features of individual electrodes. By doing this, the vastly different transient characteristics of the positive and negative electrodes within a cell, as identified in Chapter 1, may be used to analyse the polarisation distribution within a cell without the aid of a reference electrode. Assessment of a cell's polarisation distribution may be achieved by identifying the magnitude of the characteristic rapid voltage decay of the negative electrode's polarisation. This value of negative polarisation may then be subtracted from the total applied polarisation to determine the polarisation value of the positive electrode.

6.1.1 Field Cell Analysis

In this Section, the terminal response of a cell to an applied test was used to estimate the polarisation distribution within a cell that had not had a reference electrode added to it. A reference electrode was then added to the cell, and the estimated polarisations compared with the measurements taken. From the estimates and measurements of polarisation, it is concluded that the tested CYCLON cell has very little positive polarisation, and is in danger of suffering from positive electrode discharge. This differs significantly from the previously tested ESPACE cell, which was found to have poor negative polarisation. While the capacities of these two cells differ significantly, their natural open circuit polarisation decays from float may still be compared to highlight the differences in distribution of polarisation. The polarisation voltage decay profiles seen on the terminals of the two tested cells have been compared, and the optimal profile for minimum grid corrosion, and therefore maximum cell life, has been identified.

Using the data obtained from the voltage profiles on the terminals of the CYCLON cell for open circuit and various constant current discharge rates, the cell's model parameters were extracted. Using these parameters to calibrate the model, the model's response to current perturbations was then compared to the response of the test cell measured with a reference electrode.

6.1.1.1 Field Polarisation Estimation

The polarisation distribution within a cell in field service may be estimated through the analysis of the voltage profiles on the cell's terminals following the removal of the float charger. This test and analysis procedure may be applied to any 2 V cell, and requires a low rate discharge (natural open circuit decay up to discharge rates of C/1000). For this analysis, the profile of the cell's terminal voltage as it decays from the float voltage to the fully charged rest voltage is required.

In the preceding Chapters, it has been shown that upon removal of the float charger, the initial rapid decay (present within the first few minutes) is due to the polarisation decay of the negative electrode. The slower decay (taking up to 40 hours) that follows this is due to the polarisation of the positive electrode. Figure 6.7 shows the same test data as Figure 6.2 and Figure 6.3, however the displayed time and voltage have been reduced for greater clarity. The top plot of Figure 6.7

shows that following the initial and almost instantaneous decay, there is a second gradual decay of approximately three hours duration. The initial drop seen in this plot is due to the polarisation of the negative electrode, while the second slower decay is due to the polarisation of the positive.

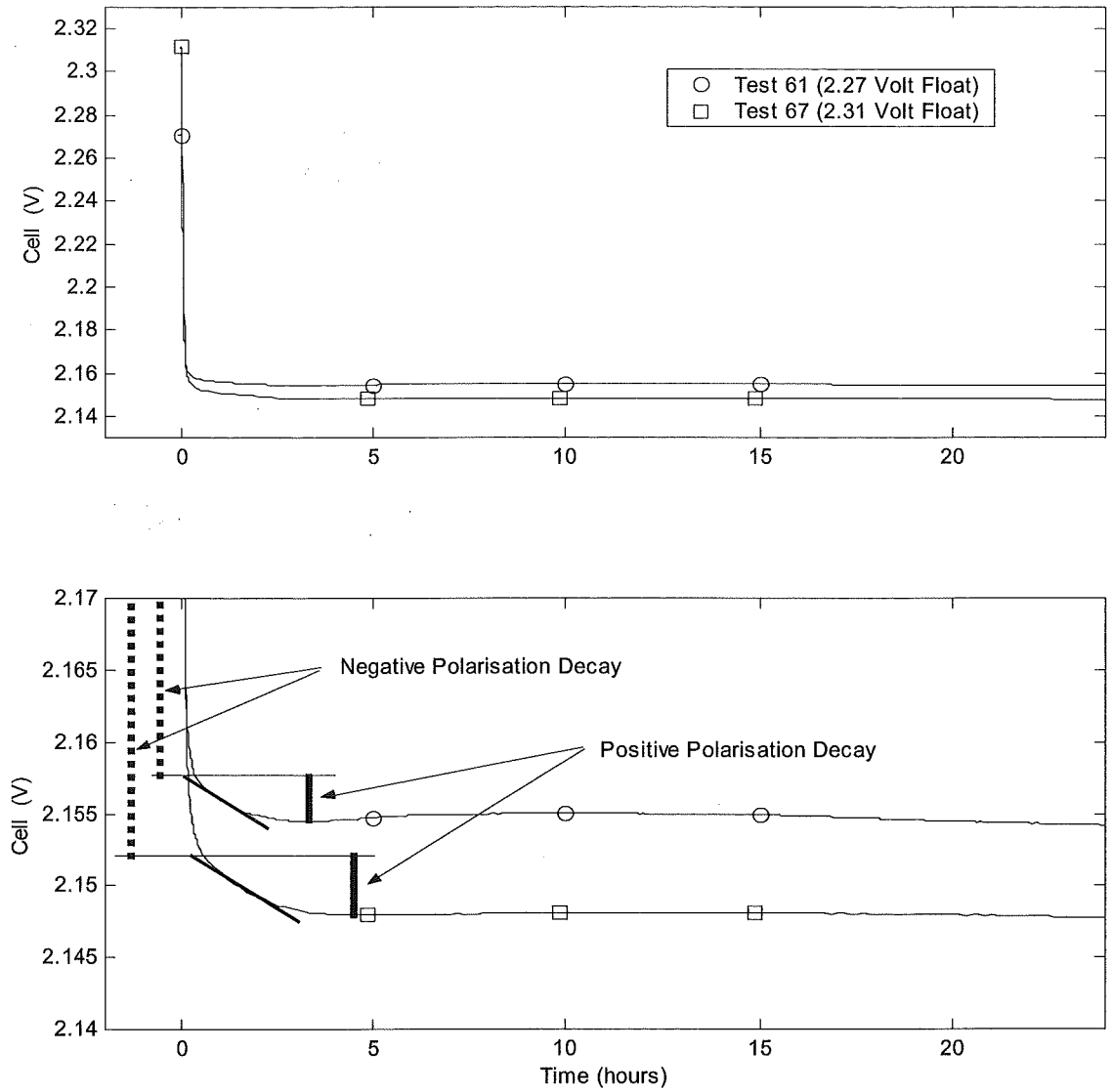

Figure 6.7 Polarisation Decay Due to the Positive and Negative Electrode

Test 61 in Figure 6.7 shows the open circuit voltage decay of the tested cell prior to the addition of a reference electrode. It can be seen that the rest voltage at which the cell settles after ten hours is approximately 2.155 V given a float voltage of 2.27 V. The 115 mV difference between these two readings is the total polarisation applied to the cell. The lower plot in Figure 6.7

shows the transition between the negative and positive polarisation decays on an amplified voltage axis. It can be seen that the positive polarisation decay of Test 61 is approximately 3 mV. With 3 mV of the 115 mV total polarisation of the cell being accounted for by the positive electrode, the negative electrode must have the remaining 112 mV. As the estimated polarisation on the positive electrode is almost non-existent, the cell is in danger of suffering from positive electrode discharge. The cell's positive electrode polarisation is well below the optimal 40 - 80 mV window for minimum grid corrosion, and as a result the cell will have a reduced life.

If the tested cell displays textbook Tafel characteristics, it is expected that increasing the float voltage of the cell should result in an increase in polarisations on both the positive and negative electrodes. The plot of Test 67 (Figure 6.7) shows the open circuit decay of the tested cell, where the float voltage preceding the discharge has been raised to 2.31 V. Through a similar analysis to that outlined in the above paragraph, it can be seen that despite the 40 mV increase in float voltage, the positive electrode's polarisation has only increased by 1 mV (estimated). The polarisation on the negative electrode is estimated to be approximately 158 mV (2.31 - 2.152), and the total polarisation for the cell at a float voltage of 2.31 V is seen to be 162 mV. The polarisation of the positive electrode accounts for the remaining 4 mV. The total polarisation at the float voltage of 2.31 V is 47 mV greater than that at 2.27 V, despite a float voltage increase of only 40 mV. The additional 7 mV is accounted for by the reduction in the fully charged open circuit rest potential of the cell, as previously discussed in this Section. This reduction in rest potential is believed to be related to the repeated testing of the cell, however attempts to verify this have not been made. From these test results, it is clear that the tested cell does not display conventional textbook Tafel characteristics.

In the previous two paragraphs, the test cell has been estimated to have extremely low positive electrode polarisation values of 3 mV and 4 mV at float voltages of 2.27 V and 2.31 V respectively. These estimates have been produced through analysis of the voltage profiles on the terminals of the cell following the removal of the float charge supply. The estimates have then been verified by subsequent measurements made using a reference electrode. Test 70 in Figure 6.2 and Figure 6.3 is essentially a replication of Test 61, however a reference electrode has been added to the cell. It can be seen in Test 70 (Figure 6.2) that the positive electrode's potential reduces by approximately 3 mV in the first hour following the removal of the float charge supply. The distribution of the applied polarisation may be estimated through analysis of a cell's terminal voltage decay profile from float charge. As polarisation data is traditionally obtained

through reference electrode testing, the developed polarisation estimation technique may be considered a virtual reference electrode.

In the preceding analysis, it has been estimated and verified through experimental measurement that the tested cell has extremely low levels of positive electrode polarisation. While low values of positive polarisation are known to promote excessive grid corrosion, if polarisation is non-existent the electrode may suffer a gradual discharge. Interestingly, during the full discharge test of this cell with a reference electrode in situ (Test 69 in Figure 6.1), the cell is seen to be positive limited, i.e. the positive electrode rolls off rapidly at the end of the discharge, while the negative electrode's profile remains consistent. As there are several reasons for the occurrence of this positive limitation, no direct conclusions linking the low or non-existent positive polarisation to the positive limited discharge can be drawn. However, a positive limited discharge would be expected if the positive electrode was not fully charged.

6.1.1.2 Polarisation Discharge Profiles

In this Chapter, the verification testing undertaken with the CYCLON cell has concluded that the cell has extremely low values of positive electrode polarisation at the recommended and elevated float voltages. The testing undertaken for the development of the model used a very different cell design, and during this testing it was seen that the tested ESPACE cell had low values of negative electrode polarisation at the recommended float voltage.

It has been shown in this work that the discharge of the negative electrode's polarisation is significantly faster than the discharge of the positive polarisation. When the natural open circuit polarisation decay profiles of the two tested cells are compared, the differences in the discharge profiles are easily seen. Figure 6.8 compares the polarisation decay of the tested CYCLON and ESPACE cells. It can be seen that as the CYCLON cell has virtually no positive electrode polarisation, within the first few minutes of removing the float charge supply, the cell's voltage collapses to close to its rest potential. Following this, very slight positive polarisation decay lasting approximately three hours is seen. The polarisation decay of the ESPACE cell differs considerably. In the top plot of Figure 6.8, the dual slope discharge profile is not apparent, however when the time axis is expanded in the lower plot, two distinct components in the polarisation decay profile are evident. In this case, the faster initial decay indicates that there is

approximately 19 mV (2.297 – 2.278 V) of negative electrode polarisation. The slower decay of about 35 hours indicates that there is approximately 151 mV (2.278 – 2.127 V) of positive polarisation. As both electrodes of the ESPACE cell have significant levels of polarisation at this float voltage, both electrodes should remain fully charged. However, as the positive polarisation for this cell is significantly greater than the 40 - 80 mV window for minimum grid corrosion, maximum cell life may not be realised. The excessive polarisation on the positive electrode will also cause an increased rate of overcharge gassing. If this exceeds the limit that can be recombined within the cell, gas loss through venting will result. This may cause the cell to fail prematurely through dryout.

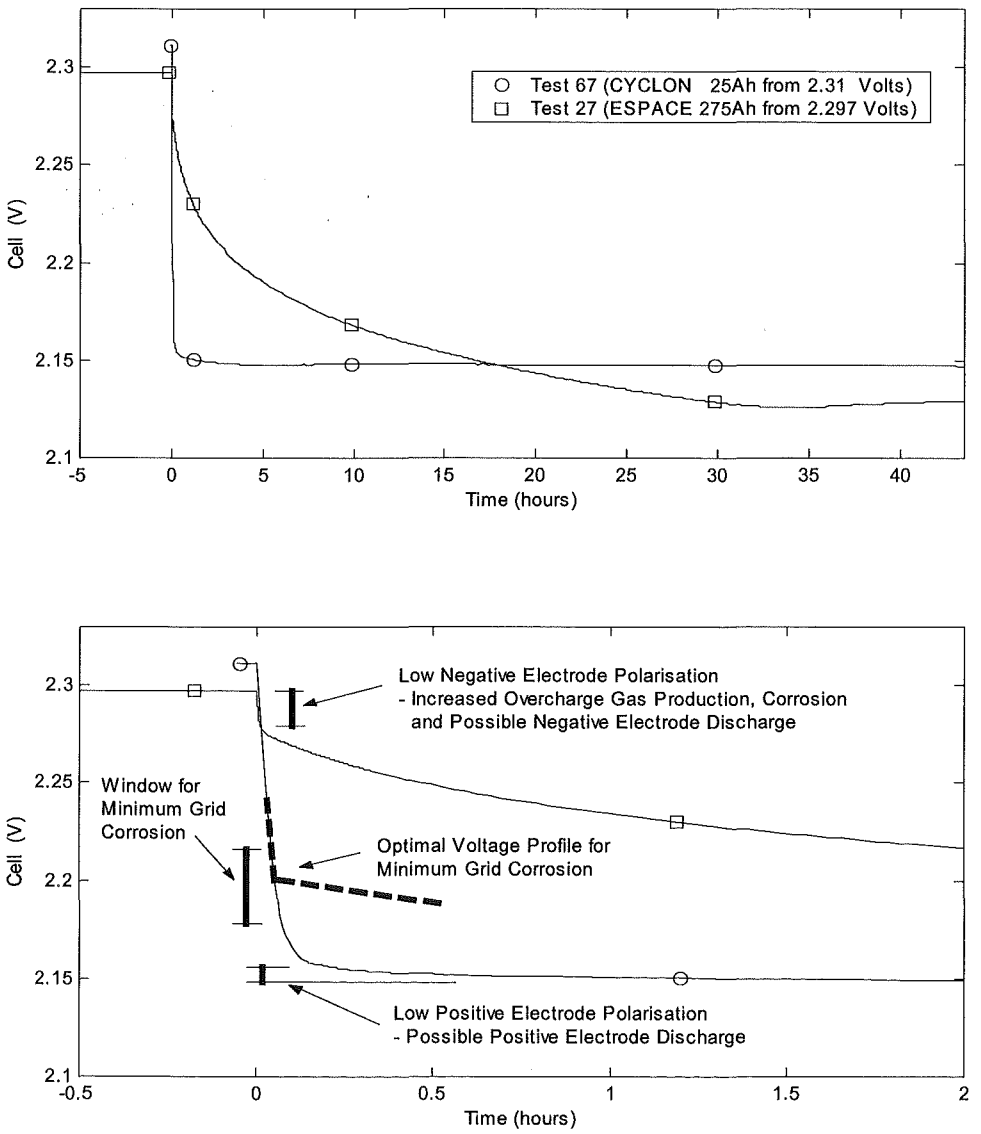

Figure 6.8 Low Negative, Low Positive, and Optimal Polarisation Discharge Profiles

For maximum cell life, the break point in the polarisation decay profile, which indicates the change from or end of the negative polarisation decay, should ideally occur at approximately 40 - 80 mV above the fully charged rest potential of the cell. The dashed line in the lower plot of Figure 6.8 indicates the ideal voltage decay profile.

6.1.1.3 Cell Model

Using only steady state values of voltage and current, along with the transient voltage profile measured on the terminals of the cell, sufficient parameters have been extracted to allow the model developed in Section 5 to be calibrated to the test cell. It has been previously indicated in this Chapter that there has been a gradual decay in the potential of the positive electrode throughout this series of testing. This has produced an offset in the terminal voltages recorded in the testing undertaken without a reference electrode, and those recorded in the testing with a reference electrode in place. To account for this voltage difference, two slightly different models of the cell have been generated. Table 6.2 lists the two sets of model parameters used for the simulations, and Figure 6.9 shows the Tafel plots of the cell models and the non-linear resistors used to produce their steady state Tafel characteristics. The differences between the two models are generated from the specification of the cell's fully charged rest potential, and the level of positive polarisation at the specified float voltage. These differing parameters are highlighted by '•' symbols in Table 6.2. The effects of these model changes do not significantly alter the Tafel plot for the models as shown in Figure 6.9 a) and b). While only two characteristic parameters have been changed in the two models, many of the calculated values of the models' components have changed slightly as a consequence.

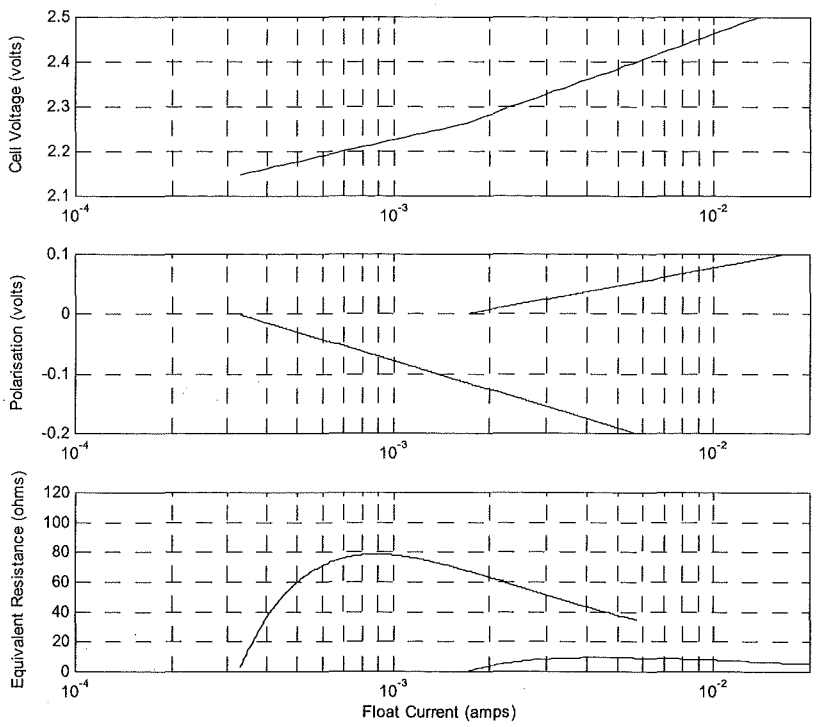

a) Model A

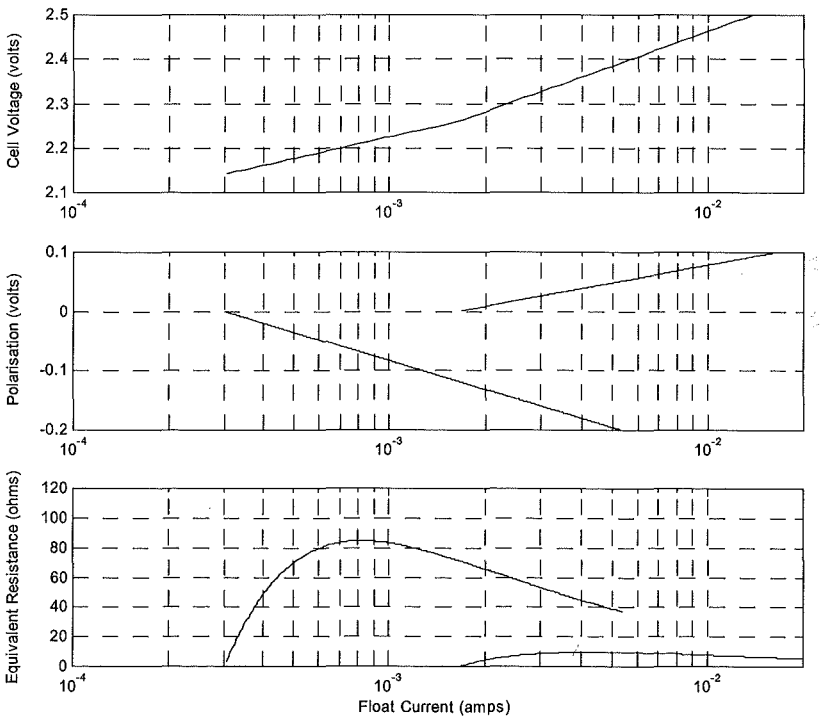

b) Model B

Figure 6.9 Tafel Plot and Equivalent Tafel Resistors

Model A	Cyclon_25ah_t66.dat	Model B	Cyclon_25ah_t75.dat
25.000000	% cell_capacity	25.000000	% cell_capacity
10.000000	% discharge_time -not reqd	10.000000	% discharge_time -not reqd
2.270000	% float_voltage -not reqd	2.270000	% float_voltage -not reqd
0.001800	% float_current -not reqd	0.001800	% float_current -not reqd
• 0.003000	% pos_polarisation @float -not reqd	• 0.004000	% pos_polarisation @float -not reqd
1.930000	% empty_open_cct_rest_volt -not reqd	1.930000	% empty_open_cct_rest_volt -not reqd
• 2.148000	% full_open_cct_rest_volt -not reqd	• 2.142000	% full_open_cct_rest_volt -not reqd
75.000000	% pos_bulk_percent -not reqd	75.000000	% pos_bulk_percent -not reqd
0.524112	% hg_hg2so4_offset_voltage wrt center	0.522648	% hg_hg2so4_offset_voltage wrt center
1.611000	% volt_ochg_start_pos	1.606500	% volt_ochg_start_pos
0.537000	% volt_ochg_start_neg	0.535500	% volt_ochg_start_neg
550458.715596	% c_bulk_p	566037.735849	% c_bulk_p
1651376.146789	% c_bulk_n	1698113.207547	% c_bulk_n
1238.532110	% c_ochg_p	1273.584906	% c_ochg_p
4.128440	% c_ochg_n	4.245283	% c_ochg_n
0.100000	% pos_ochg_slope	0.100000	% pos_ochg_slope
0.001680	% pos_ochg_int -not reqd	0.001642	% pos_ochg_int -not reqd
0.277473	% pos_ochg_1a	0.278473	% pos_ochg_1a
0.160000	% neg_ochg_slope	0.160000	% neg_ochg_slope
0.000325	% neg_ochg_int -not reqd	0.000302	% neg_ochg_int -not reqd
0.558156	% neg_ochg_1a	0.563156	% neg_ochg_1a
0.001000	% full_chg_acid_res	0.001000	% full_chg_acid_res
0.000010	% pos_metal_res	0.000010	% pos_metal_res
0.000010	% neg_metal_res	0.000010	% neg_metal_res
959.009778	% pos_self_dischg_res	978.606790	% pos_self_dischg_res
1653.681168	% neg_self_dischg_res	1772.094877	% neg_self_dischg_res

Table 6.2 Parameters Used for Modelling the CYCLON Cell

The key parameters for the calibration of the model are the cell capacity (25 Ah), the float voltage and current (2.27 V and 1.8 mA), the positive polarisation (3 mV and 4 mV in models A and B), and the open circuit rest voltages (2.155 and 2.149 V in models A and B). These parameters were obtained either from direct measurement or from the open circuit voltage decay profiles seen on the cell's terminals. A value of 1.93 V was obtained from the application manual for this cell type, and used for the fully discharged open circuit voltage. This parameter does not greatly affect the float characteristics of the model. With the exception of the 'neg_ochg_fraction' and the 'neg_ochg_slope', parameters specifying the cell were not changed from default values. The 'neg_ochg_fraction' and the 'neg_ochg_slope' were changed to provide a more realistic replication of the cell's transient response to the current perturbation testing shown in Figure 6.11 and Figure 6.12. The 'neg_ochg_fraction' was reduced from a default value of 5e-5, to 1e-5. This reduced the capacitance associated with the negative electrode's overcharge, and consequently reduced the transient response time. The 'neg_ochg_slope' was increased from a default value of 120 mV per decade, to 160 mV per decade, resulting in an increase in the voltage swing of the cell for a given signal current.

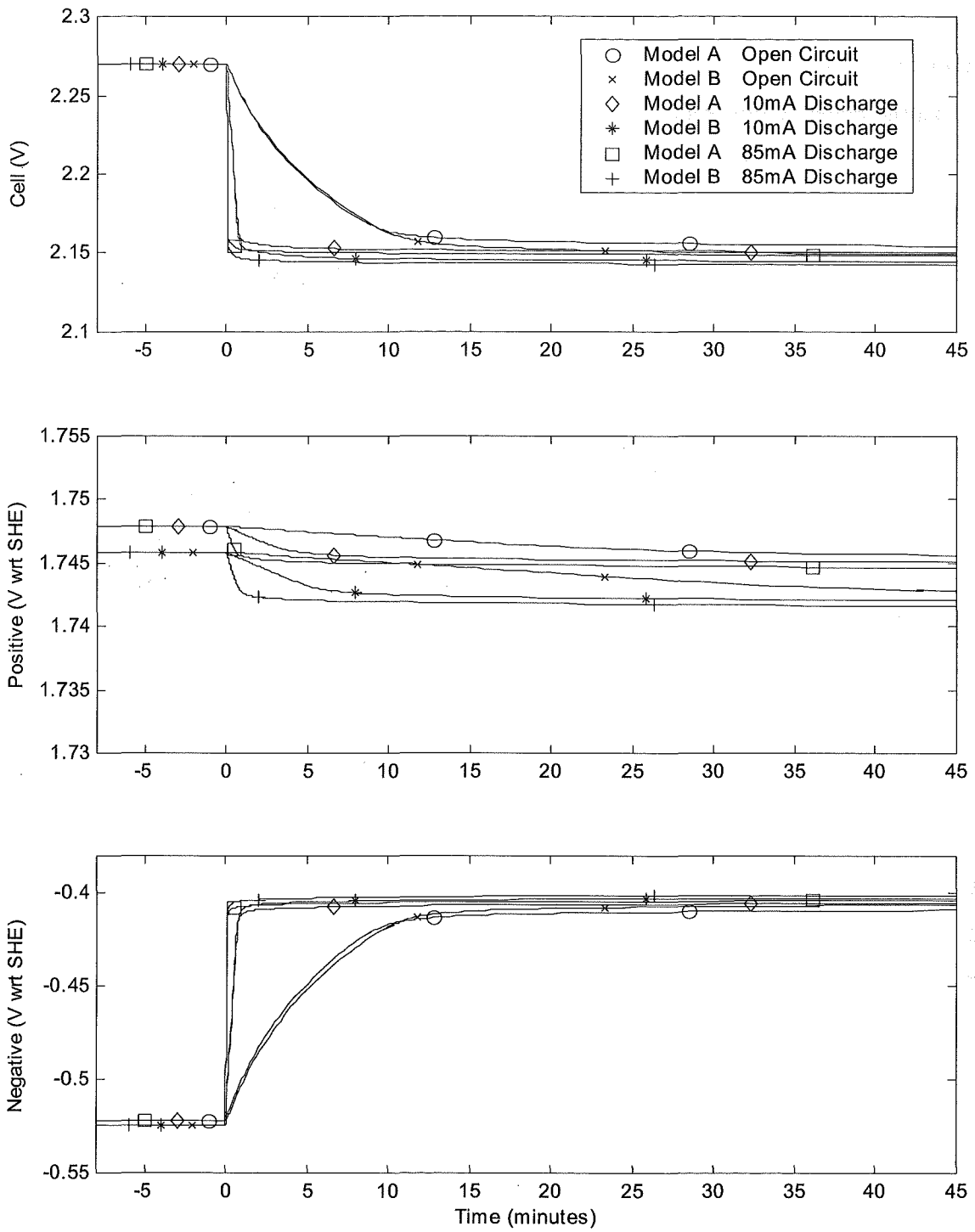

Figure 6.10 Simulated Polarisation Discharge Profiles Using Model A and Model B

Figure 6.10 shows simulated polarisation decay profiles of the CYCLON cell for the two models. This figure may be compared with measured test data plots shown in Figure 6.4. Considering the very limited amount of model training or calibration data, the response of the model to the various discharge rates is very close to the response seen in the test data. It can be seen that the negative electrode supports almost the entire (120 mV) polarisation supplied to the cell, while the positive has extremely low levels of polarisation. The open circuit decay of the models' polarisation appear to have a slightly longer duration than is seen in the test data, however the simulated 10 and 85 mA discharges show a similar duration to the experimental data.

The difference between the two simulation models (A and B) is shown through the slight difference in the potentials to which the cell settles on comparison of like discharge rates. Comparing the reference electrode testing of Figure 6.4 to the simulations using model B in Figure 6.10, the potentials of the simulated electrodes prior to the discharge are low by approximately 5 mV. While this is a pleasing result, determining the exact potential of each electrode is not as important as assessing the polarisation (difference between the float and rest potentials) on each electrode. Considering the calibration parameters for the models were obtained from the terminal characteristics of the cell, the polarisation decays of each electrode are clearly visible in the simulations, and these appear very similar to that measured with a reference electrode.

When the plots in Figure 6.4 are analysed, it may initially be assumed that the reduction in the cell's settling potential with increasing discharge rates is due to internal resistance voltage drops. However, it has been previously established that throughout the testing, there has been a continuous gradual decay of the positive electrode's potential. A constant offset voltage is apparent between similar tests in the two series of experimental testing, due to the consistent time intervals between these tests. However the latter tests in each series, performed at higher discharge rates, have reduced potentials due to the continuous gradual decay of the positive electrode's potential. As both simulation models remain consistent, this effect is not seen (or expected) in Figure 6.10. The effects of internal resistance are negligible at the indicated discharge rates.

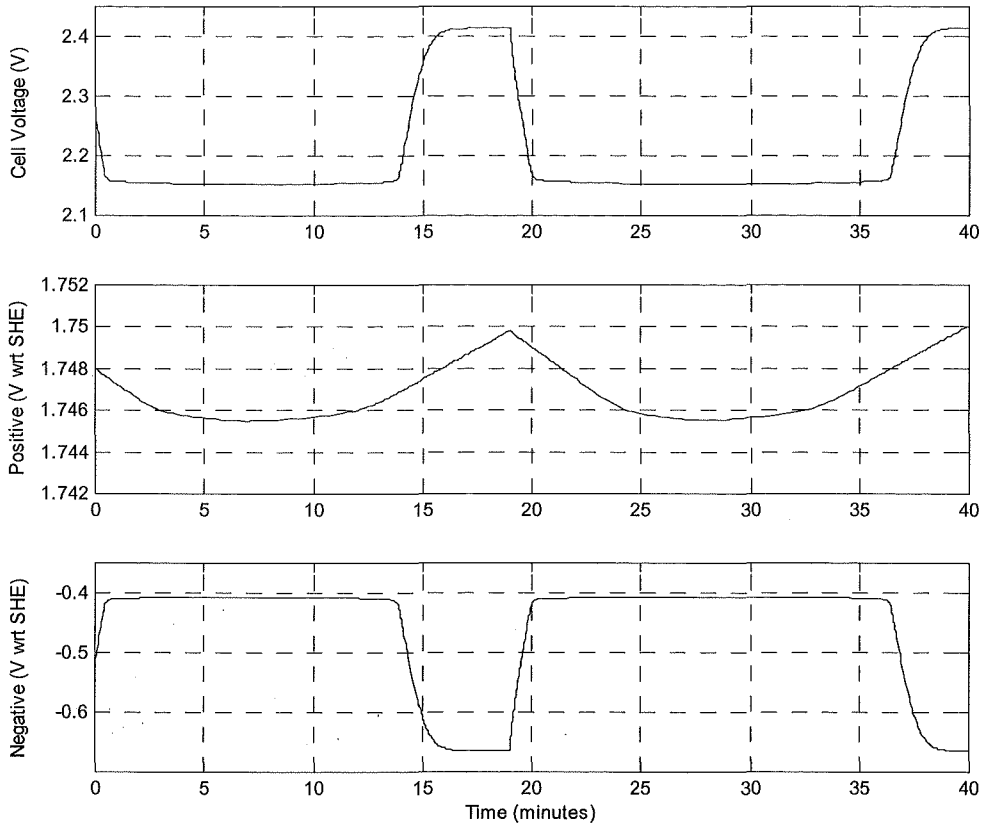

Figure 6.11 Simulated Response of Model A to ± 14 mA Current Injection

Figure 6.11 shows the response of the developed model when a 14 mA current signal is simulated. The cell specific data file used to calibrate the model has been previously described and detailed as 'Model A' in Table 6.2. This simulation may be compared to experimental test results shown in the plot of Test 66 in Figure 6.6. When the simulations of the cell's voltage profile are compared to the measured test data, it can be seen that similar underlying characteristics exist overall. Some differences are seen around the point where the negative electrode makes the transition between the bulk storage and overcharge regions of operation. This transition is seen to be more abrupt in the simulation than in the experimental data. However, the magnitude and limits of the cell's voltage, along with the voltage rate of change, are similar in both the simulation and the experimental data.

As the experimental data of Test 66 was gathered without a reference electrode, comparisons between the simulated electrode characteristics and experimental characteristics cannot be

directly made. As expected, the simulation shows that almost the entire cell terminal response is due to the response of the negative electrode. However the positive electrode does not show the expected triangular response seen in previous simulations and experimental data. The dish shaped characteristic of the positive electrode seen in Figure 6.11 is due to the low polarisation level further decaying to the point where the electrode begins to enter its bulk charge region of operation.

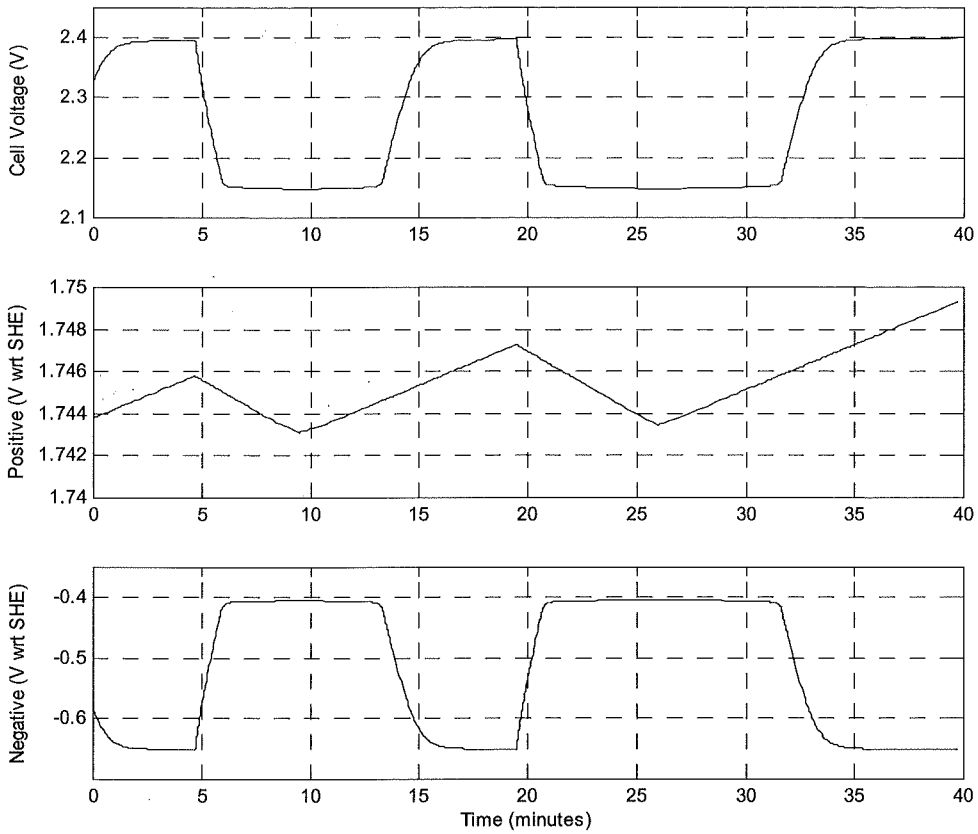

Figure 6.12 Simulated Response of Model B to ± 11 mA Current Injection

Figure 6.12 shows the response of the developed model when an 11 mA current signal is simulated. The cell specific data file used to calibrate the model has been previously described and detailed as 'Model B' in Table 6.2. This simulation may be compared to experimental test results shown in the plot of Test 75 in Figure 6.6. Many similarities are seen when the simulated voltage profiles of the cell and each electrode are compared to the experimental data, making it clear that the model reproduces the underlying characteristics of each electrode within the cell. The model closely estimates both the amplitudes and the characteristic profiles of each electrode

within the cell. While it can be seen that the simulated magnitude and rate of change of the positive electrode is similar to that of the measured data, overall the simulated potential of the positive electrode is approximately 10 mV higher than the measured data. It is also seen that there are slight differences in the terminal response of the simulation and the measured terminal voltage response of the cell. Better tuning or calibration of the model to replicate the measured response of a cell should further improve the accuracy of the model's estimations of each electrode's response and potential. However, considering that the values of the components within this model were extracted almost entirely from conventional voltage and current measurements made external to the cell, the accuracy and ability of the model to estimate the internal voltage distribution is very valuable. Effectively, when the model is calibrated to replicate both the steady state and transient responses seen on the terminals of a cell, the estimates produced by the model act as a virtual reference electrode for the tested cell.

The structure of the float charge model and the interaction of components within this model were developed with data obtained from a vastly different cell design, capacity, and mode of operation (low negative polarisation compared with low positive polarisation). The close correlation between measured and simulated responses (of each electrode and the cell as a whole) shown in this series of tests highlights that the dominant underlying features of the float charge region of operation have been identified and appropriately modelled. With very limited calibration data, the model developed in Chapters 4 and 5 of this thesis has been adapted to a cell of very different design, capacity, and float charge operating point. Despite the differing cell type, the simulated response of each electrode (and the cell) remains in close agreement with the measured data.

6.2 Applications

In this thesis an analysis of the float charge operation of VRLA cells has been undertaken. Two goals for float charge have been identified: 1) Ensuring the battery remains fully charged, and 2) Maximising the life of the battery. Through appropriate distribution of the polarisation applied to the cell by the float charge, both of the identified goals of float charge may be realised simultaneously. However, the cell's design and construction largely determine the manner in which this applied polarisation is distributed within the cell. To a much lesser extent, the total polarisation applied to a cell may be controlled in an attempt to optimise the level of polarisation on individual electrodes within the cell.

Through modelling the steady state and transient characteristics of each electrode within a cell, a test and analysis technique has been developed that estimates the polarisation distribution within a float-charging VRLA cell. While the outcome of this test produces similar information to that obtained through reference electrode testing, the test does not use any form of reference electrode, and may be applied to any standard 2 V VRLA cell without any modification to the cell.

It is understood that many long life VRLA cells suffer from low or no polarisation on the negative electrode. This mode of operation produces several mechanisms that impact on a cell's life expectancy. If the float voltage is not appropriately adjusted, the low negative polarisation will produce increased positive polarisation, thus raising the level of life-limiting positive grid corrosion, and also the rate of overcharge gas production. If gas production is excessive, gas venting and premature failure through dryout can result. Low or non-existent negative electrode polarisation may also result in a gradual discharge of the electrode to the point where the available capacity of the cell does not meet the load requirements, forcing replacement of the cell.

The problems that lead to the premature failure of some VRLA cells have been described in this work, and a simple field useable test and analysis procedure for identifying these problems and measuring the success of the applied float charge has been developed. As this work has focused on the identification of these float charge problems, and the development of an analysis procedure suitable for widespread field use, the strategies or techniques that may be used to attempt to correct problem cells have not been thoroughly investigated. Section 6.2.3 suggests future work that could be undertaken in this control area now that the float assessment tools have been developed.

While the test and analysis procedure was primarily developed for the early detection of float charge problems so that corrective action might be taken before cell damage becomes apparent, there may be many other uses for the developed model and polarisation estimation technique. Section 6.2.1 suggests possible uses of the developed float charge model, along with future work and improvements that may be made to the model. Section 6.2.2 describes some alternative applications or uses of the developed test procedure that estimates the distribution of polarisation within a cell.

6.2.1 Model Uses

The developed float charge model may have many alternative uses besides the intended assessment of cells on float charge in the field. Some of these uses may include provision of simulations for product development and testing, or tracking variations in a cell throughout its life by detailing variations in component values within the developed model. The latter suggestion may provide a timely indication that the end of battery life is imminent, allowing replacement batteries to be purchased prior to the battery failure occurring.

Due to the low voltage of a single VRLA cell, a number of cells are normally connected in series to form a 'string' in order to achieve useable voltages. As the string length is increased, the equalisation or uniformity of cell voltages tends to be reduced. To equal the 400 – 600 V DC provided by some UPS batteries, some two to three hundred 2 V cells must be series connected. The developed float charge model may also be serially stacked to simulate the operation of such long strings, however a slight spread will need to be specified for parameters such as float voltage, current, and polarisation. This spread in component values may be defined for best or worst case, or a random spread may be simulated within a specified window. With the modelling of a string of slightly different cells, battery-monitoring algorithms, string level optimisation, control techniques, and cell level equalisation methods and techniques may be simulated, assessed, and optimised.

If sufficient information is gathered during testing or general battery operation, the model may be accurately calibrated for each cell. Over time, the unchanged model will highlight variations in the operational characteristics of the cell, as these change. Re-calibration of the model will highlight the components of the model affected by the changes in the cell. Depending on the model components that have altered, the cause of the change may be determined, and possibly linked to age, operation, or cell faults. However, as the developed model targets the float region of VRLA battery operation, in its present configuration some of the traditional failure modes, such as grid corrosion, may not be appropriately modelled. Further work is necessary to improve the model's representation of the bulk charge and discharge regions of operation if a complete assessment is required. The traditional (designed) cell failure mode is grid corrosion, which causes an increase in the internal resistance of the cell, and eventually limits the current that can be supplied by the cell for a given voltage drop. Internal resistance problems are best

highlighted through high rate charge or discharge tests, as these high rate tests tend to be used to indicate capacity related SOH or remaining life. The developed test assesses the float operation of cells. The accuracy of this assessment improves as the discharge rate is reduced. As the best results are produced from open circuit decay, internal resistance does not have a large influence on the developed test. The developed model essentially assesses the SOC while the cell is float charged. While it is understood that the float voltage variation between cells in the same string may be significant when the cells are new, this variation converges to a low value for the majority of the cell's useful life, and then diverges towards the end of life. Further work is required to determine whether the developed float charge model may be used to assess the changes in float characteristics as cells age, and to establish whether this may then be used to indicate imminent cell failure.

6.2.2 Test Procedure Uses

The developed polarisation estimation test may have many applications besides the intended use of assessing cells in field service. The conventional method of assessing polarisation distribution in a laboratory involves the use of a reference electrode, however as a VRLA cell operates as a sealed unit, the addition of a reference electrode to a cell always has the potential to modify the cell's characteristics. It was seen in the first series of tests, using the ESPACE cell, that large variances in cell characteristics were produced through inconsistencies in the negative electrode Tafel line (intercept point). Atmospheric oxygen entering the cell through leaks in the case is said to have a depolarising effect on the negative electrode. Puncturing the cell's case to add a reference electrode must therefore increase the possibility of producing such leaks. As the developed polarisation assessment technique does not require any modification to the cell, the chances of altering the cell's characteristics must be reduced. The developed test may replace or supplement conventional laboratory reference electrode testing used during the development and design verification of new products. The polarisation estimation test may be extremely useful during accelerated life testing undertaken at elevated temperatures, where the use and maintenance of reference electrodes is difficult.

The developed polarisation estimation test procedure may also be used to verify the operation of cells after their manufacture, before they leave the factory. As newly manufactured cells are likely to have excessively wet separators, the paths through the separator required for oxygen

recombination may not be fully developed. A new cell may therefore operate as a flooded cell until sufficient gas has vented, and the separator has dried to the point where recombination gas paths are developed. As flooded cells are expected to have well polarised negative electrodes, the absence of this may highlight electrolyte-filling problems, or possibly case sealing problems. The voltage decay profiles measured on cell terminals for open circuit or low rate discharges may be used to indicate product consistency.

6.2.3 Float Charge Optimisation

Without knowledge of the polarisation distribution within a cell, any attempt to optimise the float charge must be based on historical data from other cells of similar type, generic empirical rules of thumb, or recommendations from laboratory based testing of the same cell type. As no simple or practical method of assessing the polarisation of standard cells was available, individual cell based float charge optimisation has not been possible.

In this thesis a model of the float charge region of operation of a VRLA cell has been presented, and a test and analysis technique has been developed to provide an estimate of the polarisation distribution within any standard 2 V VRLA cell. While this model was essential for the development and verification of the test and analysis technique, a calibrated model is not essential for analysis of a cell's polarisation. The developed testing technique requires only the cell's polarisation decay profile for polarisation estimation.

As the majority of this work has focused on developing the tools necessary to obtain polarisation estimations, little work has been undertaken on optimisation techniques and strategies to ensure both float charge goals are achieved. For a well designed cell that displays consistent textbook Tafel characteristics, the optimisation should be simple and uncomplicated. However with cells identified to be suffering from electrode polarisation problems (either positive or negative), the optimisation may be more complicated. The two cells extensively tested in this thesis were both shown to have poor electrode polarisation distributions. When the float voltage was varied on both of these cells, unexpected redistribution of the applied polarisation resulted.

It is believed that a large number of VRLA cells in field service suffer from electrode polarisation problems, the most predominant of which is negative electrode discharge. Further

work is required to determine appropriate control strategies to that ensure the cell is maintained in a fully charged state, and that maximum life for the defective cell is realised. For example, two courses of action may be available should a cell be proven to be suffering from a gradual discharge of the negative electrode. It must be determined whether it is more beneficial to: a) raise the float voltage in an attempt to polarise the negative electrode, at the expense of increased positive grid corrosion and possible dryout resulting from gas venting, or b) reduce the float voltage, giving the positive electrode optimal polarisation for minimal grid corrosion, and perform regular boost charges to ensure that the negative electrode is periodically fully charged.

When cells are charged in a series string, a spread in the terminal voltages of individual cells is often seen. The developed polarisation estimation technique may be used to assess the benefits or disadvantages of various cell voltage equalisation schemes. The advantages of natural voltage (no equalisation), uniform voltage equalisation, and optimal voltage for each cell using individual positive polarisation values may be compared to determine the scheme that best fulfils the float charge goals for the entire string.

Temperature compensation is a common technique that is used when cells are operated at temperatures either higher or lower than the designed operating point. While temperature compensation may reduce overcharge gas production levels and the possibility of thermal runaway, it does not maintain an optimal polarisation for minimum grid corrosion. Because the developed polarisation estimation assessment technique is unaffected by temperature, the polarisation at the compensated float voltage may be assessed following initial application of the recommended temperature compensation. This will determine whether the float voltage is appropriate, and whether the goals of float charge have been achieved.

Conventionally, a specific single float charge voltage is recommended for a given cell type, regardless of its age. The developed polarisation assessment technique will allow an optimal float voltage to be maintained throughout the life of the cell. This may compensate for cell characteristic variations due to age, or operational history. Further work would be required to assess the advantages or disadvantages of such an optimisation system.

A simple tool has been developed to provide an assessment of the polarisation distribution within any standard 2 V VRLA cell. With the information provided by this test, many float charge optimisation schemes may be assessed and compared. The developed tool will identify cells

with float charge problems before permanent damage is done, and also provide a measure of the success of the float charge, allowing the effectiveness of any correction or optimisation techniques to be assessed. As a tool is now available to assess the operation of VRLA cells on long-term float charge in field service, float charge problems may be identified promptly. This allows corrective action to be taken in the early stages, before the problems escalate to levels where unrecoverable damage is sustained by the cell.

7 Conclusions

In many applications a continuous supply of power is critical to the success of the application. Telecommunications systems are no exception to this, and as such their power systems typically utilise large Valve Regulated Lead Acid (VRLA) storage batteries to ensure that critical equipment has a continuous power supply in the event of a disruption to the primary AC power supply. In areas that have a reliable power supply, months or even years may pass before a disruption to the AC power occurs and the storage batteries are required to power the load. During this often lengthy time of limited activity, the storage battery must be maintained in a fully charged state. As all lead acid batteries have a relatively high self-discharge rate, a 'float charge' is necessary to counteract this.

Two goals of float charge have been identified: 1) Counteract the natural self-discharge of the battery and indefinitely maintain it in a fully charged state, and 2) Maximise the life of the battery. Traditionally, a float voltage for a given cell design is determined and recommended by the battery manufacturer. This float voltage is then applied largely unchecked to cells in field service throughout their useful life. The critical parameter relating to successful float charge is electrode polarisation, and in particular, the polarisation on the positive electrode. Theoretically, positive electrode polarisation is a function of cell voltage, however many cell designs do not display textbook characteristics. As a result, the applied (recommended) float voltage may not achieve the identified float charge goals. To address polarisation problems during float charge, several polarisation based float charge systems have been published. All of these systems require cell modification to provide a third terminal so that polarisation can be directly measured or calculated. Despite many battery monitoring and testing systems presently being available in the market place, there are no systems that provide polarisation estimates or measurements for cells in field service. Consequently, there is no method of verifying whether the applied float charge is successful, or whether problems exist.

7.1 Achievements

In recent times there have been several claims of battery monitoring or analysis advantages through the use of impedance based measurement techniques. In this work, impedance testing

was initially explored for its potential to reveal information about the polarisation distribution within a float charging VRLA cell. To facilitate this testing on any cell in a battery string, an optically isolated impedance acquisition interface unit was designed and built. This allowed standard ground-referenced automated test equipment to be used for signal generation and data acquisition. Through this testing it was found that while 'small signal' impedance measurements and prior knowledge of a cell's characteristics may be used to determine the region of operation (polarisation existence), such impedance measurements cannot determine the distribution of polarisation within a cell. Large signal impedance testing is invalid as the state (impedance) of the cell changes throughout a test cycle. These changes were found to be an increasing capacitance below the nominal float voltage, and an increasing resistance above this voltage. While small signal impedance techniques may be useful for the identification of a degraded cell and the estimation of remaining life, impedance alone does not reveal covert information about the cell's polarisation distribution.

An automated test system has also been developed during the course of this research, which provides facilities for using reference electrodes in VRLA batteries. This automated test system is controlled from Matlab on a Windows based PC, and allows both steady state and transient testing to be undertaken. While the core of the test system utilises commercially available automated test equipment such as scanning multimeters, DC power supplies, and electronic loads, a number of specialised pieces of equipment were also developed to supplement that which is commercially available. The specialised test equipment designed and developed during the course of this research included an optically isolated impedance acquisition interface unit, a precision current shunt amplifier, a precision water-bath temperature controller, and a low power constant current electronic load.

To aid analysis and understanding of VRLA battery float operation, an electrical equivalent model has been developed around the cell's float charge region of operation. While this model has a layout similar to a cell's physical composition, it is not based on or intended to represent the chemical reactions occurring within a cell. Characteristic features of a cell replicated by the model may however be interpreted as changes in the cell's chemical reactions. The responses (transient and steady state) of both electrodes within a cell are modelled separately, and the sum of these replicates the terminal response of a cell. The models for each electrode are essentially identical, and differ only by component values. The key components of each electrode are the dual-value capacitor and the non-linear (Tafel-like) overcharge resistor. Model calibration is

achieved through steady state voltage and current values measured at the terminals of the cell, and the transient voltage profile seen on the cell's terminals when a current perturbation is applied. The calibrated model replicates both the steady state and transient responses of a cell's terminals by modelling the individual electrodes. As the model estimates the response of each electrode within a standard unmodified cell, it essentially produces a virtual reference electrode for the cell. Typically, the electrode polarisation estimations are accurate to within 10 mV.

A test and analysis procedure capable of producing an estimate of a float charged cell's polarisation distribution has been developed from the large signal impedance testing and resulting float charge model. While the model was used in the development and verification of the polarisation estimation test procedure, it is not required for the estimation. The estimation is based on analysis of the voltage decay profile produced when the float charger is removed from the cell, or when a very low discharge rate (less than C/1000) is applied. The procedure utilises the vastly different time responses for the polarisation decay of each electrode to estimate their polarisations. Following the removal of the float charger, the negative electrode's potential typically decays to its fully charged rest potential within several minutes. The polarisation decay of the positive electrode is typically measured in hours. The developed test does not require prior knowledge of the cell. However, if the fully charged rest voltage of the given cell type is known, the test duration may be reduced to the length of time taken by the negative electrode's polarisation to decay. Using only the terminal response of the cell, polarisation estimates are typically accurate to within 10 mV. The developed polarisation estimation procedure can identify cells suffering from float charge imbalance problems, or assist in float voltage optimisation. Float charge imbalance problems typically result in the gradual discharge of a single electrode within a cell, while outwardly the cell appears to be fully charged.

7.2 Further Work

As the developed model was targeted at the float charge region of VRLA cell operation, a conscious effort was made to limit the calibration required for the model. As a result, the model produces a very basic representation of the main charge-discharge reactions. For completeness, improved modelling of this bulk charge storage region of operation could be investigated. Similarly, during reference electrode testing a small Coup de Fouet-like voltage overshoot and recovery was sometimes seen on the negative electrode as its polarisation decayed to the rest

potential. As the characteristics of this feature did not appear to be consistent and typically had a small magnitude (up to 10 mV), it has not been modelled. However, for improved model accuracy and completeness, further work could be undertaken to identify the cause of this.

As almost all of the energy supplied to a VRLA cell during steady state float charge must eventually be dissipated as heat, resistance is the obvious choice of model component. A non-linear resistor was therefore developed to produce Tafel characteristics. This equivalent Tafel resistance is shown to have a maximum (peak) value at polarisations similar to those claimed by battery chemists as producing the minimum rate of positive grid corrosion. The influences on the location (polarisation and current) of this peak resistance value have been discussed in Section 5.1.1.1. At this stage, the similarities between polarisations of peak equivalent resistance and minimum grid corrosion are considered entirely coincidental, and no investigation of a correlation between these phenomena has been undertaken. Further work may investigate the possible relationship between the locations of peak equivalent resistance and the minimum rate of grid corrosion. Should a relationship be verified, an invaluable tool for establishing the optimal polarisation for maximum cell life will be provided.

The majority of this research has focused on the development of a model and associated tools to determine the float charge status of cells in field service. For a cell operating with 'textbook' characteristics, optimisation of the float voltage should be relatively straightforward. The optimal strategy for the correction or treatment of polarisation problems that may be identified by the developed procedure has not been investigated. The cumulative effects of small float charge imbalance problems (typically resulting in negative plate discharge) can eventually cause premature cell failure. It is perceived that regular low-level corrective action or maintenance may alleviate or even prevent this failure mode. Now that a polarisation analysis tool is available, future work could be undertaken investigating the treatment or optimisation of cells that have been identified as having float charge problems. Similarly, optimisation of the float voltage for variations in cell age and operating temperature may also be investigated.

Appendix A

Simulation Software

vrla_part_size

```
% vrla_part_size
%
% Used to create parts data file vor VRLA cell float simulations
% P. Hunter 13/2/03
%

%%%%% Fill in this first section only %%%%%%%%%%%%%%%%%%%%%%%%%%%%%%%%%%%%%%%%%%%%%%%%%%%

batt_data_file = ('2hi_275_2v2.dat'); % name of output data file

cell_capacity  = 275;               % Ah
discharge_time = 10;                % hours -not really reqd as:
                                    %   I = C dV / dt  therefore  C = I dt / dV
                                    %   I = cell_capacity / discharge_time
                                    %   dt = discharge_time(hrs) * 3600(seconds)
empty_open_cct_rest_volt = 1.900;   % Volts (Typically 1.9 - 1.95 volts)
full_open_cct_rest_volt  = 2.140;   % Volts (Typically 2.08 - 2.16 volts
                                    %   - J. Electro chem 143 #3 March 1996)
float_voltage            = 2.200;   % Volts Typically 2.23 - 2.3 volts
float_current            = 0.022;   % Amps @ above floatV (Typ cell_capacity /1000 to 10 000)
pos_polarisation         = 0.025;   % Volts (Ideally 30 to 70mV) 0.105
pos_ochg_slope           = 0.103;   % Volts/decade 70-140mV   0.08 .085 ??
neg_ochg_slope           = 0.131;   % Volts/decade 0.120      0.040-dud cell??
                                    %%% neg intercept, and float polarisation are calculated
                                    % pg 240 Berndt oxygen evolution (positive) 0.07 to 0.14
                                    % hydrogen evolution always 0.12
                                    % but really require totals:
                                    %   total  pos == oxygen + corrosion  &&  oxygen dominant
                                    %   total  neg == hydrogen + oxygen reduction
pos_bulk_percent         = 75;      % percent of discharge volt shift due to positive
                                    %   50% == same pos as neg...
pos_ochg_fraction        = 0.003;   % 0.003   typical -may need tweek to suit cell type
neg_ochg_fraction        = 0.00005; % 0.00005 typical -may need tweek to suit cell type

full_chg_acid_res        = 0.001 ;  % ohms resistance of acid when fully charged
pos_metal_res            = 0.00001; % ohms
neg_metal_res            = 0.00001; % ohms

%%%%% calculations %%%%%%%%%%%%%%%%%%%%%%%%%%%%%%%%%%%%%%%%%%%%%%%%%%%%%%%%%%%%%%%%%%%%

%% equivalent capacitor  I=C dv/dt %%
plate_voltage_change =  full_open_cct_rest_volt - empty_open_cct_rest_volt; % dV
cap_equiv = (cell_capacity * 3600) / plate_voltage_change;     % Farads
c_bulk_p  = 1 / (1 / cap_equiv * (pos_bulk_percent/100));      % Farads
c_bulk_n  = 1 / (1 / cap_equiv * (1 - pos_bulk_percent/100));  % Farads

c_ochg_p = pos_ochg_fraction * cap_equiv;    % Farads -a fraction of the total equivalent capacity
c_ochg_n = neg_ochg_fraction * cap_equiv;    % Farads -a fraction of the total equivalent capacity

v_oc_st_p = (pos_bulk_percent/100) * full_open_cct_rest_volt;        % volt at start of pos overcharge
v_oc_st_n = 1* (1 - pos_bulk_percent/100) * full_open_cct_rest_volt; % volt at start of neg overcharge

hg_hg2so4_normal = 0.494;%  Fraction of full chg SS opencct voltage for ref-e -tweekable?
hg_hg2so4_offset = (hg_hg2so4_normal - (1 - pos_bulk_percent/100)) * full_open_cct_rest_volt;

%%%%%%%%%%%%%%%%%%%%%%%%%%%%%%%%%%%%%%%%%%%%%%%%%%%%%%%%%%%%%%%%%%%%%%%%%%%%%%%%%%%%%%%
pos_ochg_int =  10^((pos_ochg_slope*log10(float_current)-pos_polarisation)/pos_ochg_slope); % Amps
pos_ochg_1a  = pos_ochg_slope*log10(1)+(-1*pos_ochg_slope*log10(float_current) + pos_polarisation);

neg_polarisation = float_voltage - pos_polarisation - full_open_cct_rest_volt; % volts
neg_ochg_int =   10^((neg_ochg_slope*log10(float_current)-neg_polarisation)/neg_ochg_slope); % Amps
neg_ochg_1a  = neg_ochg_slope*log10(1)+(-1*neg_ochg_slope*log10(float_current) + neg_polarisation);

pos_sd_res   =  v_oc_st_p / pos_ochg_int;  % positive self discharge resistor value
neg_sd_res   =  v_oc_st_n / neg_ochg_int;  % negative self discharge resistor value

%%%%% Not reqd just used to check values are correct %%%%%%%%%%%%%%%%%%%%%%%%%%%%%%%%%%%%
%platesum = v_oc_st_p - v_oc_st_n
%justtocheck = 1/(1/c_bulk_p + 1/c_bulk_n)
pos_pol = [0.001:0.001:0.200]; %polarisation V
neg_pol = pos_pol;
pos_1a = pos_ochg_1a;
neg_1a = neg_ochg_1a;
pos_slope = pos_ochg_slope;
neg_slope = neg_ochg_slope;
rnl_ochg_p = pos_pol ./(10.^((-pos_pol+pos_1a)./-pos_slope)); % ochg nlr floatcurrents.m
rnl_ochg_n = neg_pol ./(10.^((-neg_pol+neg_1a)./-neg_slope)); % ochg nlr floatcurrents.m

pos_i = pos_pol ./ rnl_ochg_p;
```

```
neg_i = neg_pol ./ rnl_ochg_n;


i_min = min(min(pos_i),min(neg_i))
i_max = max(max(pos_i),max(neg_i))
if i_max > 1
   i_max =1
end

steps = 100;
float_i = rot90(logspace(log10(i_min),log10(i_max),steps),-1);

[fiy,fix] = size (float_i)
qaz = 1

while qaz <= fiy
   if float_i(qaz,1) < pos_ochg_int,
      float_i(qaz,2) = 0;
   else
      float_i(qaz,2) = (float_i(qaz,1)*((-1*pos_slope.*log10(float_i(qaz,1)))-pos_1a)./ -float_i(qaz,1));
   end

   if float_i(qaz,1) < neg_ochg_int,
      float_i(qaz,3) = 0;
   else
      float_i(qaz,3) = (float_i(qaz,1)*((-1*neg_slope.*log10(float_i(qaz,1)))-neg_1a)./ -float_i(qaz,1));
   end

   float_i(qaz,4) = v_oc_st_p + v_oc_st_n +float_i(qaz,2)+float_i(qaz,3);

   qaz = qaz+1;
end


%%%%%%%%%%%%%%%%%%%%%%%%%%%%%%%%%%%%%%%%%%%%%%%%%%%%%%%%%%%%%%%%%%%%%%%%%%%%%%%%%%%%%%%%%%%%%%%%%%%%%%%%%%%%%%
ref_e = 0.658
pos_open_cct = 1.74
neg_open_cct = 0.4

%%% Used to plot (check) tafel points prior to discharge testing %%%
%%% test_no  current  voltage  neg  pos %%%
test_data = ...
[  27 0.3562 2.2969 1.0661 1.2308;
   28 0.3586 2.2969 1.0717 1.2253;
   29 0.3481 2.2969 1.0713 1.2256;
   30 0.3349 2.2968 1.0778 1.2191;
   31 0.3133 2.2962 1.0816 1.2146;
   %32 0.0733 2.0979 1.0515 1.0464;
   %33 0.0756 2.0982 1.0470 1.0512;
   %34 0.0529 2.0984 1.0458 1.0526;
   %35 0.0486 2.0984 1.0446 1.0538;
   %36 0.0499 2.0977 1.0512 1.0466;
   37 0.0328 2.1981 1.0991 1.0990;
   38 0.0226 2.1984 1.0973 1.1011;
   39 0.0225 2.1983 1.0953 1.1031;
   40 0.0219 2.1984 1.0930 1.1054;
   41 0.0217 2.1983 1.0915 1.1067;
   44 0.4645 2.3473 1.1075 1.2397;
   45 0.4482 2.3477 1.1057 1.2420;
   46 0.3573 2.3476 1.1110 1.2366;
   47 0.4622 2.3477 1.1078 1.2399;
   48 0.4331 2.3477 1.1068 1.2409];

test_data (:,4) =  test_data (:,4) - ref_e;
test_data (:,5) =  test_data (:,5) + ref_e;
%%%%%%%%%%%%%%%%%%%%%%%%%%%%%%%%%%%%%%%%%%%%%%%%%%%%%%%%%%%%%%%%%%%%%%%%%%%%%%%%%%%%%%%%%%%%%%%%%%%%%%%%%%%%%
plotst = 0.0001;
plotfin = 0.02;
figure(6)
clf
subplot(3,1,1)
semilogx(float_i(:,1), float_i(:,4),'k')
grid on
hold on
%semilogx(test_data(:,2), test_data(:,3),'k*')
%xlabel ('Float Current (amps)')
ylabel ('Cell Voltage (volts)')
hold off
axis([plotst plotfin 2.1 2.5])


subplot(3,1,2)
semilogx(pos_i,pos_pol,'k')
hold on
semilogx(neg_i,-1.*pos_pol,'k')
%semilogx(test_data(:,2), test_data(:,5) -pos_open_cct,'k*')
%semilogx(test_data(:,2), -1.*test_data(:,4) + neg_open_cct,'k*')
grid on
%xlabel ('Float Current (amps)')
ylabel ('Polarisation (volts)')
axis([plotst plotfin -0.2 0.1])

subplot(3,1,3)
semilogx(pos_i,rnl_ochg_p,'k')
hold on
semilogx(neg_i,rnl_ochg_n,'k')
grid on
xlabel ('Float Current (amps)')
ylabel ('Equivalent Resistance (ohms)')
axis([plotst plotfin 0 120])
```

```
%%%%%%%%%%%%%%%%%%%%%%%%%%%%%%%%%%%%%%%%%%%%%%%%%%%%%%%%%%%%%%%%%%%%%%%%%%%%%%%%%%%%%%%%%%%%%%%%
fid=fopen(batt_data_file,'r+'); % r+  read and write (do not create)
if fid ~= -1,                    % -1  == file exists
   yn = input('File exists, Do you want to over write it? (press Y to overwrite)  ','s');
   if yn == 'y'
      fid=fopen(batt_data_file,'w'); % write (create if necessary);
   else
      ('Please rename output file ')
      break
   end
else
   fid=fopen(batt_data_file,'w'); % w write (create if necessary)
end

% Rest of the data in XXXX.XXXX format
results_format = (' %15.6f');
saveform = [  results_format ('  %% cell_capacity \n \n')];
fprintf(fid, saveform, cell_capacity );

%%%%%%%%%%%%%%%%%%%%%%%%%%%%%%%%%%%%%%%%%%%%%%%%%%%%%%%%%%%%%%%%%%%%%%%%%%%%%%%%%%%%%%%%%%%%
saveform = [  results_format ('  %% discharge_time -not reqd \n')];
fprintf(fid, saveform, discharge_time );
saveform = [  results_format ('  %% float_voltage -not reqd \n')];
fprintf(fid, saveform, float_voltage );
saveform = [  results_format ('  %% float_current -not reqd \n')];
fprintf(fid, saveform, float_current );
saveform = [  results_format ('  %% pos_polarisation @float -not reqd \n')];
fprintf(fid, saveform, pos_polarisation );
saveform = [  results_format ('  %% empty_open_cct_rest_volt -not reqd \n')];
fprintf(fid, saveform, empty_open_cct_rest_volt );
saveform = [  results_format ('  %% full_open_cct_rest_volt -not reqd \n')];
fprintf(fid, saveform, full_open_cct_rest_volt );
saveform = [  results_format ('  %% pos_bulk_percent -not reqd \n \n')];
fprintf(fid, saveform, pos_bulk_percent );
%%%%%%%%%%%%%%%%%%%%%%%%%%%%%%%%%%%%%%%%%%%%%%%%%%%%%%%%%%%%%%%%%%%%%%%%%%%%%%%
saveform = [  results_format ('  %% hg_hg2so4_offset_voltage wrt center \n')];
fprintf(fid, saveform, hg_hg2so4_offset );
saveform = [  results_format ('  %% volt_ochg_start_pos \n')];
fprintf(fid, saveform, v_oc_st_p );
saveform = [  results_format ('  %% volt_ochg_start_neg \n\n')];
fprintf(fid, saveform, v_oc_st_n );
%%%%%%%%%%%%%%%%%%%%%%%%%%%%%%%%%%%%%%%%%%%%%%%%%%%%%%%%%%%%%%%%%%
saveform = [  results_format ('  %% c_bulk_p \n')];
fprintf(fid, saveform, c_bulk_p );
saveform = [  results_format ('  %% c_bulk_n \n')];
fprintf(fid, saveform, c_bulk_n );
saveform = [  results_format ('  %% c_ochg_p \n')];
fprintf(fid, saveform, c_ochg_p );
saveform = [  results_format ('  %% c_ochg_n \n \n')];
fprintf(fid, saveform, c_ochg_n );
%%%%%%%%%%%%%%%%%%%%%%%%%%%%%%%%%%%%%%%%%%%%%%%%%%%%%%%%%%%%%%%%%%
saveform = [  results_format ('  %% pos_ochg_slope \n')];
fprintf(fid, saveform, pos_ochg_slope );
saveform = [  results_format ('  %% pos_ochg_int -not reqd \n')];
fprintf(fid, saveform, pos_ochg_int );
saveform = [  results_format ('  %% pos_ochg_1a \n')];
fprintf(fid, saveform, pos_ochg_1a );
saveform = [  results_format ('  %% neg_ochg_slope \n')];
fprintf(fid, saveform, neg_ochg_slope );
saveform = [  results_format ('  %% neg_ochg_int -not reqd \n')];
fprintf(fid, saveform, neg_ochg_int );
saveform = [  results_format ('  %% neg_ochg_1a \n\n')];
fprintf(fid, saveform, neg_ochg_1a );
saveform = [  results_format ('  %% full_chg_acid_res \n')];
fprintf(fid, saveform, full_chg_acid_res );
saveform = [  results_format ('  %% pos_metal_res \n')];
fprintf(fid, saveform, pos_metal_res );
saveform = [  results_format ('  %% neg_metal_res \n')];
fprintf(fid, saveform, neg_metal_res );
saveform = [  results_format ('  %% pos_self_dischg_res \n')];
fprintf(fid, saveform, pos_sd_res );
saveform = [  results_format ('  %% neg_self_dischg_res \n')];
fprintf(fid, saveform, neg_sd_res );

fclose(fid);
```

diff_vrla.m

```
function [dot] = diff_vrla(t,ic,options,sup,battdata)
%
% 25/1/02 Original model -negative electrode only. P.M.H.
% 20/1/03 converted to generic form
% Model of VRLA Cell at full charged / overcharged state
% - using the Parallel variable capacitor
%       /nonlinear resistor model for both +ve and -ve plate
% - joined by asid resistor
% - with single parallel self discharge resistor for each electrode
%
% 21/1/03 changed to seperate positive and neg self-discharge resistors
%    split acid resistors and added positive and negative metal resistors
% 19/2/03 rearranged order of calculatins to be more logical - no real changes

global plotres internals
persistent tlast next % reqd only to indicate sim progress on screen

%%%%% Set-up initial conditions %%%%%%%%%%%%%%%%%%%%%%%%%%%%%%%%%%%%%%%%%%%%%%%%%%%%%%%%%%%%
v2 = ic(1);       % positive plate voltage (from initial conditions)
v5 = ic(2);       % negative plate voltage (from initial conditions)
iset = sup(1,1);  % supply current
vset = sup(1,2);  % supply voltage

%%%%% Positive plate %%%%%%%%%%%%%%%%%%%%%%%%%%%%%%%%%%%%%%%%%%%%%%%%%%%%%%%%%%%%%%%%%%%%%%%
v_oc_st_p = battdata(10,1);   % voltage for start of positive overcharge
v_ochgtrans_p = 0.01;         % 0.03? % voltage range for transition (bulk to ochg)
c_bulk_p  = battdata(12,1);   % farads - bulk charge capacitance
c_oc_p    = battdata(14,1);   % farads - overcharge capacitance 350

pos_slope = battdata(16,1);   % V / Decade
pos_int   = battdata(17,1);   % Amps
pos_1a    = battdata(18,1);   % polarisation at 1a

v_oc_p    = v_oc_st_p + v_ochgtrans_p; % voltage 4 complete overcharge transistion
pos_pol = v2 - v_oc_st_p;
rnl_ochg_p = pos_pol /(10^((-pos_pol+pos_1a)/-pos_slope)); % ochg nlr floatcurrents.m

%%%%% negative plate %%%%%%%%%%%%%%%%%%%%%%%%%%%%%%%%%%%%%%%%%%%%%%%%%%%%%%%%%%%%%%%%%%%%%%
v_oc_st_n = battdata(11,1);   % voltage for start of negative overcharge
v_ochgtrans_n = 0.04;         % 0.01? % voltage range for bulk to ochg transition
c_bulk_n  = battdata(13,1);   % farads - bulk charge capacitance
c_oc_n    = battdata(15,1);   % farads - overcharge capacitance 350

neg_slope = battdata(19,1);   % V /Decade
neg_int   = battdata(20,1);   % Amps
neg_1a    = battdata(21,1);   % polarisation at 1a

v_oc_n    = v_oc_st_n + v_ochgtrans_n; % voltage 4 complete overcharge transistion
neg_pol = v5 - v_oc_st_n;
rnl_ochg_n = neg_pol /(10^((-neg_pol+neg_1a)/-neg_slope)); % ochg nlr floatcurrents.m

%%%%% other %%%%%%%%%%%%%%%%%%%%%%%%%%%%%%%%%%%%%%%%%%%%%%%%%%%%%%%%%%%%%%%%%%%%%%%%%%%%%%
full_chg_acid_res = battdata(22,1);  % total resistance of acid
r_pos_metal       = battdata(23,1);
r_neg_metal       = battdata(24,1);
r_pos_sd          = battdata(25,1);  % pos self discharge resistance
r_neg_sd          = battdata(26,1);  % neg self discharge resistance
hg_hg2so4_offset  = battdata(9,1);   % offset to give readings correct RE values

%%%%% Variable Capacitor positive %%%%%%%%%%%%%%%%%%%%%%%%%%%%%%%%%%%%%%%%%%%%%%%%%%%%%%%%%%
power_p = 5;
if v2 < v_oc_st_p
   cap_p = c_bulk_p;
elseif v2 >= v_oc_st_p & v2 < v_oc_p
   fraction_p = 1-((v2 - v_oc_st_p) / v_ochgtrans_p);
   cap_p = (c_bulk_p - c_oc_p + 1)^(fraction_p^power_p) + c_oc_p -1;
elseif v2 >= v_oc_p,
   cap_p =c_oc_p;
else
   fail
end

%%%%% Variable Capacitor negative%%%%%%%%%%%%%%%%%%%%%%%%%%%%%%%%%%%%%%%%%%%%%%%%%%%%%%%%%%%
power_n = 5;
if v5 < v_oc_st_n
   cap_n = c_bulk_n;
elseif v5 >= v_oc_st_n & v5 < v_oc_n
   fraction_n = 1-((v5 - v_oc_st_n) / v_ochgtrans_n);
   cap_n = (c_bulk_n - c_oc_n + 1)^(fraction_n^power_n) + c_oc_n -1;
elseif v5 >= v_oc_n,
   cap_n =c_oc_n;
else
   fail
end

%%%%% Acid specific gravity %%%%%%%%%%%%%%%%%%%%%%%%%%%%%%%%%%%%%%%%%%%%%%%%%%%%%%%%%%%%%%%%
if v2 > v_oc_st_p,
   sg_v2 = v_oc_st_p;
else
   sg_v2 = v2;
end
if v5 > v_oc_st_n,
   sg_v5 = v_oc_st_n;
else
   sg_v5 = v5;
end
```

```
%%%%%%%%%%%%%%%%%%%%%%% good fit up to sg == 1.3 @ 20 deg C pg 144 Berndt
acid_shape   = 2.15;  % power func to alter shape of condictivity curve
acid_sg_c_pk = 1.235; % SG value at which conductivity pk occurs
acid_c_pk_v  = 0.76;  % value of peak condictivity
%%%%%%%%%%%%%%%%%%%%%%%
full_sg = v_oc_st_p + v_oc_st_n - 0.85;  % specific gravity of full batt
full_spec_cond =  acid_c_pk_v .* (((abs(full_sg-acid_sg_c_pk)).^acid_shape)...
   ./ (-1*(abs(1-acid_sg_c_pk)).^acid_shape) +1 );
full_spec_res = 1 / full_spec_cond;
res_factor = full_spec_res / full_chg_acid_res;
sg = sg_v2 + sg_v5 - 0.85;          % Rule of thumb specific gravity = ocv - 0.85
if sg < 1.001
   sg = 1.001;
end
spec_conduct =  acid_c_pk_v .* (((abs(sg-acid_sg_c_pk)).^acid_shape)...
   ./ (-1*(abs(1-acid_sg_c_pk)).^acid_shape) +1 );
spec_res = 1 / spec_conduct;
r_acid_total = spec_res / res_factor;
r_pos_acid = r_acid_total / 2;
r_neg_acid = r_pos_acid;

%%%%% voltage or current control %%%%%%%%%%%%%%%%%%%%%%%%%%%%%%%%%%%%%%%%%%%%%%%%%%%%%%%%%%%%
if (vset-v2-v5) < iset*(r_pos_metal + r_neg_metal + r_pos_acid + r_pos_acid),
   is = (vset-v2-v5)/(r_pos_metal + r_neg_metal + r_pos_acid + r_pos_acid);
else
   is = iset; % current under current control
end

%%%%% Limits %%%%% Not necessary if all is ok... %%%%%%%%%%%%%%%%%%%%%%%%%%%%%%%%%%%%%%%%%%%
rnl_ochg_min = 0.000000001;
if rnl_ochg_p < rnl_ochg_min,
   rnl_ochg_p = rnl_ochg_min;
end
if rnl_ochg_n < rnl_ochg_min,
   rnl_ochg_n = rnl_ochg_min;
end
%%%%% self discharge %%%%%%%%%%%%%%%%%%%%%%%%%%%%%%%%%%%%%%%%%%%%%%%%%%%%%%%%%%%%%%%%%%%%%%%
i_self_p = v2 / r_pos_sd;
i_self_n = v5 / r_neg_sd;

%%%%% makes overcharge zenner action %%%%%%%%%%%%%%%%%%%%%%%%%%%%%%%%%%%%%%%%%%%%%%%%%%%%%%%
irnl_p = (v2 - v_oc_st_p)/rnl_ochg_p - i_self_p;
if irnl_p < 0,
   irnl_p = 0;
end
irnl_n = (v5 - v_oc_st_n)/rnl_ochg_n - i_self_n;
if irnl_n < 0,
   irnl_n = 0;
end

%%%%% Acid and metal voltage drops %%%%%%%%%%%%%%%%%%%%%%%%%%%%%%%%%%%%%%%%%%%%%%%%%%%%%%%%%%
v1 = is * r_pos_metal;
v6 = is * r_neg_metal;
v3 = is * r_pos_acid;
v4 = is * r_neg_acid;

%%%%% display progress on screen... %%%%%%%%%%%%%%%%%%%%%%%%%%%%%%%%%%%%%%%%%%%%%%%%%%%%%%%%
if length(next) == 0,
   next = plotres;
end
if (tlast < next) & (t >= next),
   next = floor(t/plotres) * plotres + plotres
end
tlast = t;

%%%%% the actual diff calcs %%%%%%%%%%%%%%%%%%%%%%%%%%%%%%%%%%%%%%%%%%%%%%%%%%%%%%%%%%%%%%%%%

dot(1,1) = (is - i_self_p - irnl_p)/cap_p ; %dv/dt for v2
dot(2,1) = (is - i_self_n - irnl_n)/cap_n ; %dv/dt for v5

%%%%% storing internal values as sim progresses %%%%%%%%%%%%%%%%%%%%%%%%%%%%%%%%%%%%%%%%%%%%
icap_p  = cap_p * dot(1,1);
icap_n  = cap_n * dot(2,1);

[y,x] = size (internals);
nextint = y+1;
internals(nextint,1) = t;
internals(nextint,2) = is;
internals(nextint,3) = v1;
internals(nextint,4) = v2;
internals(nextint,5) = v3;
internals(nextint,6) = v4;
internals(nextint,7) = v5;
internals(nextint,8) = v6;
internals(nextint,9) = i_self_p;
internals(nextint,10) = icap_p;
internals(nextint,11) = irnl_p;
internals(nextint,12) = i_self_n;
internals(nextint,13) = icap_n;
internals(nextint,14) = irnl_n;
internals(nextint,15) = rnl_ochg_p;
internals(nextint,16) = rnl_ochg_n;
internals(nextint,17) = cap_p;
internals(nextint,18) = cap_n;
internals(nextint,19) = r_acid_total;
internals(nextint,20) = v1 + v2 + v3 - hg_hg2so4_offset;
internals(nextint,21) = v4 + v5 + v6 + hg_hg2so4_offset;
internals(nextint,22) = sg;
```

vrla_float_sim.m

```
% vrla_float_sim.m
% vrla float simulator
%
% Runs and plots 5 different simulations
%  5 discharge rate (defined through sw1 to sw5)
%

clear all
global plotres internals
battdata = load('2hi_275_2v2.dat'); % battery data file
plotres = 100000;      % not reqd - indicates sim progress...

%% initial state conditions
v1 = battdata(10,1) + battdata(5,1) % float IC pos OCV + polarisation
v2 = battdata(3,1) - v1             % Float V - pos
ic1 = [v1 v2];

% CHARGE / DISCHARGE TIMES %%%%%%%%%%%%%%%%%%%%%%%%%%%%%%%%%%%%%%%%%%%%
%% Format: Time current voltage...   (set like bench top supply)

time = 2;                % 'hours' 2;% 'minutes' 3;% 'seconds'

f_v = 2.198;             % float voltage
sw1 =...                 % open cct (0 amp)
[-86400      1.5   f_v;
-0.000001    1.5   f_v;
 0           0     3;
390000       1     3];

sw2 =...                 % 10 mA discharge
[-86400      1.5   f_v;
-0.000001    1.5   f_v;
 0          -0.01  3;
390000       1     3];

sw3 =...                 % 100 mA discharge
[-86400      1.5   f_v;
-0.000001    1.5   f_v;
 0          -0.10  3;
390000       1     3];

sw4 =...                 % 1 A discharge
[-86400      1.5   f_v;
-0.000001    1.5   f_v;
 0          -1     3;
390000       1     3];

sw5 =...                 % 10 A discharge
[-86400      1.5   f_v;
-0.000001    1.5   f_v;
 0          -10    3;
390000       1     3];


for this_sw = 1 : 1 : 5,
   if this_sw == 1,
      switching = sw1,
   elseif this_sw == 2,
      switching = sw2,
   elseif this_sw == 3,
      switching = sw3,
   elseif this_sw == 4,
      switching = sw4,
   elseif this_sw == 5,
      switching = sw5,
   else
      error('problem')
   end

   [sy sx] = size(switching);
   results = [];
   internals =[];
   row = 1;
   while row < sy,
      if switching(row,1) >= switching(row+1,1),
         bad_time = switching(row+1,1)
         error ('   Time must be greater than previous')
         return
      end
      row =row+1;
   end

   %%%%%%%%%%%%%%%%%%%%%%%%%%%%%%%%%%%%%%%%%%%%%%%%%%%%%%%%%%%%%%%%%%%%
   options = odeset('RelTol',1e-9,'AbsTol',[1e-7],'MaxStep',600);% 9 7
   %%% max step reqd when voltage dependant resistances change quickly
   %%%    and capacitor has const slope due to const I
   %%%       as dvdt const ode solver has big time step...
   row = 1;
   while row < sy
      tspan =[switching(row,1) switching((row+1),1)];
      supply = [switching(row,2),switching(row,3)];
      if row == 1
         ic = ic1;
      else
         ic = [lastv1 lastv2];
      end
```

```
      [t,x] = ode15s ('diff_vrla',tspan,ic,options,supply,battdata);
      [thisy thisx] = size(x);
      [resultsy resultsx] = size(results);

      results(((resultsy+1):(resultsy+thisy)), 1) = t;
      results(resultsy+1:resultsy+thisy, 2:thisx+1) = x(:,1:2);
      lastv1 = x(thisy,1);
      lastv2 = x(thisy,2);
      row = row +1;
   end

   if time == 1,
      t=t./3600;
      internals(:,1) = internals(:,1)/3600;
   elseif time == 2,
      t=t./60;
      internals(:,1) = internals(:,1)/60;
   end  %must be in seconds

   %%%%% filters out 'Simulation hunting' %%%%%%%%%%%%%%%%%%%
   int_len = size(internals,1);
   filt_int = [];
   line = 1;
   while line < int_len,
      if internals(line,1) < min(internals(line+1:int_len,1)),
         filt_int_len  = size(filt_int,1);
         filt_int(filt_int_len +1,:) = internals(line,:);
      end
      line = line + 1;
   end


   if this_sw == 1,
      filt_int_1 = internals;
   elseif this_sw == 2,
      filt_int_2 = internals;
   elseif this_sw == 3,
      filt_int_3 = internals;
   elseif this_sw == 4,
      filt_int_4 = internals;
   elseif this_sw == 5,
      filt_int_5 = internals;
   else
      error('problem')
   end

   this_sw = this_sw+1
end


%%%%%%%%%%%%%%%%%%%%%%%%%%%%%%%%%%%%%%%%%%%%%%%%%%%%%%%%%%%%%%%%
filt_int = filt_int_1; % set to plot internal internal data

figure (1)
clf
hold on
subplot(3,2,1)
hold on
plot(filt_int(:,1),filt_int(:,4),'b')
grid on
legend ('Pos Cap V')
hold off

subplot(3,2,2)
hold on
plot(filt_int(:,1),filt_int(:,7),'b')
grid on
legend ('Neg Cap V')

subplot(3,2,3)
hold on
plot(filt_int(:,1),filt_int(:,15),'b')
grid on
legend ('Rnl P ')
hold off

subplot(3,2,4)
hold on
plot(filt_int(:,1),filt_int(:,16),'b')
grid on
legend ('Rnl N ')
hold off

subplot(3,2,5)
hold on
plot(filt_int(:,1),filt_int(:,17),'b')
grid on
legend ('Cap P')
hold off

subplot(3,2,6)
hold on
plot(filt_int(:,1),filt_int(:,18),'b')
grid on
legend ('Cap N')
hold off

%%%%%%%%%%%%%%%%%%%%%%%%%%%%%%%%%%%%%%%%%%%%%%%%%%%%%%%%%%%%%%%%
figure (2)
clf
hold on
subplot(3,1,1)
```

```
hold on
plot(filt_int(:,1),filt_int(:,20)+filt_int(:,21),'k') ;
plot(filt_int(:,1),filt_int(:,22),'b') ;
legend ('Cell voltage','SG')

subplot(3,1,2)
hold on
plot(filt_int(:,1),filt_int(:,2),'k') ;
legend ('Charge Current')

subplot(3,1,3)
hold on
plot(filt_int(:,1),filt_int(:,19),'b') ;
legend ('Acid resistance')
%plot(results(:,1),(results(:,2)+ results(:,3)))
%legend ('combined Cap voltgges')


%%%%%%%%%%%%%%%%%%%%%%%%%%%%%%%%%%%%%%%%%%%%%%%%%%%%%%%%%%%%%%%%%%%%%%%%%%%%%%%
figure (3)
clf
hold on
subplot(2,1,1)
hold on
plot(filt_int(:,1),filt_int(:,2),'k') ;
plot(filt_int(:,1),filt_int(:,9),'m') ;
plot(filt_int(:,1),filt_int(:,10),'r') ;
plot(filt_int(:,1),filt_int(:,11),'b') ;
grid on
legend ('i supply','i selfdisc pos','i cap pos','i ochg pos')
hold off

subplot(2,1,2)
hold on
plot(filt_int(:,1),filt_int(:,2),'k') ;
plot(filt_int(:,1),filt_int(:,12),'m') ;
plot(filt_int(:,1),filt_int(:,13),'r') ;
plot(filt_int(:,1),filt_int(:,14),'b') ;
legend ('i supply','i selfdisc neg','i cap neg','i ochg neg')
grid on
hold off

%%%%%%%%%%%%%%%%%%%%%%%%%%%%%%%%%%%%%%%%%%%%%%%%%%%%%%%%%%%%%%%%%%%%%%%%%%%%%%%
figure (4)
clf
hold on
%she = 0.658;
subplot (3,1,1)
hold on
plot(filt_int(:,1),filt_int(:,20)+filt_int(:,21),'k')
grid on
legend ('Cell')

subplot (3,1,2)
hold on
plot(filt_int(:,1),(filt_int(:,20)),'k')
grid on
legend ('Positive Electrode wrt HgHg_2SO_4')

subplot (3,1,3)
hold on
plot(filt_int(:,1),(-1*filt_int(:,21)),'k')
grid on
legend ('Negative Electrode wrt HgHg_2SO_4')

%%%%%%%%%%%%%%%%%%%%%%%%%%%%%%%%%%%%%%%%%%%%%%%%%%%%%%%%%%%%%%%%%%%%%%%%%%%%%%%
she = 0.658;

D1_marks = [0.6;8];
D2_marks = [0.8;4];
D3_marks = [0.7;6];
D4_marks = [0.3;5];
D5_marks = [0.2];

[D1x D1y] = marker (D1_marks, filt_int_1(:,1), filt_int_1(:,20)+filt_int_1(:,21));
[D2x D2y] = marker (D2_marks, filt_int_2(:,1), filt_int_2(:,20)+filt_int_2(:,21));
[D3x D3y] = marker (D3_marks, filt_int_3(:,1), filt_int_3(:,20)+filt_int_3(:,21));
[D4x D4y] = marker (D4_marks, filt_int_4(:,1), filt_int_4(:,20)+filt_int_4(:,21));
[D5x D5y] = marker (D5_marks, filt_int_5(:,1), filt_int_5(:,20)+filt_int_5(:,21));

[D1px D1py] = marker (D1_marks, filt_int_1(:,1), (filt_int_1(:,20)+ she));
[D2px D2py] = marker (D2_marks, filt_int_2(:,1), (filt_int_2(:,20)+ she));
[D3px D3py] = marker (D3_marks, filt_int_3(:,1), (filt_int_3(:,20)+ she));
[D4px D4py] = marker (D4_marks, filt_int_4(:,1), (filt_int_4(:,20)+ she));
[D5px D5py] = marker (D5_marks, filt_int_5(:,1), (filt_int_5(:,20)+ she));

[D1nx D1ny] = marker (D1_marks, filt_int_1(:,1),(-1*filt_int_1(:,21) + she));
[D2nx D2ny] = marker (D2_marks, filt_int_2(:,1),(-1*filt_int_2(:,21) + she));
[D3nx D3ny] = marker (D3_marks, filt_int_3(:,1),(-1*filt_int_3(:,21) + she));
[D4nx D4ny] = marker (D4_marks, filt_int_4(:,1),(-1*filt_int_4(:,21) + she));
[D5nx D5ny] = marker (D5_marks, filt_int_5(:,1),(-1*filt_int_5(:,21) + she));
%%%%%%%%%%%%%%%%%%%%%%%%%%%%%%%%%%%%%%%%%%%%%%%%%%%%%%%%%%%%%%%%%%%%%%%%%%%%%%%
figure (5)
clf
hold on

subplot (3,1,1)
plot(D1x, D1y,'k*')
hold on
plot(D2x, D2y,'k+')
plot(D3x, D3y,'kx')
plot(D4x, D4y,'ks')
```

```
plot(D5x, D5y,'kd')

plot(filt_int_1(:,1), filt_int_1(:,20)+filt_int_1(:,21),'k')
plot(filt_int_2(:,1), filt_int_2(:,20)+filt_int_2(:,21),'k')
plot(filt_int_3(:,1), filt_int_3(:,20)+filt_int_3(:,21),'k')
plot(filt_int_4(:,1), filt_int_4(:,20)+filt_int_4(:,21),'k')
plot(filt_int_5(:,1), filt_int_5(:,20)+filt_int_5(:,21),'k')
%grid on
legend('Open Circuit','10mA','100mA','1A','10A')
axis([-1 10 2.11 2.2])
ylabel('Cell (V)')

subplot (3,1,2)
plot(D1px, D1py,'k*')
hold on
plot(D2px, D2py,'k+')
plot(D3px, D3py,'kx')
plot(D4px, D4py,'ks')
plot(D5px, D5py,'kd')

plot(filt_int_1(:,1), (filt_int_1(:,20)+ she),'k')
plot(filt_int_2(:,1), (filt_int_2(:,20)+ she),'k')
plot(filt_int_3(:,1), (filt_int_3(:,20)+ she),'k')
plot(filt_int_4(:,1), (filt_int_4(:,20)+ she),'k')
plot(filt_int_5(:,1), (filt_int_5(:,20)+ she),'k')
%grid on
%legend
axis([-1 10 1.68 1.77])
ylabel('Positive (V wrt SHE)')

subplot (3,1,3)
plot(D1nx, D1ny,'k*')
hold on

plot(D2nx, D2ny,'k+')
plot(D3nx, D3ny,'kx')
plot(D4nx, D4ny,'ks')
plot(D5nx, D5ny,'kd')
%grid on
plot(filt_int_1(:,1),(-1*filt_int_1(:,21) + she),'k')
plot(filt_int_2(:,1),(-1*filt_int_2(:,21) + she),'k')
plot(filt_int_3(:,1),(-1*filt_int_3(:,21) + she),'k')
plot(filt_int_4(:,1),(-1*filt_int_4(:,21) + she),'k')
plot(filt_int_5(:,1),(-1*filt_int_5(:,21) + she),'k')
ylabel ('Negative (V wrt SHE)')
axis([-1 10 -0.45 -0.36])

if time == 1
   xlabel ('Time (hours)')
elseif time == 2,
   xlabel ('Time (minutes)')
elseif time == 3
   xlabel ('Time (seconds)')
end
```

Appendix B

Reference Electrode Data - TR200

RADIOMETER COPENHAGEN
RADIOMETER ANALYTICAL S.A.
72 rue d'Alsace
69627 VILLEURBANNE CEDEX, France
TACUSSEL Electronique
Tél : +33 78 03 38 38 - Fax : +33 78 68 88 12

MERCUROUS SULPHATE REFERENCE ELECTRODES

TR200 **Fixed cable electrode**
XR200 to XR240 **Screw cap electrodes**

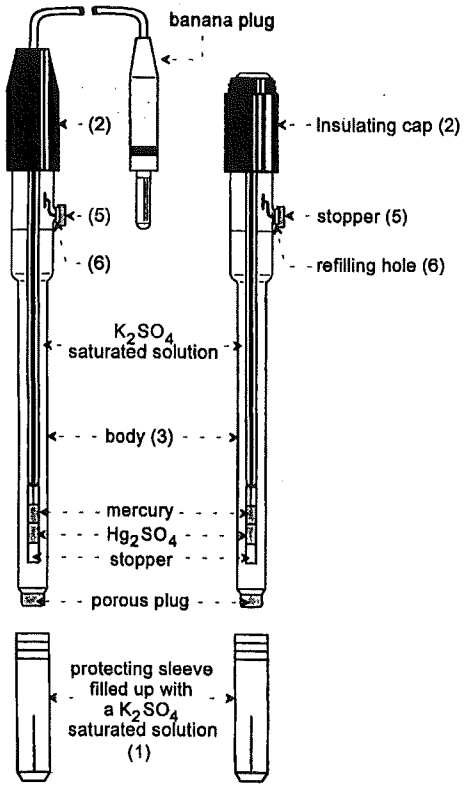

TECHNICAL SPECIFICATIONS OF MERCUROUS SULPHATE REFERENCE ELECTRODES

- Temperature measurement range : 0 to 70°C
- Potential value of the $Hg/Hg_2SO_4/K_2SO_4$ system versus the potential at 25°C of the Normal Hydrogen Electrode: +658 mV.

SETTING UP

- Remove the protecting tube (1) from the electrode.
- Rinse the electrode with demineralized water, while doing this operation, take care not to wet the cap (2).
- Check that the electrode body (3) is not damaged (not cracked or broken).
- Remove stopper (5) which closes the electrode refilling hole (6), before each measurement series. This stopper will be replaced after measurements.
- Check that the level of the filling solution of the reference element is at about 5 mm below the electrode refilling hole (5). If necessary, refill the electrode with a K_2SO_4 saturated solution (RADIOMETER reference for 500 ml: KS160).
- Shake the electrode holding it at its head and with the active tip down. This is done in order to get rid of any air bubble which can be trapped inside the electrode.

MAINTENANCE

- The electrode clogging is a major cause of faulty measurements.
- The electrodes should be rinsed with demineralized water and dried with absorbent paper after each use.
- Between 2 measurements, keep the electrode in its protecting tube filled up with the refilling solution. Renew frequently the filling liquid of that protecting tube.
- Check frequently that the filling solution of the electrode is saturated. If necessary, refill it with a new solution and add it a few crystals of K_2SO_4 in order to saturate the solution.
- In case of deposits which clog the active tip of the electrode, clean the electrode with :
  - a solution of acid (HCl 0,1N, HNO_3 30%): mineral salt deposits, etc.
  - a solution of pepsin at 5% (RADIOMETER reference KS400): protein deposits (milk, cheese, serums, etc.). Duration of treatment: 1 to 2 hours.
  - a solution of thio urea (RADIOMETER reference: KS410): for porous plugs contaminated with $S^=$ and Ag^+. Duration of treatment: a few hours until the porous plug turns white.
  - a solution of a wetting reagent (Teepol, Triton X100, etc.) or an organic solvent (alcohol, acetone, etc.): fat and oil deposits, etc.

  After this treatment, rinse carefully the active tip with demineralized water. The porous plug of the electrode can be cleaned using a fine abrasive paper.

Potentials (mV) of Hg/Hg_2SO_4 reference versus Standard Hydrogen Electrode	
TEMPERATURE °C	**HG/HG2SO4 REF in SAT K2SO4**
0	671.8
5	667.6
10	663.5
15	659.4
20	655.3
25	651.3
30	647.3
35	643.3
40	639.2
45	635.1
50	630.9
55	626.6
60	622.6

(Data Supplied by RADIOMETER Pacific)

Appendix C

List of Float Charge Tests Performed

Notes

The configuration file (commented onto each line of test data) may contain more detailed information of the test instrumentation set-up.

Tafel Testing < = float24 floatconfig1 == y m d h m s 7at 8ct 9i 10v 11+ve 12-ve
float25 >>> Tafel Testing floatconfig1 == y m d h m s 7at 8ct 9i 10v 11-ve 12+ve
Transient Testing (added high current shunt) floatconfig2 == y m d h m s 7at 8ct 9i 10i 11cv 12-ve 13+ve
floatconfig3 ==

Measurement wires were swapped during a shift...

To simplify data analysis, multiple pass – automated testing has been broken down and saved in sub tests e.g. Test21.dat has been saved as test21a.dat, test21b.dat, test21c.dat... with relevant data for each test stage.

File	Cell Type	Cells Used	Plot with	Temp	Test Type	Comment
float_1.dat	2HI275	F1	tafelplot_rev	21	SS (Tafel)	No reference electrode –stabilisation testing
float_2.dat	2HI275	F1	tafelplot_rev	21	SS (Tafel)	No reference electrode –more stabilisation testing
float_3.dat	2HI275	F1	tafelplot_rev	21	SS (Tafel)	No reference electrode –more stabilisation testing
float_4.dat	2HI275	F1	tafelplot_rev	21	SS (Tafel)	No reference electrode Increasing ~7mV steps from open circuit Current must settle to < 1mA / 10min *Suspect Tafel plots in papers produced by incrementing I instead of V – in my test V is a function of I, but in papers I is a function of V
float_5.dat	2HI275	F1	tafelplot_rev	21	SS (Tafel)	Added reference electrode Increasing ~7mV steps from open circuit Increased current settle to < 1mA / hour *Suspect Tafel plots in papers produced by incrementing I instead of V – in my test V is a function of I, but in papers I is a function of V
float_6.dat	2HI275	F1	cont_float_rev	21	transient	floatconfig1.m logging @ 10min intervals to see if 'spike' in previous tests reduces (settles) to a lower current value
float_7.dat	2HI275	F1	cont_float_rev	21	transient	floatconfig1.m logging @ 2second intervals step voltage change 2.27 >> 2.32 V for 1Hr 2.32 >> 2.27 (supply has a diode so effectively open circuit)
float_8.dat	2HI275	F1	cont_float1	21	transient	floatconfig2.m - extra 'high current' shunt added A series of short (approx 4aH) 100A discharges with a 10A current controlled recharge (no V limit) 500mA current controlled boost Open ccted for a few days >> open cct potential
float_9.dat	2HI275	F1	tafelplot_rev	21	SS (Tafel)	floatconfig1.m - stability reduced again, was: i_stab was 0.0001667 (1ma / 600s) >> 1.388e-7 currentstabtime was 600 >> 1800 seconds cell open ccted for weekend before test started, reference electrode inserted at 9am, test started at 10am

float_10.dat	2HI275	F1	Tafelplot_rev	21	SS (Tafel)	floatconfig1.m Cell sat open ccted for 3 days before starting this test Current incremented 0 > 400mA in steps of 7.2mA voltage settles to < 0.0001V in 1800 seconds
float11.dat	2HI275	F1	Cont_float1	21	Transient	foatconfig2.m Put cell in box with bubble-rap to dampen ambient temp fluctuations charged at 2.27 V no ref electrode added ref electrode then open ccted
float12.dat	2HI275	F1	Tafelplot_rev	21	SS (Tafel)	floatconfig1.m redoing float_10... incrementing I and waiting for V to settle
float13.dat	2HI275	F1	Tafelplot_rev	21	SS (Tafel)	floatconfig1.m incrementing V and waiting for I to settle
float14.dat	2HI275	F1	Tafelplot_rev	21	SS (Tafel)	Starting at high voltage and decreasing the voltage through out the test i.e. running test backwards *test interrupted/stopped for approx 1 day in the middle then restarted
float15.dat	2HI275	F1	Tafelplot_rev	21	SS (Tafel)	Redoing test 14 Voltage controlled – backwards high voltage and decreasing the voltage through out the test i.e. running test backwards
float16.dat	2HI275	F1	Tafelplot_rev	21	SS (Tafel)	Current controlled – backwards starting at 400mA and decreasing to 0
Float_17.???						
Float_18.???						
Float_19.???						
float20.dat	2HI275	F1 All	Cont_float_all	21	Transient + - 100mA single cell	floatconfig3.m String test – cell #7 from neg in string(F19) replaced with reference electrode cell (F1) before test –overnight float charge Long test – divided into a to g below
float20a.dat	2HI275	F1	Cont_float_all	21	Transient + - 100mA single cell	3 hr discharge @ 68 amps to 1.8Vpc - + 100mA bypass on cell #7 from neg
float20b.dat	2HI275	F1	Cont_float_all	21	Transient + - 100mA single cell	0.1C recharge 30A>>10A - + 100mA bypass on cell #7 from neg
float20c.dat	2HI275	F1	Cont_float_all	21	Transient + - 100mA single cell	0.1C recharge 10A>>1A - + 100mA bypass on cell #7 from neg
float20d.dat	2HI275	F1	Cont_float_all	21	Transient + - 100mA single cell	0.1C recharge 1A>> float - + 100mA bypass on cell #7 from neg
float20e.dat	2HI275	F1	Cont_float_all	21	Transient NO BYPASS	Bulk Float
float20f.dat	2HI275	F1	Cont_float_all	21	Transient	Manual -+ 1 amp bypass
float20g.dat	2HI275	F1	Cont_float_all	21	Transient NO BYPASS	Open circuit decay
float21.dat	2HI275	F1	Cont_float_all	21	Transient	floatconfig3.m NO REFERENCE ELECTRODE Ref electrode removed and plugged hole bypass unit on cell F1 and set to maintain2.27Volts floated 24Hrs then open ccted approx 35 days
float22.dat	2HI275	F1	Cont_float_all	21	Transient	floatconfig3.m NO REFERENCE ELECTRODE on float approx 23days – a couple of power cuts >> open ccted cell #7 (F1) appears more sensitive to temp...
float23.dat	2HI275	F1 All XX	Cont_float_all	21	Transient	floatconfig3.m NO REFERENCE ELECTRODE Ambient and cell temp sensors accidentally swapped Overnight float – 3Hr discharge to 1.8Vpc (68Amps) Const I const V Recharge to get reference (base line) before selecting new cell for ref E testing

float24.dat	2HI275	F1 All	cont_float_all	21	Transient	floatconfig3.m NO REFERENCE ELECTRODE Ambient and cell temp sensors accidentally swapped Open cct selfdischarge ~50 hours then recharged - used 'Power Zenner' ~70hrs to limit cell 1 voltage - Accidental self discharge
float25.dat	2HI275	F23	cont_float_plot	21	Transient	1st shift floatconfig2.m open cct discharge with reference electrode before tafel test 26 101 Amb T, 102 Cell T, 118 cell V, 119 –ve plate, 120 +ve plate, shunt 1 200mV 200A (not used (temp readings??...)), shunt 2 is the 1 ohm resistor
float26.dat	2HI275	F23	tafelplot	22-	SS (Tafel)	floatconfig1.m
float26a.dat	2HI275	F23	tafelplot	22.5 23.8	SS (Tafel)	floatconfig1.m re running last part of test 26 (2.25 – 2.45 volts)
float26all.dat	2HI275	F23	tafelplot	22.5 23.8	SS (Tafel)	floatconfig1.m All test 26 data
float26fix.dat	2HI275	F23	tafelplot	22.5 23.8	SS (Tafel)	floatconfig1.m Best data from all of test 26
float27.dat	2HI275	F23	cont_float_plot	23.4	Transient	floatconfig2.m 2.3 volt float - open cct discharge
float28.dat	2HI275	F23	cont_float_plot	23.4	Transient	floatconfig2.m 2.3 volt float – 10mA discharge
float29.dat	2HI275	F23	cont_float_plot	23.4	Transient	floatconfig2.m 2.3 volt float – 100mA discharge
float30.dat	2HI275	F23	cont_float_plot	23.4	Transient	floatconfig2.m 2.3 volt float – 1A discharge
float31.dat	2HI275	F23	cont_float_plot	24.2	Transient	floatconfig2.m 2.3 volt float – 10A discharge
float32a.dat	2HI275	F23	cont_float_plot	22	Transient	floatconfig2.m 2.15 volts ~ open cct voltage
float32.dat	2HI275	F23	cont_float_plot	22	Transient	floatconfig2.m 2.1 volt float – open cct discharge discharged ~20% of battery to get below 2.1 volts
float33.dat	2HI275	F23	cont_float_plot	23	Transient	floatconfig2.m 2.1 volt float – 10mA discharge bogus shunt 1 readings (was using load for another test)
float34.dat	2HI275	F23	cont_float_plot	22.3	Transient	floatconfig2.m 2.1 volt float – 100mA discharge
float35.dat	2HI275	F23	cont_float_plot	23.3	Transient	floatconfig2.m 2.1 volt float – 1A discharge
float36.dat	2HI275	F23	cont_float_plot	23.2	Transient	floatconfig2.m 2.1 volt float – 10A discharge for 1 Hr All 200mV 200A shunt information is bogus (shunt was being used in a different test)
float37.dat	2HI275	F23	cont_float_plot	21.6	Transient	floatconfig2.m 2.2-volt float – open cct discharge bypassed Vsence filter resistors with inductors to remove DC off set error on HP6652a power supply
float38.dat	2HI275	F23	cont_float_plot	21	Transient	floatconfig2.m 2.2-volt float – 10mA discharge test failed
float38a.dat	2HI275	F23	cont_float_plot	2.9	Transient	floatconfig2.m 2.2-volt float – 10mA discharge
float39.dat	2HI275	F23	cont_float_plot	21.5	Transient	floatconfig2.m 2.2-volt float – 100mA discharge
float40.dat	2HI275	F23	cont_float_plot	21.1	Transient	floatconfig2.m 2.2-volt float – 1A discharge
float41.dat	2HI275	F23	cont_float_plot	21.7	Transient	floatconfig2.m 2.2-volt float – 10A discharge
float42.dat	2HI275	F23	cont_float_plot	22	Transient	floatconfig2.m 2.27 volts – 10A discharge Appears to have about 80mV neg polarisation??? Has battery characteristics changed? >> redo Tafel
float43.dat	2HI275	F23	tafelplot	21-	SS (Tafel)	>> problems at low –ve polarisations - inconsistent with transient test
float44.dat	2HI275	F23	cont_float_plot	23	Transient	floatconfig2.m 2.35 volt float – open cct discharge

float45.dat	2HI275	F23	Cont_float_plot	22	Transient	floatconfig2.m 2.35 volt float –10mA discharge
float46.dat	2HI275	F23	Cont_float_plot	21.9	Transient	floatconfig2.m 2.35 volt float – 100mA discharge Shunt 1 data is bogus
float47.dat	2HI275	F23	Cont_float_plot	23.5	Transient	Moved down stairs... Ref E adaptor / seal went missing >> delay while new one is made – (early shunt 1 data bogus charging the string) floatconfig2.m 2.35 volt float – 1A discharge
float48.dat	2HI275	F23	Cont_float_plot	22.4	Transient	floatconfig2.m 2.35 volt float – 10A discharge
float49.dat	2HI275	F23	Cont_float_plot	21	Transient	Open circuit decay from 2.35volts
float50.dat	2HI275	F23	Tafelplot	24.5	Tafel	tafel plot
float51.dat	2HI275	F23	Cont_float_plot	25	Transient	Overnight open circuit decay after tafel then transition from 25 to 35 deg C
float52.dat	2HI275	F23	Tafelplot	35	Tafel	tafel plot, added absolute current stabilisation, added continuous log file (float 52cont.dat)
float52cont.dat	2HI275	F23	Cont_float	35	Transient Tafel	transient (settling of) all the tafel points
float53.dat	2HI275	F23	Cont_float_plot	35	Transient	decay after tafel then transition from 35 to 45 deg C
float54.dat	2HI275	F23	Tafelplot	45	Tafel	tafel plot, added absolute current stabilisation, Increased stabilisation time from 1800s to 3600s
float54cont.dat	2HI275	F23	Cont_float	45	Transient Tafel	transient (settling of) all the tafel points
float55.dat	2HI275	F23	Cont_float_plot	45	Transient	decay after tafel then transition from 45 to 25 deg C
float56.dat	2HI275	F23	Tafelplot	25	Tafel	repeating test 50 with settings of 54
float56cont.dat	2HI275	F23	Cont_float	25	Transient Tafel	repeating test 50 with settings of 54
float57.dat	2HI275	F23	Cont_float_plot	25	Transient	decay after tafel and transition from 25 to 35 deg C
float58.dat	2HI275	F23	Tafelplot	35	Tafel	repeating test 52 with settings of 54
float58cont.dat	2HI275	F23	Cont_float	35	Transient Tafel	repeating test 52 with settings of 54
float59.dat	2HI275	F23	Cont_float_plot	25	Transient	float discharge 5hrs @ 46.5A to 1.8V >> 100% recharge @ 34A then 8 A Float 250 hrs >> open circuit decay
float60.dat	Cyclon 25Ah	-	Cont_float_plot	25.6	Transient	float 2.27V for 70 hrs discharge 3hrs @ 7.5A to 1.75V << 100% recharge @ 7.5A to 2.45V for 6 hrs Float 150 hrs at 2.27
float61.dat	Cyclon 25Ah	-	Cont_float_plot	25.5	Transient	open circuit decay from 2.27V for 45hrs recharge 7.5mA 50hrs (no V limit) float 2.27V for 80hrs
float62.dat	Cyclon 25Ah	-	Cont_float_plot	25.5	Transient	discharge 6.5hrs @ 10mA recharge @ 7.5mA to float 2.27V Float 50 hrs @2.27
float63.dat	Cyclon 25Ah	-	Cont_float_plot	26	Transient	discharge 5hrs @ 85mA recharge @ 100mA to float Float 80 hrs @2.27 - shunt1 reading are 4 different test
float64.dat	Cyclon 25Ah	-	Cont_float_plot	26	Transient	discharge 0.9hrs @ 800mA recharge @ 1A to float Float 75 hrs @2.27 change float to 2.31 for 15 hrs
float65.dat	Cyclon 25Ah	-	Cont_float_plot	26	Transient	discharge 5hrs @ 10mA from 2.31V recharge @ 10mA to float @ 2.31 V Float 250 hrs @2.31V shunt 1 is for the 24Volt string – not this test

float66.dat	Cyclon 25Ah	-	Cont_float_plot	26.5	Transient	discharge and recharge @ +- 14mA Float @ 2.31 V 20hrs shunt 1 is for the 24Volt string – not this test
float67.dat	Cyclon 25Ah	-	cont_float_plot	26.5	Transient	Open circuit decay from Float @ 2.31 V 100 hrs shunt 1 is for the 24Volt string – not this test
float68.dat	Cyclon 25Ah	-	cont_float_plot	26.5	Transient	Added reference electrode Recharged @100mA 1.5hrs then 300mA 2.35V for 40hrs float 45hrs at 2.27V shunt 1 is for the 24Volt string – not this test
float69.dat	Cyclon 25Ah	-	cont_float_plot	26.7	Transient	Repeat of test 60 discharge 3hrs @ 7.5A to 1.75V << 100% recharge @ 7.5A to 2.45V for 6 hrs Float 150 hrs at 2.27
float70.dat	Cyclon 25Ah	-	cont_float_plot	26.4	Transient	open circuit decay from 2.27V for 45hrs recharge 7.5mA 70hrs (no V limit) float 2.27V for 80hrs shunt1 reading are 4 different test
float71.dat	Cyclon 25Ah	-	cont_float_plot	26	Transient	discharge 6.5hrs @ 10mA recharge @ 7.5mA to float 2.27V Float 50 hrs @2.27 shunt1 reading are 4 different test
float72.dat	Cyclon 25Ah	-	cont_float_plot	26.8	Transient	discharge 3.5hrs @ 85mA recharge @ 100mA to float Float 180 hrs @2.27 - shunt1 reading are 4 different test
float73.dat	Cyclon 25Ah	-	cont_float_plot	25.6	Transient	discharge 1.4hrs @ 490mA recharge @ 1A to float 2.31 Float 95 hrs @2.31 shunt1 reading are 4 different test
float74.dat	Cyclon 25Ah	-	cont_float_plot	26	Transient	discharge 6hrs @ 10mA from 2.31V recharge @ 10mA to float @ 2.31 V Float 120 hrs @2.31V shunt 1 is for the 24Volt string – not this test
float75.dat	Cyclon 25Ah	-	cont_float_plot	25.5	Transient	discharge and recharge @ +- 11mA Float @ 10mA for 3.5hrs ~2.4volt 11mA discharge 190 hrs shunt 1 is for the 24Volt string – not this test
float76.dat	Cyclon 25Ah	-	cont_float_plot	26	Transient	recharge @ 2.35V for 195 hrs open cct decay 10 weeks shunt 1 is for the 24Volt string – not this test

Appendix D

Isolated Impedance Measurement

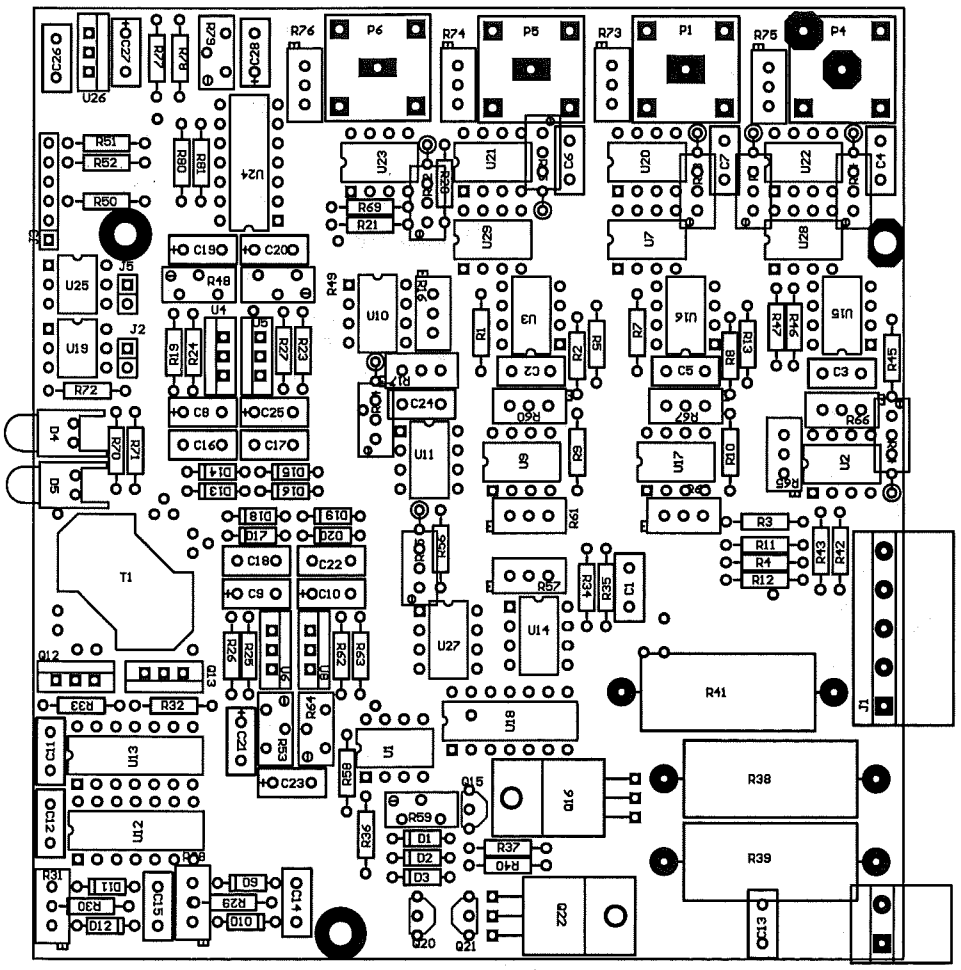

Component Layout

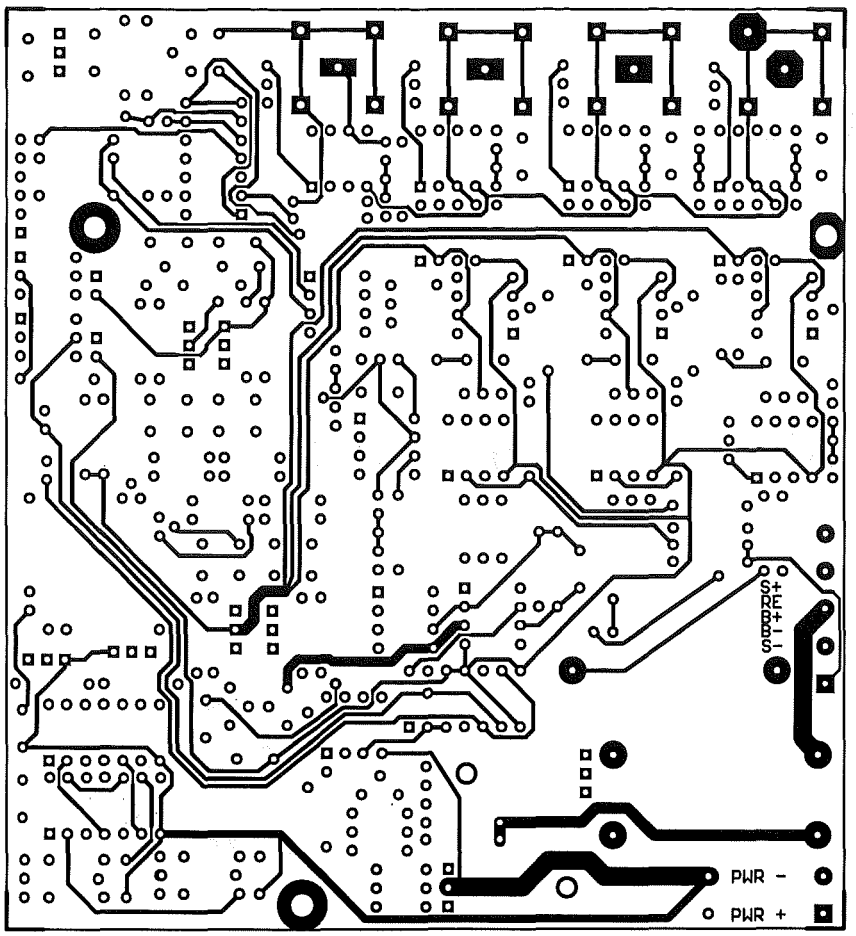

Top Copper

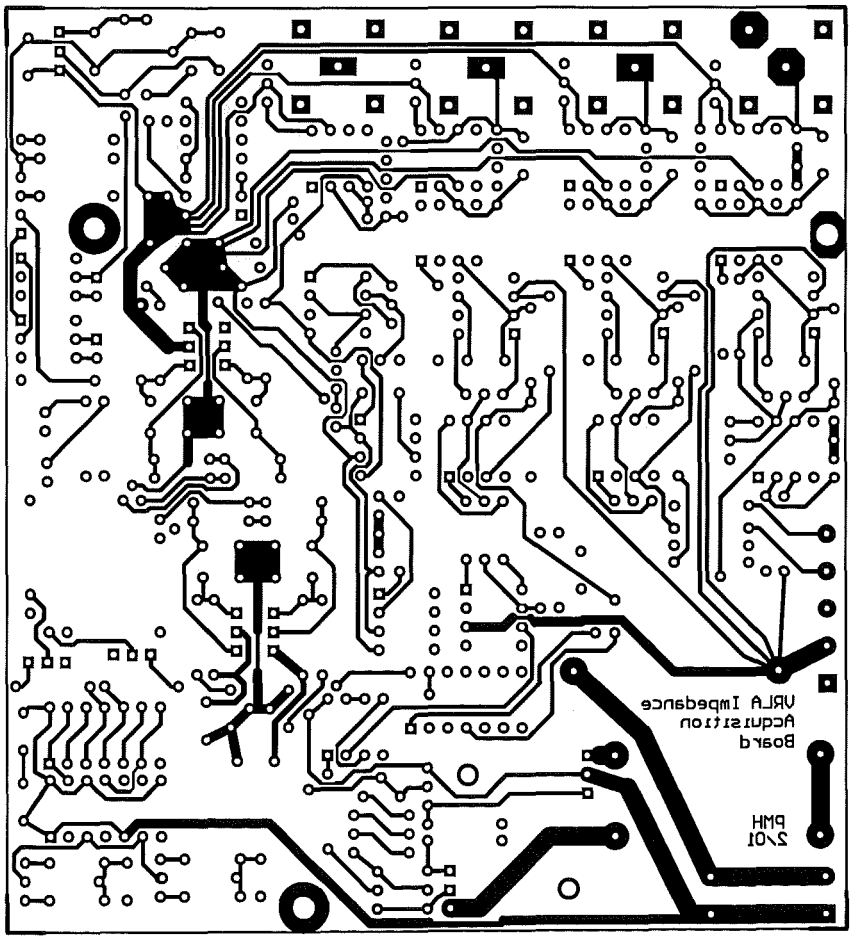

Bottom Copper

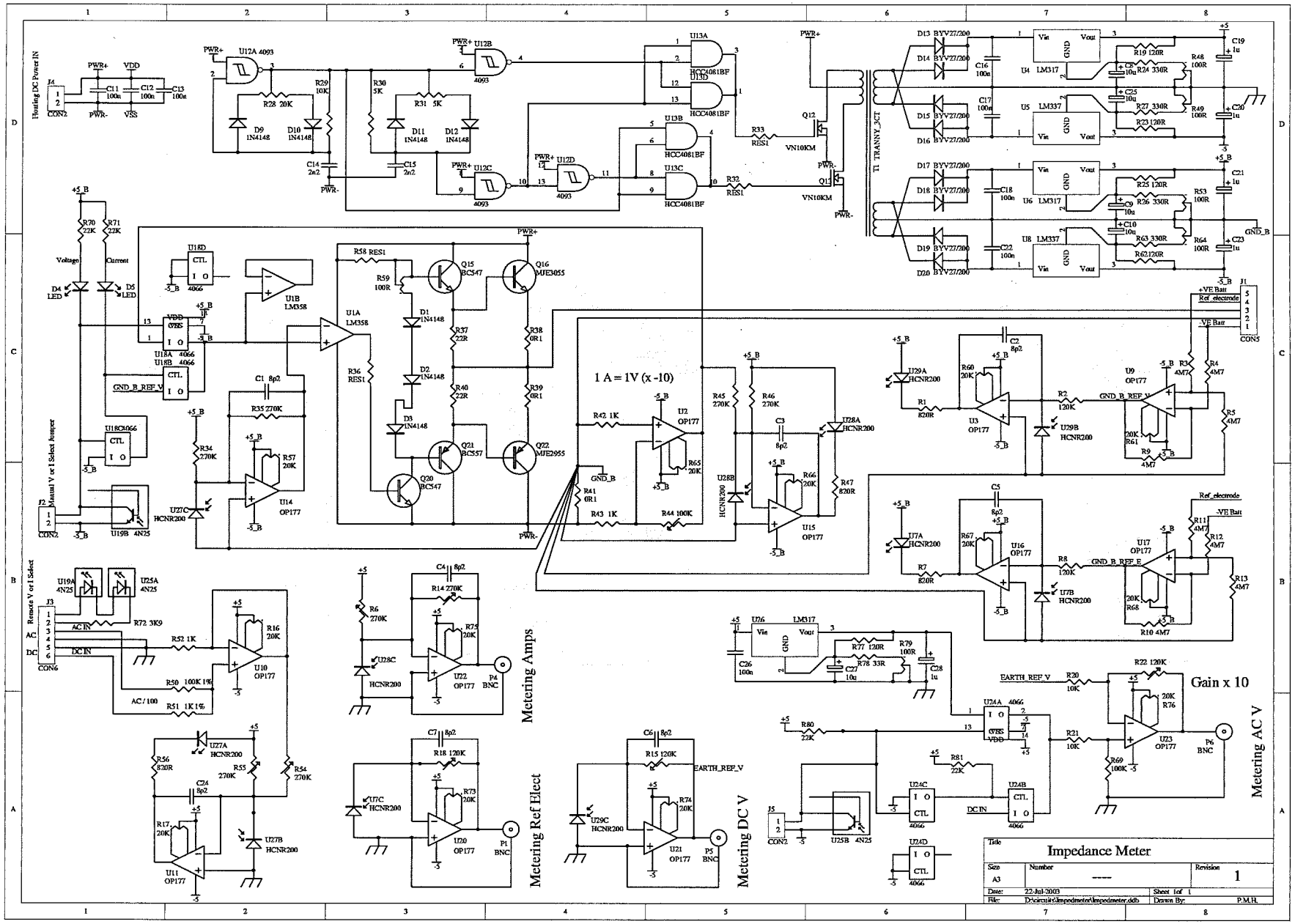
Heating DC Power IN
PWR+
VDD
PWR-
VSS
Metering Amps
Metering Ref Elect
Metering DC V
Metering AC V
Gain x 10
1 A = 1V (x -10)
Impedance Meter
Number
Revision
Date: 22-Jul-2003
Sheet 1of 1
Drawn By: P.M.H.

Precision Current Shunt Amplifier

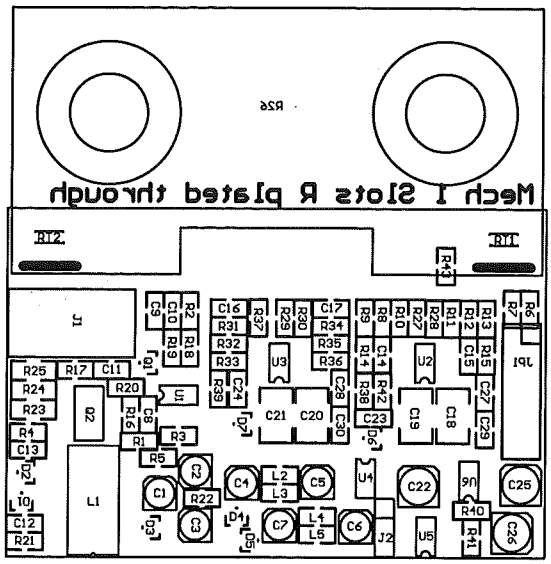

Component Layout

(Components on bottom side, viewed from below)

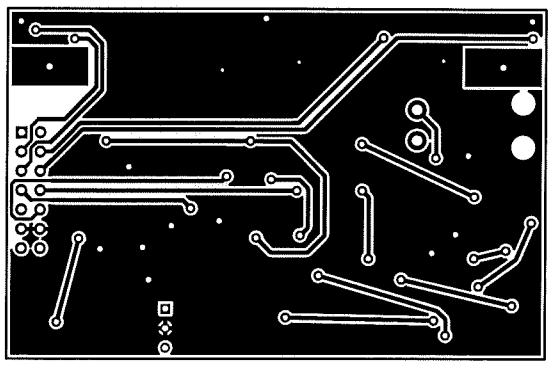

Top Copper

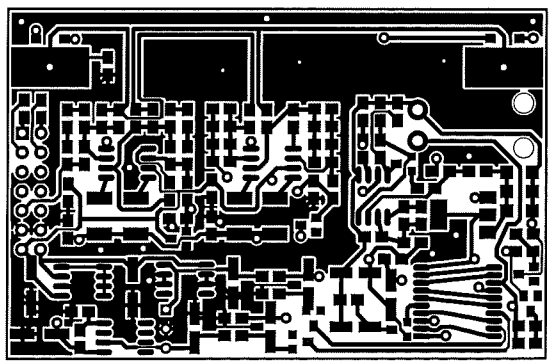

Bottom Copper (viewed through PCB)

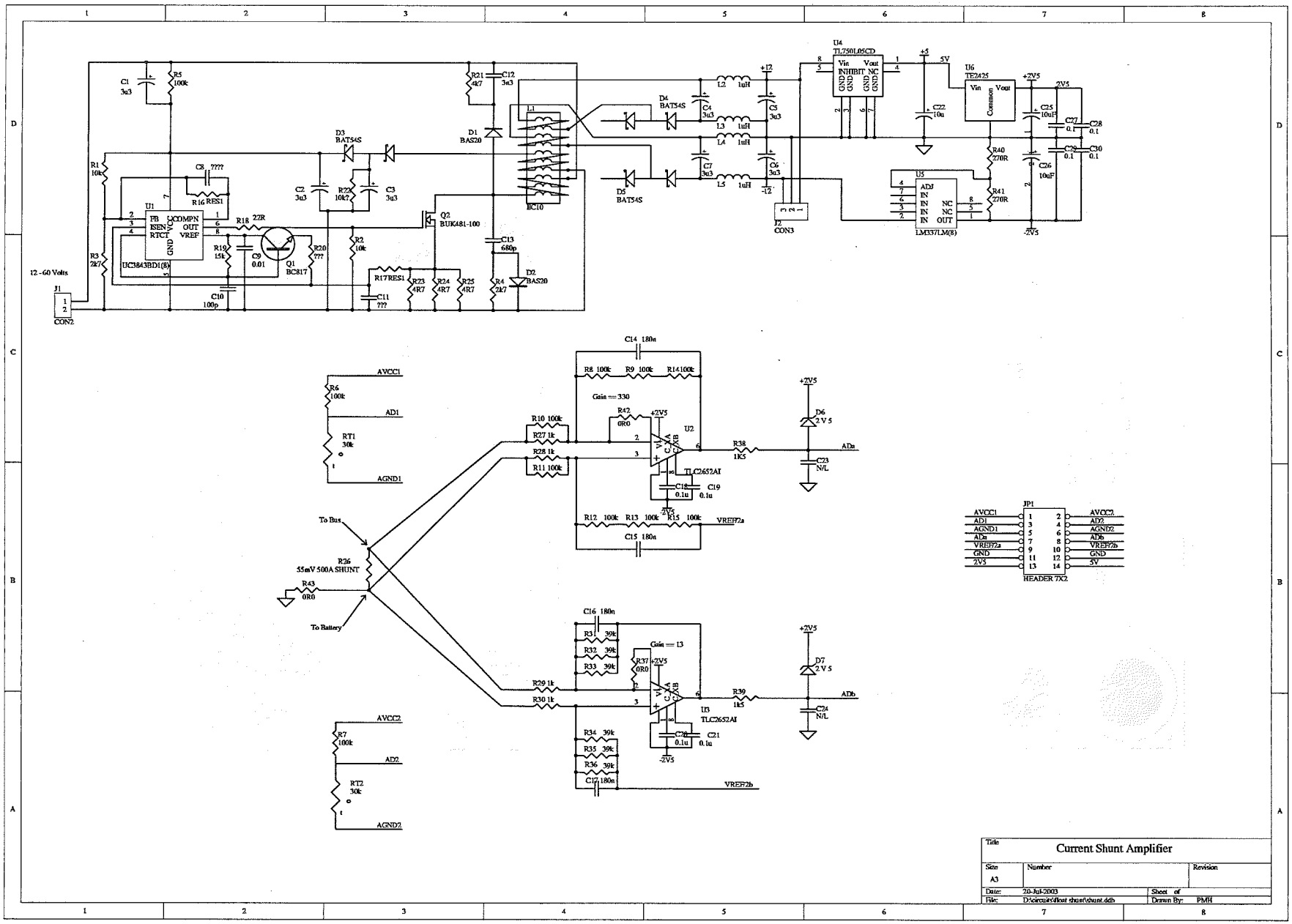

Title: Current Shunt Amplifier

Size	Number	Revision
A3		
Date: 20-Jul-2003	Sheet of	
File: D:\circuits\float shunt\shunt.ddb	Drawn By: PMH	

Temperature Controller

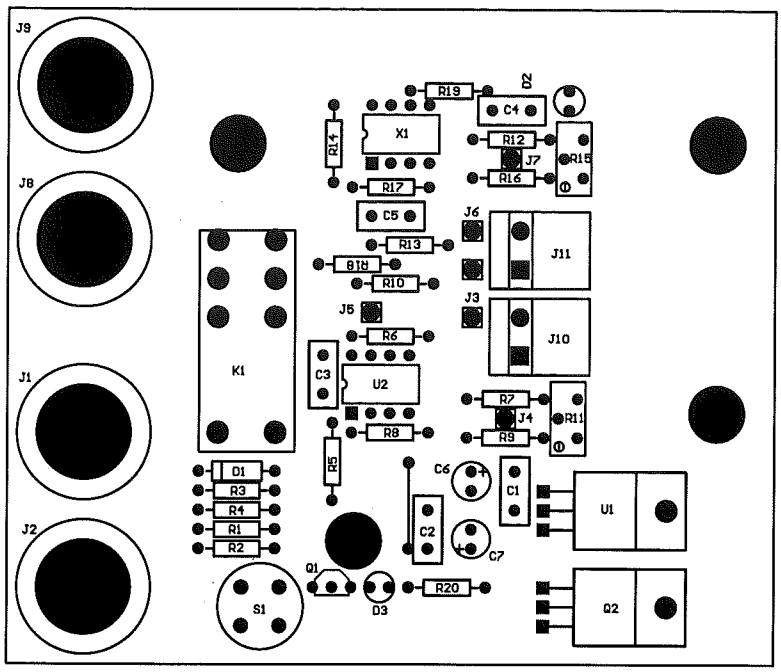

Component Layout

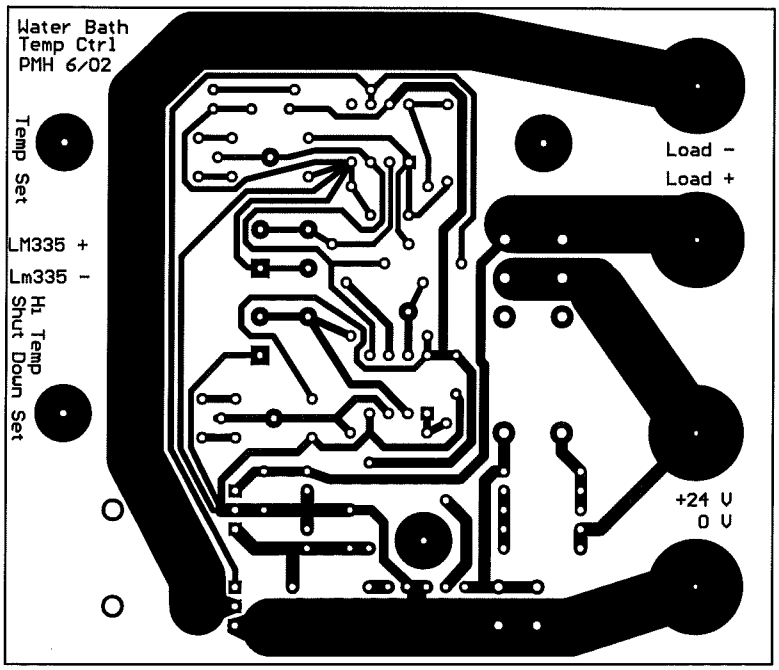

Bottom Copper (viewed from below)

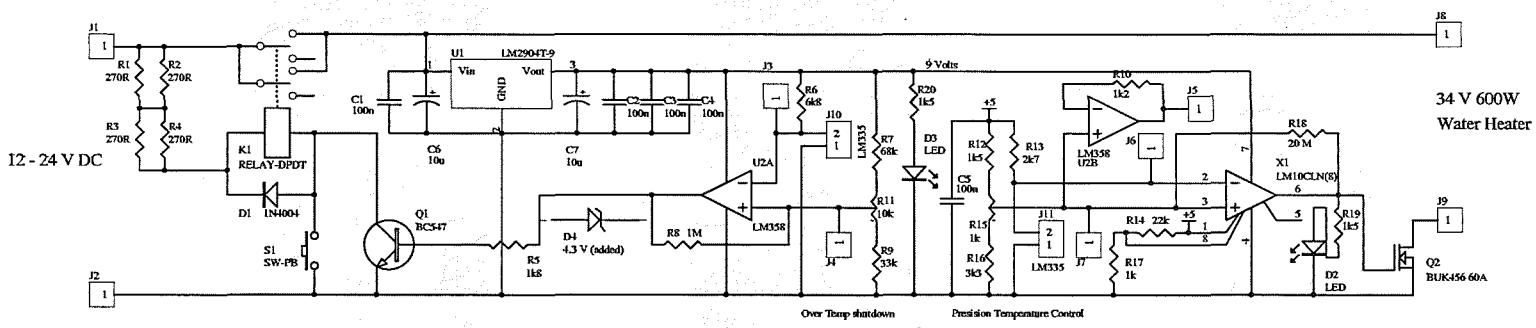

Title: Temperature Controller			
Size: B	Number		Revision
Date:	21-Jul-2003	Sheet of	
File:	D:\circuits\temperr\tempctrl.ddb	Drawn By:	PMH

Constant Current Load

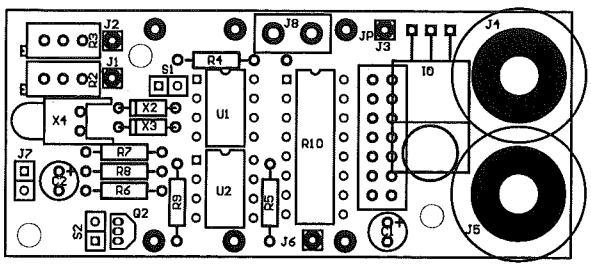

Component Layout

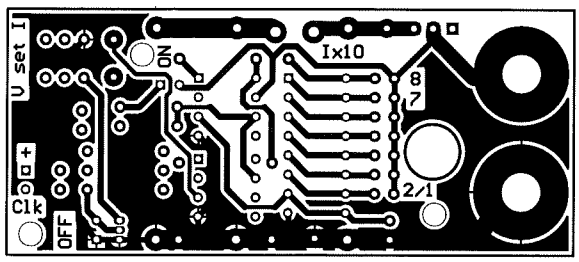

Top Copper

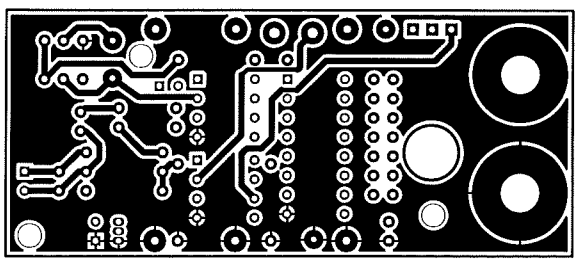

Bottom Copper (viewed through PCB)

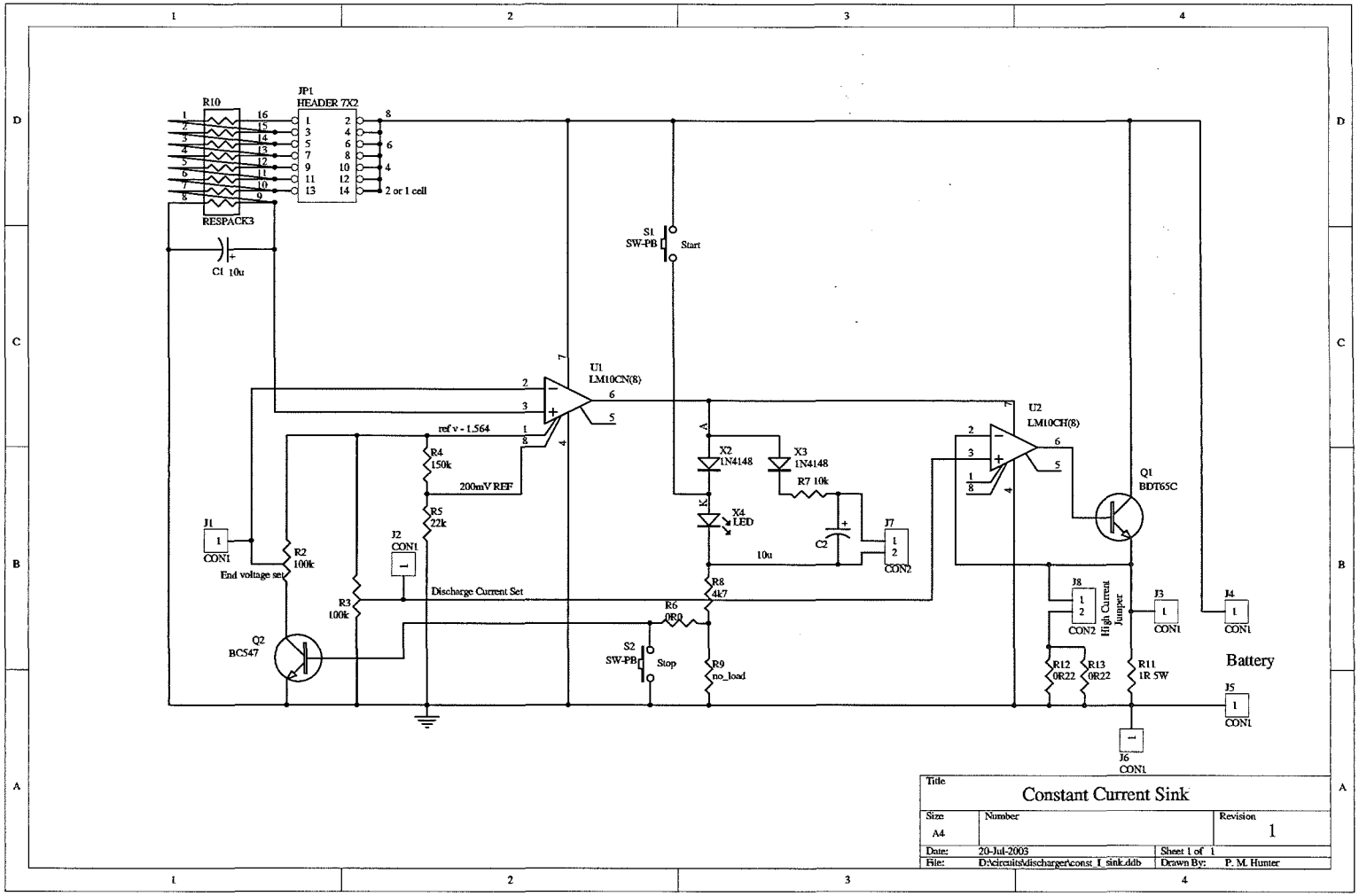
R10
RESPACK3
JP1
HEADER 7X2
2 or 1 cell
C1 10u
S1
SW-PB
Start
U1
LM10CN(8)
ref v - 1.564
R4
150k
200mV REF
R5
22k
J1
CON1
End voltage set
R2
100k
J2
CON1
Discharge Current Set
R3
100k
Q2
BC547
X2
1N4148
X3
1N4148
R7 10k
X4
LED
C2
10u
J7
CON2
R8
4k7
R6
0R0
S2
SW-PB
Stop
R9
no_load
U2
LM10CH(8)
Q1
BDT65C
J8
CON2
High Current Jumper
J3
CON1
J4
CON1
Battery
R12
0R22
R13
0R22
R11
1R 5W
J5
CON1
J6
CON1
Title
Constant Current Sink
Size
A4
Number
Revision
1
Date:
20-Jul-2005
Sheet 1 of 1
File:
D:\circuits\discharger\const_I_sink.ddb
Drawn By:
P. M. Hunter